ISSN 2686-7575 (Online)

ТОНКИЕ ХИМИЧЕСКИЕ ТЕХНОЛОГИИ

Fine Chemical Technologies

- Theoretical Basis of Chemical Technology
- Chemistry and Technology of Organic Substances
- Chemistry and Technology of Medicinal Compounds and Biologically Active Substances
- Biochemistry and Biotechnology
- Synthesis and Processing of Polymers and Polymeric Composites
- Chemistry and Technology of Inorganic Materials
- Analytical Methods in Chemistry and Chemical Technology
- Mathematical Methods and Information Systems in Chemical Technology

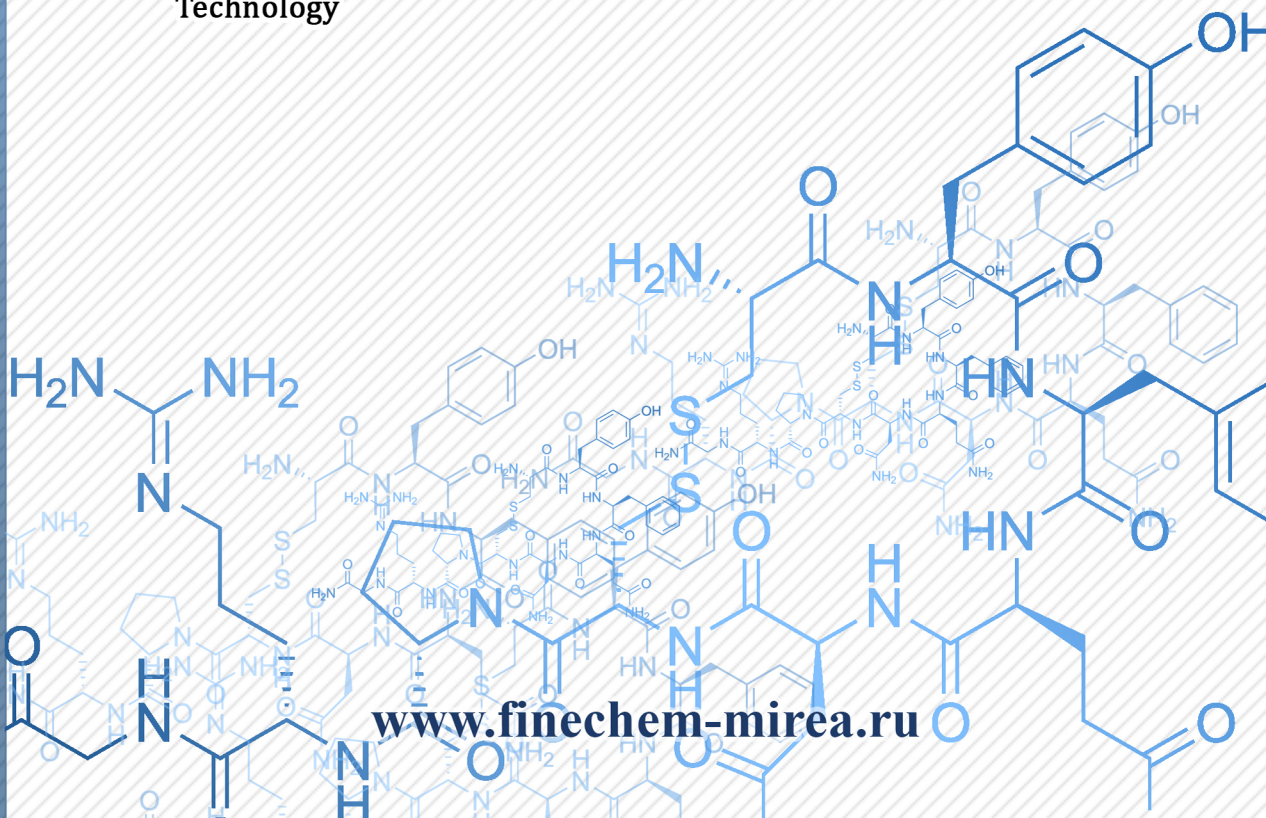

20(3)

2025

www.finechem-mirea.ru

ISSN 2686-7575 (Online)

ТОНКИЕ ХИМИЧЕСКИЕ ТЕХНОЛОГИИ

Fine Chemical Technologies

- Theoretical Basis of Chemical Technology
- Chemistry and Technology of Organic Substances
- Chemistry and Technology of Medicinal Compounds and Biologically Active Substances
- Biochemistry and Biotechnology
- Synthesis and Processing of Polymers and Polymeric Composites
- Chemistry and Technology of Inorganic Materials
- Analytical Methods in Chemistry and Chemical Technology
- Mathematical Methods and Information Systems in Chemical Technology

Tonkie Khimicheskie Tekhnologii =
Fine Chemical Technologies.
Vol. 20, No. 3, 2025

Тонкие химические технологии =
Fine Chemical Technologies.
Том 20, № 3, 2025

https://doi.org/10.32362/2410-6593-2025-20-3
www.finechem-mirea.ru

Tonkie Khimicheskie Tekhnologii =
Fine Chemical Technologies
2025, Vol. 20, No. 3

The peer-reviewed scientific and technical journal Fine Chemical Technologies highlights the modern achievements of fundamental and applied research in the field of fine chemical technologies, including the theoretical basis of chemical technology, chemistry and technology of medicinal compounds and biologically active substances, organic substances and inorganic materials, biochemistry and biotechnology, synthesis and processing of polymers and polymeric composites, analytical and mathematical methods and information systems in chemistry and chemical technology.

Founder and Publisher

Federal State Budget
Educational Institution of Higher Education
"MIREA – Russian Technological University"
78, Vernadskogo pr., Moscow, 119454, Russian Federation.
Publication frequency: bimonthly.
The journal was founded in 2006. The name was Vestnik MITHT until 2015 (ISSN 1819-1487).

The journal is included into the List of peer-reviewed science press of the State Commission for Academic Degrees and Titles of the Russian Federation.

The journal is indexed: SCOPUS, DOAJ, Chemical Abstracts, Science Index, RSCI, Ulrich's International Periodicals Directory

86, Vernadskogo pr., Moscow, 119571, Russian Federation.
Phone: +7 (499) 600-80-80 (#31288)
E-mail: *seredina@mirea.ru*

The registration number ПИ № ФС 77-74580 was issued in December 14, 2018 by the Federal Service for Supervision of Communications, Information Technology, and Mass Media of Russia

The subscription index of *Pressa Rossii*: **36924**

The Editorial Board's viewpoint may not coincide with the viewpoint of the authors of the articles published in the journal.

Тонкие химические технологии =
Fine Chemical Technologies
2025, том 20, № 3

Научно-технический рецензируемый журнал «Тонкие химические технологии» освещает современные достижения фундаментальных и прикладных исследований в области тонких химических технологий, включая теоретические основы химической технологии, химию и технологию лекарственных препаратов и биологически активных соединений, органических веществ и неорганических материалов, биохимию и биотехнологию, синтез и переработку полимеров и композитов на их основе, аналитические и математические методы и информационные системы в химии и химической технологии.

Учредитель и издатель

федеральное государственное бюджетное
образовательное учреждение высшего образования
«МИРЭА – Российский технологический университет»
119454, РФ, Москва, пр-т Вернадского, д. 78.
Периодичность: один раз в два месяца.
Журнал основан в 2006 году. До 2015 года издавался под названием «Вестник МИТХТ» (ISSN 1819-1487).

Журнал входит в Перечень ведущих рецензируемых научных журналов ВАК РФ.

Индексируется: SCOPUS, DOAJ, Chemical Abstracts, РИНЦ (Science Index), RSCI, Ulrich's International Periodicals Directory

РФ, 119571, Москва, пр. Вернадского, 86, оф. Р-108.
Тел.: +7 (499) 600-80-80 (#31288)
E-mail: *seredina@mirea.ru*

Регистрационный номер и дата принятия решения о регистрации СМИ: ПИ № ФС 77-74580 от 14.12.2018 г. СМИ зарегистрировано Федеральной службой по надзору в сфере связи, информационных технологий и массовых коммуникаций (Роскомнадзор)

Индекс по Объединенному каталогу «Пресса России»: **36924**

Мнение редакции может не совпадать с мнением авторов публикуемых в журнале статей.

Ivan A. Novakov – Academician at the RAS, Dr. Sci. (Chem.), Professor, President of the Volgograd State Technical University, Volgograd, Russian Federation.
Scopus Author ID 7003436556, ResearcherID I-4668-2015, http://orcid.org/0000-0002-0980-6591, *president@vstu.ru.*

Alexander N. Ozerin – Corresponding Member of the RAS, Dr. Sci. (Chem.), Professor, Enikolopov Institute of Synthetic Polymeric Materials of the RAS, Moscow, Russian Federation.
Scopus Author ID 7006188944, ResearcherID J-1866-2018, https://orcid.org/0000-0001-7505-6090, *ozerin@ispm.ru.*

Tapani A. Pakkanen – PhD, Professor, Department of Chemistry, University of Eastern Finland, Joensuu, Finland.
Scopus Author ID 7102310323, *tapani.pakkanen@uef.fi.*

Armando J.L. Pombeiro – Academician at the Academy of Sciences of Lisbon, PhD, Professor, President of the Center for Structural Chemistry of the Higher Technical Institute of the University of Lisbon, Lisbon, Portugal.
Scopus Author ID 7006067269, ResearcherID I-5945-2012, https://orcid.org/0000-0001-8323-888X, *pombeiro@ist.utl.pt.*

Dmitrii V. Pyshnyi – Corresponding Member of the RAS, Dr. Sci. (Chem.), Professor, Institute of Chemical Biologyand Fundamental Medicine, Siberian Branch of the RAS, Novosibirsk, Russian Federation.
Scopus Author ID 7006677629, ResearcherID F-4729-2013, https://orcid.org/0000-0002-2587-3719, *pyshnyi@niboch.nsc.ru.*

Alexander S. Sigov – Academician at the RAS, Dr. Sci. (Phys. and Math.), Professor, President of MIREA – Russian Technological University, Moscow, Russian Federation.
Scopus Author ID 35557510600, ResearcherID L-4103-2017, *sigov@mirea.ru.*

Alexander M. Toikka – Dr. Sci. (Chem.), Professor, Institute of Chemistry, Saint Petersburg State University, St. Petersburg, Russian Federation.
Scopus Author ID 6603464176, ResearcherI D A-5698-2010, http://orcid.org/0000-0002-1863-5528, *a.toikka@spbu.ru.*

Andrzej W. Trochimczuk – Dr. Sci. (Chem.), Professor, Faculty of Chemistry, Wrocław University of Science and Technology, Wrocław, Poland.
Scopus Author ID 7003604847, *andrzej.trochimczuk@pwr.edu.pl.*

Aslan Yu. Tsivadze – Academician at the RAS, Dr. Sci. (Chem.), Professor, A.N. Frumkin Institute of Physical Chemistry and Electrochemistry of the RAS, Moscow, Russian Federation.
Scopus Author ID 7004245066, ResearcherID G-7422-2014, *tsiv@phyche.ac.ru.*

Новаков Иван Александрович – академик РАН, д.х.н., профессор, президент Волгоградского государственного технического университета, Волгоград, Российская Федерация.
Scopus Author ID 7003436556, ResearcherID I-4668-2015, http://orcid.org/0000-0002-0980-6591, *president@vstu.ru.*

Озерин Александр Никифорович – член-корр. РАН, д.х.н., профессор, Институт синтетических полимерных материалов им. Н.С. Ениколопова РАН, Москва, Российская Федерация.
Scopus Author ID 7006188944, ResearcherID J-1866-2018, https://orcid.org/0000-0001-7505-6090, *ozerin@ispm.ru.*

Пакканен Тапани – PhD, профессор, Департамент химии, Университет Восточной Финляндии, Йоенсуу, Финляндия.
Scopus Author ID 7102310323, *tapani.pakkanen@uef.fi.*

Помбейро Армандо – академик Академии наук Лиссабона, PhD, профессор, президент Центра структурной химии Высшего технического института Университета Лиссабона, Португалия.
Scopus Author ID 7006067269, ResearcherID I-5945-2012, https://orcid.org/0000-0001-8323-888X, *pombeiro@ist.utl.pt.*

Пышный Дмитрий Владимирович – член-корр. РАН, д.х.н., профессор, Институт химической биологии и фундаментальной медицины Сибирского отделения РАН, Новосибирск, Российская Федерация.
Scopus Author ID 7006677629, ResearcherID F-4729-2013, https://orcid.org/0000-0002-2587-3719, *pyshnyi@niboch.nsc.ru.*

Сигов Александр Сергеевич – академик РАН, д.ф.-м.н., профессор, президент МИРЭА – Российского технологического университета, Москва, Российская Федерация.
Scopus Author ID 35557510600, ResearcherID L-4103-2017, *sigov@mirea.ru.*

Тойкка Александр Матвеевич – д.х.н., профессор, Институт химии, Санкт-Петербургский государственный университет, Санкт-Петербург, Российская Федерация.
Scopus Author ID 6603464176, Researcher ID A-5698-2010, http://orcid.org/0000-0002-1863-5528, *a.toikka@spbu.ru.*

Трохимчук Андржей – д.х.н., профессор, Химический факультет Вроцлавского политехнического университета, Вроцлав, Польша.
Scopus Author ID 7003604847, *andrzej.trochimczuk@pwr.edu.pl.*

Цивадзе Аслан Юсупович – академик РАН, д.х.н., профессор, Институт физической химии и электрохимии им. А.Н. Фрумкина РАН, Москва, Российская Федерация.
Scopus Author ID 7004245066, ResearcherID G-7422-2014, *tsiv@phyche.ac.ru.*

Contents

CHEMISTRY AND TECHNOLOGY OF ORGANIC SUBSTANCES

193 *Yulianna G. Borisova, Shakhobiddin Sh. Dzhumaev, Rimma M. Sultanova, Gul'nara Z. Raskil'dina, Simon S. Zlotskii*
Synthesis and anticorrosive activity of *tert*-amines containing cycloacetal or *gem*-dichlorocyclopropane fragments and quaternary ammonium salts on their basis

203 *Yulia F. Ivanova, Vladimir V. Emelyanov , Svetlana V. Levanova, Yuri N. Telnov*
Determination of the enthalpy of evaporation of pentaerythritol esters of various structures using gas chromatographic retention characteristics

215 *Vu Thanh Binh, Nguyen Thanh Hoa, Do Ngoc Khue, Nguyen Khanh Hung, Dao Duy Hung*
Evaluation of the catalytic effect of potassium tungstate in green decontamination for detoxification of 2-chloroethyl phenylsulfide (2-CEPS)

BIOCHEMISTRY AND BIOTECHNOLOGY

223 *Elena V. Pikurova, Anatoly N. Boyandin, Dmitry R. Serebryakov, Natalya L. Ertiletskaya, Olesya V. Anishchenko, Anna A. Sukhanova*
Use of ion-exchange resins for purification of L-lactic acid-containing *Rhizopus oryzae* fermentation broth

SYNTHESIS AND PROCESSING OF POLYMERS AND POLYMERIC COMPOSITES

237 *Eugene S. Bochkarev, Daria M. Zapravdina, Yaroslav P. Kuznetsov, Iurii M. Mkrtchian, Vladimir V. Burmistrov , Marat A. Vaniev*
The effect of ureas and their sulfur and selenium-containing analogs on the vulcanization and thermo-oxidative resistance of elastomers based on nitrile butadiene rubber

CHEMISTRY AND TECHNOLOGY OF INORGANIC MATERIALS

253 *Nikolay V. Grechishnikov, Elena E. Nikishina*
Synthesis of complex oxides Eu_2O_3–Gd_2O_3–$Zr(Hf)O_2$ using microwave radiation and study of their properties

264 *Bogdan D. Chernyshev, Igor V. Schetinin*
Formation of the microstructure and properties of strontium hexaferrite magnets using powder injection molding

ANALYTICAL METHODS IN CHEMISTRY AND CHEMICAL TECHNOLOGY

276 *Adnan Alsayed, Anastasiya A. Prezhedromirskaya , Elizaveta A. Shnyak, Stanislav A. Kedik*
Quantitative determination of 8-methoxypsoralene in mild dosage form by high-performance liquid chromatography

ERRATUM

289 *Elena D. Avdonina, Kristina A. Pervoykina, Ludmila V. Verkhovskaya, Dmitriy N. Shcherbinin, Natalia Yu. Viskova, Irina S. Kruzhkova, Maria A. Ilina, Larisa V. Kudriavtseva, Lyudmila V. Kolobukhina, Maksim M. Shmarov, Natalya A. Antipyat, Alexander L. Gintsburg, Igor N. Tyurin*
Erratum to the article "Production of the recombinant hemagglutinin protein of the swine influenza virus A/H1N1 and analysis of its physicochemical and antigenic properties"

СОДЕРЖАНИЕ

ХИМИЯ И ТЕХНОЛОГИЯ ОРГАНИЧЕСКИХ ВЕЩЕСТВ

193 *Ю.Г. Борисова, Ш.Ш. Джумаев, Р.М. Султанова, Г.З. Раскильдина, С.С. Злотский*
Синтез и антикоррозионная активность *трет*-аминов, содержащих циклоацетальный или *гем*-дихлорциклопропановый фрагмент, и четвертичных аммониевых солей на их основе

203 *Ю.Ф. Иванова, В.В. Емельянов, С.В. Леванова, Ю.Н. Тельнов*
Определение энтальпии испарения сложных эфиров пентаэритрита различного строения с использованием газохроматографических характеристик удерживания

215 *Vu Thanh Binh, Nguyen Thanh Hoa, Do Ngoc Khue, Nguyen Khanh Hung, Dao Duy Hung*
Evaluation of the catalytic effect of potassium tungstate in green decontamination for detoxification of 2-chloroethyl phenylsulfide (2-CEPS)

БИОХИМИЯ И БИОТЕХНОЛОГИЯ

223 *Е.В. Пикурова, А.Н. Бояндин, Д.Р. Серебряков, Н.Л. Ертилецкая, О.В. Анищенко, А.А. Суханова*
Применение ионообменных смол для очистки ферментационного бульона *Rhizopus oryzae*, содержащего L-молочную кислоту

СИНТЕЗ И ПЕРЕРАБОТКА ПОЛИМЕРОВ И КОМПОЗИТОВ НА ИХ ОСНОВЕ

237 *Е.С. Бочкарёв, Д.М. Заправдина, Я.П. Кузнецов, Ю.М. Мкртчян, В.В. Бурмистров, М.А. Ваниев*
Исследование влияния мочевин и их серо- и селенсодержащих аналогов на вулканизацию и термоокислительную стойкость эластомеров на основе бутадиен-нитрильного каучука

ХИМИЯ И ТЕХНОЛОГИЯ НЕОРГАНИЧЕСКИХ МАТЕРИАЛОВ

253 *Н.В. Гречишников, Е.Е. Никишина*
Синтез сложных оксидов Eu_2O_3–Gd_2O_3–$Zr(Hf)O_2$ с применением микроволнового излучения и исследование их свойств

264 *Б.Д. Чернышев, И.В. Щетинин*
Формирование структуры и свойств магнитов на основе гексаферрита стронция, полученных с помощью технологии Powder Injection Molding

АНАЛИТИЧЕСКИЕ МЕТОДЫ В ХИМИИ И ХИМИЧЕСКОЙ ТЕХНОЛОГИИ

276 *А. Алсайед, А.А. Прежедромирская, Е.А. Шняк, С.А. Кедик*
Количественное определение 8-метоксипсоралена в мягкой лекарственной форме методом высокоэффективной жидкостной хроматографии

ИСПРАВЛЕНИЯ

289 *Е.Д. Авдонина, К.А. Первойкина, Л.В. Верховская, Д.Н. Щербинин, Н.Ю. Вискова, И.С. Кружкова, М.А. Ильина, Л.В. Кудрявцева, Л.В. Колобухина, М.М. Шмаров, Н.А. Антипят, А.Л. Гинцбург, И.Н. Тюрин*
Исправление к статье «Получение и анализ физико-химических и антигенных свойств рекомбинантного белка геммагглютинина вируса свиного гриппа A/H1N1»

Tonkie Khimicheskie Tekhnologii = Fine Chemical Technologies.
2025;20(3):193–202
ISSN 2686-7575 (Online)

Chemistry and technology of organic substances
Химия и технология органических веществ

UDC 547.464.7
https://doi.org/10.32362/2410-6593-2025-20-3-193-202
EDN UAWQXG

RESEARCH ARTICLE

Synthesis and anticorrosive activity of *tert*-amines containing cycloacetal or *gem*-dichlorocyclopropane fragments and quaternary ammonium salts on their basis

Yulianna G. Borisova✉, **Shakhobiddin Sh. Dzhumaev, Rimma M. Sultanova, Gul'nara Z. Raskil'dina, Simon S. Zlotskii**
Ufa State Petroleum Technological University, Ufa, 450064 Russia
✉ *Corresponding author, e-mail: yulianna_borisova@mail.ru*

Abstract

Objectives. The work set out to synthesize tertiary amines comprising derivatives of morpholine and piperidine containing a 1,3-dioxolane or *gem*-dichlorocyclopropane fragment, as well as quaternary ammonium salts based on them. In order to determine the process conditions (duration and temperature of the reaction) under which the maximum possible yield of the target quaternary ammonium salts is achieved, the effect of the halide structure on the yield of *tert*-amines and their subsequent salts was evaluated. The study also aimed to establish the structural and spatial structure of the obtained carbo- and heterocyclic amines and salts based on them, as well as to evaluate the anticorrosive properties of the obtained products in a hydrogen sulfide medium.

Methods. The target compounds, such as tertiary amines and quaternary ammonium salts (QAS), were obtained by classical methods of organic synthesis consisting of alkylation and condensation of the corresponding amines of various structures. Preparation of QAS was carried out using a microwave system for organic synthesis via microwave activation on a Sineo device (China). The qualitative and quantitative composition of the reaction masses was determined using gas–liquid chromatography (Crystal 2000 hardware and software complex), while mass spectroscopy was carried out on a Chromatec-Crystal 5000M device with a NIST 2012 database). A Bruker AM-500 device having operating frequencies of 500 and 125 MHz was used to perform nuclear magnetic resonance spectroscopy.

Results. Tertiary amines containing a cycloacetal or *gem*-dichlorocyclopropane fragment were obtained under thermal heating conditions. By carrying out their condensation in excess halides using microwave radiation, new quaternary ammonium salts were synthesized with a yield close to quantitative. Anticorrosive activity was estimated for the obtained cyclic compounds. 4-Allyl-4-[2-(1,3-dioxolan-2-yl)-ethyl]morpholinium chloride was determined to have the maximum protective effect in a hydrogen sulfide medium with a protection level of 91%.

Conclusions. Tertiary amines containing a cycloacetal or *gem*-dichlorocyclopropane fragment were obtained under the proposed conditions. Such substances are in demand as intermediates in the synthesis of quaternary ammonium salts having anticorrosive activity.

Keywords
alkylation, microwave radiation, quaternary ammonium salt, corrosion

Submitted: 05.09.2024
Revised: 31.01.2025
Accepted: 31.03.2025

For citation
Borisova Yu.G., Dzhumaev Sh.Sh., Sultanova R.M., Raskil'dina G.Z., Zlotskii S.S. Synthesis and anticorrosive activity of *tert*-amines containing cycloacetal or *gem*-dichlorocyclopropane fragments and quaternary ammonium salts on their basis. *Tonk. Khim. Tekhnol.* = *Fine Chem. Technol*. 2025;20(3):193–202. https://doi.org/10.32362/2410-6593-2025-20-3-193-202

НАУЧНАЯ СТАТЬЯ

Синтез и антикоррозионная активность *трет*-аминов, содержащих циклоацетальный или *гем*-дихлорциклопропановый фрагмент, и четвертичных аммониевых солей на их основе

Ю.Г. Борисова✉, Ш.Ш. Джумаев, Р.М. Султанова, Г.З. Раскильдина, С.С. Злотский

Уфимский государственный нефтяной технический университет, Уфа, 450064 Россия

✉ *Автор для переписки, e-mail: yulianna_borisova@mail.ru*

Аннотация

Цели. Синтезировать третичные амины — производные морфолина и пиперидина, содержащие 1,3-диоксолановый или *гем*-дихлорциклопропановый фрагмент, а также четвертичные аммониевые соли на их основе. Оценить влияние строения галогенидов на выход *трет*-аминов и их последующих солей. Определить условия (длительность и температуру реакции) проведения процесса, при которых достигается максимально возможный выход целевых четвертичных аммониевых солей. Установить структурное и пространственное строение полученных карбо- и гетероциклических аминов и солей на их основе, а также оценить антикоррозионные свойства полученных продуктов в сероводородной среде.

Методы. Целевые соединения, такие как третичные амины и четвертичные аммониевые соли (ЧАС), были получены классическими способами органического синтеза — алкилированием и конденсацией соответствующих аминов различного строения. Получение ЧАС было осуществлено с использованием микроволновой системы для проведения органических синтезов методом микроволновой активации на приборе «Sineo» (Китай). Качественный и количественный состав реакционных масс были определены газожидкостной хроматографией (на аппаратно-программном комплексе «Кристалл 2000»), масс-спектроскопией (на приборе «Хроматэк-Кристалл 5000М» с базой NIST 2012) и спектроскопией ядерного магнитного резонанса (на приборе «Bruker AM-500» с рабочими частотами 500 и 125 МГц).

Результаты. В условиях термического нагрева получены третичные амины, содержащие циклоацетальный или *гем*-дихлорциклопропановый фрагменты, конденсация которых в избытке галогенидов с использованием микроволнового излучения позволила синтезировать новые четвертичные аммониевые соли с выходом, близким к количественному. Для полученных циклических соединений была оценена антикоррозионная активность. Определено, что максимальным защитным эффектом в сероводородной среде обладает 4-аллил-4-[2-(1,3-диоксолан-2-ил)этил]морфолиниум хлорид, который имеет степень защиты, равную 91%.

Выводы. В предложенных условиях были получены третичные амины, содержащие циклоацетальный или *гем*-дихлорциклопропановый фрагменты. Третичные амины служат промежуточными продуктами в синтезе четвертичных аммониевых солей, обладающих антикоррозионной активностью.

Ключевые слова

алкилирование, микроволновое излучение, четвертичная аммониевая соль, коррозия

Поступила: 05.09.2024
Доработана: 31.01.2025
Принята в печать: 31.03.2025

Для цитирования

Борисова Ю.Г., Джумаев Ш.Ш., Султанова Р.М., Раскильдина Г.З., Злотский С.С. Синтез и антикоррозионная активность *трет*-аминов, содержащих циклоацетальный или *гем*-дихлорциклопропановый фрагмент, и четвертичных аммониевых солей на их основе. *Тонкие химические технологии*. 2025;20(3):193–202. https://doi.org/10.32362/2410-6593-2025-20-3-193-202

INTRODUCTION

Cyclic amines such as morpholine, piperazine, and piperidine, which are widely used in the synthesis of a wide range of biologically active products, are produced on an industrial scale [1–3]. The tertiary amines and their derivatives containing 1,3-dioxacycloalkane or *gem*-dichlorocyclopropane fragments obtained on their basis exhibit various forms of biological activity, such as antifungal (fungicidal), bactericidal (biocidal), herbicidal, etc. [4, 5]. Nitrogen-containing heterocyclic compounds are additionally used in the design and synthesis of quaternary ammonium salts (QAS) with antimicrobial properties [6, 7]. It should be noted that QAS containing *gem*-dichlorocyclopropane fragment exhibit antibacterial activity against *Escherichia coli*,

Klebsiella pneumoniae, *Staphylococcus aureus*, *Acinobacter Baumanii* [8]. Prof. A. Vereshchagin, who synthesized QAS on the basis of cyclic acetals of pyridine aldehyde and hydroxypyridine esters, established their ability to inhibit the growth of gram-positive and gram-negative bacteria, fungi, and some viruses in low concentrations [9–11]. The series of works by Acad. A.L. Maksimov *et al.* demonstrate various applications of acetals in petrochemistry [12–14]. For example, cyclic acetals, which are well dispersed in lubricating compositions, can be used as active high-octane components of anti-wear additives in diesel fuel and other energy carriers to reduce the corrected diameter of the wear spot [15–17]. Heterocycles and their analogs or derivatives (esters, amides and salts) have antioxidant properties and inhibit acid corrosion of metals [18, 19].

Thus, the synthesis of new QAS containing 1,3-dioxacycloalkane and *gem*-dichlorocyclopropane structures seems to be important and relevant in terms of the creation of new petrochemical reagents and pharmacological preparations.

We previously showed that quaternary ammonium salts derived from 2-chloromethyl-*gem*-dichlorocyclopropane and 4-chloromethyl-1,3-dioxolane are catalytic in the *O*-alkylation reaction of 2,2-dimethyl-4-oxymethyl-1,3-dioxolane with allyl chloride [20].

In the present study, new *tert*-amines and salts based on them were prepared using 1,1-dichloro-2-(chloromethyl)-2-methylcyclopropane and 2-bromoethyl-1,3-dioxolane to evaluate the anticorrosion activity of the obtained compounds.

MATERIALS AND METHODS

During the process of analyzing reaction masses, the mass spectra of compounds were recorded on the Chromatek-Crystal 5000M hardware-software complex (*Chromatek*, Russia) with the NIST 2012 database (*National Institute of Standards and Technology*, USA). The analysis conditions were as described in the article [9]. The electron impact ionization method was used to obtain mass spectra of compounds. ^{1}H and ^{13}C nuclear magnetic resonance (NMR) spectra were recorded on a Bruker AM-500 spectrometer (*Bruker Corporation*, USA) with operating frequencies of 500 and 125 MHz, respectively; the used solvent was deuterated chloroform $CDCl_3$. Chemical shifts are given on the δ scale (ppm) relative to tetramethylsilane as internal standard. The spin-spin interaction constants (*J*) are given in Hz.

1,1-Dichloro-2-(chloromethyl)-2-methylcyclopropane **3** was prepared by dichlorocarbenylation of 2-methyl-3-chloropropene-1 (CAS 1563-47-3) under interfacial catalysis conditions following a similar procedure as presented in [9]. Morpholine (CAS 110-91-8), piperidine (CAS 110-89-4) and 2-bromoethyl-1,3-dioxolane **4** (CAS 4360-63-8) are commercially available reagents.

Synthesis of compounds 5–7 under thermal heating conditions

The flask was loaded with 0.002 mol of amine (0.17 g of morpholine or piperidine), 0.004 mol of halide (0.69 g of 1,1-dichloro-2-(chloromethyl)-2-methylcyclopropane **3** or 0.72 g of 2-bromoethyl-1,3-dioxolane **4**) and 20 mL of dimethylformamide. The reaction mixture was stirred at 100°C for 8–11 h until complete conversion of the amine (control by gas–liquid chromatography). The mixture was washed with water, extracted with methylene chloride, and evaporated. The target product was isolated by vacuum distillation.

4-[2,2-Dichloro-1-methylcyclopropyl)methyl]-morpholine **5**. Colorless liquid. $T_{boil.}$ = 98–99°C (5 mm Hg). Yield 90% (0.40 g). ^{1}H NMR spectrum, δ, ppm (*J*, Hz): 1.32 d (2H, CH_2, *J* 4.14), 1.67 s (3H, CH_3), 2.43 d (4H, $2CH_2$, *J* 4.14), 2.57 d (2H, CH_2, *J* 12.74), 3.71 d (4H, $2CH_2$, *J* 4.11). ^{13}C NMR, δ_C, ppm: 19.98 (CH_3), 28.61 (C), 31.23 (CH_2), 53.32 (2 CH_2), 62.79 (CH_2), 66.75 (C), 66.97 ($2CH_2$). Mass spectrum *m*/*z* (I_{rel}, %): 222.98/224.99/226.99 (15/10/4), 187.99/190.02 (13/4), 127.02/129.02 (18/5), 124.06 (30), 99.89/101.05 (100/27), 84.99/87.00 (30/10), 73.03/74.91 (18/5), 56.00 (60).

1-[2,2-Dichloro-1-methylcyclopropyl)methyl]-piperidine **6**. Colorless liquid. $T_{boil.}$ = 93–95°C (5 mm Hg). Yield 93% (0.41 g). ^{1}H NMR spectrum, δ, ppm (*J*, Hz): 1.10 d (2H, CH_2, *J* 6.03), 1.65 s (3H, CH_3), 1.64–1.75 m (6H, $3CH_2$), 2.33 dd (4H, $2CH_2$, *J* 8.8), 2.61 d (2H, CH_2, *J* 12.01). ^{13}C NMR, δ_C, ppm: 19.81 (CH_3), 23.01 (CH_2), 23.55 ($2CH_2$), 28.73 (C), 31.26 (CH_2), 57.39 ($2CH_2$), 62.81 (CH_2), 66.71 (C). Mass spectrum *m*/*z* (I_{rel}, %): 221.01/223.01/225.01 (10/6/2), 186.01/188.01 (10/5), 138.07 (30), 124.06 (30), 97.92/99.08 (100/31), 83.02/85.03 (30/6), 69.06/71.05 (28/8), 55.00 (55).

4-[2-(1,3-Dioxolan-2-yl)ethyl]morpholine **7**. Colorless liquid. $T_{boil.}$ = 101–102°C (5 mm Hg). Yield 95% (0.35 g). ^{1}H NMR spectrum, δ, ppm (*J*, Hz): 1.82–1.85 m (2H, CH_2), 2.39–2.44 m (6H, $3CH_2$), 3.65–3.68 m (4H, $2CH_2$), 3.80 d (2H, CH_2, *J* 3.67), 3.91 d (2H, CH_2, *J* 3.73), 4.88 t (1H, CH, *J* 9.56). ^{13}C NMR, δ_C, ppm: 30.99 (CH_2), 40.96 (CH_2), 53.64 ($2CH_2$), 64.80 ($2CH_2$), 66.84 ($2CH_2$), 103.13 (CH). Mass spectrum *m*/*z* (I_{rel}, %): 188.14 (2), 114.06 (100), 101.09 (25), 86.00 (22), 70.02 (52), 56.03 (44).

Synthesis of compounds 11–13 under microwave heating conditions

The flask was loaded with 0.002 mol of *tert*-amine (0.44 g of amine **5** or **6** or 0.37 g of amine **7**), 0.004 mol (0.68 g of benzyl bromide **8**, 0.58 g of amyl bromide **9** or 0.3 g of allyl chloride **10**) and 20 mL of methyl isobutyl ketone. The reaction mixture was stirred under microwave irradiation (MWI) conditions at 30°C for 2–4 h until precipitation. The mixture was filtered off, the residue on the filter was washed with hexane (2 × 100 mL) and dried under vacuum.

4-Benzyl-4-[-2,2-dichloro-1-methylcyclopropyl)-methyl]morpholinium bromide **11**. Brown powder. $T_{melt.}$ = 167°C. Yield 95% (0.75 g). ^{1}H NMR spectrum, δ, ppm (*J*, Hz): 1.67 s (3H, CH_3), 1.65 d (1H, CH_a, ^2J 7.7), 1.90 d (1H, CH_a, *J* 7.4), 3.22 d (4H, $2CH_2$, *J* 4.37), 3.49 d (2H, CH_2, *J* 10.87), 3.98 d (4H, $2CH_2$, *J* 9.98), 4.83 s (2H, CH_2), 7.55–7.61 m (5H, Ph–). ^{13}C NMR, δ_C, ppm: 19.60 (CH_3), 26.07 (C), 31.44 (CH_2), 60.00 (CH_2), 60.59 ($2CH_2$), 63.50 (CH_2), 65.99 ($2CH_2$), 129.32 (2CH), 127.07 (CH), 128.52 (2CH), 134.22 (C).

1-Butyl-1-[2,2-dichloro-1-methylcyclopropyl)-methyl]piperidinium bromide **12**. Brown powder. $T_{melt.}$ = 162°C. Yield 92% (0.66 g). ^{1}H NMR spectrum, δ, ppm (*J*, Hz): 0.93 s (3H, CH_3), 1.01 d (2H, CH_2, *J* 10.87), 1.23–1.29 m (10H, $5CH_2$), 3.57–3.61 m (4H, $2CH_2$), 3.41 d (2H, CH_2, *J* 4.77), 4.03 d (2H, CH_2, *J* 12.03). ^{13}C NMR, δ_C, ppm: 13.31 (CH_3), 19.82 (CH_2), 19.89 (CH_3), 21.56 (CH_2), 23.29 ($2CH_2$), 23.05 (CH_2), 29.34 (CH_2), 28.74 (C), 67.45 ($2CH_2$), 67.89 (CH_2), 68.41 (CH_2).

4-Allyl-4-[2-(1,3-dioxolan-2-yl)ethyl]morpholinium chloride **13**. Brown powder. $T_{melt.}$ = 145°C. Yield 98% (0.51 g). ^{1}H NMR spectrum, δ, ppm (*J*, Hz): 1.25–1.34 m (2H, CH_2), 3.03–3.12 m (6H, $3CH_2$), 3.34–3.41 m (4H, $2CH_2$), 3.80 d (2H, CH_2, *J* 5.79), 3.98 d (2H, CH_2, *J* 5.72), 5.55 d (1H, CH, *J* 6.16), 5.70 dd (2H, CH_2, *J* 10.55), 5.90–6.01 m (1H, CH). ^{13}C NMR, δ_C, ppm: 31.03 (CH_2), 43.28 (CH_2), 51.07 ($2CH_2$), 59.94 (CH_2), 63.73 ($2CH_2$), 67.56 ($2CH_2$), 103.55 (CH), 125.86 (CH_2), 127.32 (CH).

Methodology for determination of anticorrosive activity of substances in a hydrogen sulfide-containing environment

The electrochemical method was used to study the anticorrosive activity of substances. Electrochemical analysis was carried out on the Monikor-2M corrosion rate analyzer (*Akurs-M*, Russia). The device includes two electrodes made of St3 steel (properties of St3 steel, requirements to chemical composition, control methods, and data on international quality standard are listed in GOST 380-2005[1]). Prior to testing, the surface of steel electrodes was prepared using emery paper #180, followed by emery paper #240, in the direction of the electrode length. The prepared electrode samples were degreased with dimethyl ketone (*Vekton*, Russia) immediately before carrying out the test. Next, the electrodes were activated by means of three-stage washing. The test substance (volume of 0.25 mL) was dissolved in 25 mL of ethyl alcohol (*Ruskhim*, Russia). Cylindrical laboratory cells were filled with the calculated amount of 3% sodium chloride solution (*Lenreaktiv*, Russia) and purged for 30 min with nitrogen (Orenburg, Russia). After purging, the calculated amount of hydrogen sulfide water[2] and 1.25 mL of dissolved substance in alcohol were poured into the medium. Then the electrodes were immersed in an electrochemical cell pre-filled with the test medium and the corrosion rate was determined for a period of 60 min. To obtain convergent and reliable results, parallel tests of 2 cells with the same medium were performed and arithmetic mean values of the obtained corrosion rates were calculated.

The braking coefficient was calculated by the formula: $A = \frac{P_0}{P_1}$, where P_0 is the depth corrosion rate of the sample in solution without corrosion inhibitor, mm/year; P_1 is the depth corrosion rate of the sample in solution with corrosion inhibitor, mm/year.

RESULTS AND DISCUSSION

Morpholine **1** and piperidine **2** were converted to the corresponding tertiary amines **5**–**7** by *N*-alkylation of 1,1-dichloro-2-(chloromethyl)-2-methylcyclopropane **3** and 2-β-bromoethyl-1,3-dioxolane **4**, which, upon action of benzyl bromide **8**, butyl **9**, or 3-chloro-propene-1 **10**, formed the corresponding quaternary ammonium salts **11**–**13** in quantitative yields (Scheme).

Under the selected conditions (100°C, 8–11 h), the yield of tertiary amines **5**–**7** was 90–95%. Dimethylformamide was used as a solvent since its use reduces the synthesis time by 2–4 times as compared to toluene without reducing the yield and selectivity of formation of target compounds **5**–**7**.

[1] GOST 380-2005. Interstate Standard. Common quality carbon steel. Grades. Moscow: Standartinform; 2007.

[2] Hydrogen sulfide water was prepared independently by mixing sodium sulfide and table salt solutions with hydrochloric acid. The concentration of hydrogen sulfide water was determined by the titration method.

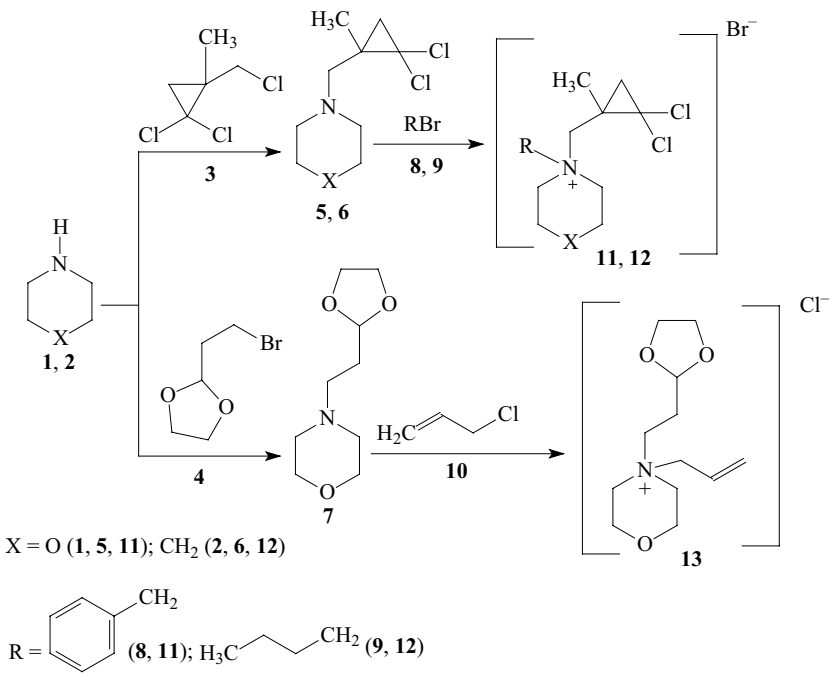

Scheme. Obtaining target salts **11**–**13**

Quaternary ammonium salts containing acetal or *gem*-dichlorocyclopropane fragments **11**–**13** were obtained by condensation of tertiary amines **5**–**7** with an excess of halides **8**–**10** in 70–90% yield. MWI was successfully used for the synthesis of these QAS to prepare salts **11**–**13** at 30°C in 2–4 h in quantitative yields; conversely, thermal heating (40–100°C) required 6–8 h (Table 1).

Amines containing carbo- and heterocyclic fragments (acetal and cyclopropane groups) and the corresponding salts obtained on their basis are known to exhibit anticorrosion properties in acidic and hydrogen sulfide-containing media and can thus be effective inhibitors of corrosion of low-carbon and low-alloy steels [21]. While continuing to conduct studies in this field, we have investigated the anticorrosion activity of the obtained *tert*-amines **5**–**7** and salts **11**–**13** in hydrogen sulfide-containing medium, which is widespread in hydrocarbon production processes.

Table 1. Condensation of tertiary amines **5**–**7** with excess halides **8**–**10** and under the influence of thermal heating and microwave radiation **11**–**13**

Initial compounds		Reaction condition		Reaction product	Yield, %	Heating type
		T, °C	Reaction time, h			
5	**8**	100	7	**11**	80	Thermal
		40	3		95	MWI
6	**9**	90	8	**12**	70	Thermal
		60	4		92	MWI
7	**10**	40	6	**13**	90	Thermal
			2		98	MWI

Note: methyl isobutyl ketone solvent.

Table 2. Protection degree and inhibition coefficient of substances **5**–**7**, **11**–**13** in hydrogen sulfide-containing environment

Compound number	Corrosion, mm/year	Protection degree, %	Inhibition coefficient
5	0.78	23	1.31
6	0.29	71	3.51
7	0.23	78	4.47
11	0.18	82	5.58
12	0.11	89	9.23
13	0.08	91	11.61

Compound **13** showed the highest anticorrosion activity with a protection degree of 91% (inhibition coefficient = 11.61). Amines **5**–**7** showed protection efficiency in the range from 23 to 78% (inhibition coefficient = 1.31–4.47). We note that the degree of protection of salts **11**–**13** slightly exceeds the similar index (50%) of reagents used in oil production [22]. This may be assumed to be due to the presence of alkyl substituents in molecules **12** and **13**, leading to an increase in hydrophilicity and solubility in the corrosive environment, which in turn, according to [23], increases the inhibitory effect of organic compounds.

CONCLUSIONS

Thus, tertiary amines containing cycloacetal or *gem*-dichlorocyclopropane fragments were obtained under thermal heating conditions. Condensation of tertiary amines in an excess of halides using MWI allowed the synthesis of new quaternary ammonium salts in near quantitative yields. The anticorrosive activity was evaluated for the tertiary amines. 4-Allyl-4-[2-(1,3-dioxolan-2-yl)ethyl]morpholinium chloride is determined to exhibit anticorrosive properties in hydrogen sulfide environment, having a protection degree equal to 91%.

Acknowledgments

The work was carried out within the framework of the State Assignment of the Ministry of Science and Higher Education of the Russian Federation in the field of scientific activity, publication No. FEUR – 2022-0007 “Petrochemical reagents, oils, and materials for thermal power engineering.”

Authors’ contributions

Yu.G. Borisova—collecting and processing material, writing the text of the article.

Sh.Sh. Dzhumaev—conducting research, reviewing publications on the topic of articles.

G.Z. Raskil’dina—collecting and processing material, statistical processing.

R.M. Sultanova—consultation on planning, methodology, and research implementation.

S.S. Zlotskii—development of the concept of scientific work, critical revision with the introduction of valuable intellectual content.

The authors declare no conflicts of interest.

REFERENCES

1. Waiker D.K., Verma A., Akhilesh G.T., Singh N., Roy A., Dilnashin H., Tiwari V., Trigun S.K., Singh S.P., Krishnamurthy S., Lama P., Davisson V.J., Shrivastava S.K. Design, Synthesis, and Biological Evaluation of Piperazine and *N*-Benzylpiperidine Hybrids of 5-Phenyl-1,3,4-oxadiazol-2-thiol as Potential Multitargeted Ligands for Alzheimer’s Disease Therapy. *ACS Chem. Neurosci.* 2023;14(11):2217–2242. https://doi.org/10.1021/acschemneuro.3c00245
2. Blake L.C., Roy A., Neul D., Schoenen F.J., Aubé J., Scott E.E. Benzylmorpholine analogs as selective inhibitors of lung cytochrome P450 2A13 for the chemoprevention of lung cancer in tobacco users. *Pharm. Res.* 2013;30(9): 2290–2302. https://doi.org/10.1007/s11095-013-1054-z

СПИСОК ЛИТЕРАТУРЫ

1. Waiker D.K., Verma A., Akhilesh G.T., Singh N., Roy A., Dilnashin H., Tiwari V., Trigun S.K., Singh S.P., Krishnamurthy S., Lama P., Davisson V.J., Shrivastava S.K. Design, Synthesis, and Biological Evaluation of Piperazine and *N*-Benzylpiperidine Hybrids of 5-Phenyl-1,3,4-oxadiazol-2-thiol as Potential Multitargeted Ligands for Alzheimer’s Disease Therapy. *ACS Chem. Neurosci.* 2023;14(11):2217–2242. https://doi.org/10.1021/acschemneuro.3c00245
2. Blake L.C., Roy A., Neul D., Schoenen F.J., Aubé J., Scott E.E. Benzylmorpholine analogs as selective inhibitors of lung cytochrome P450 2A13 for the chemoprevention of lung cancer in tobacco users. *Pharm. Res.* 2013;30(9): 2290–2302. https://doi.org/10.1007/s11095-013-1054-z

3. Brito A.F., Moreira L.K.S., Menegatti R., Costa E.A. Piperazine derivatives with central pharmacological activity used as therapeutic tools. *Fundam. Clin. Pharmacol*. 2019;33(1): 13–24. https://doi.org/10.1111/fcp.12408
4. Sun N.B., Jin J.Z., Lei C., Ke W. Synthesis, structure and biological activities of 2,2-dichloro-1-(4-ethoxyphenyl)-cyclopropanyl substituted piperidin-1-yl ketone. *Asian J. Chem*. 2013;25(7): 4067–4070. https://doi.org/10.14233/ajchem.2013.14040
5. Yakovenko E.A., Baimurzina Y.L., Raskil'dina G.Z., *et al.* Synthesis and herbicidal and antioxidant activity of a series of hetero- and carbocyclic derivatives of monochloroacetic acid. *Russ. J. Appl. Chem*. 2020;93(5):712–720. https://doi.org/10.1134/S1070427220050122
[Original Russian Text: Yakovenko E.A., Baimurzina Y.L., Raskil'dina G.Z., Zlotskii S.S. Synthesis and herbicidal and antioxidant activity of a series of hetero- and carbocyclic derivatives of monochloroacetic acid. *Zhurnal prikladnoi khimii*. 2020;93(5):705–713 (in Russ.). https://doi.org/10.31857/S0044461820050126]
6. Nadagouda M.N., Vijayasarathy P., Sin A., *et al.* Antimicrobial activity of quaternary ammonium salts: structure-activity relationship. *Med. Chem. Res*. 2022;31(10):1663–1678. https://doi.org/10.1007/s00044-022-02924-9
7. Goebel T., Ulmer D., Projahn H., Kloeckner J., Heller E., Glaser M., Holzgrabe U. In search of novel agents for therapy of tropical diseases and human immunodeficiency virus. *J. Med. Chem.* 2008;51(2):238–250. https://doi.org/10.1021/jm070763y
8. Raskil'dina G.Z., Borisova Yu.G., Vereshchagin A.N., Detusheva E.V., Sultanova R.M., Zlotskii S.S. Biological activity of quaternary ammonium salts containing 1,3-dioxolane or *gem*-dichlorocyclopropane fragment. *Rev. and Adv. in Chem*. 2024;14(1):16–21. https://doi.org/10.1134/S2634827624600105
9. Tsuji Y., Yamamoto M., Vereshchagin A.N., Dorofeev A.S., Geyvandova T.A., Agafonova I.F., Geyvandov R.K. *Dimeric Quaternary Pyridinium Salts Possessing Biocidal Activity*: Pat. WO158045. Publ. 02.10.2014.
10. Vereshchagin A.N., Frolov N.A., Konyuhova V.Y., Hansford K.A., Egorov M.P. Synthesis and microbiological properties of novel bis-quaternary ammonium compounds based on 4,4′-oxydiphenol spacer. *Mendeleev Commun.* 2019;29(5): 523–525. https://doi.org/10.1016/j.mencom.2019.09.015
11. Vereshchagin A.N., Gordeeva A.M., Frolov N.A., Proshin P.I., Hansford K.A., Egorov M.P. Synthesis and microbiological properties of novel bis-quaternary ammonium compounds based on biphenyl spacer. *Eur. J. Organ. Chem.* 2019;26: 4123–4127. https://doi.org/10.1002/ejoc.201900319
12. Samoilov V.O., Ni D.S., Goncharova A.V., *et al.* Catalytic hydrogenolysis of solketal on bifunctional catalysts with production of high octane components of motor fuels. *Russ. J. Appl. Chem.* 2020;93(1):108–117. https://doi.org/10.1134/s1070427220010127
[Original Russian Text: Samoilov V.O., Ni D.S., Goncharova A.V., Knyazeva M.I., Ramazanov D.N., Maksimov A.L. Catalytic hydrogenolysis of solketal on bifunctional catalysts with production of high octane components of motor fuels. *Zhurnal prikladnoi khimii*. 2020;93(1):121–131 (in Russ.). https://doi.org/10.31857/S0044461820010120]
13. Maximov A.L., Nekhaev A.I., Ramazanov D.N. Ethers and acetals, promising petrochemicals from renewable sources. *Pet. Chem.* 2015;55(1):1–21. https://doi.org/10.1134/S0965544115010107
[Original Russian Text: Maximov A.L., Nekhaev A.I., Ramazanov D.N. Ethers and acetals, promising petrochemicals from renewable sources. *Neftekhimiya.* 2015;55(1):3–24 (in Russ.). https://doi.org/10.7868/S0028242115010104]

3. Brito A.F., Moreira L.K.S., Menegatti R., Costa E.A. Piperazine derivatives with central pharmacological activity used as therapeutic tools. *Fundam. Clin. Pharmacol*. 2019;33(1):13–24. https://doi.org/10.1111/fcp.12408
4. Sun N.B., Jin J.Z., Lei C., Ke W. Synthesis, structure and biological activities of 2,2-dichloro-1-(4-ethoxyphenyl)-cyclopropanyl substituted piperidin-1-yl ketone. *Asian J. Chem*. 2013;25(7):4067–4070. https://doi.org/10.14233/ajchem.2013.14040
5. Яковенко Е.А., Баймурзина Ю.Л., Раскильдина Г.З., Злотский С.С. Синтез, гербицидная и антиокислительная активность ряда гетеро- и карбоциклических производных монохлоруксусной кислоты. *Журн. прикладной химии*. 2020;93(5):705–713. https://doi.org/10.31857/S0044461820050126
6. Nadagouda M.N., Vijayasarathy P., Sin A., *et al*. Antimicrobial activity of quaternary ammonium salts: structure-activity relationship. *Med. Chem. Res*. 2022;31(10):1663–1678. https://doi.org/10.1007/s00044-022-02924-9
7. Goebel T., Ulmer D., Projahn H., Kloeckner J., Heller E., Glaser M., Holzgrabe U. In search of novel agents for therapy of tropical diseases and human immunodeficiency virus. *J. Med. Chem.* 2008;51(2):238–250. https://doi.org/10.1021/jm070763y
8. Raskil'dina G.Z., Borisova Yu.G., Vereshchagin A.N., Detusheva E.V., Sultanova R.M., Zlotskii S.S. Biological activity of quaternary ammonium salts containing 1,3-dioxolane or *gem*-dichlorocyclopropane fragment. *Rev. and Adv. in Chem*. 2024;14(1):16–21. https://doi.org/10.1134/S2634827624600105
9. Tsuji Y., Yamamoto M., Vereshchagin A.N., Dorofeev A.S., Geyvandova T.A., Agafonova I.F., Geyvandov R.K. *Dimeric Quaternary Pyridinium Salts Possessing Biocidal Activity*: Pat. WO158045. Publ. 02.10.2014.
10. Vereshchagin A.N., Frolov N.A., Konyuhova V.Y., Hansford K.A., Egorov M.P. Synthesis and microbiological properties of novel bis-quaternary ammonium compounds based on 4,4′-oxydiphenol spacer. *Mendeleev Commun.* 2019;29(5):523–525. https://doi.org/10.1016/j.mencom.2019.09.015
11. Vereshchagin A.N., Gordeeva A.M., Frolov N.A., Proshin P.I., Hansford K.A., Egorov M.P. Synthesis and microbiological properties of novel bis-quaternary ammonium compounds based on biphenyl spacer. *Eur. J. Organ. Chem.* 2019;26: 4123–4127. https://doi.org/10.1002/ejoc.201900319
12. Самойлов В.О., Ни Д.С., Гончарова А.В., Князева М.И., Рамазанов Д.Н., Максимов А.Л. Каталитический гидрогенолиз зольketаля на бифункциональных катализаторах с получением высокооктановых компонентов моторных топлив. *Журн. прикладной химии*. 2020;93(1):121–131. https://doi.org/10.31857/S0044461820010120
13. Максимов А.Л., Нехаев А.И., Рамазанов Д.Н. Простые эфиры и ацетали – перспективные продукты нефтехимии из возобновляемого сырья (обзор). *Нефтехимия*. 2015;55(1):3–24. https://doi.org/10.7868/S0028242115010104
14. Дмитриев Г.С., Терехов А.В., Занавескин Л.Н., Максимов А.Л., Хаджиев С.Н. Кинетика реакции образования зольketаля в присутствии серной кислоты. *Кинетика и катализ*. 2018;59(4):488–492. https://doi.org/10.1134/S0453881118040020
15. Дмитриев Г.С., Терехов А.В., Занавескин Л.Н., Хаджиев С.Н., Занавескин К.Л., Максимов А.Л. Выбор катализатора и технологической схемы синтеза зольketаля. *Журн. прикладной химии*. 2016;89(10):1298–1304.

14. Dmitriev G.S., Terekhov A.V., Zanaveskin L.N., *et al.* Kinetics of the formation of solketal in the presence of sulfuric acid. *Kinet. Catal.* 2018;59(4):504–508. https://doi.org/10.1134/S002315841804002X
[Original Russian Text: Dmitriev G.S., Terekhov A.V., Zanaveskin L.N., Maksimov A.L., Khadzhiev S.N. Kinetics of the formation of solketal in the presence of sulfuric acid. *Kinetika i kataliz.* 2018;59(4):488–492 (in Russ.). https://doi.org/10.1134/S0453881118040020]
15. Dmitriev G.S., Terekhov A.V., Zanaveskin L.N., *et al.* Choice of a catalyst and technological scheme for synthesis of solketal. *Russ. J. Appl. Chem.* 2016;89(10):1619–1624. https://doi.org/10.1134/S1070427216100094
[Original Russian Text: Dmitriev G.S., Terekhov A.V., Zanaveskin L.N., Khadzhiev S.N., Zanaveskin K.L., Maksimov A.L. Choice of a catalyst and technological scheme for synthesis of solketal. *Zhurnal prikladnoi khimii*. 2016;89(10):1298–1304 (in Russ.).]
16. Dzhumaev Sh.Sh., Sakhabutdinova G.N., Stankevich K.E. Synthesis of some alcohols-based heterocyclic compounds and investigation of their influence on the lubricability of diesel fuel. *Bashkirskii khimicheskii zhurnal = Bashkir Chem. J.* 2023;30(2):85–88 (in Russ.). https://doi.org/10.17122/bcj-2023-2-85-88
17. Oparina L.A., Kolyvanov N.A., Ganina A.A., *et al.* Aryl butyl acetals as oxygenate octane-enhancing additives for motor fuels. *Pet. Chem.* 2020;60(1):134–139. https://doi.org/10.1134/S0965544120010107
[Original Russian Text: Oparina L.A., Kolyvanov N.A., Ganina A.A., D'yachkova S.G. Aryl butyl acetals as oxygenate octane-enhancing additives for motor fuels. *Neftekhimiya.* 2020;60(1):148–153 (in Russ.). https://doi.org/10.31857/S0028242120010104]
18. Mamlieva A.V., Mikhailova N.N., Shavshukova S.Yu. Corrosion inhibitors based on cyclic acetals and their derivatives. *NefteGazoKhimiya = Oil & Gas Cheymistry*. 2020;1:30–33 (in Russ.). https://doi.org/1024411/2310-8266-2020-10103
19. Raskil'dina G.Z., Ishmetova D.V., Sokov S.A., *et al.* Cytotoxic and antioxidant activity of a series of 4-methylene-1,3-dioxolanes acetals. *Pharm. Chem. J.* 2024;58(4):631–633. https://doi.org/10.1007/s11094-024-03187-x
[Original Russian Text: Raskil'dina G.Z., Ishmetova D.V., Sokov S.A., Golovanov A.A. Cytotoxic and antioxidant activity of a series of 4-methylene-1,3-dioxolanes acetals. *Khimiko-Farmatsevticheskii Zhurnal*. 2024;58(4):32–34 (in Russ.). https://doi.org/10.30906/0023-1134-2024-58-4-32-34]
20. Sakhabutdinova G.N., Yakovenko E.A., Raskil'dina G.Z., *et al.* Synthesis and Catalytic activity of quaternary ammonium salts containing *gem*-dichlorocyclopropane and 1,3-dioxolane fragments. *Russ. J. Appl. Chem*. 2020;93(7):967–972. https://doi.org/10.1134/s1070427220070046
[Original Russian Text: Sakhabutdinova G.N., Yakovenko E.A., Raskil'dina G.Z., Zlotskii S.S. Synthesis and Catalytic activity of quaternary ammonium salts containing *gem*-dichlorocyclopropane and 1,3-dioxolane fragments. *Zhurnal prikladnoi khimii*. 2020;93(7):952–957 (in Russ.). https://doi.org/10.31857/S004446182007004X]
21. Latypova F.N., Vildanov F.Sh., Chanyshev R.R., Zlotskii S.S. Chemistry of cyclic acetals and their analogues in the work of scientific schools D.L. Rakhmankulova. *Izv. Vyssh. Uchebn. Zaved. Khim. Khim. Tekhnol. = ChemChemTech.* 2015;58(8):3–21 (in Russ.).
16. Джумаев Ш.Ш., Сахабутдинова Г.Н., Станкевич К.Е. Синтез некоторых гетероциклических соединений на основе спиртов и исследование их влияния на смазывающую способность дизельного топлива. *Башкирский хим. журнал*. 2023;30(2):85–88. https://doi.org/10.17122/bcj-2023-2-85-88
17. Опарина Л.А., Колыванов Л.А., Ганина А.А., Дьячкова С.Г. Арилбутилацетали-октаноповышающие оксигенатные добавки к моторным топливам. *Нефтехимия*. 2020;60(1):148–153. https://doi.org/10.31857/S0028242120010104
18. Мамлиева А.В., Михайлова Н.Н., Шавшукова С.Ю. Ингибиторы коррозии на основе циклических ацеталий и их производных. *НефтеГазоХимия*. 2020;1:30–33. https://doi.org/10.24411/2310-8266-2020-10103
19. Раскильдина Г.З., Ишметова Д.В., Соколов С.А., Голованов А.А. Цитотоксическая и антиоксидантная активность ряда ацеталий 4-метилен-1,3-диоксоланов. *Химико-фармацевтический журн*. 2024;58(4):32–34. https://doi.org/10.30906/0023-1134-2024-58-4-32-34
20. Сахабутдинова Г.Н., Яковенко Е.А., Раскильдина Г.З., Злотский С.С., Синтез и каталитическая активность четвертичных аммонийных солей, содержащих *гем*-дихлорциклопропановый и 1,3-диоксолановый фрагменты. *Журн. прикладной химии*. 2020;93(7):952–957. https://doi.org/10.31857/S004446182007004X
21. Латыпова Ф.Н., Вильданов Ф.Ш., Чанышев Р.Р., Злотский С.С. Химия циклических ацеталий и их аналогов в работах научной школы Д.Л. Рахманкулова. *Изв. вузов. Химия и хим. технология*. 2015;58(8):3–21.
22. Гаймалетдинова Г.Л., Латыпова Д.Р., Латыпов О.Р., Исмаков Р.А., Миннимухаметова Э.Р., Мулюков Р.А. Исследование антикоррозионных свойств реагента комплексного действия, применяемого в качестве присадки к буровому раствору. *Нефтяная провинция.* 2022;3(31):163–178. https://doi.org/10.25689/NP.2022.3.163-178
23. Verma C., Ebenso E.E., Quraishi M.A., Hussain C.M. Recent developments in sustainable corrosion inhibitors: design, performance and industrial scale applications. *Mater. Adv.* 2021;2(12):3806–3850. https://doi.org/10.1039/d0ma00681e

22. Gaimaletdinova G.L., Latypova D.R., Latypov O.R., Ismakov R.A., Minnimukhametova E.R., Mulyukov R.A. Study of the anticorrosion properties of a complex action reagent used as a drilling mud additive. *Neftyanaya Provintsiya*. 2022;3(31): 163–178 (in Russ.). https://doi.org/10.25689/NP.2022.3.163-178
23. Verma C., Ebenso E.E., Quraishi M.A., Hussain C.M. Recent developments in sustainable corrosion inhibitors: design, performance and industrial scale applications. *Mater. Adv.* 2021;2(12):3806–3850. https://doi.org/10.1039/d0ma00681e

About the Authors

Yulianna G. Borisova, Cand. Sci. (Chem.), Teacher, Department of General, Analytical and Applied Chemistry, Ufa State Petroleum Technological University (1, Kosmonavtov ul., Ufa, 450064, Russia). E-mail: yulianna_borisova@mail.ru. Scopus Author ID 56526865000, ResearcherID P-9744-2017, RSCI SPIN-code 3777-0375, https://orcid.org/0000-0001-6452-9454

Shakhobiddin Sh. Dzhumaev, Cand. Sci. (Chem.), Laboratory Engineer, Department of General, Analytical and Applied Chemistry, Ufa State Petroleum Technological University (1, Kosmonavtov ul., Ufa, 450064, Russia). E-mail: shakhob2993@mail.ru. Scopus Author ID 7801627714, ResearcherID HLH-5542-2023, RSCI SPIN-code 4999-3682, https://orcid.org/0000-0002-1938-1478

Gul'nara Z. Raskil'dina, Dr. Sci. (Chem.), Professor, Department of General, Analytical and Applied Chemistry, Ufa State Petroleum Technological University (1, Kosmonavtov ul., Ufa, 450064, Russia). E-mail: graskildina444@mail.ru. Scopus Author ID 56069888400, ResearcherID F-1619-2017, RSCI SPIN-code 2183-3333, https://orcid.org/0000-0001-9770-5434

Rimma M. Sultanova, Dr. Sci. (Chem.), Professor, Department of General, Analytical and Applied Chemistry, Ufa State Petroleum Technological University (1, Kosmonavtov ul., Ufa, 450064, Russia). E-mail: rimmams@yandex.ru. Scopus Author ID 6602738038, RSCI SPIN-code 8208-6060, https://orcid.org/0000-0001-6719-2359

Simon S. Zlotskii, Dr. Sci. (Chem.), Professor, Head of the Department of General, Analytical and Applied Chemistry, Ufa State Petroleum Technological University (1, Kosmonavtov ul., Ufa, 450064, Russia). E-mail: nocturne@mail.ru. Scopus Author ID 6701508202, ResearcherID W-6564-2018, RSCI SPIN-code 6529-3323, https://orcid.org/0000-0001-6365-5010

Об авторах

Борисова Юлианна Геннадьевна, к.х.н., преподаватель кафедры общей, аналитической и прикладной химии, ФГБОУ ВО «Уфимский государственный нефтяной технический университет» (450064, Россия, г. Уфа, ул. Космонавтов, д. 1). E-mail: yulianna_borisova@mail.ru. Scopus Author ID 56526865000, ResearcherID P-9744-2017, SPIN-код РИНЦ 3777-0375, https://orcid.org/0000-0001-6452-9454

Джумаев Шахобиддин Шамсидинович, к.х.н., инженер-лаборант кафедры общей, аналитической и прикладной химии, ФГБОУ ВО «Уфимский государственный нефтяной технический университет» (450064, Россия, г. Уфа, ул. Космонавтов, д. 1). E-mail: shakhob2993@mail.ru. Scopus Author ID 7801627714, ResearcherID HLH-5542-2023, SPIN-код РИНЦ 4999-3682, https://orcid.org/0000-0002-1938-1478

Раскильдина Гульнара Зинуровна, д.х.н., профессор кафедры общей, аналитической и прикладной химии, ФГБОУ ВО «Уфимский государственный нефтяной технический университет» (450064, Россия, г. Уфа, ул. Космонавтов, д. 1). E-mail: graskildina444@mail.ru. Scopus Author ID 56069888400, ResearcherID F-1619-2017, SPIN-код РИНЦ 2183-3333, https://orcid.org/0000-0001-9770-5434

Султанова Римма Марсельевна, д.х.н., профессор кафедры общей, аналитической и прикладной химии, ФГБОУ ВО «Уфимский государственный нефтяной технический университет» (450064, Россия, г. Уфа, ул. Космонавтов, д. 1). E-mail: rimmams@yandex.ru. Scopus Author ID 6602738038, SPIN-код РИНЦ 8208-6060, https://orcid.org/0000-0001-6719-2359

Злотский Семен Соломонович, д.х.н., заведующий кафедрой общей, аналитической и прикладной химии, ФГБОУ ВО «Уфимский государственный нефтяной технический университет» (450064, Россия, г. Уфа, ул. Космонавтов, д. 1). E-mail: nocturne@mail.ru. Scopus Author ID 6701508202, ResearcherID W-6564-2018, SPIN-код РИНЦ 6529-3323, https://orcid.org/0000-0001-6365-5010

Translated from Russian into English by H. Moshkov
Edited for English language and spelling by Thomas A. Beavitt

Tonkie Khimicheskie Tekhnologii = Fine Chemical Technologies.
2025;20(3):203–214
ISSN 2686-7575 (Online)

Chemistry and technology of organic substances
Химия и технология органических веществ

UDC 543.544.43+544.016
https://doi.org/10.32362/2410-6593-2025-20-3-203-214
EDN VFQXIM

RESEARCH ARTICLE

Determination of the enthalpy of evaporation of pentaerythritol esters of various structures using gas chromatographic retention characteristics

Yulia F. Ivanova, Vladimir V. Emelyanov✉, Svetlana V. Levanova, Yuri N. Telnov
Samara State Technical University, Samara, 443100 Russia
✉ *Corresponding author, e-mail: koraks95@mail.ru*

Abstract

Objectives. The work set out to prepare and chromatographically analyze pentaerythritol esters, use gas chromatography to determine the Kováts logarithmic retention indices and enthalpies of sorption, and evaluate the enthalpy of evaporation of pentaerythritol tetraesters based on linear correlations with enthalpies of sorption and logarithmic retention indices.

Methods. The synthesis was carried out in an isothermal stirred reactor at T = 393.2 K at a molar ratio of pentaerythritol to carboxy lic acid of 1 : 4 in self-catalysis mode to avoid side reactions that occur during aggressive acid catalysis. The obtained samples were analyzed using Chromatec Analytic hardware and software complex based on a Kristall-2000M chromatograph equipped with a capillary column (60 m × 0.32 mm × 0.5 μm) having BP-1 grafted stationary phase (100% dimethylpolysiloxane). The analysis conditions were as follows: isothermal mode; column temperature, 433.2–603.2 K; evaporator and detector temperatures, 623.2 K; gas flow split, 1 : 50; carrier gas, helium; volume of injected sample, 0.15 μL; diluent of reaction samples, methanol.

Results. For the first time, the values of the Kováts retention indices and enthalpies of sorption were found for 31 pentaerythritol esters of various structures (mono-, di-, tri-, and tetramethanoates; 2-methylpentanoates; 4-methylpentanoates; 2,2-dimethylbutanoates; 2-ethylbutanoates; octanoates; nanoates; and decanoates). The obtained correlation equations were used to estimate the enthalpy of evaporation of pentaerythritol tetraesters (for 7 compounds, data were obtained for the first time).

Conclusions. The retention parameters were found as linear dependencies with a high degree of correlation ($R^2 > 0.99$) in the studied temperature range (433.2–603.2 K). The enthalpies of evaporation calculated based on the enthalpies of sorption and logarithmic retention indices within the limits of error of the correlation dependencies coincide with the literature data and the values predicted by the quantitative structure–property relationship method. The obtained data can be used to design units for separating multicomponent mixtures and identify these compounds.

Keywords
pentaerythritol esters, retention indices, enthalpy of evaporation, esterification, sorption

Submitted: 31.10.2024
Revised: 11.12.2024
Accepted: 08.04.2025

For citation
Ivanova Yu.F., Emelyanov V.V., Levanova S.V., Telnov Yu.N. Determination of the enthalpy of evaporation of pentaerythritol esters of various structures using gas chromatographic retention characteristics. *Tonk. Khim. Tekhnol. = Fine Chem. Technol.* 2025;20(3):203–214. https://doi.org/10.32362/2410-6593-2025-20-3-203-214

НАУЧНАЯ СТАТЬЯ

Определение энтальпии испарения сложных эфиров пентаэритрита различного строения с использованием газохроматографических характеристик удерживания

Ю.Ф. Иванова, В.В. Емельянов✉, С.В. Леванова, Ю.Н. Тельнов

Самарский государственный технический университет, Самара, 443100 Россия

✉ *Автор для переписки, e-mail: koraks95@mail.ru*

Аннотация

Цели. Получение и хроматографический анализ сложных эфиров пентаэритрита; определение логарифмических индексов удерживания Ковача и энтальпий сорбции с помощью газовой хроматографии; оценка энтальпии испарения тетраэфиров пентаэритрита на основе линейных корреляций с энтальпиями сорбции и логарифмическими индексами удерживания.

Методы. Синтез проводили в изотермическом реакторе смешения при соотношении пентаэритрит : карбоновая кислота = 1 : 4 (мольн.), в режиме самокатализа во избежание протекания побочных превращений, имеющих место при агрессивном кислотном катализе, при T = 393.2 K. Анализ полученных образцов проводили с использованием программно-аппаратного комплекса «Хроматэк-Аналитик» на базе хроматографа «Кристалл-2000М», оснащенного капиллярной колонкой (60 м × 0.32 мм × 0.5 мкм) с привитой неподвижной фазой BP-1 (100% диметилполисилоксан). Условия анализа: изотермический режим; температура колонки 433.2–603.2 K; температуры испарителя и детектора одинаковы и равны 623.2 K; деление газового потока 1 : 50; газ носитель — гелий; объем вводимой пробы — 0.15 мкл; для разбавления реакционных проб применяли метанол.

Результаты. Впервые получены значения индексов удерживания Ковача и энтальпий сорбции для 31 сложного эфира пентаэритрита различной структуры (моно-, ди-, три- и тетраформиатов, 2-метилпентаноатов, 4-метилпентаноатов, 2,2-диметилбутаноатов, 2-этилбутаноатов, октаноатов, наноатов, деканоатов). Получены корреляционные уравнения, позволившие оценить энтальпию испарения для тетраэфиров пентаэритрита (для 7 соединений данные получены впервые).

Выводы. Значения параметров удерживания представляют собой линейные зависимости с высокой степенью корреляции (R^2 > 0.99) в исследованном температурном диапазоне (433.2–603.2 K). Рассчитанные энтальпии испарения в пределах погрешности корреляционных зависимостей на основе энтальпий сорбции и логарифмических индексов удерживания совпадают с литературными и прогнозируемыми по методу Quantitative Structure-Property Relationship значениями. Полученные данные могут быть использованы для проектирования узлов разделения многокомпонентных смесей и идентификации данных соединений.

Ключевые слова

сложные эфиры пентаэритрита, индексы удерживания, энтальпии испарения, этерификация, сорбция

Поступила: 31.10.2024
Доработана: 11.12.2024
Принята в печать: 08.04.2025

Для цитирования

Иванова Ю.Ф., Емельянов В.В., Леванова С.В., Тельнов Ю.Н. Определение энтальпии испарения сложных эфиров пентаэритрита различного строения с использованием газохроматографических характеристик удерживания. *Тонкие химические технологии*. 2025;20(3):203–214. https://doi.org/10.32362/2410-6593-2025-20-3-203-214

INTRODUCTION

Pentaerythritol esters are of great interest to various sectors of global industry. This is mainly due to the possibility of varying the chemical and/or physical properties of these esters by introducing various numbers of acid fragments of a particular structure to permit their use as plasticizers for polymer products, alkyd resins, lubricants, stationary chromatographic phases, and nonionic surfactants [1–6].

The mass application of plasticizers is limited by a number of requirements imposed by technical and economic standards: absence of odor and color, commercial availability, and thermodynamic compatibility with the polymer material [7]. As a rule, such requirements are met by pentaerythritol esters of linear and an iso structure having an average molecular weight in the range of 400–800 g/mol [8]. In this case, the most significant effect is exhibited by compounds of branched structure, which have a higher resistance

to emission from the polymer in comparison with their isomers of linear structure.

To create optimal technologies for obtaining ester products, reliable data on the enthalpies of evaporation are required, which are used in the design of reaction units or separation units [9]. Experimental determination is based on obtaining the saturated vapor pressure by various methods: direct (ebulliometry), indirect (transpiration), etc. However, this entails certain difficulties, since the classical ebulliometric method is unsuitable for compounds with low thermal stability (which clearly manifests itself for branched ester structures); moreover, when using the transpiration method, the experiment can be extremely lengthy due to the high molecular weight of the ester [10, 11].

Recently, modeling methods have become increasingly important, allowing for rapid estimation of the enthalpy of evaporation with a sufficient accuracy based on reliable retention parameters of compounds obtained under gas chromatography conditions [12].

The purpose of this work was to obtain and chromatographically analyze pentaerythritol esters, determine the Kováts retention indices for a number of unstudied pentaerythritol esters of various structures, determine the enthalpies of sorption, and estimate the enthalpies of evaporation for tetraethers by prediction based on experimental correlations.

EXPERIMENTAL

Synthesis of pentaerythritol esters

The objects of the study were pentaerythritol esters for which there are no reference descriptions of retention indices under gas-liquid chromatography conditions. Pentaerythritol esters of the following acids were studied: formic (98%, *neoFroxx GmbH*, Germany), 2-methylpentanoic (98%, *Merck*, Germany), 4-methylpentanoic (99%, *Sigma-Aldrich*, USA), 2,2-dimethylbutanoic (98%, *Acros Organics*, USA), 2-ethylbutanoic (99%, *Acros Organics*, USA), octanoic (99%, *Sigma-Aldrich*, USA), nonanoic (99%, *Sigma-Aldrich*, USA), and decanoic (99%, *Sigma-Aldrich*, USA), which were synthesized according to the following scheme:

The syntheses were carried out at a molar ratio of alcohol to carboxylic acid of 1 : 4 in order to obtain products of all degrees of substitution. The experimental equipment was a jacketed reactor (*RULLAB*, Russia) connected to a reflux condenser. The reactor was thermostated by circulating PMS-200 polymethylsiloxane (*Acros Organics*, USA) using a circulating oil thermostat (*Huber*, Germany). The reaction temperature was 393 K. The process was conducted in the self-catalysis mode to avoid side reactions that occur during aggressive acid catalysis.

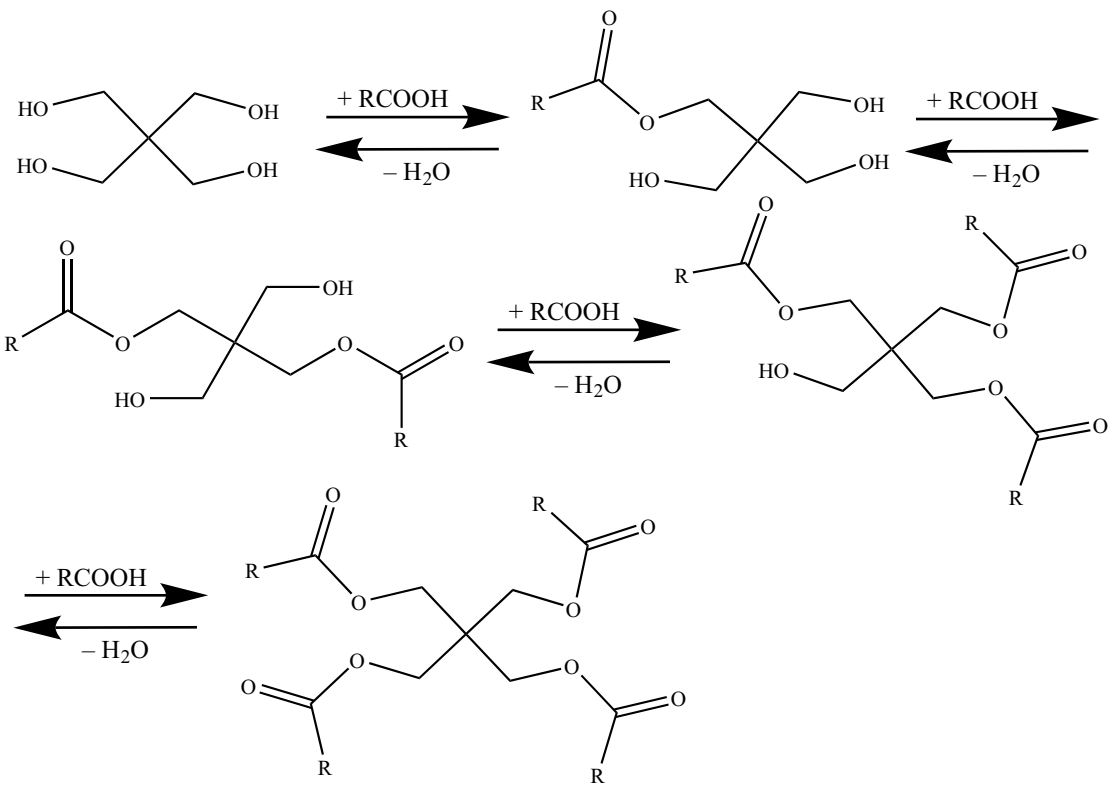

Scheme. Synthesis of pentaerythritol esters

The reaction system was stirred with a magnetic stirrer (*Heidolph*, Germany). The reaction was performed until the signals of all four possible products appeared (monoesters, diesters, triesters, and tetraesters). The conversion of pentaerythritol was determined by kinetic monitoring of the reaction by changing the chromatographic signals with time (gradual depletion of alcohol and increase and decrease in concentrations in a series of mono-, di-, tri- and tetrasubstituted products).

Analysis of reaction mixture

The obtained samples were analyzed using the Chromatec Analytic hardware and software complex based on a Kristall-2000M chromatograph (*Chromatec*, Russia) equipped with a capillary column (60 m × 0.32 mm × 0.5 μm) with BP-1 grafted stationary phase (100% dimethylpolysiloxane, *Chromatec*, Russia). Analysis conditions were as follows: isothermal mode; column temperature, 433.2–603.2 K; injector temperature, 623.2 K; detector temperature, 623.2 K; gas flow split, 1 : 50; carrier gas, helium; injected sample volume, 0.15 μL; diluent for reaction samples, methanol (*Acros Organics*, USA); concentration range of the measured compounds, 0.2–0.6 mg/mL. The asymmetry factor of chromatographic peaks was 1, thus eliminating the possibility of overloading the chromatographic column, as well as its physical modification, which could lead to distortion of retention index values [13, 14].

Determination of retention indices

The retention indices and enthalpies of sorption were determined by the following equations [15]:

$$I_x = \frac{\ln(t'_x) - \ln(t'_z)}{\ln(t'_{z+1}) - \ln(t'_z)} \cdot 100 + 100z, \quad (1)$$

$$\ln(k) = \frac{\Delta\bar{S}_{\text{sorb}}}{R} - \frac{\Delta\bar{U}_{\text{sorb}}}{RT}, \quad (2)$$

$$k = \frac{t_{\text{R}} - t_{\text{D}}}{t_{\text{D}}}, \quad (3)$$

$$\Delta\bar{H}_{\text{sorb}}\left(T_{\text{av}}\right) = \Delta\bar{U}_{\text{sorb}}\left(T_{\text{av}}\right) - RT, \quad (4)$$

where I_x is the retention index of the substance under study; t'_x, t'_z, and t'_{z+1} are the reduced retention times of the sample under study (subscript x) and normal alkanes with the number of carbon atoms z and $z + 1$, respectively; $R = 8.3145$ J/(mol · K) is the universal gas constant; t_{R} is the absolute retention time of the substance under study; t_{D} is the dead retention time; k is the retention factor; $\Delta\bar{U}_{\text{sorb}}$ is the internal energy of sorption at the average temperature of the experiment; $\Delta\bar{S}_{\text{sorb}}$ is the entropy of sorption at the average temperature of the experiment; $\Delta\bar{H}_{\text{sorb}}$ is the enthalpy of sorption at the average temperature of the experiment; and T_{av} is the average temperature of the experiment.

The experimental values of the enthalpies of sorption were reduced to a temperature of 298.2 K using the equation

$$\Delta H_{\text{sorb}}\left(298.2\text{K}\right) = \\ = \Delta\bar{H}_{\text{sorb}}\left(T_{\text{av}}\right) + \left(-\Delta_{\text{liq}}^{\text{vap}} C_P^{\circ}\right)\left(298.2 - T_{\text{av}}\right), \quad (5)$$

where $\Delta_{\text{liq}}^{\text{vap}} C_P^{\circ}$ is the heat capacity of the liquid–vapor phase transition, predicted using the method that we proposed previously [16] based on modified Randić indices.

RESULTS AND DISCUSSION

Retention indices

For all compounds in the temperature range of 433.2–603.2 K (all studied temperature modes are given in Table 1), it was possible to achieve a clear separation of the components of the analyzed samples. The only exception was pentaerythritol monodecanoates, which may be due to the similar retention times of normal alkanes.

The confidence interval in determining the retention indices as determined in 3–4 measurements was no more than 0.2.

Table 1 presents the experimental values of the logarithmic retention indices and their temperature dependencies.

One of the known dependencies relating the logarithmic retention index with the structure of the compound is the correlation relative to the number of carbon atoms in the acid fragment of the ester in the case of linear structure. For this, it is necessary to have data for determining the retention index at the same temperature. As such a temperature, the value of 513.2 K was chosen based on the published data [17], as well as due to the fact that this temperature is within the studied range (433.2–603.2 K), which allows for a satisfactory approximation to 513.2 K.

The dependence of the retention indices on the number of carbon atoms in the acid fragment (Fig. 1) demonstrates good linearization ($R^2 = 0.999$), indicating the adequacy of the obtained results.

Table 1. Experimental values of retention indices of pentaerythritol esters

No.	T, K / I_i				$I_{513.2}$	$\Delta I/\Delta T$	a^*	b^*	R^2
Monoesters									
Methanoate	*433.2* 1272.2	*443.2* 1279.5	*453.2* 1285.0	*463.2* 1290.4	1320.8	6.1	0.6011	1012.4	0.994
2-Methylpentanoate	*523.2* 1912.7	*533.2* 1920.5	*543.2* 1928.3	*553.2* 1935.2	1905.3	7.5	0.7533	1518.8	0.999
4-Methylpentanoate	*523.2* 1989.0	*533.2* 1997.0	*543.2* 2004.9	*553.2* 2014.1	1980.5	8.4	0.8323	1553.4	0.999
2,2-Dimethylbutanoate	*503.2* 1750.6	*513.2* 1750.6	*523.2* 1750.7	*533.2* 1750.8	1750.6	0.1	0.0067	1747.2	0.999
2-Ethylbutanoate	*513.2* 1572.2	*523.2* 1576.4	*533.2* 1581.3	*543.2* 1585.3	1572.2	4.4	0.4438	1344.4	0.999
Octanoate	*573.2* 2113.2	*583.2* 2122.1	*593.2* 2130.7	*603.2* 2139.8	2060.1	8.9	0.8848	1606.0	0.999
Nanoate	*573.2* 2233.0	*583.2* 2242.6	*593.2* 2252.0	*603.2* 2262.4	2174.4	9.8	0.9759	1673.5	0.999
Diesters									
Methanoate	*433.2* 1452.6	*443.2* 1457.4	*453.2* 1461.7	*463.2* 1466.8	1490.1	4.7	0.4680	1249.9	0.999
2-Methylpentanoate	*513.2* 2166.7	*523.2* 2172.9	*533.2* 2183.4	*543.2* 2188.9	2166.7	7.4	0.7720	1770.3	0.985
4-Methylpentanoate	*523.2* 2285.4	*533.2* 2289.8	*543.2* 2293.9	*553.2* 2299.4	2280.6	4.7	0.4603	2044.4	0.996
2,2-Dimethylbutanoate	*503.2* 2092.6	*513.2* 2102.6	*523.2* 2110.8	*533.2* 2121.6	2102.6	9.7	0.9528	1613.2	0.998
2-Ethylbutanoate	*513.2* 2067.5	*523.2* 2074.3	*533.2* 2079.7	*543.2* 2086.8	2067.5	6.4	0.6337	1742.4	0.997
Octanoate	*573.2* 2723.4	*583.2* 2729.3	*593.2* 2735.1	*603.2* 2742.3	2685.7	6.3	0.6253	2364.8	0.997
Nanoate	*573.2* 2919.4	*583.2* 2925.7	*593.2* 2932.0	*603.2* 2938.2	2881.8	6.3	0.6280	2559.4	0.999
Decanoate	–	–	*593.2* 3113.0	*603.2* 3119.7	3059.7	2.7	0.6670	2117.4	–
Triesters									
Methanoate	*433.2* 1506.7	*443.2* 1509.7	*453.2* 1512.7	*463.2* 1516.2	1532.0	3.2	0.3178	1368.9	0.999
2-Methylpentanoate	*513.2* 2491.7	*523.2* 2494.6	*533.2* 2497.1	*543.2* 2499.6	2491.7	2.6	0.2617	2357.5	0.999
4-Methylpentanoate	*523.2* 2588.9	*233.2* 2591.0	*543.2* 2593.5	*553.2* 2595.7	2586.6	2.3	0.2292	2469.0	0.999
2,2-Dimethylbutanoate	*503.2* 2385.7	*513.2* 2391.2	*523.2* 2396.3	*533.2* 2401.7	2391.2	5.3	0.5318	2118.1	0.999

Table 1. Continued

No.	T, K / I_i				$I_{513.2}$	$\Delta I/\Delta T$	a^*	b^*	R^2
2-Ethylbutanoate	*513.2* 2329.7	*523.2* 2332.1	*533.2* 2334.0	*543.2* 2336.4	2329.7	2.2	0.2207	2216.5	0.999
Octanoate	*573.2* 3273.9	*583.2* 3275.0	*593.2* 3276.4	*603.2* 3277.6	3266.5	1.2	0.1236	3203.0	0.998
Nanoate	*573.2* 3555.4	*583.2* 3558.0	*593.2* 3560.6	*603.2* 3563.1	3540.2	2.6	0.2548	3409.4	0.999
Decanoate	*573.2* 3840.3	*583.2* 3841.4	*593.2* 3842.7	*603.2* 3843.7	3833.4	1.1	0.1150	3774.4	0.998
Tetraesters									
Methanoate	*433.2* 1537.3	*443.2* 1538.5	*453.2* 1540.3	*463.2* 1541.5	1548.7	1.4	0.1440	1474.8	0.995
2-Methylpentanoate	*513.2* 2751.5	*523.2* 2750.8	*533.2* 2749.7	*553.2* 2747.7	2751.5	−0.9	−0.0967	2801.3	0.996
4-Methylpentanoate	*523.2* 2881.7	*533.2* 2879.7	*543.2* 2877.5	*553.2* 2875.5	2883.8	−2.1	−0.2089	2991.0	0.999
2,2-Dimethylbutanoate	*503.2* 2616.8	*513.2* 2619.3	*523.2* 2621.8	*533.2* 2624.6	2619.3	2.6	0.2593	2486.3	0.999
2-Ethylbutanoate	*513.2* 2650.2	*523.2* 2649.8	*533.2* 2649.4	*543.2* 2649.0	2650.2	−0.4	−0.0415	2671.5	0.999
Octanoate	*573.2* 3737.9	*583.2* 3733.5	*593.2* 3729.8	*603.2* 3725.7	3761.8	−4.1	−0.4015	3967.9	0.999
Nanoate	*573.2* 4102.3	*583.2* 4098.2	*593.2* 4094.1	*603.2* 4090.0	4126.9	−4.1	−0.4072	4335.6	0.999
Decanoate	*573.2* 4430.6	*583.2* 4426.0	*593.2* 4421.2	*603.2* 4416.5	4459.1	−4.7	−0.4729	4701.7	0.999

* The coefficients a and b are derived from the temperature dependence $I = aT + b$ of the logarithmic retention indices, where T is the temperature of the chromatographic column, K.

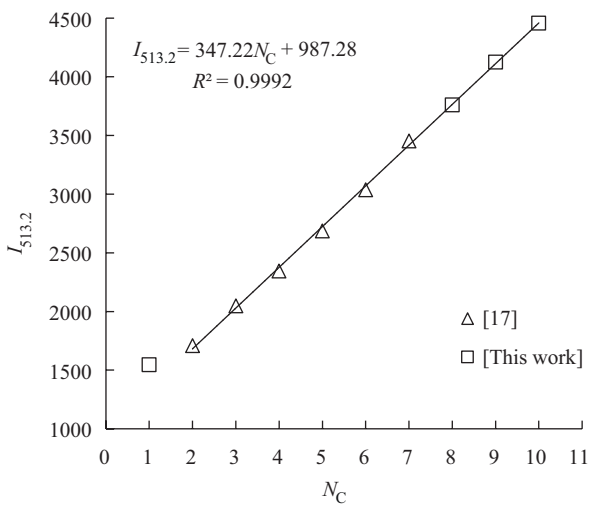

Fig. Dependence of the retention indices of pentaerythritol tetraesters of linear structure at a temperature of 513.2 K on the number of carbon atoms in the acid fragment

Enthalpies of sorption and prediction of enthalpy of evaporation

Table 2 presents the results of calculation of enthalpy of sorption.

Analysis of the enthalpies of sorption when reduced to a temperature of 298.2 K showed that the dependence of the enthalpy of sorption on the number of substituted hydroxyl groups has a linear anamorphosis for esters with different acid fragments indicating an additive contribution of the methylene fragment to the enthalpy value. At the same time, the enthalpies of sorption of pentaerythritol methanoates under error conditions have similar values, which is probably due to the absence of a methylene fragment.

The general equation (except for methanoates) describing the relationship between the retention index

Table 2. Experimental values of enthalpies of sorption of pentaerythritol esters

No.	$-\Delta_{liq}^{vap}C_P^{\circ}$, J/(mol K)	T_{av}, K	$-\Delta\bar{H}_{sorb}(T_{av})$, kJ/mol	$-\Delta H_{sorb}^{\circ}(298.2)$, kJ/mol
Monoesters				
Methanoate	193.0	448.2	49.8 ± 3.9	80.8 ± 6.6
2-Methylpentanoate	219.5	538.2	60.1 ± 4.9	112.8 ± 9.2
4-Methylpentanoate	219.7	538.2	68.6 ± 0.4	121.4 ± 0.8
2,2-Dimethylbutanoate	215.6	518.2	63.6 ± 0.2	111.0 ± 0.3
2-Ethylbutanoate	219.7	528.2	62.0 ± 0.7	112.5 ± 1.2
Octanoate	236.1	588.2	76.6 ± 0.5	145.0 ± 0.9
Nanoate	243.2	588.2	79.8 ± 1.3	150.3 ± 2.6
Diesters				
Methanoate	180.1	448.2	54.8 ± 2.7	81.8 ± 4.1
2-Methylpentanoate	224.4	528.2	75.6 ± 1.0	127.2 ± 1.6
4-Methylpentanoate	224.9	538.2	76.2 ± 0.7	130.1 ± 1.2
2,2-Dimethylbutanoate	217.3	523.2	69.9 ± 0.4	118.8 ± 0.6
2-Ethylbutanoate	224.8	528.2	72.3 ± 0.6	124.0 ± 1.0
Octanoate	253.3	588.2	81.8 ± 0.6	155.3 ± 1.3
Nanoate	265.9	588.2	85.7 ± 1.2	162.8 ± 2.4
Decanoate	278.7	598.2	85.8	169.4
Triesters				
Methanoate	167.2	448.2	57.5 ± 3.1	82.6 ± 4.5
2-Methylpentanoate	224.7	528.2	86.2 ± 0.8	137.9 ± 1.2
4-Methylpentanoate	225.4	538.2	86.0 ± 0.6	140.1 ± 1.0
2,2-Dimethylbutanoate	214.3	518.2	80.6 ± 0.1	127.8 ± 0.1
2-Ethylbutanoate	225.2	528.2	83.9 ± 0.8	135.6 ± 1.2
Octanoate	265.5	588.2	98.2 ± 0.9	175.2 ± 1.7
Nanoate	283.4	588.2	103.6 ± 1.1	185.8 ± 2.1
Decanoate	301.8	598.2	103.7	194.3
Tetraesters				
Methanoate	154.2	448.2	60.0 ± 2.9	83.1 ± 4.1
2-Methylpentanoate	221.8	530.7	93.2 ± 0.7	144.7 ± 1.1
4-Methylpentanoate	222.8	538.2	96.7 ± 0.7	150.2 ± 1.1
2,2-Dimethylbutanoate	208.3	518.2	89.1 ± 0.1	134.9 ± 0.2
2-Ethylbutanoate	222.6	528.2	93.4 ± 0.6	144.6 ± 0.9
Octanoate	274.4	588.2	112.9 ± 0.9	192.5 ± 1.6
Nanoate	297.7	588.2	120.6 ± 1.6	206.9 ± 2.9
Decanoate	321.5	598.2	130.5 ± 1.9	227.0 ± 3.4

reduced to a single temperature and the sorption enthalpy has the form:

$$-\Delta H^{\circ}_{\text{sorb}}(298.2) = \\ = -6.682N_i + 0.047I_{513.2} + 40.371, \left(R^2 = 0.965\right), \quad (6)$$

where N_i is the number of substituted hydroxyl groups in the pentaerythritol molecule for compound i: monoester (N = 1), diester (N = 2), triester (N = 3), and tetraester (N = 4). The characteristics of the predictive ability of the obtained equation are the following: maximum deviation, 14.3; mean error of predicted values, 4.1; and standard deviation of error, 3.9.

The enthalpies of evaporation can be found using linear correlations relative to the chromatographic retention parameters:

$$\Delta H^{\circ}_{\text{evap}}(298) = f\left(I_T\right),$$

$$\Delta H^{\circ}_{\text{evap}}(298) = f\left(-\Delta H^{\circ}_{\text{sorb}}(298.2)\right),$$

where I_T is the retention index of the compound at a certain temperature T, K.

Using the literature values of enthalpies of evaporation and enthalpies of sorption of some pentaerythritol tetraesters [17, 18], we obtained the following correlation equations:

$$\Delta H^{\circ}_{\text{evap}}(298) = \\ = 0.0367I_{513.2} + 43.387, \ \left(R^2 = 0.991\right), \quad (7)$$

$$\Delta H^{\circ}_{\text{evap}}(298) = \\ = -0.824\Delta H^{\circ}_{\text{sorb}}(298) + 27.055, \ \left(R^2 = 0.994\right). \quad (8)$$

Table 3 compares the values of the enthalpies of evaporation of pentaerythritol tetraesters with the values predicted by the quantitative structure–property relationship (QSPR) method [19].

The obtained values of the enthalpy of evaporation are at a level acceptable for technical calculations. Deviations from the data obtained by the QSPR method and literature data on pentaerythritol tetraesters are 3–6%.

Table 3. Values of the enthalpies of evaporation of pentaerythritol tetraesters, obtained by various methods

Component	$\Delta H^{\circ}_{\text{evap}}(298)$, kJ/mol			
	This work		Literature data	Additive method QSPR [21]
	(7)	(8)		
Methanoate	100.3 ± 2.0	95.5 ± 1.6	–	102.2 ± 2.8
Ethanoate	105.4 ± 0.8	105.0 ± 1.7	106.9 ± 1.8 [18]	106.6 ± 3.0
Propionate	118.1 ± 0.9	117.6 ± 1.9	115.0 ± 2.1 [18]	115.7 ± 3.2
Butanoate	129.8 ± 1.0	129.9 ± 2.1	129.8 ± 2.3 [18]	127.4 ± 3.6
2-Methylpropanoate	123.2 ± 1.0	123.7 ± 2.0	122.8 ± 2.5 [18]	121.8 ± 3.4
Pentanoate	142.9 ± 1.1	143.5 ± 2.4	144.2 ± 2.3 [18] 134.0 ± 1.9 [18]	141.1 ± 4.0
3-Methylbutanoate	135.7 ± 1.1	135.0 ± 2.2	137.4 ± 2.4 [18]	135.7 ± 3.8
2,2-Dimethylpropionate	125.1 ± 1.0	126.2 ± 2.1	125.2 ± 2.5 [18]	125.9 ± 3.5
Caproate	156.4 ± 1.3	155.0 ± 2.6	155.4 ± 3.0 [18]	155.1 ± 4.3
2-Methylpentanoate	144.4 ± 2.8	146.2 ± 2.4	–	149.4 ± 4.2
4-Methylpentanoate	149.3 ± 2.9	150.7 ± 2.5	–	150.1 ± 4.2
2,2-Dimethylbutanoate	139.6 ± 2.7	138.1 ± 2.3	–	139.9 ± 3.9

Table 3. Continued

Component	$\Delta H^{\circ}_{evap}(298)$, kJ/mol			
	This work		Literature data	Additive method QSPR [21]
	(7)	(8)		
2-Ethylbutanoate	140.7 ± 2.8	146.1 ± 2.4	–	149.9 ± 4.2
Heptanoate	168.5 ± 1.6	169.2 ± 2.8	168.5 ± 2.8 [18] 167.5 ± 2.3 [20]	170.3 ± 4.8
Octanoate	181.6 ± 3.6	185.6 ± 3.1	–	186.2 ± 5.2
Nanoate	195.0 ± 3.8	197.4 ± 3.3	193.6 ± 2.0 [20]	202.4 ± 5.7
Decanoate	207.2 ± 4.1	214.0 ± 3.5	–	219.1 ± 6.1

CONCLUSIONS

After experimentally determining the Kováts retention indices, the enthalpies of sorption were estimated for 31 pentaerythritol esters of various structures. The retention indices are described by linear dependencies with a high degree of correlation ($R^2 > 0.99$) in the studied temperature range (433.2–603.2 K). Using the correlation equations, the enthalpies of evaporation of pentaerythritol tetraesters were estimated (for seven of these, data were obtained for the first time). The calculated enthalpies of evaporation coincide with the literature data and the values predicted by the QSPR method within the limits of error of the correlation equations. The obtained data can be used to design units for separating multicomponent mixtures and identify these compounds.

Acknowledgments

The research was supported by the Russian Science Foundation, grant No. 24-79-00158, https://rscf.ru/project/24-79-00158.

Authors' contributions

Yu.F. Ivanova—experiment execution, data processing, writing the article.

V.V. Emelyanov—experiment execution, data processing, writing the article.

S.V. Levanova—data processing, writing the article.

Yu.N. Telnov—experiment execution.

The authors declare that they have no conflicts of interest that require disclosure in this article.

REFERENCES

1. Howell B.A., Alrubayyi A., Ostrander E.A. Thermal properties of charring plasticizers from the biobased alcohols, pentaerythritol and 3,5-dihydroxybenzoic acid. *J. Therm. Anal. Calorim.* 2019;138(25):2661–2668. https://doi.org/10.1007/s10973-019-08311-8
2. Piskarev V.V., Viktorova E.A. Modern alkyd paints, their properties, composition, use in design and range of applications. *Vestnik Kazanskogo tekhnologicheskogo universiteta = Herald of Kazan Technological University*. 2014;17(17):89–91 (in Russ.).
3. Minyaeva O.A., Kupriyanova N.P., Grigorieva U.A. Effect of nonionic surfactants as emulsifiers on the melting temperature of soft medicinal forms basis. *Sovremennye problemy nauki i obrazovaniya = Modern Problems of Science and Education*. 2015;1(1):1978 (in Russ.).
4. Kurganov A.A., Victorova E.P., Kanateva E.Yu. Monolithic capillary columns based on pentaerythritol acrylates for molecular-size-based separations of synthetic polymers. *J. Sep. Sci*. 2015;38(13):2223–2228. https://doi.org/10.1002/jssc.201500211

СПИСОК ЛИТЕРАТУРЫ

1. Howell B.A., Alrubayyi A., Ostrander E.A. Thermal properties of charring plasticizers from the biobased alcohols, pentaerythritol and 3,5-dihydroxybenzoic acid. *J. Therm. Anal. Calorim.* 2019;138(25):2661–2668. https://doi.org/10.1007/s10973-019-08311-8
2. Пискарев В.В., Викторова Е.А. Современные алкидные краски, их свойства, состав, использование в дизайне и спектр применения. *Вестник Казанского технологического университета*. 2014;17(17):89–91.
3. Миняева О.А., Куприянова Н.П., Григорьева У.А. Влияние добавок неионогенных ПАВ в качестве эмульгаторов на температуру плавления основы мягких лекарственных форм. *Современные проблемы науки и образования*. 2015;1(1):1978.
4. Kurganov A.A., Victorova E.P., Kanateva E.Yu. Monolithic capillary columns based on pentaerythritol acrylates for molecular-size-based separations of synthetic polymers. *J. Sep. Sci*. 2015;38(13):2223–2228. https://doi.org/10.1002/jssc.201500211

5. Kucherenko E.V., Melnik D.M., Korolev A.A., *et al.* Monolithic Capillary Columns Based on Pentaerythritol Tetraacrylate for Peptide Analysis. *Russ. J. Phys. Chem. A.* 2015; 89(9):1688–1692. https://doi.org/10.7868/S0044453715090198
[Original Russian Text: Kucherenko E.V., Melnik D.M., Korolev A.A., Kanateva A.Yu., Pirogov A.V., Kurganov A.A. Monolithic Capillary Columns Based on Pentaerythritol Tetraacrylate for Peptide Analysis. *Zhurnal Fizicheskoi Khimii.* 2015;89(9):1478–1483 (in Russ.). https://doi.org/10.7868/S0044453715090198]
6. Tonkonogov B.P., Popova K.A., Hurumova A.F. Perspective of using esters as a national production as bases of oils for the aircraft equipment. *Trudy Rossiiskogo gosudarstvennogo universiteta nefti i gaza imeni I.M. Gubkina = Proceedings of Gubkin University.* 2015;278(1):109–120 (in Russ.).
7. Silman A.V., Niyazbakiev I.I., Smirnova Yu.K. Phthalate-free plasticizers. In: *Modern Scientific Research: Problems and Solutions: A collection of materials of the International Scientific and Practical Conference*. St. Petersburg; 2020. P. 59–62 (in Russ.).
8. Wypych G. *Handbook of Plasticizers*: 2nd ed. Toronto: Chemtech Publishing; 2012. 748 p.
9. Ryzhkin D.A., Raeva V.M. Comparison of methods for calculating the enthalpy of vaporization of binary azeotropic mixtures. *Fine Chem. Technol*. 2024;19(4):279–292. https://doi.org/10.32362/2410-6593-2024-19-4-279-292
10. Krasnykh E.L., Druzhinina Y.A., Portnova S.V., Smirnova Y.A. Vapor pressure and enthalpy of vaporization of trimethylolpropane and carboxylic acids esters. *Fluid Phase Equilib*. 2018;462:111–117. https://doi.org/10.1016/j.fluid.2018.01.018
11. Nesterova T.N., Nazmutdinov A.G., Tsvetkov V.S., Rozhnov A.M., Roshchupkina I.Yu. Vapour pressures and enthalpies of vaporization of alkylphenols. *J. Chem. Thermodyn.* 1990;22(4):365–377. https://doi.org/10.1016/0021-9614(90)90122-7
12. Wu E., Sinha S., Yang C., Zhang M., Acree W.E. Abraham Solvation Parameter Model: Calculation of L Solute Descriptors for Large C_{11} to C_{42} Methylated Alkanes from Measured Gas–Liquid Chromatographic Retention Data. *Liquids.* 2022;2(3):85–105. https://doi.org/10.3390/liquids2030007
13. Zenkevich I.G., Olisov D.A. Effects of the Discrimination of Sample Composition with the Use of Split Injection into Gas Chromatographic Capillary Columns. *J. Anal. Chem.* 2019;74(Suppl 1):32–38. https://doi.org/10.1134/S1061934819070190
[Original Russian Text: Zenkevich I.G., Olisov D.A. Effects of the Discrimination of Sample Composition with the Use of Split Injection into Gas Chromatographic Capillary Columns. *Zhurnal Analiticheskoi Khimii.* 2019;74(7):40–47 (in Russ.). https://doi.org/10.1134/S0044450219070223]
14. Zenkevich I.G., Pavlovskii A.A. Anomalous temperature dependence of gas chromatographic retention indices of polar compounds on nonpolar phases. *Russ. J. Phys. Chem. A.* 2016;90(5):1074–1080. https://doi.org/10.1134/S0036024416040336
[Original Russian Text: Zenkevich I.G., Pavlovskii A.A. Anomalous temperature dependence of gas chromatographic retention indices of polar compounds on nonpolar phases. *Zhurnal Fizicheskoi Khimii*. 2016;90(5):792–799 (in Russ.). https://doi.org/10.7868/S0044453716040348]

5. Кучеренко Е.В., Мельник Д.М., Королев А.А., Канатьева А.Ю., Пирогов А.В., Курганов А.А. Монолитные капиллярные колонки на основе тетраакрилата пентаэритрита для хроматографического анализа пептидов. *Журн. физ. химии.* 2015;89(9):1688–1692. https://doi.org/10.7868/S0044453715090198
6. Тонконогов Б.П., Попова К.А., Хурумова А.Ф. Перспективы применения сложных эфиров отечественного производства в качестве основ масел для авиационной техники. *Труды Российского государственного университета нефти и газа имени И.М. Губкина.* 2015;278(1):109–120.
7. Сильман А.В., Ниязбакиев И.И., Смирнова Ю.К. Бесфталатные пластификаторы. В сб.: *Современные научные исследования: проблемы и пути их решения: сборник научных трудов по материалам Международной научно-практической конференции*. СПб: Профессиональная наука; 2020. С. 59–62.
8. Wypych G. *Handbook of Plasticizers*: 2nd ed. Toronto: Chemtech Publishing; 2012. 748 p.
9. Рыжкин Д.А., Раева В.М. Сравнение методов расчета энтальпии парообразования бинарных азеотропных смесей. *Тонкие химические технологии.* 2024;19(4):279–292. https://doi.org/10.32362/2410-6593-2024-19-4-279-292
10. Krasnykh E.L., Druzhinina Y.A., Portnova S.V., Smirnova Y.A. Vapor pressure and enthalpy of vaporization of trimethylolpropane and carboxylic acids esters. *Fluid Phase Equilib*. 2018;462:111–117. https://doi.org/10.1016/j.fluid.2018.01.018
11. Nesterova T.N., Nazmutdinov A.G., Tsvetkov V.S., Rozhnov A.M., Roshchupkina I.Yu. Vapour pressures and enthalpies of vaporization of alkylphenols. *J. Chem. Thermodyn.* 1990;22(4):365–377. https://doi.org/10.1016/0021-9614(90)90122-7
12. Wu E., Sinha S., Yang C., Zhang M., Acree W.E. Abraham Solvation Parameter Model: Calculation of L Solute Descriptors for Large C_{11} to C_{42} Methylated Alkanes from Measured Gas–Liquid Chromatographic Retention Data. *Liquids.* 2022;2(3):85–105. https://doi.org/10.3390/liquids2030007
13. Зенкевич И.Г., Олисов Д.А. Эффекты дискриминации состава проб при их дозировании в капиллярные газохроматографические колонки с делением потока. *Журн. анал. химии*. 2019;74(7):40–47. https://doi.org/10.1134/S0044450219070223
14. Зенкевич И.Г., Павловский А.А. Аномальная температурная зависимость газохроматографических индексов удерживания полярных соединений на неполярных фазах. *Журн. физ. химии.* 2016;90(5):792–799. https://doi.org/10.7868/S0044453716040348
15. Портнова С.В., Ямщикова Ю.Ф., Красных Е.Л. Характеристики удерживания и энтальпии сорбции сложных эфиров природных гидроксикарбоновых кислот на неподвижной фазе DB-1. *Журн. физ. химии.* 2019;93(3):577–583. https://doi.org/10.1134/S0044453719020225
16. Красных Е.Л., Портнова С.В. Прогнозирование изменения теплоемкости фазового перехода жидкость-пар на основе модифицированных индексов Рандича. Алканы и кислородсодержащие соединения. *Журн. структ. химии*. 2017;58(4):739–744. https://doi.org/10.15372/JSC20170409
17. Емельянов В.В., Красных Е.Л., Портнова С.В. Характеристики удерживания и энтальпии сорбции сложных эфиров пентаэритрита и кислот C_2–C_8 на неполярной неподвижной фазе. *Журн. физ. химии.* 2020;94(10):1567–1575. https://doi.org/10.31857/S004445372010009X

15. Portnova S.V., Yamshchikova Y.F., Krasnykh E.L. Retention Characteristics and Sorption Enthalpies of Esters of Natural Hydroxycarboxylic Acids on DB-1 Stationary Phase. *Russ. J. Phys. Chem. A.* 2019;93(3):577–583. https://doi.org/10.1134/S0036024419020213
[Original Russian Text: Portnova S.V., Yamshchikova Y.F., Krasnykh E.L. Retention Characteristics and Sorption Enthalpies of Esters of Natural Hydroxycarboxylic Acids on DB-1 Stationary Phase. *Zhurnal Fizicheskoi Khimii.* 2019;93(3):464–5470 (in Russ.). https://doi.org/10.1134/S0044453719020225]
16. Krasnykh E.L., Portnova S.V. Prediction of changes in the heat capacity of the liquid–vapor phase transition based on modified Randič indices. Alkanes and oxygen-containing compounds. *J. Struct. Chem.* 2017;58(4):706–711. https://doi.org/10.1134/S0022476617040096
[Original Russian Text: Krasnykh E.L., Portnova S.V. Prediction of changes in the heat capacity of the liquid–vapor phase transition based on modified Randič indices. Alkanes and oxygen-containing compounds. *Zhurnal Strukturnoi Khimii.* 2017;58(4):739–744 (in Russ.). https://doi.org/10.15372/JSC20170409]
17. Emel'yanov V.V., Krasnykh E.L., Portnova S.V. Retention indices and sorption enthalpies of pentaerythritol and C_2–C_8 acid esters on nonpolar stationary phases. *Russ. J. Phys. Chem. A.* 2020;94(10):2168–2176. https://doi.org/10.1134/S003602442010009X
[Original Russian Text: Emel'yanov V.V., Krasnykh E.L., Portnova S.V. Retention indices and sorption enthalpies of pentaerythritol and C_2–C_8 acid esters on nonpolar stationary phases. *Zhurnal Fizicheskoi Khimii.* 2020;94(10):1567–1575 (in Russ.). https://doi.org/10.31857/S004445372010009X]
18. Emel'ianov V.V., Krasnykh E.L., Portnova S.V., Levanova S.V. Synthetic oils based on pentaerythritol esters. Vapor pressure and enthalpy of vaporization. *Fuel*. 2022;312:122908. https://doi.org/10.1016/j.fuel.2021.122908
19. Krasnykh E.L., Portnova S.V. Prediction of enthalpies of vaporization based on modified Randič indices. Esters. *J. Struct. Chem.* 2016;57(3):437–445. https://doi.org/10.1134/S0022476616030033
[Original Russian Text: Krasnykh E.L., Portnova S.V. Prediction of enthalpies of vaporization based on modified Randič indices. Esters. *Zhurnal Strukturnoi Khimii.* 2016;57(3):466–474 (in Russ.). https://doi.org/10.15372/JSC20160303]
20. Razzouk A., Mokbel I., García J., Fernandez J., Msakni N., Jose J. Vapor pressure measurements in the range 10^{-5} Pa to 1 Pa of four pentaerythritol esters. Density and vapor–liquid equilibria modeling of ester lubricants. *Fluid Phase Equilib*. 2007;260(2):248–261. https://doi.org/10.1016/j.fluid.2007.07.029

18. Emel'ianov V.V., Krasnykh E.L., Portnova S.V., Levanova S.V. Synthetic oils based on pentaerythritol esters. Vapor pressure and enthalpy of vaporization. *Fuel*. 2022;312:122908. https://doi.org/10.1016/j.fuel.2021.122908
19. Красных Е.Л., Портнова С.В. Прогнозирование энтальпий испарения на основе модифицированных индексов Рандича. Сложные эфиры. *Журн. структ. химии*. 2016;57(3):466–474. https://doi.org/10.15372/JSC20160303
20. Razzouk A., Mokbel I., García J., Fernandez J., Msakni N., Jose J. Vapor pressure measurements in the range 10^{-5} Pa to 1 Pa of four pentaerythritol esters. Density and vapor–liquid equilibria modeling of ester lubricants. *Fluid Phase Equilib*. 2007;260(2):248–261. https://doi.org/10.1016/j.fluid.2007.07.029

About the Authors

Yulia F. Ivanova, Postgraduate Student, Technology of Organic and Petrochemical Synthesis Department, Samara State Technical University (244, Molodogvardeyskaya ul., Samara, 443100, Russia). E-mail: vaewa.yu@yandex.ru. RSCI SPIN-code 5226-6633, https://orcid.org/0009-0004-3508-6032

Vladimir V. Emelyanov, Cand. Sci. (Chem.), Associate Professor, Technology of Organic and Petrochemical Synthesis Department, Samara State Technical University (244, Molodogvardeyskaya ul., Samara, 443100, Russia). E-mail: koraks@mail.ru. Scopus Author ID 57219254675, RSCI SPIN-code 5802-8200, http://orcid.org/0000-0002-6228-5713

Svetlana V. Levanova, Dr. Sci. (Chem.), Professor, Honored Scientist of the Russian Federation, Professor, Technology of Organic and Petrochemical Synthesis Department, Samara State Technical University (244, Molodogvardeyskaya ul., Samara, 443100, Russia). E-mail: kinterm@mail.ru. Scopus Author ID 6701876379, ResearcherID D-6065-2014, RSCI SPIN-code 4521-0265, http://orcid.org/0000-0003-2539-8986

Yuri N. Telnov, Master Student, Samara State Technical University (244, Molodogvardeyskaya ul., Samara, 443100, Russia). E-mail: yuriy-telnov@mail.ru. https://orcid.org/0009-0004-0322-498X

Об авторах

Иванова Юлия Федоровна, аспирант, кафедра «Технология органического и нефтехимического синтеза», ФГБОУ ВО «Самарский государственный технический университет» (443100, Россия, г. Самара, ул. Молодогвардейская, д. 244). E-mail: vaewa.yu@yandex.ru. Scopus Author ID 59668481900, SPIN-код РИНЦ 5226-6633, https://orcid.org/0009-0004-3508-6032

Емельянов Владимир Владимирович, к.х.н., доцент, кафедра «Технология органического и нефтехимического синтеза», ФГБОУ ВО «Самарский государственный технический университет» (443100, Россия, г. Самара, ул. Молодогвардейская, д. 244). E-mail: koraks@mail.ru. Scopus Author ID 57219254675, SPIN-код РИНЦ 5802-8200, http://orcid.org/0000-0002-6228-5713

Леванова Светлана Васильевна, д.х.н., профессор, заслуженный деятель науки РФ, профессор, кафедра «Технология органического и нефтехимического синтеза», ФГБОУ ВО «Самарский государственный технический университет» (443100, Россия, г. Самара, ул. Молодогвардейская, д. 244). E-mail: kinterm@mail.ru. Scopus Author ID 6701876379, ResearcherID D-6065-2014, SPIN-код РИНЦ 4521-0265, http://orcid.org/0000-0003-2539-8986

Тельнов Юрий Николаевич, магистрант, ФГБОУ ВО «Самарский государственный технический университет» (443100, Россия, г. Самара, ул. Молодогвардейская, д. 244). E-mail: yuriy-telnov@mail.ru. https://orcid.org/0009-0004-0322-498X

Translated from Russian into English by V. Glyanchenko
Edited for English language and spelling by Thomas A. Beavitt

Tonkie Khimicheskie Tekhnologii = Fine Chemical Technologies.
2025;20(3):215–222
ISSN 2686-7575 (Online)

Chemistry and technology of organic substances
Химия и технология органических веществ

UDC 547+546.786+623+544
https://doi.org/10.32362/2410-6593-2025-20-3-215-222
EDN ZKHQPM

RESEARCH ARTICLE

Evaluation of the catalytic effect of potassium tungstate in green decontamination for detoxification of 2-chloroethyl phenylsulfide (2-CEPS)

Vu Thanh Binh[1,✉], Nguyen Thanh Hoa[1], Do Ngoc Khue[1], Nguyen Khanh Hung[3], Dao Duy Hung[3]

[1] *New Technology Institute, Academy of Military Science and Technology; 17 Hoang Sam, Cau Giay District, Hanoi, Vietnam*

[2] *Thuyloi University, 175 Tay Son, Dong Da District, Hanoi, Vietnam*

[3] *Chemical Corps, 26 Hoang Sam, Cau Giay District, Hanoi, Vietnam*

✉ *Corresponding author, e-mail: vuthanhbinh0979@gmail.com*

Abstract

Objectives. 2-Chloroethyl phenylsulfide (2-CEPS) is a relevant simulant of chemical warfare sulfur mustard gas (yperit) as part of an environmentally-friendly decontamination processes. This study presents the initial results of research the catalytic ability of tungstate in the conversion process of 2-CEPS.

Methods. The decontamination system employed in this study comprised hydrogen peroxide (H_2O_2), potassium tungstate acting as a metal transition salt catalyst, a surfactant, and organic solvents. The research investigated the impact of K_2WO_4 concentration on the conversion efficiency and rate of the target compound. As well as additionally exploring the influence of the substrate-to-catalyst ratio on the reaction pathway, the study evaluated the stability of the detoxifying mixture.

Results. Increasing the concentration of K_2WO_4 is shown to lead to an increase in the efficiency and conversion rate of 2-CEPS. As well as demonstrating stability and durability, the catalyst did not cause unwanted H_2O_2 breakdown. After 18 h of mixing, the conversion retained efficiency above 95% within 15 min of the reaction. The degradation kinetics follow a pseudo-first-order model, indicating that the reaction rate is directly influenced by the K_2WO_4 concentration. In addition to enhancing the oxidative capacity of the solution, increased tungstate concentration promotes the formation of undesirable sulfone byproducts.

Conclusions. The study investigated the catalytic activity of tungstate within an eco-friendly solution formulated to degrade 2-CEPS. Our findings demonstrate a strong correlation between the concentration of potassium tungstate (K_2WO_4) and the rate of 2-CEPS degradation. A key advantage of tungstate is its exceptional stability and durability as a catalyst. Efficient decontamination is ensured thanks to its minimal interference with the stability of hydrogen peroxide (H_2O_2).

Keywords

2-CEPS, yperit, chemical warfare, green decontamination solution, tungstate, catalysis

Submitted: 18.10.2024
Revised: 21.01.2025
Accepted: 17.03.2025

For citation

Vu Th.B., Nguyen Th.H., Do N.K., Nguyen Kh.H., Dao D.H. Evaluation of the catalytic effect of potassium tungstate in green decontamination for detoxification of 2-chloroethyl phenylsulfide (2-CEPS). *Tonk. Khim. Tekhnol. = Fine Chem. Technol.* 2025;20(3): 215–222. https://doi.org/10.32362/2410-6593-2025-20-3-215-222

НАУЧНАЯ СТАТЬЯ

Оценка каталитического эффекта вольфрамата калия в экологически безопасной детоксикации 2-хлорэтилфенилсульфида (2-CEPS)

Vu Thanh Binh[1,✉], Nguyen Thanh Hoa[1], Do Ngoc Khue[1], Nguyen Khanh Hung[3], Dao Duy Hung[3]

[1] *Институт Новой Технологии, Академия Военной Науки и Технологии, Ханой, Вьетнам*

[2] *Университет Туи Лой, Ханой, Вьетнам*

[3] *Химический Корпус, Ханой, Вьетнам*

✉ *Автор для переписки, e-mail: vuthanhbinh0979@gmail.com*

Аннотация

Цели. Представлены первые результаты изучения каталитической способности вольфрамата в процессе превращения 2-хлорэтилфенилсульфида (2-CEPS) — аналога иприта, сернистого иприта — в рамках экологически безопасных методов дезактивации.

Методы. Система дезактивации включала пероксид водорода (H_2O_2), вольфрамат калия (катализатор на основе соли переходного металла), поверхностно-активное вещество и органические растворители. Исследовалось влияние концентрации K_2WO_4 на эффективность и скорость превращения целевого соединения. Дополнительно изучалось соотношение субстрата и катализатора, а также стабильность детоксицирующей смеси.

Результаты. Показано, что увеличение концентрации K_2WO_4 приводит к росту эффективности и скорости превращения 2-CEPS. Катализатор продемонстрировал стабильность и долговечность, не вызывая нежелательного разложения H_2O_2. После 18 ч перемешивания степень конверсии сохранялась выше 95% в течение 15 мин реакции. Кинетика деградации соответствует модели псевдопервого порядка, что указывает на прямую зависимость скорости реакции от концентрации K_2WO_4, однако повышение концентрации вольфрамата способствует образованию нежелательных сульфоновых побочных продуктов.

Выводы. Исследована каталитическая активность вольфрамата в экологически безопасном растворе, разработанном для деградации 2-CEPS. Установлена четкая зависимость между концентрацией K_2WO_4 и скоростью разложения 2-CEPS. Ключевое преимущество вольфрамата — его исключительная стабильность и долговечность в качестве катализатора, а также минимальное влияние на стабильность H_2O_2, что обеспечивает эффективную дезактивацию.

Ключевые слова

2-хлорэтилфенилсульфид, иприт, химическое оружие, экологичный раствор для обеззараживания, вольфрамат, катализ

Поступила: 18.10.2024
Доработана: 21.01.2025
Принята в печать: 17.03.2025

Для цитирования

Vu Th.B., Nguyen Th.H., Do N.K., Nguyen Kh.H., Dao D.H. Evaluation of the catalytic effect of potassium tungstate in green decontamination for detoxification of 2-chloroethyl phenylsulfide (2-CEPS). *Тонкие химические технологии*. 2025;20(3):215–222. https://doi.org/10.32362/2410-6593-2025-20-3-215-222

INTRODUCTION

Although chemical decontamination processes based on chlorine-containing substances such as hypochlorite and chloramine are effective and cost-efficient, there are still negative impacts on human health and the environment [1]. The potential use of such compounds is additionally limited due to their high corrosiveness, which can damage equipment, weapons, and storage facilities.

Green chemistry, also known as clean chemistry or sustainable chemistry, attracts significant attention from scientists, economists, and politicians. Green chemistry focuses on designing and producing environmentally friendly products while minimizing the use and creation of hazardous substances [2]. The environmental friendliness of chemicals can be categorized into edible, contactable, and approved for use in agriculture and industry [3]. H_2O_2 is an ideal oxidizing agent, capable of oxidizing with an atomic efficiency of 47%, producing water as the only available theoretical product, and safe for storage, transportation, and use. H_2O_2 has high oxidizing properties, especially when combined with a suitable catalytic activator. Generally, there are four groups of commonly used catalytic activators: organic activators, metal ion activators, metal complexes (biomimetic), and metal salt activators. Metal salt activators are especially

interesting due to their diversity and strong catalytic abilities [4]. In 2003, Ryoji Noyori used tungstate as a catalyst for strengthening the oxidation reaction with H_2O_2. Tungstate is physiologically harmless and does not cause the decomposition of H_2O_2 [5]. In 2010, George W. Wagner demonstrated the use of molybdate metal salt activator as a catalyst to create the peroxy anion (OOH) for accelerating the oxidizing ability of H_2O_2 [6]. Environmentally-friendly organic solvent components Triton X-100 (TX-100), solvent propylene carbonate (PC), and propylene glycol (PG), were used in respective volume ratios of 10%, 10%, and 20% [7].

In the present study, we used 30% H_2O_2 as an oxidizing agent to detoxify 2-CEPS along with potassium tungstate as the catalyst/activator and organic solvents containing TX-100, PC, and PG in respective volume ratios of 10%, 10%, and 20%. Several factors affecting efficiency, speed, and conversion direction were investigated. The catalyst/substrate ratio was shown to greatly influence the conversion process and product formation trends; the tungstate catalyst in the decontamination mixture demonstrated high stability, durability, and minimal unwanted decomposition of H_2O_2.

MATERIALS AND METHODS

Chemical and equipment

Chemical

2-CEPS (98%) by *Sigma-Aldrich* (USA); H_2O_2 (30%), TX-100 (99%) by *Merck* (Germany); PC (99%), PG (99%), K_2WO_4 (99%), Na_2CO_3 (99%), Na_2SO_3 (99%) by *Macklin* (China); chloroform, methanol with suitable purity for high-performance liquid chromatography (HPLC) by *Fisher Scientific* (United Kingdom); distilled water.

Equipment

HPLC HP-1100 chromatograph (*Agilent Technologies*, USA), chromatographic column C8 (250 mm × 4.6 mm × × 5 μm), UV-VIS diode array (DAD) detector with scan range of 0–1100 nm; Agilent 5975 gas chromatography-mass spectrometer (GC–MS *Agilent Technologies*, USA), DB-5MS column (30 m × 0.32 mm × 0.25 mm); Pioneer™ precision balances *Ohaus*, USA) with 0.0001g sensitivity; MS2 minishaker (USA).

Methods

2-CEPS degradation and analytical methods

The 2-CEPS concentration during the reaction was determined according to the HPLC method. Elution was isocratic with a flow rate of 1.0 mL/min using a mixture of methanol and diluted water (70/30, *v*/*v*). At an injection volume of 10 μL, the detection wavelength was 252 nm, and the retention time was 7.188 min.

The intermediates produced during the degradation of 2-CEPS were analyzed using GC–MS chromatography. Helium with a purity above 99.999% was applied as the carrier gas at a constant flow rate of 1.0 mL/min and pressure of 60 psi. The injection was implemented in splitless mode over 1.0 min, and the injection volume was 1.0 μL. The shunt flow was set at 50.0 mL/min. The carrier gas saving time and flow rate were 2.0 min and 20.0 mL/min, respectively. The inlet temperature was held at 280°C. The optimized initial temperature of the oven was set at 40°C for 1 min, then increased at a rate of 10°C per minute to 280°C for 5 min. The substances were identified by comparing the mass spectra of the analytes with the NIST mass spectral library (*National Institute of Standards and Technology*, USA) and using fragment-matching methods [7].

Experimental setup

The reactions were carried out in 10-mL capped test tubes at room temperature (25°C). After taking organic solvents of 100 μL of TX-100, 100 μL of PC, and 200 μL of PG [3, 5], decontamination solutions were added to the test tube to make up a total volume of 1 mL. Then 20-μL 2-CEPS was added to the test tube (at a volume ratio between decontamination and reactant of 50 : 1) and the tube was agitated. At 1, 5, 10, 15, and 30-min time points, 59 μL of the sample was added to a test tube containing 1 mL of a reaction quenching mixture containing 0.2 *M* Na_2SO_3 and 0.2 *M* Na_2CO_3 and agitated. Chloroform of 2 mL was then added to the mixture and agitated for 2 min [8]. The extracted solution was filtered through a 0.22 μm filter and analyzed using HPLC to record the concentration of 2-CEPS. Intermediates were analyzed by GC–MS. After repeating each experiment 3 times, the average value was taken.

The removal efficiency (η, %) was calculated using the following formula:

$$\eta = \frac{C_0 - C_t}{C_0} \times 100\%,$$

where C_0 and C_t (ppm) are the concentrations of 2-CEPS in before and after treatment, respectively.

RESULTS AND DISCUSSION

Analyzing the effect of K_2WO_4 concentration on reaction time and conversion efficiency

Since decontaminants used in military contexts require rapid toxicity conversion, the reaction rate and conversion efficiency are the most important factors. To analyze the effect of K_2WO_4 concentration on the

degradation process of 2-CEPS, the concentration of H_2O_2 was fixed at 4.32 *M*, while K_2WO_4 concentrations were varied between 0 *M*, 0.0005 *M*, 0.00075 *M*, 0.001 *M*, and 0.0025 *M*. The results are shown in Figs. 1 and 2 and Table 1.

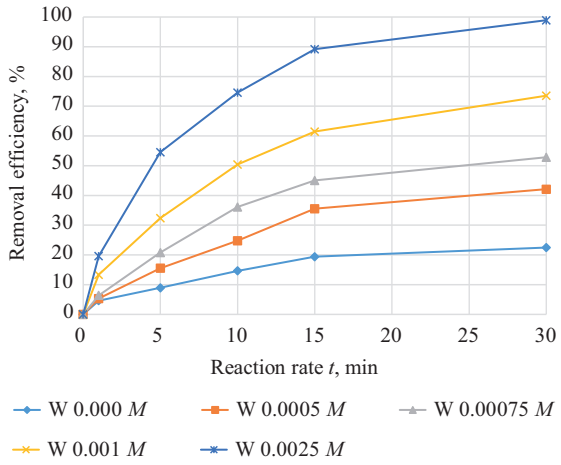

Fig. 1. Effect of K_2WO_4 concentration on removal efficiency of 2-CEPS

As shown in Fig. 1, at a fixed concentration of H_2O_2, the removal rate of 2-CEPS depends on the concentration of K_2WO_4. In the case without K_2WO_4, the conversion reaction of 2-CEPS proceeds slowly, recording an efficiency of 22.47% after 30 min. In the cases with K_2WO_4, the conversion rate increases significantly, reaching a maximum of 98.92% after 30 min at a concentration of 0.0025 *M*.

According to the analyzed K_2WO_4 concentration condition (Fig. 2), $\ln(C_t/C_0)$ decreases linearly over time (*t*), implying that the conversion reaction of 2-CEPS

Table 1. Relationship between K_2WO_4 concentration (C_{WO4}) and the rate constant of removing 2-CEPS reaction (*K*)

C_{WO4}	K	K/C_{WO4}
0.00050	0.0281	56.2
0.00075	0.0400	53.3
0.00100	0.0620	62.0
0.00250	0.1429	57.2

is based on the pseudo-first-order kinetic reaction. At the same time, Table 1 shows that the ratio K/C_{WO4} is relatively constant, around 53.3 to 62.0, implying that the reaction rate constant is first-order with respect to the concentration of K_2WO_4. This can be explained in terms of the case with K_2WO_4, where the oxidation sulfide compound process by H_2O_2 based on the metal W has two stages:

Stage 1. During the aqueous phase, the catalyst precursor K_2WO_4 is rapidly oxidized by H_2O_2, forming a bis-peroxo wolfram complex [5, 9].

$$K_2WO_4 + 2H_2O_2 \rightarrow K_2[WO(O_2)_2(OH)_2] + H_2O.$$

In this stage, the molar ratio of K_2WO_4/H_2O_2 was analyzed from 1/8640 to 1/1728. Therefore, the rate of forming complex depends on the concentration of K_2WO_4, and it can be assumed that the total K_2WO_4 has been converted to the peroxo complex.

Stage 2. The peroxo complex approaches and oxidizes the sulfide. When adding 2-CEPS, because of the volume is equal to 1/50 of the decontaminant, it quickly dissolves into the solution, supporting the peroxo to contact and react easily.

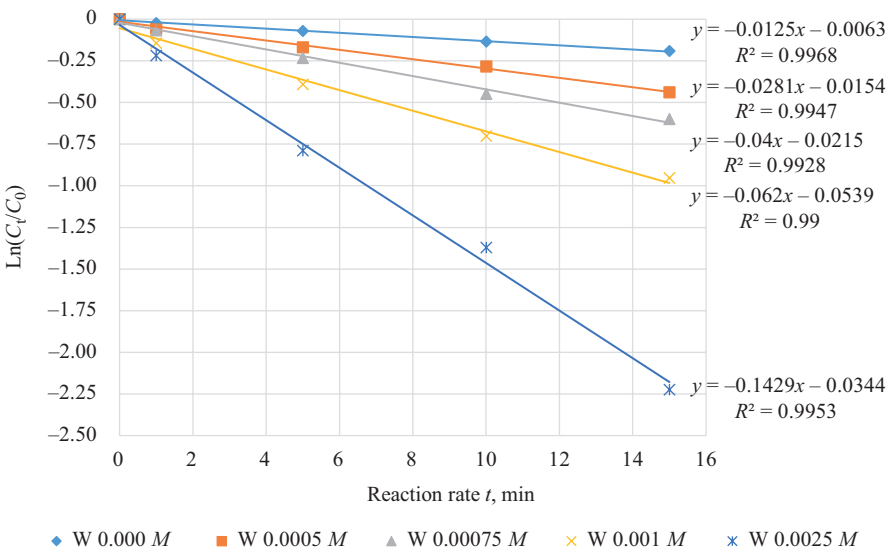

Fig. 2. Kinetic chart of $\ln(C_t/C_0)$ vs *t*

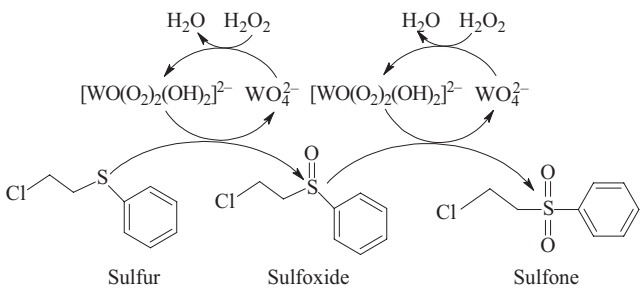

Fig. 3. 2-CEPS conversion process

In Stage 2, the molar ratio of peroxo/2-CEPS is from 1/267 to 1/54. Initially, the reaction rate records almost unchanged at this ratio due to its dependence on the peroxo concentration. However, when the concentration of 2-CEPS starts to decrease, the reaction rate becomes dependent on both the concentrations of peroxo and also 2-CEPS.

In addition to the effect of kinetic factors, some dynamic factors may also affect the conversion process, such as the velocity of movement of molecules in the solution, spatial effects, and the reaction ability between the peroxo complex and 2-CEPS in the solution.

Thus, the detoxification of 2-CEPS in solution highly depends on the concentration of K_2WO_4. At low enough concentrations, the reaction equation follows pseudo-first-order kinetics, and the rate constant is first-order depending on the concentration of K_2WO_4.

Analyzing the effect of the catalyst/substrate ratio on the detoxification process trend

The aim of the oxidation decontamination yperite process is to convert it into compounds with lower toxicity, especially sulfoxide, which has lower toxicity and does not cause blistering. At the same time, this process must avoid producing sulfone, a reaction intermediate that has high toxicity and can be formed over the oxidation process [10]. To determine the effect of the catalyst/substrate ratio leads to the trend of producing conversion product 2-CEPS, we performed the experiments as described in the Methods section with $[H_2O_2]$ = 4.32 *M* and $[K_2WO_2]$ concentrations of 0.0025 *M*, 0.01 *M*, and 0.09 *M*. The conversion products 2-CEPS were identified using the GC–MS spectral library after 15 min. The results from the GC–MS identified 6 product peaks at retention times of 14.491, 15.591, 16.956, 18.321, 18.539, and 18.736 min. Based on the mass spectra identified in Fig. 4, the substances have ion fragments with corresponding unique *m*/*z*, peak 1: ethenylsulfinyl benzene (77, 104, 125, 152); peak 2: ethenylsulfonyl benzene (77, 104, 125, 168); peak 3: methyl phenyl sulfone (65, 77, 78, 141, 156); peak 4: methylsulfinyl benzene (77, 109, 125, 172); peak 5: 2-chloroethyl sulfonyl benzene (63, 77, 125, 141, 204); peak 6: 2-phenylsulfonyl ethanol (77, 109, 125, 141), where peaks 1 and 4 are the sulfoxide family, while peaks 2, 3, 5, and 6 are the sulfone family.

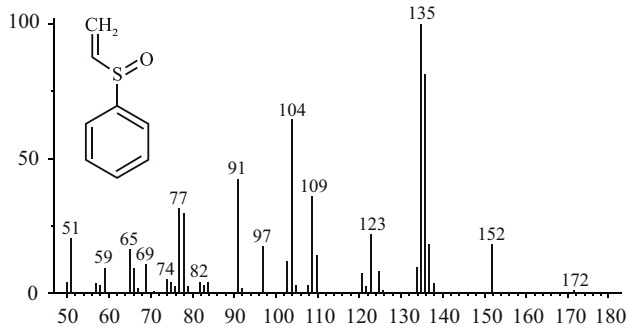

(a) Mass spectrum of ethenylsulfinyl benzene with a peak at 14.491 min

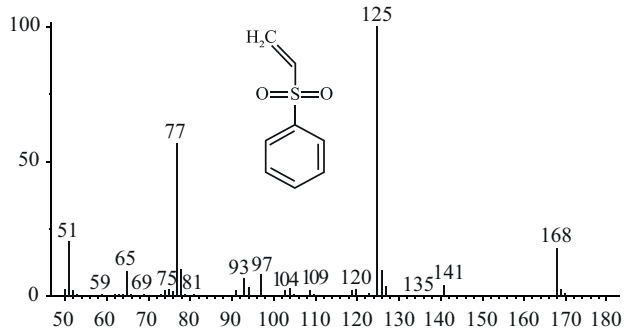

(b) Mass spectrum of ethenylsulfonyl benzene with a peak at 15.591 min

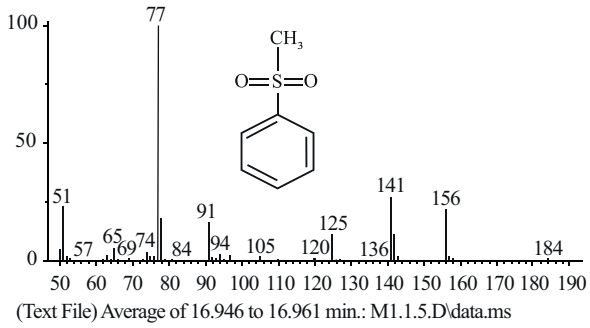

(c) Mass spectrum of methyl phenyl sulfone with a peak at 16.956 min

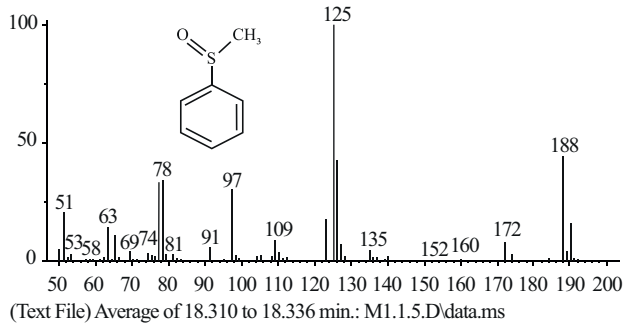

(d) Mass spectrum of methylsulfinyl benzene with a peak at 18.321 min

Fig. 3. 2-CEPS conversion process

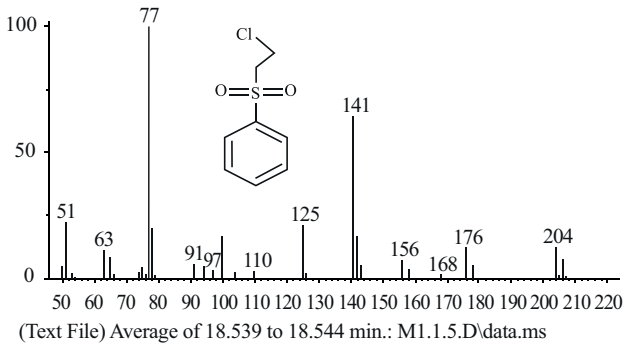

(e) Mass spectrum of 2-chloroethyl sulfonyl benzene with a peak at 18.539 min

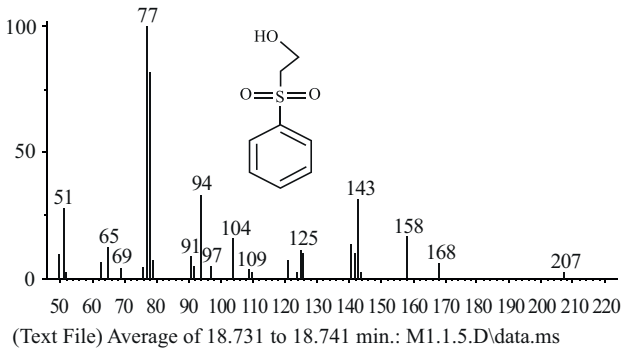

(f) Mass spectrum of 2-phenylsulfonyl ethanol with a peak at 18.736 min

Fig. 3. (Continued). 2-CEPS conversion process

As well as showing the retention time, the GC–MS in Fig. 5 visually illustrates the effect of the catalyst/substrate ratio on the formation of products. Specific data on peak height and the relative percentage of sulfoxide and sulfone family products are presented in Table 2.

According to the results given in Fig. 5 and Table 2 when the concentration of K_2WO_4 increases, the sulfoxide family products decrease from 77.59% to 6.35%, while the sulfone product family increases from 22.41% to 93.65%. This can be explained in terms of the formed bisperoxotungstate compound (A)

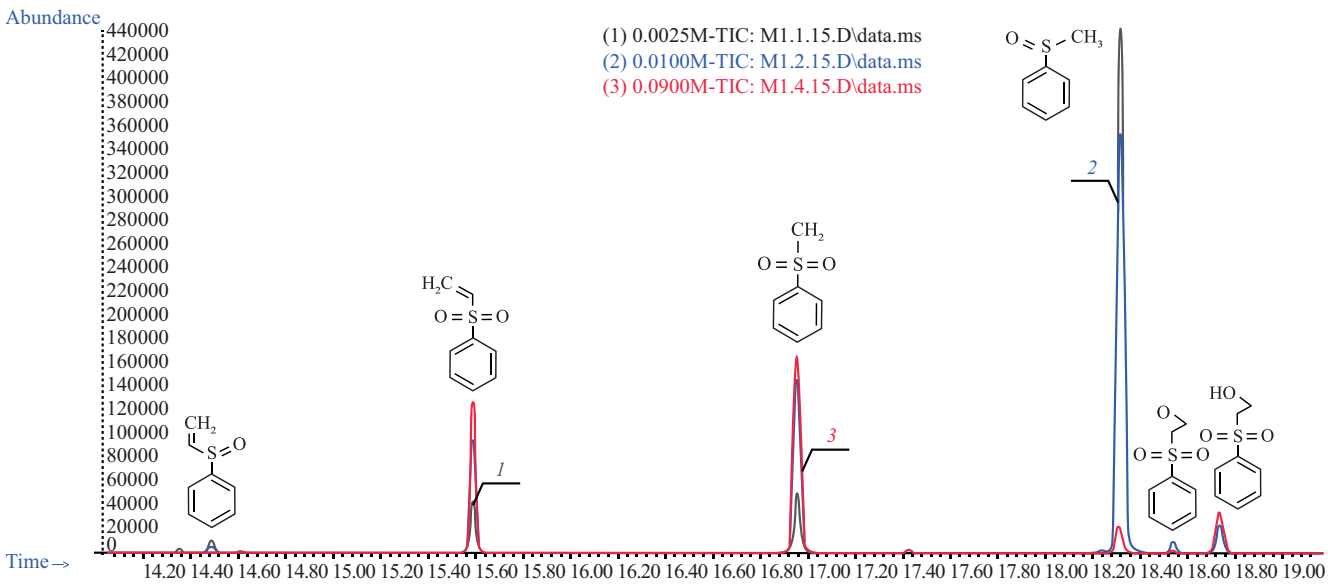

Fig. 5. GC–MS of mixture products after 15 min converting 2-CEPS

Table 2. Peak height and relative percentage of sulfoxide and sulfone products

K_2WO_4 concentration (C_M)	Peak height, h						% Sulfoxide	% Sulfone
	$h_{Peak\ 1}$	$h_{Peak\ 2}$	$h_{Peak\ 3}$	$h_{Peak\ 4}$	$h_{Peak\ 5}$	$h_{Peak\ 6}$		
0.0025	10^4	$45 \cdot 10^3$	$5 \cdot 10^4$	$44 \cdot 10^4$	10^4	$25 \cdot 10^3$	77.59	22.41
0.0100	$6 \cdot 10^3$	$95 \cdot 10^3$	$15 \cdot 10^4$	$36 \cdot 10^4$	10^4	$25 \cdot 10^3$	56.66	43.34
0.0900	0	$13 \cdot 10^4$	$168 \cdot 10^3$	$23 \cdot 10^3$	$3 \cdot 10^3$	$38 \cdot 10^3$	6.35	93.65

being in equilibrium with states B and C (Fig. 6). When the concentration of K_2WO_4 increases, so does the amount of peroxo complex A; this causes the equilibrium in the forward direction to tend to form more B and C complexes. Among them, the peroxo complex and complex C have higher oxidation activity, leading to the excessive oxidation of sulfides to sulfones.

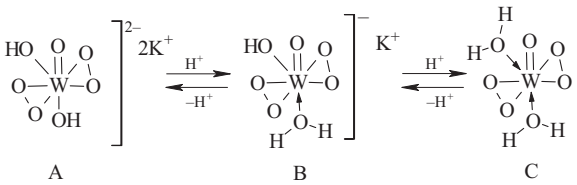

Fig. 6. Equilibrium in reaction between peroxo complexes A, B, and C

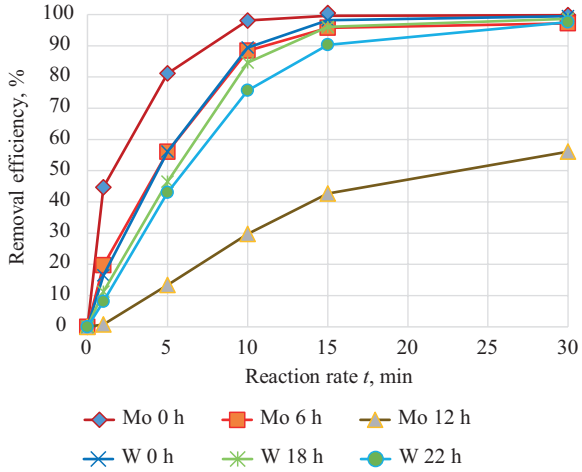

Fig. 7. Effect of mixing time on 2-CEPS conversion efficiency

Bis(2-chloroethyl) sulfide has the potential to damage skin tissue because it has a sulfur atom (S) with a high electron density that can promote the chloroethyl group to form a primary intramolecular ring, releasing chloride and forming a positively charged ethylsulfonium ring. This intermediate product reacts rapidly with nucleophilic groups of DNA, such as the 2-deoxyguanosine base, to cause skin burns. Similar substances with a chloroethyl group, such as CEPS, 2-Chloroethyl ethyl sulfide, etc., also cause blistering, but to a much lesser extent [11, 12]. Although strong oxidizing decontaminants like the oxidation system based on the K_2WO_4 catalyst will oxidize the sulfide to sulfoxide, which no longer has the ability to cause skin burns, further oxidation to highly toxic sulfone must be avoided. However, sulfone only causes skin burns upon injection. Thus, increasing the catalyst ratio increases the oxidation capability of the decontamination, but also leads to the trend of producing unwanted sulfone products [13–15].

Analyzing the durability of catalyst in green decontamination

Since decontaminant mixtures used with military-grade toxic agents typically need to be prepared hours before use, stability after mixing can be an even more important factor than the speed and effectiveness of the conversion.

We set out to research the stability of the decontamination system using $[H_2O_2]$ = 3.09 *M* and $[K_2WO_4]$ = 0.005 *M*, as well as to compare with the decontaminant based on the Molybdate catalyst system, using $[H_2O_2]$ = 4.32 *M* and $[K_2MoO_4]$ = 0.02 *M*, which was published by Wagner [3, 4, 6] and by the present authors in a previous study [7].

According to Fig. 7, the oxidation system based on the K_2MoO_4 catalyst shows very high efficiency when immediately used after mixing, recording over 99% conversion efficiency when used after 15 min. Six hours after mixing, the conversion efficiency at 15 min of reaction remains around 95%; however, after 12 h of mixing, it drops to about 42%. In contrast, the oxidation system based on the K_2WO_4 catalyst shows excellent stability: 18 h after mixing at 15 min of reaction, the recorded conversion efficiency was still over 95%. After 22 h of mixing, the conversion efficiency significantly decreases: in this case, the reaction rate is slower than the oxidation system based on the K_2MoO_4 catalyst because K_2WO_4 is chemically stable and unconvertible in the decontamination environment. The tungstate complex is especially suitable for use as a pre-catalyst because it does not cause the inefficient decomposition of H_2O_2 [16].

CONCLUSIONS

The catalytic ability of tungstate in the green chemical decontamination solution for converting 2-CEPS has been investigated. The results of the study show that the conversion process of 2-CEPS in the solution is highly dependent on the concentration of K_2WO_4. The degradation is based on a pseudo-first-order kinetic law; the reaction rate constant is first-order depending on the concentration of K_2WO_4. Increasing the concentration of the tungstate catalyst implies raising the oxidative capacity of the decontaminant, but also leads to a trend of producing unwanted sulfone products. Additionally, tungstate is an effective, highly durable catalyst, which even more importantly does not cause inefficient decomposition of H_2O_2.

Authors' contributions

Vu Thanh Binh—conducting research, collecting and processing material, and writing the text of the article.

Nguyen Thanh Hoa—conceptualization of the research paper, critical revision with the introduction of valuable intellectual content.

Do Ngoc Khue—idea of a new method, concept of the study, and planning consultations.

Nguyen Khanh Hung— experimental studies and participation in writing of the text of the article.

Dao Duy Hung—experimental studies and participation in writing of the text of the article.

All authors have read and approved the final version of the manuscript.

The authors declare no conflicts of interest.

REFERENCES

1. Altmann H.J., Richardt A. Decontamination of Chemical Warfare Agents. In: Richardt A., Blum M.M. (Eds.). *Decontamination of Warfare Agents: Tnzymatic Methods for Removal of B/C Weapons*. 2008. P. 83–115. https://doi.org/10.1002/9783527621620.ch7
2. Shea D.A. *Chemical Weapons: A Summary Report of Characteristics and Effects*. Washington, D.C: Library of Congress. Congressional Research Service; 2013. 15 p. Report. Congressional Research Service. R42862.
3. Wagner G., Procell L., Sorrick D., Hess Z., Gehring D., Henderson V., *et al*. *Development of New Decon Green* (*registered trademark*): *A How-To Guide for the Rapid Decontamination of CARC Paint*. 2008. 51 p.
4. Wagner G., Procell L., Yang Y.C., Bunton C. Molybdate/Peroxide Oxidation of Mustard in Microemulsions. *Langmuir*. 2001;17(16):4809–4811. https://doi.org/10.1021/la010334h
5. Noyori R., Aoki M., Sato K. Green oxidation with aqueous hydrogen peroxide. *Chem. Commun*. 2003;(16):1977–1986. https://doi.org/10.1039/B303160H
6. Wagner G. Hydrogen peroxide-based decontamination of chemical warfare agents. *Main Gr. Chem*. 2010;9(3):257–263. https://doi.org/10.3233/MGC-2010-0028
7. Vu Th.B., Do N.K., Ha H.N., Dao D.H., Hoang K.H., Nguyen Th.H. Research on formulating ingredients and evaluating the decomposition ability of 2-chloroethyl phenylsulfide by green decontamination based on molybdate. *J. Mil. Sci. Technol*. 2023;90(90 SE-Research Articles):94–101. https://doi.org/10.54939/1859-1043.j.mst.90.2023.94-101
8. Zhao S., Zhu Y., Xi H., Han M., Li D., Li Y., *et al*. Detoxification of mustard gas, nerve agents and simulants by peroxomolybdate in aqueous H_2O_2 solution: Reactive oxygen species and mechanisms. *J. Environ. Chem. Eng*. 2020;8(5):104221. https://doi.org/10.1016/j.jece.2020.104221
9. Aneesh K., Vusa C.S.R., Berchmans S. Enhanced peroxidase-like activity of $CuWO_4$ nanoparticles for the detection of NADH and hydrogen peroxide. *Sensors Actuators B: Chem*. 2017;253:723–730. https://doi.org/10.1016/j.snb.2017.06.175
10. Haipeng L., Jinxing Y., Yongjing L., Lihong Q., Guomin Z. Decontamination of HD by the Catalytic System of Hydrogen Peroxide Solution. *Hans J. Chem. Eng. Technol*. 2020;10(4):314–321. http://doi.org/10.12677/HJCET.2020.104040
11. Cheng X., Liu C., Yang Y., Liang L., Chen B., Yu H., Xia J., Liu S., Li Y. Advances in sulfur mustard-induced DNA adducts: Characterization and detection. *Toxicol. Lett*. 2021;344:46–57. https://doi.org/10.1016/j.toxlet.2021.03.004
12. Shakarjian M.P., Heck D.E., Gray J.P., Sinko P.J., Gordon M.K., Casillas R.P., Heindel N.D., Gerecke D.R., Laskin D.L., Laskin J.D. Mechanisms mediating the vesicant actions of sulfur mustard after cutaneous exposure. *Toxicol. Sci*. 2010;114(1):5–19. https://doi.org/10.1093/toxsci/kfp253
13. Oheix E., Gravel E., Doris E. Catalytic processes for the neutralization of sulfur mustard. *Chemistry–A Eur J.* 2021;27(1):54–68. https://doi.org/10.1002/chem.202003665
14. Popiel S., Nawała J., Dziedzic D., Gordon D., Dawidziuk B. Study on the kinetics and transformation products of sulfur mustard sulfoxide and sulfur mustard sulfone in various reaction media. *Int. J. Chem. Kinetics.* 2018;50(2):75–89. https://doi.org/10.1002/kin.21141
15. Ye X. Peroxytungstate Anions in Asymmetric Ion Pair Catalyzed Oxidations: Doctoral Thesis. Singapore: Nanyang Technological University; 2019. 198 p. https://doi.org/10.32657/10220/48123
16. Hida T., Nogusa H. Practical and versatile oxidation of alcohol using novel Na_2WO_4–H_2O_2 system under neutral conditions. *Tetrahedron*. 2009;65(1):270–274. https://doi.org/10.1016/j.tet.2008.10.056

About the Authors

Vu Thanh Binh, Postgraduate Student, Institute of New Technology, Academy of Military Science and Technology (17, Hoang Sam str., Cau Giay district, Hanoi, Vietnam). E-mail: vuthanhbinh0979@gmail.com. https://orcid.org/0009-0007-5278-0538

Nguyen Thanh Hoa, Dr. Sci. (Environm. Eng.), Faculty of Chemistry and Environment, Thuyloi University (175, Tay Son str., Dong Da district, Hanoi, Vietnam). E-mail: nthoa@tlu.edu.vn. Scopus Author ID 57204931100, https://orcid.org/0000-0001-8322-5202

Do Ngoc Khue, Dr. Sci. (Chem.), Professor, Institute of New Technology, Academy of Military Science and Technology (17, Hoang Sam str., Cau Giay district, Hanoi, Vietnam). E-mail: dnkhue@gmail.com

Nguyen Khanh Hung, Dr. Sci. (Chem. Eng.), Institute of Military Chemistry and Environment, Chemical Corps (Km8+500, Thang Long boulevard, An Khanh district, Hanoi, Vietnam). E-mail: khanhhungctet@gmail.com

Dao Duy Hung, Dr. Sci. (Chem. Eng.), Institute of Military Chemistry and Environment, Chemical Corps (Km8+500, Thang Long boulevard, An Khanh district, Hanoi, Vietnam). E-mail: daoduyhung179@gmail.com

The text was submitted by the authors in English and edited for English language and spelling by Thomas A. Beavitt

Tonkie Khimicheskie Tekhnologii = Fine Chemical Technologies.
2025;20(3):223–236
ISSN 2686-7575 (Online)

Biochemistry and biotechnology
Биохимия и биотехнология

UDC 544.726+54.058
https://doi.org/10.32362/2410-6593-2025-20-3-223-236
EDN HJIVQS

RESEARCH ARTICLE

Use of ion-exchange resins for purification of L-lactic acid-containing *Rhizopus oryzae* fermentation broth

Elena V. Pikurova[1,✉], Anatoly N. Boyandin[1,2], Dmitry R. Serebryakov[1], Natalya L. Ertiletskaya[1], Olesya V. Anishchenko[2], Anna A. Sukhanova[1]

[1] *Reshetnev Siberian State University of Science and Technology, Krasnoyarsk, 660037 Russia*

[2] *Institute of Biophysics, Siberian Branch, Russian Academy of Sciences, Federal Research Center "Krasnoyarsk Science Center SB RAS," Krasnoyarsk, 660036 Russia*

✉ *Corresponding author, e-mail: vitaelen@gmail.com*

Abstract

Objectives. The work set out to describe conditions for the purification of a model fermentation broth for cultivating the lactic acid-containing micromycete *Rhizopus oryzae* from impurities of inorganic salts using ion-exchange resins under dynamic conditions.

Methods. The solutions collected for analysis were examined using precipitation titration to determine the concentration of chlorides along with a qualitative reaction with Nessler's reagent to ascertain the presence of ammonium ions. The concentration of lactic acid was evaluated spectrophotometrically using iron(III) chloride. The total nitrogen content was determined by high-temperature catalytic combustion on a Formacs HT TOC/TN Analyzer (Netherlands). The content of trace elements and macroelements in the samples was determined using an iCAP 6300 Duo inductively coupled plasma emission spectrometer (United Kingdom).

Results. Purification of the model broth under the described conditions was carried out by successive filtration through the cation exchanger KU-2-8 in the H-form and subsequently through a mixture of weakly basic A847 and strongly basic AV-17-8 anion exchangers in the OH-form taken in a one-to-one ratio. The breakthrough of impurity ions into the solution was shown to occur after passing 30-fold and 10-fold volumes of the model broth relative to the volume of the cation-exchange and anion-exchange resins, respectively. The dynamic exchange capacity prior to breakthrough was determined as follows: 0.35 mmol-eq/cm^3 for the anion-exchange column and 1.61 mmol-eq/cm^3 for the cation-exchange column. The following parameters were defined as column regeneration modes: 3-fold excess of 2 *M* H_2SO_4, 10-fold excess of distilled H_2O for cation exchange; for anion exchange, 3-fold excess of 2 *M* NaOH and 20-fold excess of H_2O.

Conclusions. The conducted studies showed that purification of the model fermentation broth of *Rhizopus oryzae* can be successfully implemented using ion-exchange resins. The model fermentation broth passing successively through cation-exchange and anion-exchange columns was shown to be purified from impurities of mineral salts while maintaining the concentration of lactic acid.

Keywords

lactic acid, purification, cation-exchange resin, anion-exchange resin, sorption, model solution

Submitted: 19.11.2024
Revised: 24.02.2025
Accepted: 10.06.2025

For citation

Pikurova E.V., Boyandin A.N., Serebryakov D.R., Ertiletskaya N.L., Anishchenko O.V., Sukhanova A.A. Use of ion-exchange resins for purification of L-lactic acid-containing *Rhizopus oryzae* fermentation broth. *Tonk. Khim. Tekhnol. = Fine Chem. Technol.* 2025;20(3): 223–236. https://doi.org/10.32362/2410-6593-2025-20-3-223-236

НАУЧНАЯ СТАТЬЯ

Применение ионообменных смол для очистки ферментационного бульона *Rhizopus oryzae*, содержащего L-молочную кислоту

Е.В. Пикурова[1,✉], А.Н. Бояндин[1], Д.Р. Серебряков[1], Н.Л. Ертилецкая[1], О.В. Анищенко [2], А.А. Суханова[1]

[1] *Сибирский государственный университет науки и технологий им. М.Ф. Решетнева, Красноярск, 660013 Россия*

[2] *Институт биофизики Сибирского отделения Российской академии наук, Федеральный исследовательский центр "Красноярский научный центр СО РАН", Красноярск, 660036 Россия*

✉ *Автор для переписки, e-mail: vitaelen@gmail.com*

Аннотация

Цели. Подбор условий очистки модельного ферментационного бульона для культивирования микромицета *Rhizopus oryzae*, содержащего молочную кислоту, от примесей неорганических солей с использованием ионообменных смол в динамических условиях.

Методы. Отбираемые на анализ растворы исследовали титриметрическим методом (осадительное титрование) для определения концентрации хлоридов и качественной реакцией с реактивом Несслера для определения наличия иона аммония. Концентрацию молочной кислоты определяли спектрофотометрически с применением хлорида железа(III). Содержание общего азота определяли методом высокотемпературного каталитического сжигания на анализаторе Formacs HT TOC/TN Analyzer (Нидерланды). Определение содержания микро- и макроэлементов в исследуемых пробах проводили с помощью эмиссионного спектрометра с индуктивно-связанной плазмой iCAP 6300 Duo (Великобритания).

Результаты. Определили, что очистку модельного бульона в данных условиях необходимо проводить последовательным фильтрованием через катионит КУ-2-8 в Н-форме, а затем через смесь слабоосновного А847 и сильноосновного АВ-17-8 анионитов в ОН-форме, взятых в соотношении один к одному. Установили, что проскок примесных ионов в раствор наступает после прохождения 30-кратного и 10-кратного объемов модельного бульона по отношению к объему катионообменной и анионообменных смол соответственно. Определили динамическую обменную емкость до проскока, которая для анионообменной колонки составила 0.35 ммоль-экв/см^3, а для катионообменной колонки — 1.61 ммоль-экв/см^3. В качестве режимов регенерации колонок определены следующие параметры: 3-кратный избыток 2 *M* H_2SO_4, 10-кратный избыток дистиллированной H_2O для катионообменной и 3-кратный избыток 2 *M* NaOH, 20-кратный избыток H_2O для анионообменной колонок.

Выводы. Проведенные исследования показали, что очистка модельного ферментационного бульона *Rhizopus oryzae* может быть успешно реализована с применением ионообменных смол. Установлено, что этот раствор, проходя последовательно через катионообменные и анионообменные колонки, очищается от примесей минеральных солей, при этом концентрация молочной кислоты не снижается.

Ключевые слова

молочная кислота, очистка, катионит, анионит, сорбция

Поступила: 19.11.2024
Доработана: 24.02.2025
Принята в печать: 10.06.2025

Для цитирования

Пикурова Е.В., Бояндин А.Н., Серебряков Д.Р., Ертилецкая Н.Л., Анищенко О.В., Суханова А.А. Применение ионообменных смол для очистки ферментационного бульона *Rhizopus oryzae*, содержащего L-молочную кислоту. *Тонкие химические технологии*. 2025;20(3):223–236. https://doi.org/10.32362/2410-6593-2025-20-3-223-236

INTRODUCTION

Lactic acid (LA) is one of the most important chemicals used in various industries and cosmetology. Between 2019 and 2024, the demand for LA on the global market has increased at an average annual growth rate of 18.7% [1]. According to the relevant United States classification, L(+)-LA belongs to Generally Recognized As Safe (GRAS) compounds that are deemed harmless for use in food products [2–3].

The increased interest in LA can be largely attributed to the demand for polylactide, of which the former is a monomer. Polylactide or polylactic acid is widely used as a biodegradable plastic in the food industry, cosmetics, and medicine [1–7].

Fermentation is generally considered to be a preferred method for LA production as compared to chemical synthesis due to the possibility of obtaining specific LA isomers. However, extraction and separation of LA from microbial fermentation media represent relatively complex and expensive processes. Since the L-isomer is the only biologically active form of LA, i.e., capable of being quickly and completely assimilated by human or animal organisms, the main efforts in LA biosynthesis are aimed at using strains that form the L-isomer.

Various representatives of bacteria and fungi have the ability to synthesize LA. Among microscopic fungi, special attention is paid to mucoral fungi of the genus *Rhizopus*. The *R. oryzae* and *R. arrhizus* species, which can be grown on cheap and simple media with hexoses and pentoses or glycerol as a carbon source, are most resistant to low pH [8, 9].

The costs of isolating LA from fermentation broth (FB) and purification can reach 50% of the total costs of the process. Until now, the most common production method involves the neutralization of the acid formed in the biotechnological process with calcium compounds and the subsequent precipitation of calcium in the form of sulfate, which forms a large amount of gypsum, resulting in LA of low purity. Various approaches to the isolation and purification of LA aimed at overcoming these drawbacks include solvent extraction, membrane separation, ion-exchange chromatography, and reactive distillation [8, 10]. These separation technologies have both advantages and disadvantages. In any case, it is difficult to effectively separate and purify LA using a single method; in many cases, better results can be obtained by integrating several technologies.

Under actual conditions, FB purification is generally carried out over several stages, in particular, when using membrane technologies [9, 10]. Membrane filtration, which represents an important stage of LA isolation, is often used in combination with other methods to obtain high-purity LA. The first stage involves the removal of suspended particles (first of all, biomass) using ultrafiltration. The second stage can be nanofiltration, which is used to separate LA from carbohydrates (whose molecules have a higher molecular weight and are additionally binded with an additional hydration shell) and a significant portion of the salts contained in the FB. Since membrane filtration does not remove all impurity ions, further purification of the LA solution using ion exchange technology is usually required.

In recent decades, ion exchange technology has become a key technological process in various industries, resulting in a proliferation of available synthetic ion exchange materials marketed under different brands and having various properties. In Russia, as elsewhere, ion exchange filter methods for softening and purifying water are used in around 75% of cases [11, 12]. Ion exchange processes occupy an important place in the technologies for extracting almost all rare, widely dispersed, and radioactive elements, especially in the nuclear industry. Ion exchange resins are used to separate multicomponent mixtures of acids and their salts, extract and remove various metals in the metallurgical and chemical industries, as well as to purify target components in the food, pharmaceutical, and medical industries [1, 3, 11–18]. The efficiency of the separation and sorption process during ion exchange depends on the type of ion exchanger, its charge and size, structural characteristics, the size of ions in hydrated and dehydrated states, and the temperature of the environment.

There are two main approaches to the recovery and purification of LA by adsorption using ion-exchange resins. Thus, the works of various research groups demonstrate the possibility of adsorbing LA from the FB by ion-exchange resin [19–21]. This strategy involves neutralization (pH control) of the FB by exchanging lactate ions for the counterions obtained from an anion exchanger. The subsequent elution of resin-bound lactate, e.g. using 1 *M* hydrochloric acid solution, leads to complete LA extraction [22].

In the second case, a type of ion-exchange system is selected that does not sorb lactate ion or absorbs it in an amount of no more than 10%, but removes impurity ions after the FB passes through a cation exchanger and then through an anion exchanger. For example, in [23] a two-stage LA purification process was proposed: first, a strongly acidic cation exchange resin was used to convert sodium lactate obtained after fermentation into LA and remove cations present in the nutrient medium, then LA was separated from other anions from the broth using a weakly basic anion exchanger. However, one volume of cation exchanger was only sufficient for three-fold volume of the broth; subsequently, regeneration was required.

Since the extraction and separation of LA from the microbial fermentation medium are labor-intensive processes, the problem of simplifying the technology and improving the quality of purification of the target product is acute. Our research group is currently developing a highly effective strain-producer for enantiomerically pure L-LA involving optimal cultivation modes for the LA purification membrane technology (LA isolation and purification is significantly simplified due to the absence of an alkaline neutralization agent). At the second stage, the additional purification of LA from impurities of inorganic ions is carried out using ion exchange approaches.

In the present work, the ion exchange purification of LA on a model system using organic resins was studied. This approach can be used to remove impurity anions and cations from FB, while LA with a concentration of 8–10% remains in solution. The proposed process, which uses no additional chemical reagents, can be used to obtain LA as a high-purity aqueous solution, which can be subsequently concentrated to obtain LA of commercial quality (50–90%).

EXPERIMENTAL

The following reagents were used in the work: metal salts (chemically pure and analytical grade, *Khimreaktivsnab*, Russia) $K_2HPO_4 \cdot 3H_2O$, NaCl, NH_4NO_3, $MgSO_4 \cdot 7H_2O$, $ZnSO_4 \cdot 7H_2O$, NaOH, H_2SO_4, $BaCl_2$, $AgNO_3$, phenolphthalein, Nessler reagent. The following types of resins were used in the experiments: Purolite A847, AV-17-8, KU-2-8. Weakly basic gel anion exchanger Purolite A847 (*Purolite*, Romania) is manufactured in hydroxide form with a polyacrylic matrix containing a tertiary ammonium functional group (type II). This resin is an analog of AN-31, Granion AWA-G1, etc. The strongly basic gel anion exchanger AV-17-8 (GOST 20301-74[1], *Tokem*, Russia) having a matrix based on a styrene-divinylbenzene copolymer is produced in chloride form and contains a functional group of quaternary ammonium (type I). This resin is an analog of Purolite A400/A300, Lewatit M-500, Amberlite IRA 402/420, Dowex SBR-P/Maraton A, etc. Strongly acid cation gel exchanger KU-2-8 (TU 6-07-493-95, *Tokem*) produced in sodium form is a sulfonated copolymer of styrene and divinylbenzene with an SO_3H-active group. This resin is an analog of Purolite C100, Lewatit S-100, Amberlite IR-120, Amberjet 1200, Dowex HCR-S/S, Dowex Marathon C. The granule size of all the resins is 0.4–0.6 mm. These commercially available resins are widely used in various separation and purification processes in Russia.

The choice of gel-type ion exchangers is due to the fact that, when using porous anion-exchange resins, a significant proportion of LA will be retained in their pores, having an average size of 600–1500 μm.

The preparation of ion exchangers for work was carried out in accordance with GOST 10896-78[2]. The static exchange capacity of anion exchangers in the OH form was 0.9 mmol-eq/cm^3 for AV-17-8 and 1.1 mmol-eq/cm^3 for A847. The static exchange capacity of KU-2-8 in the H form was 2.1 mmol-eq/cm^3.

The model medium composition (in g/dm^3) is as follows: $K_2HPO_4 \cdot 3H_2O$ — 1.78; NaCl — 0.41; NH_4NO_3 — 2.56; $MgSO_4 \cdot 7H_2O$ — 0.074; $ZnSO_4 \cdot 7H_2O$ — 0.0086; LA — 81.25.

To prepare 1000 cm^3 of the medium, 100 cm^3 of 80% LA (sold by *Paritrade* Russia; manufactured in China) were diluted with distilled water in a 1-dm^3 measuring flask without bringing the volume to the mark. Following the addition and dissolution of pre-weighed salts, the volume was brought to the mark with distilled water. The pH value of the model FB was 1.9.

The process was studied under dynamic conditions as follows. A cotton plug was placed on the bottom of a burette (ion exchange column) with a working volume of 25 cm^3. Next, the first burette was filled with 25 cm^3 of the prepared cation exchange resin, and the second one—with anion exchange resin. The resins were placed in a swollen state. The model FB was successively passed through columns having a bed height of 350 mm and a diameter of 10 mm using the descending flow method at a rate of 5 cm^3/min. The ion and LA content, as well as the solution pH, were monitored at the outlet of the anion-exchange column. The process diagram is shown in Fig. 1a.

The column regeneration modes were investigated after completing the experiments on purifying the model FB (Fig. 1b). Thus, 100 cm^3 of 2 *M* NaOH solution were passed through an anion-exchange column containing a resin with a volume of 25 cm^3. 100 cm^3 of 2 *M* H_2SO_4 solution were passed through a cation-exchange column with a resin volume of 25 cm^3. The flow rate was 5 cm^3/min. Three portions of 33 cm^3 were collected at the outlet of each column and analyzed. Then, distilled water was passed through the columns to determine the amount of water required to

[1] GOST 20301-74. State Standard of the USSR. Ion-exchange resins. Anionites. Specifications. Moscow: Izdatelstvo standartov; 1992. https://meganorm.ru/Data2/1/4294833/4294833041.pdf. Accessed June 06, 2025.

[2] GOST 10896-78. Interstate Standard. Ion-exchange resins. Preparation of specimens for test. Moscow: IPK Izdatelstvo standartov; 1999. https://meganorm.ru/Data2/1/4294840/4294840000.pdf. Accessed June 06, 2025.

wash the resins from the regeneration solution. Samples of 25 cm^3 were collected at the outlet of each column. A total of 20 column volumes of water were passed through each column. The samples were analyzed for alkalinity (using phenolphthalein) and for sulfate ions (using barium chloride); pH was also monitored.

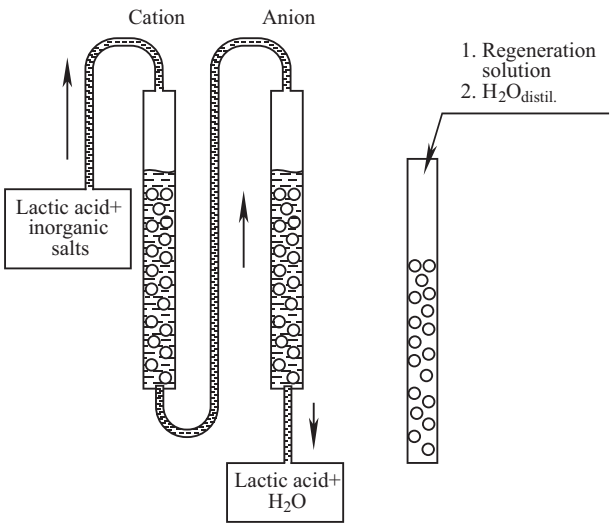

Fig. 1. (a) Scheme of ion-exchange purification of the model fermentation broth (FB) of *R. oryzae*; (b) scheme of regeneration of ion-exchange columns

The dynamic exchange capacity before breakthrough (DEC_{br}, mmol-eq/cm^3) was obtained according to the relationship presented in general form as:

$$DEC_{br} = \frac{\left(C_{init} - C_{res}\right) \cdot V_{FB}}{M_e \cdot V_{resin}}, \quad (1)$$

where C_{init} is the initial concentration of the impurity ion in the model FB, mg/dm^3; C_{res} is the residual concentration of the impurity ion at the outlet of the column, mg/dm^3; V_{FB} is the volume of the model solution that passed through the column before breakthrough, dm^3; V_{resin} is the volume of resin in the column, cm^3; M_e is the molar mass of the ion equivalent, g/mol-eq; ½Mg^{2+}, ½Zn^{2+}, NH_4^+, K^+, Na^+, Cl^-, NO_3^-, HPO_4^-, ½SO_4^{2-}.

The solutions collected for analysis were examined by the titrimetric method (precipitation titration) to determine the concentration of chlorides [RD 52.24.407-2017] (detection limit is 2 mg/dm^3) and by the qualitative reaction with Nessler reagent to determine the presence of ammonium ion. The concentration of LA was determined spectrophotometrically using iron(III) chloride [24]. The content of total nitrogen was determined by high-temperature catalytic combustion on a Formacs HT TOC/TN Analyzer (*Skalar*, Netherlands) (detection limit is 0.008 mg/dm^3).

The content of trace- and macroelements in the studied samples was determined using an iCAP 6300 Duo inductively coupled plasma (ICP) emission spectrometer (*Thermo Scientific*, United Kingdom). Samples for analysis were diluted 100-fold and acidified with hydrochloric acid (special purity grade, *Sigma Tek*, Khimki, Russia) in a ratio of 1/100. The device was calibrated using multi-element standards (ICP multi-element standard solution IV and IX, *Merck*, Germany; ICP multi-element standard solution VI, *Fluka*, Switzerland) and single-element standards P (CGP10) and Mg (CGMG10) (*Inorganic Ventures*, USA), as well as CaO and Na_2SO_4 (special purity grade). Scandium (5 mg/dm^3) (Scandium ICP standard, *Fluka*, Switzerland) was used as an internal standard. Deionized water (18 MOhm) was used to prepare calibration standards and dilute samples. Concentrated hydrochloric acid (1/100) was added to the standards. The detection limit (3×SD, mg/dm^3) was 0.003 for Ca (λ = 317.933), 0.03 for K (λ = 769.896), 0.03 for Mg (λ = 279.079), 0.03 for Na (λ = 589.592), 0.004 for P (λ = 213.618), 0.03 for S (λ = 182.034), and 0.4 for Zn (λ = 213.856), where SD is the standard deviation, and λ is the element detection wavelength, nm. A detailed description of the spectrometer characteristics is presented in [25].

The solutions pH measurements were carried out on a tabletop pH meter AQUASEARCHER™ AB41PH (*OHAUS*, China) with a resolution of 0.1 to 0.001.

RESULTS AND DISCUSSION

In this work, we studied the processes of purification of model FB using ion-exchange resins under dynamic conditions. Provided that neutralizing agents were not used, the composition of the model FB was close to the composition of the mineral medium for cultivating *R. oryzae*. Table 1 shows data on the composition of impurities in 8% LA from different manufacturers. LA purchased from *Paritrade*, Russia, was used to prepare the FB.

The adsorption capacity of ion-exchange resins with respect to impurity ions from a model FB was studied as follows. A model FB with a volume of 500 cm^3 was passed successively through a burette filled with a strongly acidic gel cationite KU-2-8 in the H-form, and then through a weakly basic gel anionite Purolite A847 in OH-form. The solution feed rate was 5 cm^3/min is concomitant with state-of-the art technological processes. Preliminary experiments showed that an increase in the flow rate decreases the breakthrough (appearance) time of ions, which increases the amount of impurities remaining in the solution after purification. At the outlet, the solution was collected for analysis in portions of 50 cm^3, which is double the volume from each ionite. Thus, the samples with the phase volume ratios V_{FB}/V_{resin} = 2, 4, 6, 8, 9, 10, 12, 14, 16, 18, and 20 were obtained.

Table 1. Elemental composition of 8% LA from various manufacturers

Type of solution	Concentration, mg/dm^3							
	Ca	K	Mg	Na	P	S	Zn	N
LA (*Paritrade*, Russia)	0.4	BDL[3]	0.1	7.9	1.1	4.7	0.1	13.7
LA (chemically pure, *NevaReaktiv*, Russia)	0.3	1.5	BDL	17.2	6.2	14.8	BDL	18.0
LA (*Panreac*, Spain)	0.1	BDL	BDL	0.5	BDL	7.2	0.0	0.7

To assess the sorption characteristics of the cation exchanger and anion exchanger, the degree of ion sorption was calculated from the V_{FB}/V_{resin} ratio (Figs. 2 and 3). It can be seen that most of the analyzed impurities are almost completely removed from the model FB with a volume of 500 cm^3 (V_{FB}/V_{resin} = 20; Figs. 2 and 3). Even in the last portion, their content did not exceed 11 mg/dm^3 (0.001%). The exception was sulfur (represented in the studied medium by sulfate ions). Even in the first fractions (V_{FB}/V_{resin} = 2–4), the sulfur content did not fall below 50 mg/dm^3 (sorption degree 80%, Fig. 3); in the subsequent ones, it even increased. This means that the efficiency of this type of anion exchanger in relation to sulfates is insufficient.

Since lactate ion is also capable of being sorbed on the anion exchanger, its concentration was monitored in each sample. According to the obtained results, following the passage of 50 cm^3 of FB, the LA concentration dropped sharply; subsequently in the sample V_{FB}/V_{resin} = 6, it was restored and its concentration further increased. This can be explained by the fact that the initial content of all anions in FB is much lower in relation to the anion exchanger capacity. As the concentration of strong acid anions increases, the weaker lactate ion passes into solution as a result of exchange for chlorides, nitrates, phosphates and sulfates.

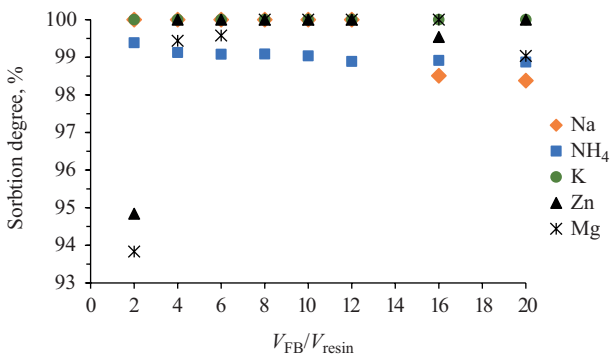

Fig. 2. Dynamics of sorption of impurity cations from a model FB by cation exchanger KU-2-8 (H)

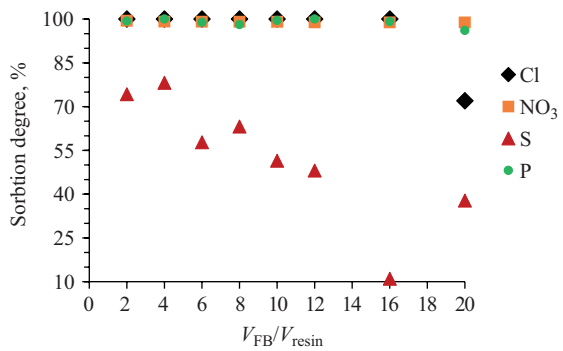

Fig. 3. Dynamics of sorption of impurity anions from a model FB by the anionite Purolite A847 (OH)

Additional qualitative analysis was performed using the Nessler method to determine ammonium ions. Since this method is sufficiently sensitive to determine microscopic amounts (up to 0.001% by volume) of ammonia, trace amounts of NH^{4+} ions were found in all samples. However, with a fairly high nitrogen concentration in the initial FB (i.e., NH^{4+} and NO^{3-} ions), its concentration in the obtained samples did not exceed 11 mg/L according to the ICP analysis data. This indicates the effectiveness of ion-exchange purification. Chloride ions begin to be detected only in the sample with a phase volume ratio of V_{FB}/V_{resin} = 20.

Next, we studied the effect of multiple passes of the model FB through ion-exchange resins on the degree of its purification. For this, we used the KU-2-8 and A847 ion exchange resins. The model FB with a volume of 250 cm^3 (a tenfold excess to the volume of each resin) was passed through the columns at a rate of 5 cm^3/min, and then returned to the original container. Fractions of 5 cm^3 were collected for analysis every hour. According to the analysis of the obtained samples (given in Table 2), most elements were almost completely removed with residual concentrations not exceeding 12 mg/dm^3. This is consistent with the data of the previous experiment for the sample V_{FB}/V_{resin} = 10.

[3] Here and below BDL means "below the detection limit."

As in the previous experiment, the sorption of sulfates was not complete, but only 50–60%. This may be due to both their very high initial concentration compared to most other elements and the insufficient specific affinity of the anion exchanger to sulfates. In addition, when carrying out purification by this method, LA losses of 6–20% are observed. Thus, multiple passing of the model FB through ion-exchange resins is ineffective and labor-intensive; since the sorption rate is quite fast, the purification was carried out in subsequent experiments by descending flow to pass the model FB once through the resins.

To assess the possibility of improving the sorption of sulfate ions, experiments were carried out using a combination of strongly basic and weakly basic gel-type anion exchangers with different ratios. AV-17-8 (OH) was chosen as the strongly basic anion exchanger. A previous study of the selectivity of the AV-17-8 anion exchanger with respect to the anions SO_4^{2-}, NO_3^-, and Cl^- [13] showed that the main factor influencing the selectivity of ion exchange is electroselectivity, i.e., the preferential sorption of ions with a higher charge—in our case, the sulfate ion. In the case of anions having the same charge, selectivity is determined by the radius of the ion and its hydration energy. It was shown in [13, 26] that increased ion size results in a decreased tendency to hydration. Therefore, a strongly basic anionite exhibits greater selectivity with respect to nitrate ions as compared to Cl ions.

In the next experiment, the first burette was filled with the KU-2-8 cation exchanger (25 cm^3), while the second was filled in turn with two types of anion exchangers such that the total volume was 25 cm^3. The ratio of the A847 and AV-17-8 anion exchangers was 50/50 or 75/25. The obtained results were compared with the data of the experiment in which only A847 was used. Samples obtained after passing 250 cm^3 (V_{FB}/V_{resin} = 10), 400 cm^3 (V_{FB}/V_{resin} = 16), 500 cm^3 (V_{FB}/V_{resin} = 20), and 600 cm^3 (V_{FB}/V_{resin} = 24) of the model FB were collected and analyzed.

It is evident from the obtained data presented in Table 3 that most elements were almost completely extracted from the solution (~100% sorption) after passing even a 24-fold excess of FB relative to the volume of each resin and that the residual concentrations ranged from 0 to 13 mg/cm^3. However, the sorption of phosphates deteriorated sharply after replacing part of the A847 anion exchanger with AV-17-8 and increasing the volume of the passed solution (experiments 2 and 3, Table 3). At the same time, the efficiency of sulfate removal increased to 94%. Thus, a 10-fold excess of the passed solution is sufficient for effective purification of the model FB. In this case, the concentration of lactate ions does not decrease. Since the lowest residual content of impurities was noted for the KU-2-8+A847/AV-17-8(50/50) system with the ratio V_{FB}/V_{resin} = 10, these parameters were used for further purification of the real solution.

Table 2. Ionic composition of samples after cyclic purification of model FB depending on time

Time, h	Concentration, mg/dm^3								
	LA, %	Ca	K	Mg	Na	P	S	Zn	N
0	8.4	1.4	586.2	15.4	190.7	261.7	224.7	3.3	942.2
1	6.6	0.4	BDL	0.1	2.6	1.9	125.6	BDL	11.7
2	7.5	0.3	BDL	BDL	2.3	4.1	117.1	BDL	8.1
4	7.9	2.8	0.1	0.1	0.8	12.5	78.6	BDL	7.7

Table 3. Ionic composition of samples depending on the ratio of phase volumes V_{FB}/V_{resin} and the type of anion exchange column

V_{FB}/V_{resin}	Concentration, mg/dm^3								
	LA, %	Ca	K	Mg	Na	P	S	N	Zn
FB	8.4	1.4	586.2	15.4	190.7	261.7	224.7	942.2	3.3
1. KU-2-8+A847(100)									
10	9.6	BDL	BDL	BDL	BDL	0.8	115.2	9.2	BDL

Table 3. Continued

V_{FB}/V_{resin}	Concentration, mg/dm^3								
	LA, %	Ca	K	Mg	Na	P	S	N	Zn
16	10.1	0.4	BDL	BDL	2.72	1.5	211.1	10.4	BDL
20	9.7	0.4	BDL	0.14	2.95	7.1	147.6	10.8	BDL
2. KU-2-8+A847/AB-17-8(50/50)									
10	9.4	BDL	BDL	0.01	1.84	3.2	13.2	9.8	BDL
16	9.2	1.6	BDL	0.04	0.20	67.6	47.9	11.0	BDL
20	8.9	0.2	BDL	0.07	1.10	126.4	11.1	11.3	BDL
24	8.9	BDL	BDL	0.07	BDL	231.3	121.8	13.0	BDL
30	8.9	BDL	BDL	BDL	6.1	544.7	11.5	29.1	BDL
3. KU-2-8+A847/AB-17-8(75/25)									
10	9.3	0.6	BDL	0.1	3.4	1.1	14.6	9.3	BDL
16	9.2	2.1	BDL	0.3	0.2	25.3	28.8	12.5	BDL
20	9.2	0.1	BDL	BDL	2.3	63.3	12.6	10.1	BDL
24	9.5	0.1	BDL	BDL	1.9	186.4	111.2	12.8	BDL

Since the cationite did not reach full adsorption capacity, the model FB was continued to be passed through the KU-2-8+A847/AV-17-8(50/50) system. According to the ICP analysis, in the sample V_{FB}/V_{resin} = 30, the concentration of only Na cations increased to 6 mg/L (Table 3, experiment 2). This will be considered as the threshold concentration (before breakthrough). This assumption does not contradict the data on the sodium ion content in industrial LA samples, whose amount varies from 0.52 to 17.2 (Table 1). Since the qualitative reaction to the ammonium ion was negative, the increase in the nitrogen amount to 29.14 (Table 3, experiment 2) is probably due to the saturation of anionite with nitrate ions and their release into the solution.

Thus, under these conditions, in the case of using KU-2-8 in the H-form, effective purification from impurity cations is possible for a model FB that is 30 times larger than the volume of the cation exchanger.

Ion-exchange purification processes are impossible without effective regeneration of the resins used. As a result of contact with a model FB containing impurities, anion-exchange resins saturated with counterions extracted from the solution are deactivated to lose their original adsorption characteristics. However, it is possible to remove sorbed ions and restore the activity of the resin layer with the help of the regeneration process. Regeneration can be carried out repeatedly with little or no loss of capacity.

Next, we regenerated the column with KU-2-8 (25 cm^3) and the anion exchange column filled with a mixture of anion exchangers AV-17-8 (~12.5 cm^3) and A847 (~12.5 cm^3) (the anion exchangers were taken in a 50/50 ratio) after an experiment, in which 750 cm^3 of model FB passed through these resins. The columns were regenerated in two stages using the technique described in the experimental section. First, a three- to four-fold excess of the regenerate solution (eluent) was passed through the cation exchanger (anion exchanger). Next, repeatedly distilled water was passed in order to remove the regeneration products and excess regeneration solution from the ion exchanger layer.

As can be seen from Tables 4 and 5, the concentration of elements in the first portion of eluates is the highest, i.e., extraction (desorption) is effective. In subsequent samples, the concentration drops sharply; therefore, the amount of eluent can be reduced to a two- to three-fold excess relative to the resin volume. From Table 4 it is clear that the solution pH is quite high with a 5- to 15-fold excess of distilled water, decreasing to 7 only after passing

Table 4. Content of elements after regeneration of anion exchange column

Stages of filtration	Concentration, mg/dm^3								pH
	Ca	K	Mg	Na	P	S	N	Zn	
Eluate, portion 1	0.5	44.4	BDL	30880.0	463.3	2383.6	6835.5	BDL	14.8
Eluate, portion 2	5.0	51.6	BDL	38844.6	41.4	143.1	3296	0.1	14.7
Eluate, portion 3	4.0	69.1	1.1	39783.9	42.6	138.4	1266	0.1	14.4
5× H_2O	–	–	–	–	–	–	–	–	14.2
10× H_2O	–	–	–	–	–	–	–	–	12.3
15× H_2O	0.3	9.8	BDL	15.9	1.33	9.6	1.1	0.1	10.0
20× H_2O	0.2	2.7	BDL	1.6	BDL	BDL	0.4	BDL	7.2

Table 5. Content of elements after regeneration of cation exchange column

Stages of filtration	Concentration, mg/dm^3							pH
	K	Mg	Na	P	S	N	Zn	
Eluate, portion 1	11666.0	175.4	3881.4	29.5	41480.0	10760.0	41.4	2.1
Eluate, portion 2	3283.5	111.9	538.9	3.9	57953.8	1607.0	27.7	2.1
Eluate, portion 3	769.5	60.5	101.5	0.8	49813.2	151.1	15.7	2.1
5× H_2O	17.6	0.1	2.7	BDL	53.4	2.7	BDL	3.7
10× H_2O	3.4	0.1	1.2	BDL	BDL	0.7	0.1	5.8
15× H_2O	4.5	BDL	1.1	BDL	BDL	0.7	BDL	6.8

a 20-fold excess of water through the column. The solution contained virtually no impurities, i.e., regeneration was effective. In the case of a cation-exchange column, a sharp decrease in sulfate ions is observed already after a 5-fold excess of distilled water (Table 5). After a 10-fold excess of water, the test solution basically does not contain ions, and its pH increases to 5.8. Thus, under these conditions, a 10-fold excess of distilled water is sufficient.

The factors affecting the useful exchange capacity of resins include:

- the type of ions removed from the aqueous solution;
- the ratio of salt components in the aqueous solution;
- the pH value;
- the height of the layer;
- the flow rate of the filtered water;
- the intensity of operation.

In practice, the ion-exchange capacity of resins is determined by the degree of their saturation. This is due to the fact that, at a certain stage, the number of breakthroughs reaches the maximum permissible level, at which the quality of purification is significantly reduced. The formula for calculating the sorption capacity is given in the experimental section.

Table 6 shows the calculated values of the dynamic exchange capacity of ion-exchange resins for each impurity element contained in the model FB before

Table 6. Dynamic exchange capacity before the breakthrough (DEC_{br}) of cation exchange and anion exchange columns

FB components	$C_{initial}$, mg/dm^3	C_{res}, mg/dm^3	DEC_{br}, mmol-eq/cm^3
K	586.21	0	0.45
Mg	15.43	0	0.04
Na	190.84	6	0.24
Zn	3.39	0	0.01
S	224.71	13.2	0.13
P	261.82	3.2	0.08
Cl	250.03	0	0.07
N (NH_4^+)	522.41	0	0.87
N (NO_3^-)	420.75	9.2	0.07
∑anions	–		0.35
∑cations			1.61

breakthrough. They were obtained based on the results of the best experiment for the anion-exchange column (Table 3, experiment 2). The ratio for the cation-exchange column V_{FB}/V_{resin} = 30, for the anion-exchange V_{FB}/V_{resin} = 10. In this work, the breakthrough value was taken to be a residual concentration of the impurity element of no more than 14 mg/L. Thus, DEC_{br} for the anion exchange column was 0.35 mmol-eq/cm^3, and for the cation exchange column, DEC_{br} was 1.61 mmol-eq/cm^3. The DEC_{br} value depends on the concentration and nature of the sorbed ions and cations, as well as on the pH of the medium, the solution filtration rate, the size of the ion exchanger grains, the ratio of the ion exchanger layer height to its width, and other factors. As a rule, its value is significantly lower than the static exchange capacity.

CONCLUSIONS

The conducted studies demonstrate that purification of the model FB of *R. oryzae* can be successfully implemented using ion-exchange resins. The model FB passed successively through cation-exchange and anion-exchange columns was shown to be purified from mineral salt impurities while maintaining the concentration of LA. In the work, a strongly acidic gel cation exchanger KU-2-8 in the H-form was used as a cation absorber. For the sorption of anions, it is necessary to use a mixture of weakly basic gel A847 anion exchanger and strongly basic gel AV-17-8 anion exchanger in the OH-form taken in a ratio of 1/1. It is shown that the breakthrough of impurity ions into the solution occurs after passing a 30-fold and 10-fold volume of the model FB relative to the volume of the cation-exchange and anion-exchange resins, respectively. For the resins used in the work, the dynamic exchange capacity before breakthrough was determined to be 0.35 mmol-eq/cm^3 for the anion-exchange column and 1.61 mmol-eq/cm^3 for the cation-exchange column.

According to the ion-exchange column regeneration parameters established in this work, the regenerate solution (eluent) must be used in an amount of two to three times excess relative to the resin volume. Then, in order to remove the regeneration products and excess regeneration solution, a 20-fold excess of distilled water must be passed through the anion-exchange column, while a 10-fold excess of distilled water is sufficient to pass through the cation-exchange column.

It is worth noting that the model medium used in the work was not subjected to preliminary nanofiltration

purification, i.e., the salt content corresponded to the original FB. Under conditions of additional nanofiltration purification, a significant increase in the productivity of ion-exchange resins can be expected, depending on the efficiency of the implemented nanofiltration process. The relevance of the work consists in the possibility of using the obtained experimental data in the development of technology for the production and purification of LA.

Acknowledgments

The research was supported by the Krasnoyarsk Regional Science Foundation and the *JSC Sibagro Biotech* partner enterprise, application No. 2023090409806.

Authors' contributions

E.V. Pikurova—methodology development, conducting experiments, analysis of literary sources, writing and editing the text of the article.

A.N. Boyandin—methodology development, conducting experiments, analysis of literary sources, writing and editing the text of the article.

D.R. Serebryakov—conducting experiments, analysis of literary sources.

N.L. Ertiletskaya—conducting experiments, analysis of literary sources.

O.V. Anishchenko—conducting experiments, determination of research objects, provision of equipment, processing experimental data, and consultation on the instrument base.

A.A. Sukhanova—scientific consulting, discussion of the results, editing the article.

The authors declare no conflict of interest.

REFERENCES

1. Din N.A.S., Lim S.J., Maskat M.Y., *et al.* Lactic acid separation and recovery from fermentation broth by ion-exchange resin: A review. *Bioresour. Bioprocess.* 2021;8(1):31. https://doi.org/10.1186/s40643-021-00384-4
2. Wee Y.J., Kim J.N., Ryu H.W. Biotechnological production of lactic acid and its recent applications. *Food Technol. Biotechnol*. 2006;44(2):163–173.
3. Li C., Gao M., Zhu W., *et al.* Recent advances in the separation and purification of lactic acid from fermentation broth. *Process Biochem.* 2021;104:142–151. https://doi.org/10.1016/j.procbio.2021.03.011
4. Ehsani M., Khodabakhshi K., Asgari M. Lactide synthesis optimization: investigation of the temperature, catalyst and pressure effects. *e-Polymers*. 2014;14(5):353–361. https://doi.org/10.1515/epoly-2014-0055
5. Bahati D., Bricha M., Semlali A., El Mabrouk K. Preparation and characterization of poly (lactic acid)-chitosan blend fibrous electrospun membrane loaded with bioactive glass nanoparticles for guided bone/tissue regeneration. *Mater. Chem. Phys.* 2024;323:129637. https://doi.org/10.1016/j.matchemphys.2024.129637
6. Nair L.S., Laurencin C.T. Biodegradable polymers as biomaterials. *Prog. Polym. Sci.* 2007;32(8–9):762–798. https://doi.org/10.1016/j.progpolymsci.2007.05.017
7. Auras R., Harte B., Selke S. An Overview of Polylactides as Packaging Materials. *Macromol. Biosci.* 2004;4(9):835–864. https://doi.org/10.1002/mabi.200400043
8. Jin B., Huang L.P., Lant P. *Rhizopus arrhizus* – a producer for simultaneous saccharification and fermentation of starch waste materials to L-(+)-lactic acid. *Biotechnol. Lett*. 2003;25:1983–1987. https://doi.org/10.1023/B:BILE.0000004389.53388.d0
9. Nyanikova G.G., Minina A., Belyaeva A.D. Influence of substratum composition on growth of fungus *Rhizopus oryzae*. *Izvestiya Sankt Peterburgskogo gosudarstvennogo tekhnologicheskogo instituta* (*tekhnicheskogo universiteta*) = *Bulletin of the St. Petersburg State Institute of Technology* (*Technical University*). 2018;45(71):82–86 (in Russ.).
10. Lee H.D., Lee M.Y., Hwang Y.S., *et al.* Separation and Purification of Lactic Acid from Fermentation Broth Using Membrane-Integrated Separation Processes. *Ind. Eng. Chem. Res.* 2017;56(29):8301–8310. https://doi.org/10.1021/acs.iecr.7b02011

СПИСОК ЛИТЕРАТУРЫ

1. Din N.A.S., Lim S.J., Maskat M.Y., *et al.* Lactic acid separation and recovery from fermentation broth by ion-exchange resin: A review. *Bioresour. Bioprocess.* 2021;8(1):31. https://doi.org/10.1186/s40643-021-00384-4
2. Wee Y.J., Kim J.N., Ryu H.W. Biotechnological production of lactic acid and its recent applications. *Food Technol. Biotechnol*. 2006;44(2):163–173.
3. Li C., Gao M., Zhu W., *et al.* Recent advances in the separation and purification of lactic acid from fermentation broth. *Process Biochem.* 2021;104:142–151. https://doi.org/10.1016/j.procbio.2021.03.011
4. Ehsani M., Khodabakhshi K., Asgari M. Lactide synthesis optimization: investigation of the temperature, catalyst and pressure effects. *e-Polymers*. 2014;14(5):353–361. https://doi.org/10.1515/epoly-2014-0055
5. Bahati D., Bricha M., Semlali A., El Mabrouk K. Preparation and characterization of poly (lactic acid)-chitosan blend fibrous electrospun membrane loaded with bioactive glass nanoparticles for guided bone/tissue regeneration. *Mater. Chem. Phys.* 2024;323:129637. https://doi.org/10.1016/j.matchemphys.2024.129637
6. Nair L.S., Laurencin C.T. Biodegradable polymers as biomaterials. *Prog. Polym. Sci.* 2007;32(8–9):762–798. https://doi.org/10.1016/j.progpolymsci.2007.05.017
7. Auras R., Harte B., Selke S. An Overview of Polylactides as Packaging Materials. *Macromol. Biosci.* 2004;4(9):835–864. https://doi.org/10.1002/mabi.200400043
8. Jin B., Huang L.P., Lant P. *Rhizopus arrhizus* – a producer for simultaneous saccharification and fermentation of starch waste materials to L-(+)-lactic acid. *Biotechnol. Lett*. 2003;25:1983–1987. https://doi.org/10.1023/B:BILE.0000004389.53388.d0
9. Няникова Г.Г., Минина А., Беляева А.Д. Влияние состава питательной среды на рост гриба *Rhizopus oryzae*. *Известия СПбГТИ* (*ТУ*). 2018;45(71):82–86.
10. Lee H.D., Lee M.Y., Hwang Y.S., *et al.* Separation and Purification of Lactic Acid from Fermentation Broth Using Membrane-Integrated Separation Processes. *Ind. Eng. Chem. Res.* 2017;56(29):8301–8310. https://doi.org/10.1021/acs.iecr.7b02011
11. Soto M.L., Moure A., Domínguez H., Parajó J.K. Recovery, concentration and purification of phenolic compounds by adsorption: A review. *J. Food Eng.* 2011;105(1):1–27. http://doi.org/10.1016/j.jfoodeng.2011.02.010

11. Soto M.L., Moure A., Domínguez H., Parajó J.K. Recovery, concentration and purification of phenolic compounds by adsorption: A review. *J. Food Eng.* 2011;105(1):1–27. http://doi.org/10.1016/j.jfoodeng.2011.02.010
12. Selitskii G.A., Galkin Yu.A. Purification of wastewater from heavy metal ions by sodium cation exchange. *Metallurgiya i mashinostroenie*. 2008;11(2):5–7 (in Russ.).
13. Saikova C.V., Pashkov G.L., Panteleeva M.V. *Reaktsionno-ionoobmennye protsessy izvlecheniya tsvetnykh metallov i sinteza dispersnykh materialov* (*Reaction-Ion-Exchange Processes of Non-Ferrous Metals Extraction and Synthesis of Dispersed Materials*). Krasnoyarsk; 2018. 198 p. (in Russ.). ISBN 978-5-7638-3856-5
14. Di N.F., Lancia A. Recovery of Tungstate from Aqueous Solutions by Ion Exchange. *Ind. Eng. Chem. Res.* 2007;46(21):6777–6782. https://doi.org/10.1021/ie061691w
15. Kabay N., Demircioğlu M., Yayli S. Günay E., Yüksel M., Sağlam M., Streat M. Recovery of Uranium from Phosphoric Acid Solutions Using Chelating Ion-Exchange Resins. *Ind. Eng. Chem. Res.* 1998;37(5):1983–1990. https://doi.org/10.1021/ie970518k
16. Elabd A.A., Zidan W.I., Abo-Aly M.M., *et al.* Uranyl ions adsorption by novel metal hydroxides loaded Amberlite IR120. *J. Environ. Radioact.* 2014;134:99–108. https://doi.org/10.1016/j.jenvrad.2014.02.008
17. Lebedev K.B. (Ed.). *Ionity v tsvetnoi metallurgii* (*Ionites in Non-Ferrous Metallurgy*). Moscow: Metallurgiya; 1975. 352 p. (in Russ.).
18. Vulikh A.I. *Ionoobmennyi sintez* (*Ion-Exchange Synthesis*). Moscow: Khimiya; 1973. 231 p. (in Russ.).
19. Zhang Y., Qian Z., Liu P., Liu L., Zheng Z., Ouyang J. Efficient *in situ* separation and production of L-lactic acid by *Bacillus coagulans* using weak basic anion-exchange resin. *Bioprocess Biosyst. Eng*. 2018;41(2):205–212. https://doi.org/10.1007/s00449-017-1858-z
20. Rampai T., Thitiprasert S., Boonkong W., Kodama K., Tolieng V., Thongchul N. Improved lactic acid productivity by simultaneous recovery during fermentation using resin exchanger. *Asia-Pacific J. Sci. Technol.* 2016;21(2):193–199. https://doi.org/10.14456/kkurj.2016.11
21. Pradhan N., Rene E., Lens P., Dipasquale L., D'Ippolito G., Fontana A., Panico A. Adsorption behaviour of lactic acid on granular activated carbon and anionic resins: thermodynamics, isotherms and kinetic studies. *Energies*. 2017;10(5):665. https://doi.org/10.3390/en10050665
22. Boonmee M., Cotano O., Amnuaypanich S., Grisadanurak N. Improved lactic acid production by *in situ* removal of lactic acid during fermentation and a proposed scheme for its recovery. *Arab. J. Sci. Eng.* 2016;41(6):2067–2075. https://doi.org/10.1007/s13369-015-1824-5
23. González M.I., Álvarez S., Riera F.A., *et al.* Purification of Lactic Acid from Fermentation Broths by Ion-Exchange Resins. *Ind. Eng. Chem. Res*. 2006;45(9):3243–3247. https://doi.org/10.1021/ie051263a
24. Borshchevskaya L.N., Gordeeva T.L., Kalinina A.N., *et al*. Spectrophotometric determination of lactic acid. *J. Anal. Chem*. 2016;71(8):755–758. https://doi.org/10.1134/S1061934816080037
[Original Russian Text: Borshchevskaya L.N., Gordeeva T.L., Kalinina A.N., Sineokii S.P. Spectrophotometric determination of lactic acid. *Zhurnal Analiticheskoi Khimii*. 2016;71(8):787–790 (in Russ.). https://doi.org/10.7868/S004445021608003X]

12. Селицкий Г.А., Галкин Ю.А. Очистка сточных вод от ионов тяжелых металлов методом натрий-катионирования. *Металлургия и машиностроение*. 2008;11(2):5–7.
13. Сайкова С.В., Пашков Г.Л., Пантелеева М.В. *Реакционно-ионообменные процессы извлечения цветных металлов и синтеза дисперсных материалов*. Красноярск: Сиб. федер. ун-т; 2018. 198 с. ISBN 978-5-7638-3856-5
14. Di N.F., Lancia A. Recovery of Tungstate from Aqueous Solutions by Ion Exchange. *Ind. Eng. Chem. Res.* 2007;46(21):6777–6782. https://doi.org/10.1021/ie061691w
15. Kabay N., Demircioğlu M., Yayli S. Günay E., Yüksel M., Sağlam M., Streat M. Recovery of Uranium from Phosphoric Acid Solutions Using Chelating Ion-Exchange Resins. *Ind. Eng. Chem. Res.* 1998;37(5):1983–1990. https://doi.org/10.1021/ie970518k
16. Elabd A.A., Zidan W.I., Abo-Aly M.M., *et al.* Uranyl ions adsorption by novel metal hydroxides loaded Amberlite IR120. *J. Environ. Radioact.* 2014;134:99–108. https://doi.org/10.1016/j.jenvrad.2014.02.008
17. *Иониты в цветной металлургии*; под ред. К.Б. Лебедева. М.: Металлургия; 1975. 352 с.
18. Вулих А.И. *Ионообменный синтез*. М.: Химия; 1973. 231 с.
19. Zhang Y., Qian Z., Liu P., Liu L., Zheng Z., Ouyang J. Efficient *in situ* separation and production of L-lactic acid by *Bacillus coagulans* using weak basic anion-exchange resin. *Bioprocess Biosyst. Eng*. 2018;41(2):205–212. https://doi.org/10.1007/s00449-017-1858-z
20. Rampai T., Thitiprasert S., Boonkong W., Kodama K., Tolieng V., Thongchul N. Improved lactic acid productivity by simultaneous recovery during fermentation using resin exchanger. *Asia-Pacific J. Sci. Technol.* 2016;21(2):193–199. https://doi.org/10.14456/kkurj.2016.11
21. Pradhan N., Rene E., Lens P., Dipasquale L., D'Ippolito G., Fontana A., Panico A. Adsorption behaviour of lactic acid on granular activated carbon and anionic resins: thermodynamics, isotherms and kinetic studies. *Energies*. 2017;10(5):665. https://doi.org/10.3390/en10050665
22. Boonmee M., Cotano O., Amnuaypanich S., Grisadanurak N. Improved lactic acid production by *in situ* removal of lactic acid during fermentation and a proposed scheme for its recovery. *Arab. J. Sci. Eng.* 2016;41(6):2067–2075. https://doi.org/10.1007/s13369-015-1824-5
23. González M.I., Álvarez S., Riera F.A., *et al.* Purification of Lactic Acid from Fermentation Broths by Ion-Exchange Resins. *Ind. Eng. Chem. Res*. 2006;45(9):3243–3247. https://doi.org/10.1021/ie051263a
24. Борщевская Л.Н., Гордеева Т.Л., Калинина А.Н., Синеокий С.П. Спектрофотометрическое определение молочной кислоты. *Журн. анал. химии.* 2016;71(8):787–790. https://doi.org/10.7868/S004445021608003X
25. Anishchenko O.V., Tolomeev A.P., Ivanova E.A., Drobotov A.V., Kolmakova A.A., Zuev I.V., Gribovskaya I.V. Accumulation of elements by submerged (*Stuckenia pectinate* (L.) Börner) and emergent (*Phragmites australis* (Cav.) Trin. ex Steud.) macrophytes under different salinity levels. *Plant Physiol. Biochem*. 2020;154:328–340. https://doi.org/10.1016/j.plaphy.2020.05.019
26. Кокотов Ю.А. *Иониты и ионный обмен*. Л.: Химия; 1980. 150 с.

25. Anishchenko O.V., Tolomeev A.P., Ivanova E.A., Drobotov A.V., Kolmakova A.A., Zuev I.V., Gribovskaya I.V. Accumulation of elements by submerged (*Stuckenia pectinate* (L.) Börner) and emergent (*Phragmites australis* (Cav.) Trin. ex Steud.) macrophytes under different salinity levels. *Plant Physiol. Biochem*. 2020;154:328–340. https://doi.org/10.1016/j.plaphy.2020.05.019
26. Kokotov Yu.A. *Ionity i ionnyi obmen* (*Ionites and Ion Exchange*). Leningrad: Khimiya; 1980. 150 p. (in Russ.).

About the Authors

Elena V. Pikurova, Cand. Sci. (Chem.), Researcher, Laboratory of High-Molecular Compounds, Reshetnev Siberian State University of Science and Technology (31, pr. Imeni Gazety Krasnoyarskii Rabochii, Krasnoyarsk, 660037, Russia). E-mail: vitaelen@gmail.ru. Scopus Author ID 56016899300, ResearcherID D-5117-2014, RSCI SPIN-code 7570-9876, https://orcid.org/0000-0001-7558-6358

Anatoly N. Boyandin, Cand. Sci. (Biol.), Senior Researcher, Laboratory of High-Molecular Compounds, Reshetnev Siberian State University of Science and Technology (31, pr. Imeni Gazety Krasnoyarskii Rabochii, Krasnoyarsk, 660037, Russia). E-mail: boyandin@biopolymer.pro. Scopus Author ID 6507584996, ResearcherID H-1641-2016, RSCI SPIN-code 7990-1174, https://orcid.org/0000-0002-9190-2792

Dmitry R. Serebryakov, Postgraduate Student, Engineer, Laboratory of High-Molecular Compounds, Reshetnev Siberian State University of Science and Technology (31, pr. Imeni Gazety Krasnoyarskii Rabochii, Krasnoyarsk, 660037, Russia). E-mail: di-plo-doc@yandex.ru. RSCI SPIN-code 2770-0929, https://orcid.org/0009-0007-8619-238X

Natalya L. Ertiletskaya, Postgraduate Student, Junior Researcher, Laboratory of High-Molecular Compounds, Reshetnev Siberian State University of Science and Technology (31, pr. Imeni Gazety Krasnoyarskii Rabochii, Krasnoyarsk, 660037, Russia). E-mail: natalya.ertiletskaya@gmail.com. Scopus Author ID 57781636600, RSCI SPIN code 1735-2461, https://orcid.org/0000-0003-2626-893X

Olesya V. Anishchenko, Cand. Sci. (Biol.), Head of the Analytical Laboratory, Institute of Biophysics of the Siberian Branch at the Russian Academy of Sciences (50, Akademgorodok, Krasnoyarsk, 660036, Russia). E-mail: hydrakr@rambler.ru. Scopus Author ID 6507556442, RSCI SPIN-code 5213-7769, https://orcid.org/0000-0002-1976-599X

Anna A. Sukhanova, Cand. Sci. (Biol.), Senior Researcher, Laboratory of High-Molecular Compounds, Reshetnev Siberian State University of Science and Technology (31, pr. Imeni Gazety Krasnoyarskii Rabochii, Krasnoyarsk, 660037, Russia). E-mail: shumilova.ann@mail.ru. Scopus Author ID 57292697300, RSCI SPIN-code 8540-6543, https://orcid.org/0000-0002-5830-1450

Об авторах

Пикурова Елена Витальевна, к.х.н., научный сотрудник, лаборатория «Высокомолекулярные соединения», Сибирский государственный университет науки и технологий имени академика М.Ф. Решетнёва (СибГУ имени академика М.Ф. Решетнёва) (660013, Россия, Красноярск, пр-т имени газеты Красноярский Рабочий, д. 31). E-mail: vitaelen@gmail.ru. Scopus Author ID 56016899300, ResearcherID D-5117-2014, SPIN-код РИНЦ 7570-9876, https://orcid.org/0000-0001-7558-6358

Бояндин Анатолий Николаевич, к.б.н., старший научный сотрудник, лаборатория «Высокомолекулярные соединения», Сибирский государственный университет науки и технологий имени академика М.Ф. Решетнёва (СибГУ имени академика М.Ф. Решетнёва) (660013, Россия, Красноярск, пр-т имени газеты Красноярский Рабочий, д. 31). E-mail: boyandin@biopolymer.pro. Scopus Author ID 6507584996, ResearcherID H-1641-2016, SPIN-код РИНЦ 7990-1174, https://orcid.org/0000-0002-9190-2792

Серебряков Дмитрий Русланович, аспирант, инженер, лаборатория «Высокомолекулярные соединения», Сибирский государственный университет науки и технологий имени академика М.Ф. Решетнёва (СибГУ имени академика М.Ф. Решетнёва) (660013, Россия, Красноярск, пр-т имени газеты Красноярский Рабочий, д. 31). E-mail: di-plo-doc@yandex.ru. SPIN-код РИНЦ 2770-0929, https://orcid.org/0009-0007-8619-238X

Ертилецкая Наталья Леонидовна, аспирант, младший научный сотрудник, лаборатория «Высокомолекулярные соединения», Сибирский государственный университет науки и технологий имени академика М.Ф. Решетнёва (СибГУ имени академика М.Ф. Решетнёва) (660013, Россия, Красноярск, пр-т имени газеты Красноярский Рабочий, д. 31). E-mail: natalya.ertiletskaya@gmail.com. Scopus Author ID 57781636600, SPIN-код РИНЦ 1735-2461, https://orcid.org/0000-0003-2626-893X

Анищенко (Барсукова) Олеся Валерьевна, к.б.н., заведующий аналитической лабораторией, Институт биофизики Сибирского отделения Российской академии наук (660036, Россия, Красноярск, Академгородок, 50). E-mail: hydrakr@rambler.ru. Scopus Author ID 6507556442, SPIN-код РИНЦ 5213-7769, https://orcid.org/0000-0002-1976-599X

Суханова Анна Алексеевна, к.б.н., старший научный сотрудник, лаборатория «Высокомолекулярные соединения», Сибирский государственный университет науки и технологий имени академика М.Ф. Решетнёва (СибГУ имени академика М.Ф. Решетнёва) (660013, Россия, Красноярск, пр-т имени газеты Красноярский Рабочий, д. 31). E-mail: shumilova.ann@mail.ru. Scopus Author ID 57292697300, SPIN-код РИНЦ 8540-6543, https://orcid.org/0000-0002-5830-1450

Translated from Russian into English by M. Povorin
Edited for English language and spelling by Thomas A. Beavitt

Tonkie Khimicheskie Tekhnologii = Fine Chemical Technologies.
2025;20(3):237–252
ISSN 2686-7575 (Online)

Synthesis and processing of polymers and polymeric composites
Синтез и переработка полимеров и композитов на их основе

UDC 661.17
https://doi.org/10.32362/2410-6593-2025-20-3-237-252
EDN JPYWRA

RESEARCH ARTICLE

The effect of ureas and their sulfur- and selenium-containing analogs on the vulcanization and thermo-oxidative resistance of elastomers based on nitrile butadiene rubber

Eugene S. Bochkarev, Daria M. Zapravdina, Yaroslav P. Kuznetsov, Iurii M. Mkrtchian, Vladimir V. Burmistrov ✉, Marat A. Vaniev

Volgograd State Technical University, Volgograd, 400005 Russia

✉ *Corresponding author, e-mail: w_tovn@mail.ru, vburmistrov@vstu.ru*

Abstract

Objectives. The study set out to investigate the effect of ureas and their sulfur- and selenium-containing analogs on the vulcanization of elastomeric materials based on nitrile butadiene rubber and their resistance to thermo-oxidative aging.

Methods. The properties of the molecules of ureas under study were calculated by the MM+ quantum chemical method of molecular mechanics and PM3 semiempirical method using the HyperChem 8.0 software. Vulcanization of rubbers and total crosslink density were studied using the rotorless vulcanization method with a MonTech MDR 3000 Professional rheometer. The dynamic characteristics of vulcanized rubbers were investigated in accordance with ASTM D6601-02 and D5992-96 standards. The efficiency of the studied antioxidants against thermo-oxidative aging was evaluated in accordance with GOST 9.024-74. Infrared (IR) spectra of samples were recorded with an FT-801 Fourier-transform IR spectrometer (Russia) according to the attenuated total reflection method.

Results. For the first time, a study was conducted on the efficiency of 1-(3-chlorophenyl)-3-phenylurea, 1-(3-chlorophenyl)-3-phenylthiourea, and 1-(3-fluorophenyl)-3-phenylselenourea as antioxidants for elastomers under conditions of thermo-oxidative aging. The effect of these substances on the vulcanization characteristics and total crosslink density of materials based on nitrile butadiene rubber was investigated.

Conclusions. The values of electron affinity energy and its sign were shown to accurately predict the possibility of using individual molecules as accelerators of the vulcanization process or antioxidants. With a change in the electron affinity energy from 0.051 (urea) to −1.115 (thiourea) and −1.365 eV (selenourea), the time to the start of vulcanization was shown to change from 15 to 3 and 2 min, respectively. As a result of thermo-oxidative aging of rubbers based on BNKS-28 AN rubber without a stabilizer and with 1-(3-chlorophenyl)-3-phenylurea, 1-(3-chlorophenyl)-3-phenylthiourea, and 1-(3-fluorophenyl)-3-phenylselenourea, the total crosslink density changes by 33%, 23%, 25%, and 29%, respectively. In this connection, the use of 1-(3-chlorophenyl)-3-phenylurea somewhat improves the stability of rubbers to thermo-oxidative aging, whereas 1-(3-chlorophenyl)-3-phenylthiourea and 1-(3-fluorophenyl)-3-phenylselenourea do not worsen this property when introduced into the rubber compound.

Keywords

elastomers, urea, thiourea, selenourea, nitrile butadiene rubber, vulcanization, thermo-oxidative resistance

Submitted: 21.10.2024
Revised: 16.12.2024
Accepted: 08.04.2025

For citation

Bochkarev E.S., Zapravdina D.M., Kuznetsov Ya.P., Mkrtchian I.M., Burmistrov V.V., Vaniev M.A. The effect of ureas and their sulfur- and selenium-containing analogs on the vulcanization and thermo-oxidative resistance of elastomers based on nitrile butadiene rubber. *Tonk. Khim. Tekhnol. = Fine Chem. Technol*. 2025;20(3):237–252. https://doi.org/10.32362/2410-6593-2025-20-3-237-252

НАУЧНАЯ СТАТЬЯ

Исследование влияния мочевин и их серо- и селенсодержащих аналогов на вулканизацию и термоокислительную стойкость эластомеров на основе бутадиен-нитрильного каучука

Е.С. Бочкарёв, Д.М. Заправдина, Я.П. Кузнецов, Ю.М. Мкртчян, В.В. Бурмистров ✉, М.А. Ваниев

Волгоградский государственный технический университет, Волгоград, 400005 Россия

✉ *Автор для переписки, e-mail: w_tovn@mail.ru, vburmistrov@vstu.ru*

Аннотация

Цели. Исследование влияния мочевин и их серо- и селенсодержащих аналогов на вулканизацию эластомерных материалов на основе бутадиен-нитрильного каучука и на их стойкость термоокислительному старению.

Методы. Квантово-химическими методами молекулярной механики ММ+ и с помощью полуэмпирического метода PM3 проведен расчет исследуемых молекул мочевины и ее аналогов в программном комплексе HyperChem 8.0. Вулканизацию резин и оценку общей плотности сшивки изучали методом безроторной вулканометрии на реометре MonTech MDR 3000 Professional. Исследование динамических характеристик вулканизованных резин проводили в соответствии с ASTM D6601-02 и D5992-96. Эффективность исследуемых противостарителей к термоокислительному старению проводили по ГОСТ 9.024-74. Инфракрасные (ИК) спектры образцов получены на ИК-Фурье спектрометре ФТ-801 (Россия) методом нарушенного полного внутреннего отражения.

Результаты. Впервые проведено исследование эффективности действия 1-(3-хлорфенил)-3-фенил мочевины, 1-(3-хлорфенил)-3-фенил тиомочевины и 1-(3-фторфенил)-3-фенил селеномочевины в качестве антиоксидантов для эластомеров в условиях термоокислительного старения. Изучено влияние указанных соединений на вулканизационные характеристики и общую плотность сшивки материалов на основе бутадиен-нитрильного каучука.

Выводы. Установлено, что значения энергии сродства к электрону и ее знак позволяют прогнозировать возможность использования отдельных молекул в качестве ускорителей процесса вулканизации или антиоксидантов. Показано, что при изменении энергии сродства к электрону от 0.051 (мочевина) до −1.115 (тиомочевина) и −1.365 эВ (селеномочевина) время до начала вулканизации изменяется от 15 до 3 и 2 мин соответственно. В результате термоокислительного старения резин на основе каучука БНКС-28 АН без стабилизатора с 1-(3-хлорфенил)-3-фенил мочевиной, 1-(3-хлорфенил)-3-фенил тиомочевиной и 1-(3-фторфенил)-3-фенил селеномочевиной значение общей плотности сшивки изменяется в ряду 33%, 23%, 25% и 29% соответственно. В этой связи сделан вывод, что применение 1-(3-хлорфенил)-3-фенил мочевины несколько улучшает стабильность резин при термоокислительном старении, а 1-(3-хлорфенил)-3-фенил тиомочевина и 1-(3-фторфенил)-3-фенил селеномочевина не ухудшают данный показатель при введении в резиновую смесь.

Ключевые слова

эластомеры, мочевина, тиомочевина, селеномочевина, бутадиен-нитрильный каучук, вулканизация, термоокислительная стойкость

Поступила: 21.10.2024
Доработана: 16.12.2024
Принята в печать: 08.04.2025

Для цитирования

Бочкарёв Е.С., Заправдина Д.М., Кузнецов Я.П., Мкртчян Ю.М., Бурмистров В.В., Ваниев М.А. Исследование влияния мочевин и их серо- и селенсодержащих аналогов на вулканизацию и термоокислительную стойкость эластомеров на основе бутадиен-нитрильного каучука. *Тонкие химические технологии*. 2025;20(3):237–252. https://doi.org/10.32362/2410-6593-2025-20-3-237-252

INTRODUCTION

Exposure to high temperatures and oxygen changes the initial properties of elastomers depending on the composition of their ingredients [1, 2]. Aromatic amines, substituted phenols, phosphorous acid esters, and organosilicon compounds are widely used in industry as antioxidants for elastomeric materials [3–6]. However, the above-mentioned groups of antioxidants have fairly high values of saturated vapor pressure and are poorly soluble in rubber, which limits their use in the food and medical industries. As a rubber stabilizer for the food industry, 2,2-methylene-bis(4-methyl-6-*tert*-butylphenol), better known as Agidol 2[1], is commonly used. The use of D,L-camphor anils as heat stabilizers was studied in [7]. Other potentially interesting options for use as heat stabilizers may include compounds of sulfur- or selenium-containing carboxyalkylphenols based on selenium-containing analogs of phenozan (3-(3,5-di-*tert*-butyl-4-hydroxyphenyl)propionic acid) [8] and compounds based on 2,3-camphorquinone.

Modern computational systems allow one to evaluate compatibility and predict interactions between polymer macromolecules under the action of various aggressive factors [9]. A method was developed for selecting components of elastomer compositions based on quantum-chemical modeling [10]. The relationship of the total energy of the system, which was determined by quantum-chemical calculation methods, including dynamic testing methods, with relaxation parameters allows the effect of additives on the properties of whole elastomer compositions to be predicted.

The aim of this work was to investigate the influence of ureas and their sulfur- and selenium-containing analogs on the vulcanization of elastomeric materials based on nitrile butadiene rubber and on their resistance to thermo-oxidative aging.

EXPERIMENTAL

Figure 1 presents the structural formulas of the studied compounds obtained by the syntheses described in the literature [11–13], as well as their notation.

The objects of the study comprised two groups of samples:

(1) Samples of rubber compounds based on BNKS-28 AN synthetic nitrile butadiene rubber (Specification TU 38.30313-2006) that was obtained by suspension polymerization at low temperatures (A) and contained a noncoloring antioxidant (N), without additives of the compounds shown in Fig. 1. Such objects have the letter ***K*** in the notation. Rubber samples containing 4 parts by weight (pbw) of 1-(3-chlorophenyl)-3-phenylurea, 1-(3-chlorophenyl)-3-phenylthiourea, or 1-(3-fluorophenyl)-3-phenylselenourea per 100 pbw of rubber are designated as ***KO***, ***KS***, and ***KSe***, respectively.

(2) Samples of rubber compounds based on BNKS-28 AN commercial rubber that do not contain a filler. They were produced on laboratory rollers 320 160/160 (*Yarpolimermash*, USSR) by sequential introduction of the recipe ingredients. The vulcanization activator was a combination of zinc oxide (4 pbw) and stearic acid (2 pbw). The crosslinking agent was sulfur (2 pbw). The vulcanization accelerator was *N*-cyclohexyl-2-benzothiazole sulfenamide (1.5 pbw). Such samples have the letter ***P*** in their notation. In turn, elastomers containing 1-(3-chlorophenyl)-3-phenylurea, 1-(3-chlorophenyl)-3-phenylthiourea, or 1-(3-fluorophenyl)-3-phenylselenourea in an amount of 4 pbw per 100 pbw of rubber are assigned the notation ***PO***, ***PS***, and ***PSe***, respectively. The objects of comparison were rubbers containing the standard antiaging agent *N*-isopropyl-*N*′-phenyl-1,4-phenylenediamine (4 pbw) and the vulcanization accelerator *N*-cyclohexyl-2-benzothiazole sulfenamide (1.5 pbw) with the notation ***IPPD*** and ***CBS***, respectively. The dosage of the studied compounds was selected in such a way as to obtain differences in the exhibited properties of rubbers while taking into account the fact that ***IPPD*** has a low saturated vapor pressure (0.00046 kPa at 90°C) and a boiling point (166°C) close to the vulcanization temperature (150°C). Further increase is impractical since it leads to migration of the antiaging agent from the rubber matrix [14]. For better dispersion, the antiaging agents were introduced first, and then the remaining ingredients of the rubber mixture were added in the order they are mentioned in the text.

The preliminarily obtained chemical compounds were characterized using quantum-chemical methods for calculating the properties of molecules in the HyperChem 8.0 software[2] (*Hypercube Inc*, USA). The geometry of the molecules was optimized using the MM+ molecular mechanics method, and then the PM3 (Parameterized Model, revision 3) semiempirical method was used to calculate the diagrams of energy levels, the lowest unoccupied molecular orbital (LUMO),

[1] Technical Information. Vulkanox BKF / Lanxess. 2004. http://www.symtake.com/tw/uploads/filelist/1000/2/1382580948_c0a80afd82d4d906.pdf. Accessed April 10, 2024.

[2] HyperChem Professional 8.0. http://www.hypercubeusa.com/. Accessed February 25, 2025.

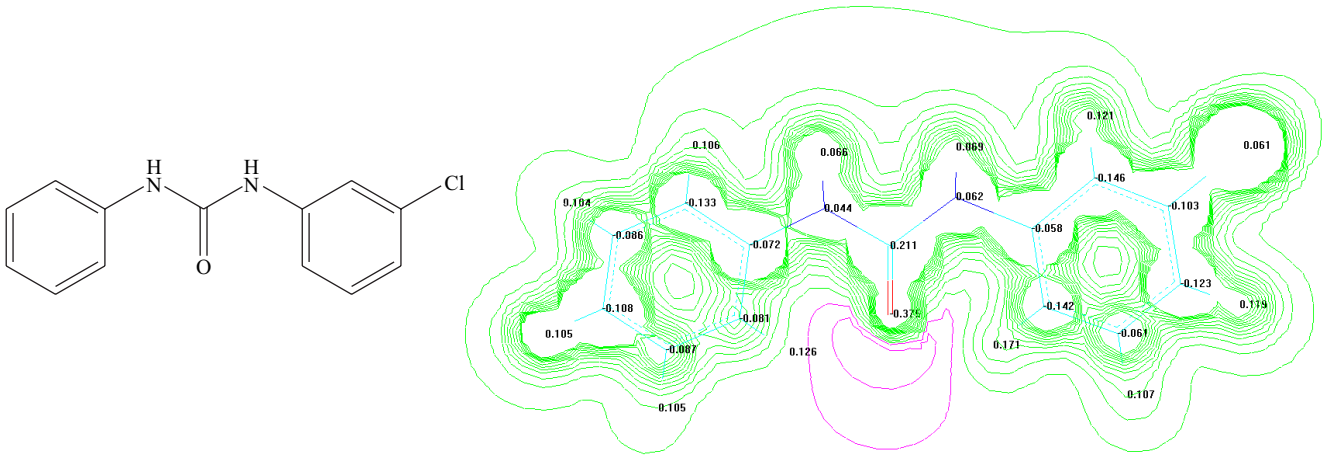

1-(3-Chlorophenyl)-3-phenylurea (***O***) [12]

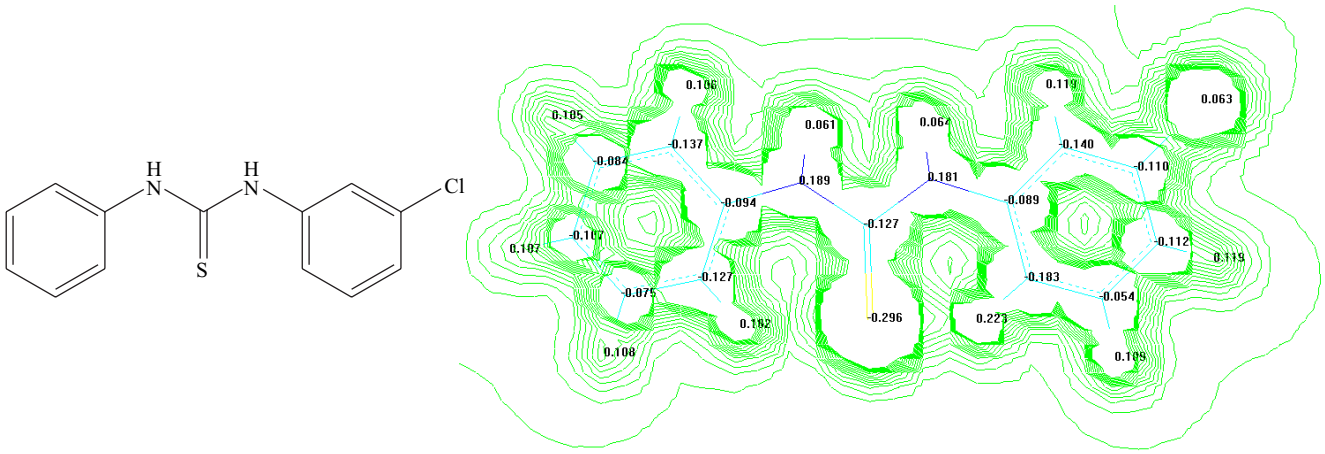

1-(3-Chlorophenyl)-3-phenylthiourea (***S***) [13]

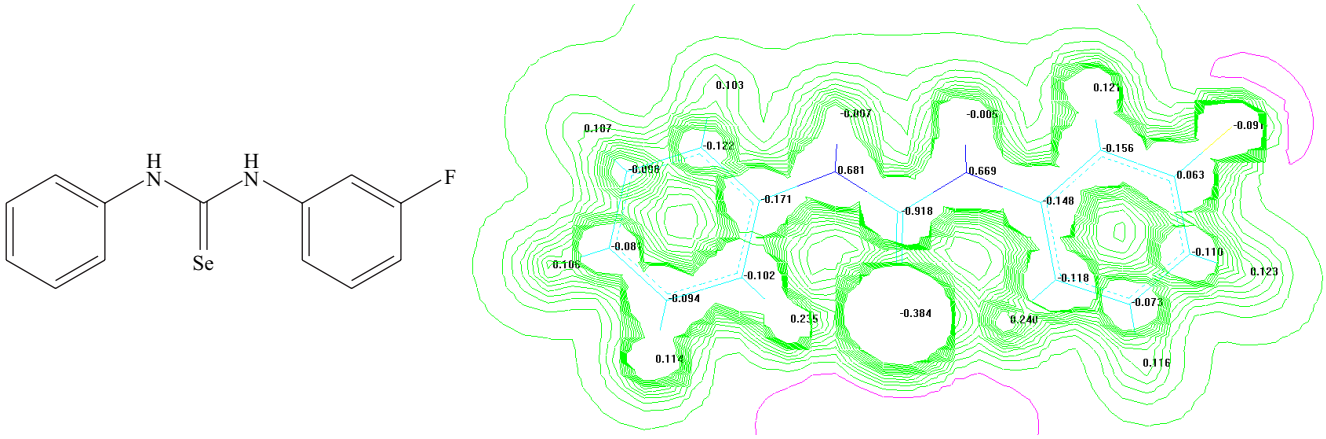

1-(3-Fluorophenyl)-3-phenylselenourea (***Se***) [14]

(a) (b)

Fig. 1. (a) Structures, and (b) charge distributions and electronic densities of the studied molecules

and the highest occupied molecular orbital (HOMO), as well as the thermodynamic parameters: enthalpy, entropy, and heat capacity of the compounds. By comparing the shapes and excitation energies ΔE_{exc} of these frontier molecular orbitals, a conclusion can be drawn about the nucleophilicity or electrophilicity of the molecules under study. Characteristics were also calculated for the system of the molecules under study together with nitrile butadiene rubber to assess their compatibility from the changes in the total energies of the system and individual substances.

The vulcanization of rubbers was investigated by the rotorless vulcanization method with a MonTech MDR 3000 Professional rheometer

(*MonTech*, Germany) at a temperature of 150°C in accordance with GOST R 54547-2011[3]. Using this rheometer, the total crosslink density ν_{tot} of vulcanized rubber samples was found under shear deformation conditions at 100°C from the change in the storage modulus depending on the shear strain in accordance with the ASTM D6601-02[4] standard and the described procedure [15]. In this case, the relationship between the parameter ν_{tot} and the equilibrium dynamic modulus is determined in accordance with the kinetic theory of rubber elasticity [16] using the equation

$$\nu_{tot} = \frac{G_\infty}{3RT}, \quad (1)$$

where ν_{tot} is the total crosslink density, mol/cm^3; G_∞ is the equilibrium dynamic modulus, Pa; R is the universal gas constant (R = 8.314 J/(mol·K)); T is the test temperature (373.15 K).

The dynamic characteristics of vulcanized rubbers were studied in accordance with ASTM D6601-02 and ASTM D5992-96[5] using a MonTech MDR 3000 Professional rheometer in dynamic moving die rheometer mode. The conditions for conducting dynamic tests were selected from those recommended by the standard: temperature 100°C and oscillation frequency 10 Hz. The change in dynamic moduli after thermal-oxidative aging at 90°C for 72 h in an oven was also assessed. In this case, the corresponding temperature was added to the notation, e.g., ***PO90***.

The physical and mechanical characteristics of vulcanized rubbers were evaluated in accordance with GOST 270-75[6]. The efficiency of the studied antioxidants to thermo-oxidative aging was determined at a temperature of 100°C for 72 h according to GOST 9.024-74[7].

IR spectra of the samples were recorded with an FT-801 Fourier transform infrared (FTIR) spectrometer (*NPF SIMEKS*, Russia) by the attenuated total reflection method on a ZnSe crystal in the wavelength range λ = 550–4000 cm^{-1} with a resolution of 4 cm^{-1}.

RESULTS AND DISCUSSION

Tables 1 and 2 present the results of calculations of the properties of ureas and their ***S***- and ***Se***-containing analogs by the PM3 semiempirical method in comparison with standard compounds used as vulcanization accelerators and antioxidants.

The obtained values of the energies of the LUMO molecular orbital were used to find the electron affinity energies, which are related by density functional theory, as well as to determine such parameters as the dipole moment and the charge distribution and electron density on the amine groups. The presence of reaction sites of the synthesized compounds can be assumed based on these parameter values. These parameters are also of interest due to the vulcanization of nitrile butadiene rubber during thermos-oxidative aging due to the lone pair of electrons on the nitrogen atom. At the same time, by varying the functional groups in the urea molecule to obtain ***S***- and ***Se***-containing analogs with the same number of electrons on the outer energy levels (ns^2, np^4) and different energies of the levels, it is possible to influence the mobility of hydrogen atoms at the amino group. Note that, for antiaging agents and antiozonants (Agidol-2 and ***IPPD***), the electron affinity energy is positive; i.e., the addition of an electron is accompanied by the release of energy, whereas the vulcanization accelerator ***CBS*** demonstrates a negative value. It can be assumed that the ***S*** and ***Se*** compounds, for which the energies are −1.115 and −1.365 eV, respectively, will accelerate vulcanization, with the latter acting to a greater extent. In addition, these compounds can have canonical mesomeric thio- and selenoamide forms, carrying a negative charge on the sulfur atom and a positive charge on the nitrogen atoms of the amidine fragment. In turn, the sulfur/selenium atom is a strong nucleophilic site, which allows these compounds to act as sulfur/selenium donors and consequently as a crosslinking agent [17]. At the same time, the compound ***O*** has an electron affinity energy of 0.051 eV and does not exhibit nucleophile properties; therefore, it will not react with the nitrile group. The electronic

[3] GOST R 54547-2011. National Standard of the Russian Federation. Rubber compounds. Measurement of vulcanization characteristics using rotorless cure meters. Moscow: Standartinform; 2018.

[4] ASTM D6601-02. Standard Test Method for Rubber Properties—Measurement of Cure and After-Cure Dynamic Properties Using a Rotorless Shear Rheometer. https://www.astm.org/d6601-02.html. DOI: 10.1520/D6601-02. Accessed February 25, 2025.

[5] ASTM D5992-96(2018). Standard Guide for Dynamic Testing of Vulcanized Rubber and Rubber-Like Materials Using Vibratory Methods. https://www.astm.org/d5992-96r18.html. DOI: 10.1520/D5992-96R18. Accessed February 25, 2025.

[6] GOST 270-75. Interstate Standard. Rubber. Method of the determination elastic and tensile stress-strain properties. Moscow: IPK Izdatelstvo standartov; 1978.

[7] GOST 9.024-74. State Standard of the USSR. Unified system of corrosion and ageing protection. Rubbers. Methods of heat ageing stability determination. Moscow: Izdatelstvo standartov; 1986.

structure shows (Fig. 1) that this compound has a lone pair of electrons, which prevents any reaction with the nitrile group. However, during heating with sulfur, such an electron-pair donor can react with it to form thiourea, which will affect the vulcanization rate.

Calculation of the properties of the model of the rubber–molecule system begins with finding the state with the minimum potential energy, which usually corresponds to the equilibrium geometry of the atoms. Figure 2 presents the results of calculating the minimum energies of the compounds under study in comparison with the standard antioxidant ***IPPD*** using molecular dynamics methods.

Various physicochemical parameters of the rubber–molecule system can be calculated on the basis of the determination of the electron density distribution in the molecules together with the bond force constants. From Fig. 2, which depicts the change in the kinetic and potential energy with time for the compounds under study in the BNKS rubber environment, it can be seen that the values of the change in the potential energy of the ***O*** compound are similar to those of the standard antiaging agent ***IPPD***. Replacing the heteroatom with sulfur and selenium in the compounds leads to a decrease in this parameter. First of all, we note that high-molecular-weight compounds have limited molecular mobility. The formation of a transition complex is accompanied by rehybridization of the carbon atoms of the rubber backbone from sp^3 to sp^2 hybridization state, which is limited by structural relaxation. Higher values of the potential energy show that an activated complex having an optimal energetically favorable structure does

Table 1. Results of quantum-chemical calculation of the enthalpy *H*, entropy *S*, heat capacity C_p, and energies of molecular orbitals HOMO and LUMO of molecules*

Compound	*H*, kJ/mol	S^{298}, kJ/(mol·K)	C_p, kJ/(mol·K)	LUMO, eV	HOMO, eV	ΔE_{exc}, eV	Dipole moment *D*	Nitrogen atom charge
BNKS-28 AN	284.8	0.9823	0.4959	0.664	−9.657	10.32	–	−0.077
Urea	−171.7	0.2724	0.0586	1.061	−9.618	10.68	4.071	−0.017
O	67.2	0.4676	0.2026	0.051	−8.921	8.97	2.512	0.045
S	344.3	0.5526	0.2872	−1.115	−8.614	7.49	4.376	0.189
Se	158.0	0.4631	0.2095	−1.365	−8.234	6.86	4.493	0.277
IPPD	148.9	0.5122	0.2473	0.224	−8.179	8.40	2.116	0.031
Agidol-2	−278.0	0.4945	0.2583	0.397	−8.723	9.12	1.425	–
CBS	143.5	0.5152	0.2440	−0.878	−8.911	8.03	2.025	−0.105

* HOMO is the highest occupied molecular orbital, LUMO is the lowest unoccupied molecular orbital, and $\Delta E_{exc} = E_{LUMO} - E_{HOMO}$ is the difference of the energies of the orbitals.

Table 2. Estimation of changes in the total energy of rubber–compound systems

Compound	*E*, kJ/mol	E_{NBR}, kJ/mol	E_{system}, kJ/mol	Δ*E*, kJ/mol	Solubility of compound in rubber
O	−226352	−385474	−643961	−32134.8	Soluble
S	−244968	−385474	−633457	−3014.7	Soluble
Se	−257781	−385474	−646345	−3089.71	Soluble
IPPD	−229879	−385474	−618360	−3006.74	Soluble

Note: *E* are the calculated energies of individual compounds under study, E_{NBR} are the calculated energies of nitrile butadiene rubber, E_{system} are the calculated energies of mixtures of nitrile butadiene rubber with compounds under study in a box simulating the volume of rubber, and $\Delta E = E + E_{NBR} - E_{system}$.

not have time to form during the oxidation reaction with oxygen at high temperatures. In this connection, the ***O*** compound can be expected to exhibit antioxidant properties that prevent the thermo-oxidative destruction of macromolecules, but do not prevent the structuring of rubber at nitrile groups.

Changes in the energies of the system and individual substances showed that negative energy values suggest that the polymer–substance system may exhibit self-organization capabilities and consequent compatibility.

Figure 3 illustrates the effect of ureas and their ***S***- and ***Se***-containing analogs at a temperature of 150°C on the structuring of BNKS-28 AN rubber without a vulcanizing group and for rubber compounds vulcanized with a standard sulfur-containing system.

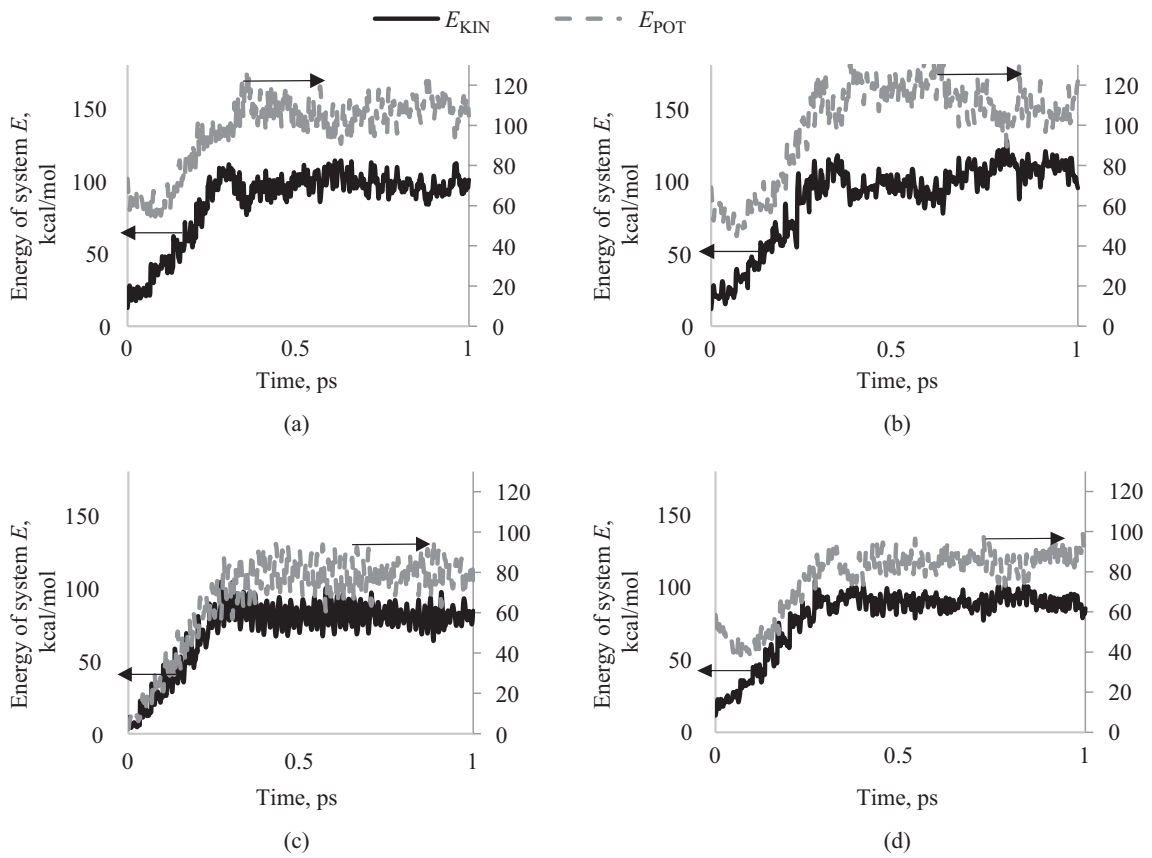

Fig. 2. Calculated minimum values of kinetic energy E_{KIN} and potential energy E_{POT} of (a) the standard antioxidant ***IPPD***, (b) urea ***O***, and (c) ***S***-containing and (d) ***Se***-containing analogs in rubber

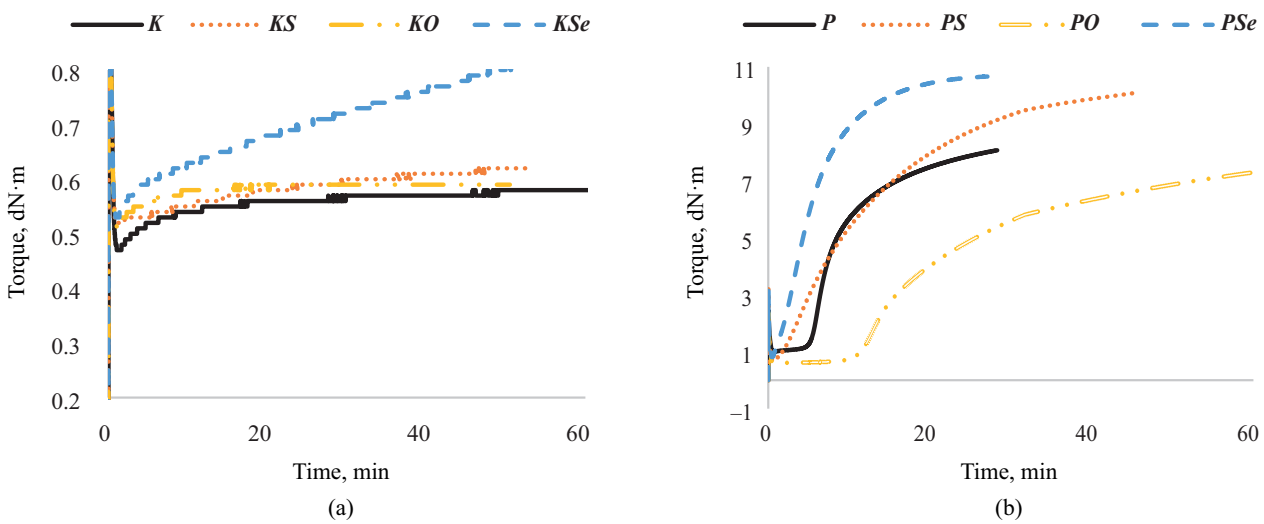

Fig. 3. Torque versus time for BNKS-28 AN rubber with the urea analogs under study (a) without a vulcanizing system and (b) with the ***CBS***–sulfur vulcanizing system

The dependencies in Fig. 3a show that the ***Se*** compound causes structuring of nitrile butadiene rubber (***KSe*** sample) even in the absence of a crosslinking agent. To a somewhat lesser extent, an increase in torque is also observed upon the introduction of a sulfur-containing analog of urea into the rubber.

Since the presence of the vulcanization accelerator ***CBS*** can lead to side reactions during the vulcanization of rubbers containing oligomeric unsaturated polyketone [18], we assessed the effect of urea and its sulfur- and selenium-containing analogs on vulcanization. Upon the introduction of the synthesized products into rubber compounds containing a vulcanizing system (Fig. 3b), it was noted that the ***S***- and ***Se***-containing analogs of urea (in the composition of the ***PS*** and ***PSe*** samples) caused a decrease in the parameter "time to the onset of vulcanization" from 6 to 3 and 2 min, respectively. In addition, the maximum torques of the vulcanizates increased from 8 to 10 daN·m for both additives. In this regard, we note that these compounds act as vulcanization coagents during the formation of the elastomer structure.

For the ***O*** compound, we noted the opposite effect. The use of this compound together with the ***CBS***–sulfur vulcanizing system led to an increase in the prevulcanization time of rubbers from 6 to 15 min and a subsequent decrease in the torque and total vulcanization rate. The experimental vulcanization data confirm the assumptions based on the results of the quantum-chemical calculation in HyperChem 8.0.

Figure 4 shows the physical and mechanical characteristics of vulcanized rubbers and their change after aging at 100°C for 72 h.

The results of the assessment of the parameters "engineering tensile strength" and "relative elongation at break" (Figs. 4a and 4b) and their changes after aging show that the introduction of the ***S***- and ***Se***-containing analogs of urea increases the tensile strength of rubbers. The introduction of the ***O*** compound has an insignificant effect on this parameter. However, in all cases, the sign of the change in the engineering tensile strength was reversed, and in the case of rubbers containing the ***O*** compound, this parameter changed to a lesser extent. Here it is likely that the introduced additives shift the process toward the destruction of macromolecules, thus preventing crosslinking along the nitrile groups of the rubber. The change in the relative elongation at break after aging somewhat decreased for rubbers containing the compounds under study.

For the obtained mixtures of rubber with urea and its ***S***- and ***Se***-containing analogs, as well as rubbers based on them, the changes in storage modulus G' and loss modulus G'' were estimated. Figure 5 demonstrates the effect of urea and its ***S***- and ***Se***-containing analogs on the change in the storage and loss moduli of rubber (assessed in accordance with ASTM D6601-02) after its exposure in rheometer molds at a temperature of 150°C for 4 h.

It can be seen from Fig. 5 that prolonged exposure of BNKS-28 AN rubber to an elevated temperature (150°C for 4 h) results in a significant increase in the storage modulus and loss modulus due to crosslinking along the nitrile groups of the rubber (see Fig. 6). However, as seen from the slightly reduced values of the storage and loss moduli, the presence of ***S***, ***Se***, or ***O*** in the rubber slows down this process. At the same time, the total crosslink density after exposure to the above temperature changes by 18% for BNKS-28 AN and 8% in the case of using the ***O*** compound (Table 3). Here, it is important to note that the total crosslink density ν_{tot} is the sum of the physical crosslink density ν_{ph} and the chemical crosslink density ν_{ch}, and

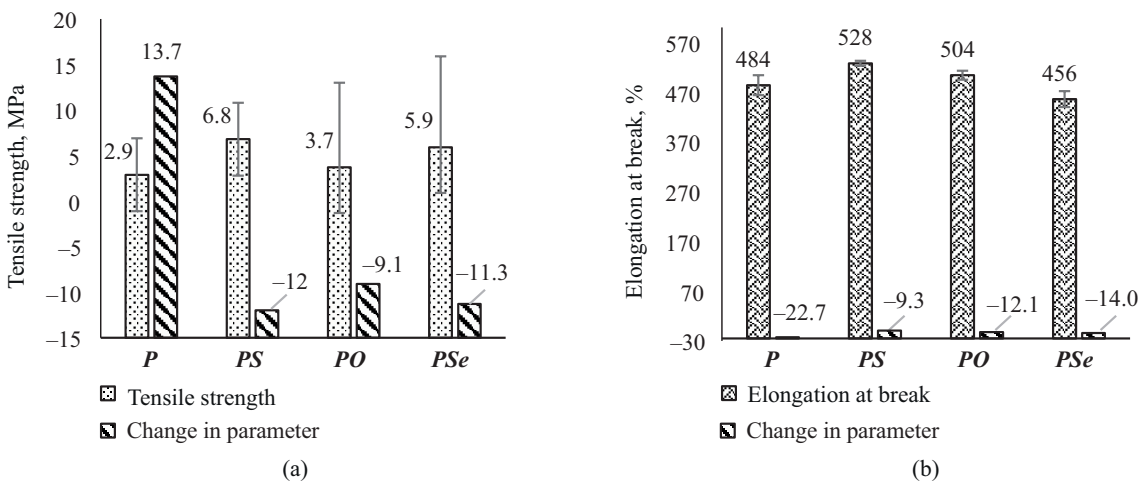

Fig. 4. Effect of the studied urea analogs on (a) engineering tensile strength and (b) relative elongation at break and their changes after thermo-oxidative aging at 100°C for 72 h

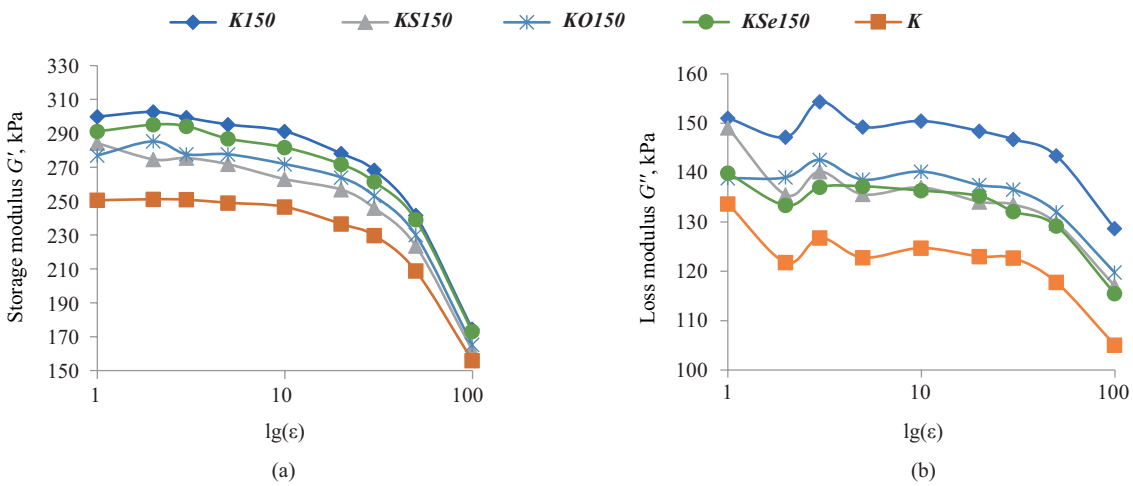

Fig. 5. (a) Storage modulus G' and (b) loss modulus G'' versus logarithm ε of shear strain

Table 3. Effect of the studied compounds on the total crosslink density ν_{tot} in rubbers and elastomers before and after exposure to elevated temperatures

Exposure of rubber compounds to 150°C for 4 h				
Rubber compound	***K150***	***KO150***	***KS150***	***KSe150***
$\nu_{tot}\cdot10^{-3}$, mol/cm^3	0.33	0.30	0.30	0.32
Rubber	***P***	***PO***	***PS***	***PSe***
$\nu_{tot}\cdot10^{-3}$, mol/cm^3	0.87	0.81	0.95	0.94
Aging of rubbers at 90°C for 72 h				
Rubber	***P90***	***PO90***	***PS90***	***PSe90***
$\nu_{tot}\cdot10^{-3}$, mol/cm^3	1.16	1.02	1.20	1.22

Note: the total crosslink density of rolled BNKS-28 AN rubber is $0.28\cdot10^{-3}$ mol/cm^3.

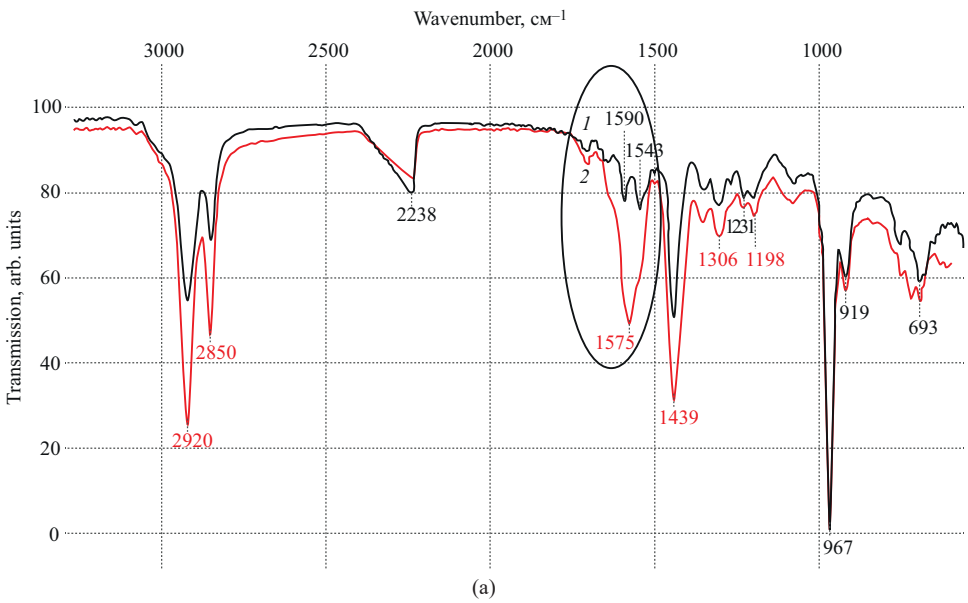

Fig. 6. FTIR spectra before (*1*, black) and after (*2*, red) aging of rubbers containing (a) 1-(3-chlorophenyl)-3-phenylurea (***KO*** and ***KO150***), (b) 1-(3-chlorophenyl)-3-phenylthiourea (***KS*** and ***KS150***), and (c) 1-(3-fluorophenyl)-3-phenylselenourea (***KSe*** and ***KSe150***)

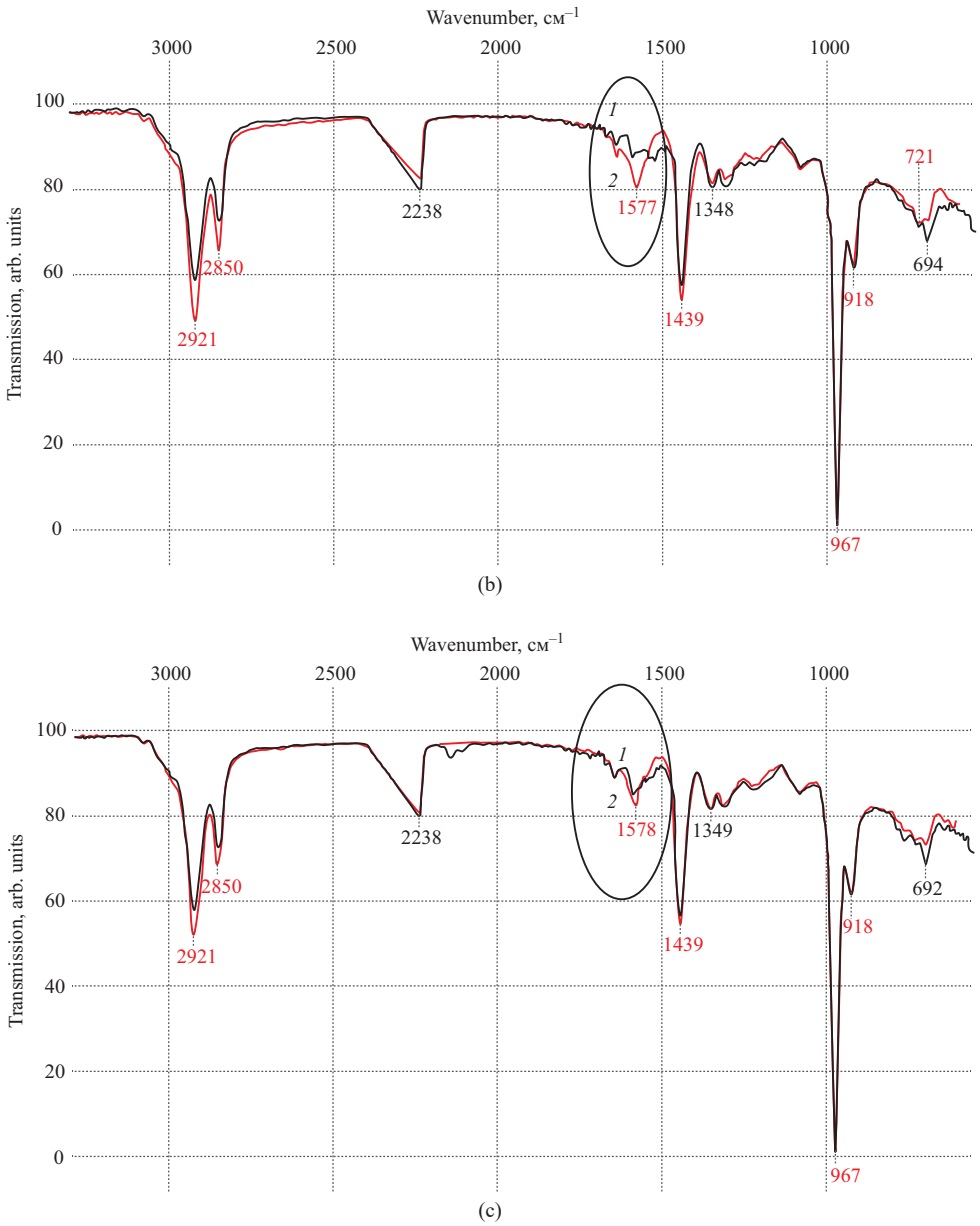

Fig. 6. FTIR spectra before (*1*, black) and after (*2*, red) aging of rubbers containing (a) 1-(3-chlorophenyl)-3-phenylurea (***KO*** and ***KO150***), (b) 1-(3-chlorophenyl)-3-phenylthiourea (***KS*** and ***KS150***), and (c) 1-(3-fluorophenyl)-3-phenylselenourea (***KSe*** and ***KSe150***)

the primary ν_{tot} value estimated for noncrosslinked rubber is determined by the physical intertwining of macromolecules. Exposure of BNKS-28 AN rubber to a temperature of 150°C leads to the processes of destruction of the rubber macromolecules and their crosslinking by nitrile groups, with the latter being predominant. As a result of the structuring of the macromolecules, the rubber lost its ability to dissolve in toluene and chloroform, thus preventing an assessment of the change in the characteristic viscosity. At the same time, the FTIR spectra (Fig. 6) show a significant increase in the spectral band in the region of 1575–1590 cm^{-1}, which characterizes the formation of a C=N–C crosslink.

Despite the insignificant change in the degree of crosslinking for the rubber with urea after exposure to an elevated temperature (***KO150***), the passband at 1592 cm^{-1} (C=N–C group) demonstrated a significant increase. At the same time, there was a decrease in the band of the nitrile group of the rubber at 2250 cm^{-1}. For the ***S***-containing analog of urea, the increase in the passband at 1592 cm^{-1} (C=N–C group) and decrease in the band of the nitrile group of the rubber at 2250 cm^{-1} were exhibited to a lesser extent. In the case of using the ***Se***-analog of urea in the rubbers based on nitrile butadiene rubber, the chemical crosslinking of its macromolecules is probably due to the ability of the above compound to act as a donor of crosslinking agents,

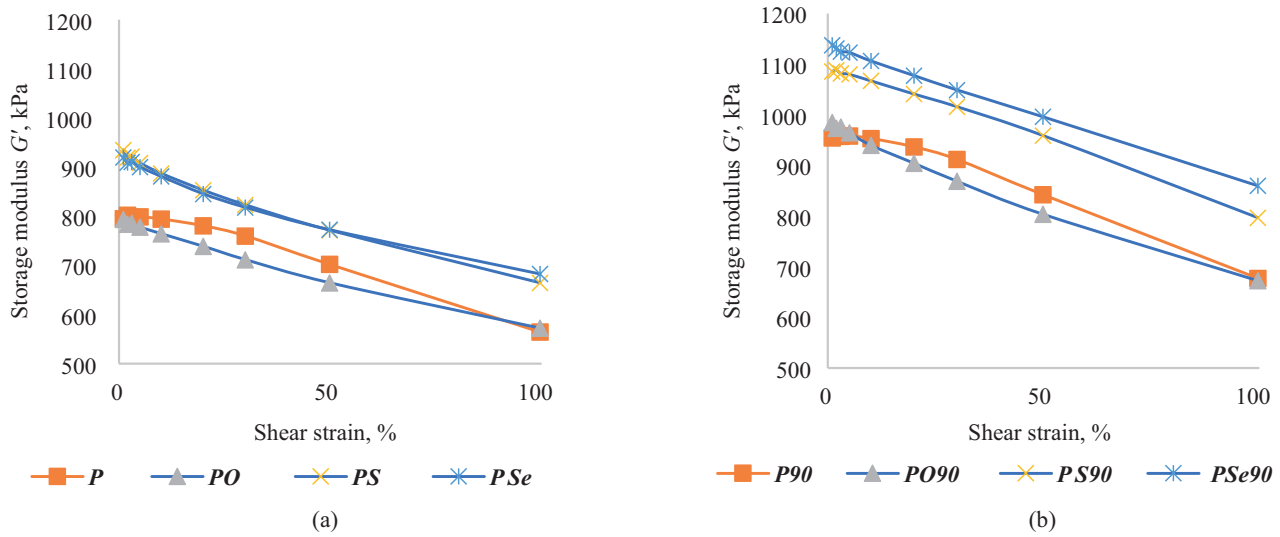

Fig. 7. Storage moduli G' (a) before and (b) after aging at 90°C for 72 h of the unfilled rubbers (***P*** and ***P90***) and rubbers containing 1-(3-chlorophenyl)-3-phenylurea (***PO*** and ***PO90***), 1-(3-chlorophenyl)-3-phenylthiourea (***PS*** and ***PC90***), and 1-(3-fluorophenyl)-3-phenylselenourea (***PSe*** and ***PSe90***)

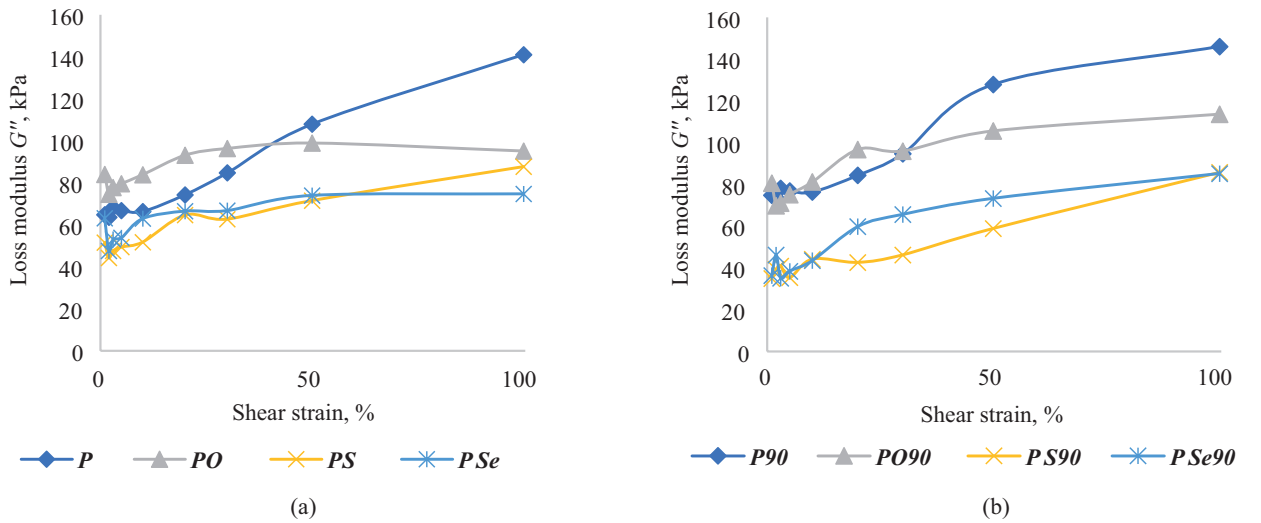

Fig. 8. Loss moduli G'' (a) before and (b) after aging at 90°C for 72 h of the unfilled rubbers (***P*** and ***P90***) and the rubbers containing 1-(3-chlorophenyl)-3-phenylurea (***PO*** and ***PO90***), 1-(3-chlorophenyl)-3-phenylthiourea (***PS*** and ***PC90***), and 1-(3-fluorophenyl)-3-phenylselenourea (***PSe*** and ***PSe90***)

rather than to the formation of C=N–C crosslinking at nitrile groups.

Similarly, the change in dynamic properties before and after aging at 90°C for 72 h was carried out in rubbers containing the ***CBS***–sulfur vulcanizing group (Figs. 7 and 8).

The rubbers containing the ***S***- and ***Se***-containing analogs of ureas demonstrate a significant increase in the storage modulus in comparison with the unfilled rubbers (Fig. 7). For the ***PO*** rubber, the modulus value remained virtually unchanged. After thermo-oxidative aging of the rubbers, an increase in the storage modulus was noted for all rubbers (Fig. 7b). In the presence of the vulcanizing group, the storage moduli of the ***S***- and ***Se***-containing urea analogs significantly increase. The change in the loss modulus due to shear deformation is shown in Fig. 8.

The dependencies in Fig. 8a indicate that the dissipation of mechanical energy into thermal energy is due to an increase in the component of the complex modulus. The introduction of urea and its ***S***- and ***Se***-containing analogs leads to a decrease in the dissipation of mechanical energy into thermal energy due to a higher total crosslink density, which increases

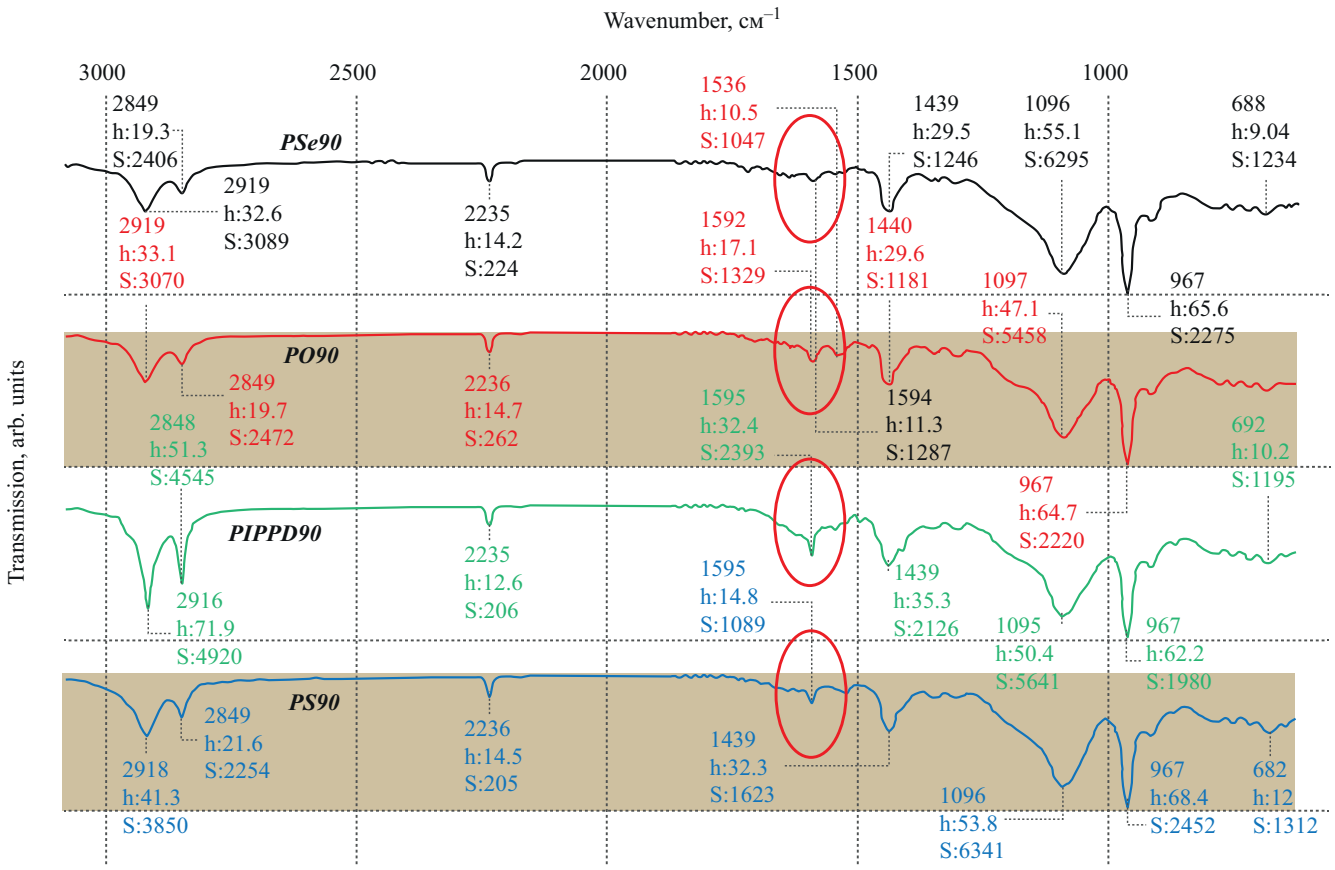

Fig. 9. FTIR spectra of rubber based on BNKS-28 AN after thermo-oxidative aging

from $0.87 \cdot 10^{-3}$ mol/cm^3 for BNKS-28 rubbers without additives to $0.94 \cdot 10^{-3}$ mol/cm^3 for the ***S***- and ***Se***-containing analogs. The loss modulus after thermo-oxidative aging (Fig. 8b) also increases to a greater extent for the ***PO90*** rubbers. In this case, the total crosslink density after thermo-oxidative aging of rubbers changes from 33%, 23%, 25%, and 29% for the rubbers ***P90***, ***PO***, ***PS90***, and ***PSe90***, respectively. This demonstrates a certain stabilizing effect of the used urea compounds. However, as indicated by the FTIR spectra, the protective action mechanisms are of a different nature (Fig. 9).

As in the case with rubber, the FTIR spectra show an increase in the transmission band in the region of 1590–1595 cm^{-1}. However, for the rubbers containing selenium (***PSe90***), no peak in this region is observed after aging, while for the analog containing sulfur, this peak is characterized by a less significant increase.

Comparing the obtained calculated data on the electron affinity energy for urea and its ***S***- and ***Se***-containing analogs (Table 1) with the total crosslink densities of the corresponding rubbers (Table 3), we note their similar trend. Namely, the decrease in the electron affinity energy in the series of the studied compounds from 0.051 and −1.115 to −1.365 eV (for ***O***, ***S***, and ***Se***, respectively) leads to an increase in the total crosslink density of the corresponding rubber samples ***PO***, ***PS***, and ***PSe*** from 23% and 25% to 29%, respectively.

CONCLUSIONS

The study has shown that 1-(3-chlorophenyl)-3-phenylurea, 1-(3-chlorophenyl)-3-phenylthiourea, and 1-(3-fluorophenyl)-3-phenylselenourea exhibit activity as vulcanization accelerators and heat stabilizers of rubbers. The values and sign of electron affinity energy obtained by quantum chemical calculations can be used to predict the possibility of using individual molecules as vulcanization accelerators. At the same time, with increasing magnitude of negative electron affinity energy, the vulcanization rate in the main period increases along with a decrease in the time before the onset of vulcanization. For example, with a change in the electron affinity energy from 0.051 (urea) to −1.115 (thiourea) and −1.365 eV (selenourea), the time before the onset of vulcanization changes

from 15 to 3 and 2 min, respectively. In the case of using selenourea, according to the results of IR spectroscopy, no cyclization of nitrile groups of rubber is observed either. As a result of thermo-oxidative aging of rubbers based on BNKS-28 AN rubber without a stabilizer and with 1-(3-chlorophenyl)-3-phenylurea, 1-(3-chlorophenyl)-3-phenylthiourea, and 1-(3-fluorophenyl)-3-phenylselenourea, the total crosslink density changes in the series 33%, 23%, 25%, and 29%, respectively. In turn, the change in tensile strength after thermo-oxidative aging is +13%, −9%, −12%, and −11.3% for the rubber samples ***P***, ***PO***, ***PS***, and ***PSe***, respectively. In this regard, we note that the use of 1-(3-chlorophenyl)-3-phenylurea somewhat improves the stability of rubbers during thermal-oxidative aging, whereas 1-(3-chlorophenyl)-3-phenylthiourea and 1-(3-fluorophenyl)-3-phenylselenourea do not worsen this parameter when introduced into the rubber compound.

Acknowledgments

The work was supported by the Volgograd State Technical University, the development program of “Priority 2030”, the scientific project No. 1/656-24.

Authors’ contributions

E.S. Bochkarev—design of the research concept, planning and conducting experimental studies, processing the data obtained, preparation of the data obtained for publication.

D.M. Zapravdina—design of the research concept, planning and conducting experimental studies, processing the data obtained, preparation of the data obtained for publication.

Ya.P. Kuznetsov—conducting the experiment, data processing, and analysis of the results.

I.M. Mkrtchian—conducting IR research.

V.V. Burmistrov—design of the research concept, development of the experiment, discussion and analysis of the results, writing the text of the article.

M.A. Vaniev—consultation on conducting individual stages of the study, scientific editing.

The authors declare no conflicts of interest.

REFERENCES

1. Gaidadin A.N., Petryuk I.P., Kosterin D.V. Evaluation of kinetic parameters of high-temperature aging of rubbers based on ethylene-propylene rubber. *Vestnik Kazanskogo tekhnologicheskogo universiteta = Bulletin of the Kazan Technological University*. 2014;17(1):169–171 (in Russ).
2. Khankishiyeva R.F. The improvement of physical and mechanical properties of sealers based on nitrile-butadiene rubber and combination of nano-metal oxides. *SOCAR Proceedings*. 2020;3:174–182. https://doi.org/10.5510/OGP20200300459
3. Dorofeev A.N., Zemskii D.N. New stabilizers based on *p*-phenylene diamine for tire rubbers. *Kauchuk i Rezina*. 2016;5:30–33 (in Russ).
4. Akhmadullin R.M., Karimov I.A., Akhmetshin I.F., Kotyrev E.A., Alimanov D.V., Nadelyaev K.L. Study of the stabilizing efficiency of thermal stabilizers bisphenol-5 and vulcanox BKF at production of butadiene acrylonitrile rubber. *Kauchuk i Rezina*. 2017;76(4):210–213 (in Russ).
5. Chirkova Yu.N., Dorofeev A.N., Gaifetdinov R.R. Effect provided by *N*-phenyl, *N′*-oxyalkyl-*p*-phenylenediamine-based stabilizers upon the thermo-oxidation and ozone ageing stability of rubbers. *Vestnik Tekhnologicheskogo universiteta = Herald of Technological University*. 2018;21(3):98–102 (in Russ.).
6. Martynova Y.Z., Khairullina V.R., Nasretdinova R.N., *et al.* Determination of the chain termination rate constants of the radical chain oxidation of organic compounds on antioxidant molecules by the QSPR method. *Russ. Chem. Bull.* 2020;69(9): 1679–1691. https://doi.org/10.1007/s11172-020-2948-7
[Original Russian Text: Martynova Yu.Z., Khairullina V.R., Nasretdinova R.N., Garifullina G.G., Mitsukova D.S., Gerchikov A.Ya., Mustafin A.G. Determination of the chain termination rate constants of the radical chain oxidation of organic compounds on antioxidant molecules by the QSPR method. *Izvestiya Akademii nauk. Seriya khimicheskaya*. 2020;9:1679–1691 (in Russ.).]

СПИСОК ЛИТЕРАТУРЫ

1. Гайдадин А.Н., Петрюк И.П., Костерин Д.В. Оценка кинетических параметров высокотемпературного старения резин на основе этиленпропиленового каучука. Вестник Казанского технологического университета. 2014;17(1):169–171.
2. Khankishiyeva R.F. The improvement of physical and mechanical properties of sealers based on nitrile-butadiene rubber and combination of nano-metal oxides. *SOCAR Proceedings*. 2020;3:174–182. https://doi.org/10.5510/OGP20200300459
3. Дорофеев А.Н., Земский Д.Н. Оксипропилированные ароматические диамины – стабилизаторы шинных резин. *Каучук и резина*. 2016;5:30–33.
4. Ахмадуллин Р.М., Каримов И.А., Ахметшин И.Ф., Котырев Е.А., Алиманов Д.В., Наделяев К.Л. Исследование стабилизирующей эффективности термостабилизаторов бисфенол-5 и вулканокс BKF при производстве бутадиен-нитрильного каучука. *Каучук и резина*. 2017;76(4): 210–213.
5. Чиркова Ю.Н., Дорофеев А.Н., Гайфетдинов Р.Р. Влияние стабилизаторов класса *N*-фенил, *N′*-оксиалкил-*п*-фенилендиамин на стойкость резин к термоокислительному и озонному старению. *Вестник Технологического университета*. 2018;21(3):98–102.
6. Мартынова Ю.З., Хайруллина В.Р., Насретдинова Р.Н., Гарифуллина Г.Г., Мицукова Д.С., Герчиков А.Я., Мустафин А.Г. Определение констант скорости обрыва цепи радикально-цепного окисления органических соединений на молекулах антиоксидантов методом QSPR. *Известия Академии наук. Серия химическая*. 2020;9:1679–1691.
7. Вернигора А.А., Нилидин Д.А., Давиденко А.В., Фан Нгок Ту, Губин С.Г., Губина Е.В., Ваниев М.А., Новаков И.А. Влияние анилов D,L-камфоры на термоокислительную стойкость резины на основе бутадиенни-трильного каучука. *Известия ВолгГТУ*. 2021;252(5):47–52. https://doi.org/10.35211/1990-5297-2021-5-252-47-52

7. Vernigora A.A., Nilidin D.A., Davidenko A.V., Fan Ngok Tu, Gubin S.G., Gubina E.V., Vaniev M.A., Novakov I.A. Influence of anyles D,L-camphora on thermal oxidating stability of butadiene rubber based elastomer. *Izvestiya VolgGTU = Izvestia VSTU*. 2021;252(5):47–52 (in Russ). https://doi.org/10.35211/1990-5297-2021-5-252-47-52
8. Kholshin S.V., Yagunov S.E., Kandalintseva N.V., *et al.* Synthesis of new selenium-containing analogs of phenozan acid. *Russ. Chem. Bull.* 2019;68(12):2374–2376. https://doi.org/10.1007/s11172-019-2715-9
[Original Russian Text: Kholshin S.V., Yagunov S.E., Kandalintseva N.V., Prosenko A.E. Synthesis of new selenium-containing analogs of phenozan acid. *Izvestiya Akademii nauk. Seriya khimicheskaya*. 2019;12:2374–2376 (in Russ.).]
9. Averina A.E., Laptev A.B., Nesterov A.S., Sarvaeva G.A., Nikolaev E.V. Application of quantum-chemical calculations to evaluate the aging processes of polyethylene terephthalate under the influence of climate. *Aviatsionnye materialy i tekhnologii = Aviation Materials and Technologies*. 2020;3(60):47–56 (in Russ.). https://doi.org/10.18577/2071-9140-2020-0-3-47-56
10. Valiev H.H., Vorobyev V.V., Karnet Yu.N., Kornev Yu.V., Yumaschev O.B. Application of quantum-chemical modeling results in experimental investigations of silicone composites. *Mater. Phys. Mechan.* 2017;32(3):293–297.
11. Siddique M.U.M., McCann G.J.P., Sonawane V., Horley N., Williams I.S., Joshi P., Chaudhuri B. Biphenyl urea derivatives as selective CYP1B1 inhibitors. *Org. Biomol. Chem.* 2016;14(38):8931–8936. https://doi.org/10.1039/C6OB01506A
12. Serrano J.L., Soeiro P.F., Reis M.A., Boto R.E.F., Silvestre S., Almeida P. Synthesis and process optimization of symmetric and unsymmetric barbiturates C5-coupled with 2,1-benzisoxazoles. *Mol. Diver*. 2020;24(1):155–166. https://doi.org/10.1007/s11030-019-09937-4
13. Kuznetsov Ya.P., Rasskazova E.V., Pitushkin D.A., *et al.* Synthesis and Properties of *N*,*N*′-Disubstituted Ureas and Their Isosteric Analogs Containing Polycyclic Fragments: XI. 1-[(Adamantan-1-yl)alkyl]-3-arylselenoureas. *Russ. J. Org. Chem.* 2021;57(7): 1036–1046. https://doi.org/10.1134/S1070428021070022
[Original Russian Text: Kuznetsov Ya.P., Rasskazova E.V., Pitushkin D.A., Eshtukov A.V., Vasipov V.V., Burmistrov V.V., Butov G.M. Synthesis and Properties of *N*,*N*′-Disubstituted Ureas and Their Isosteric Analogs Containing Polycyclic Fragments: XI. 1-[(Adamantan-1-yl)alkyl]-3-arylselenoureas. *Zhurnal organicheskoi khimii*. 2021;57(7):929–941 (in Russ.). https://doi.org/10.31857/S0514749221070028]
14. Reznichenko S.V., Morozov Yu.L. (Eds.). *Bol'shoi spravochnik rezinshchika. Kauchuki i ingredienty* (*Large Rubber Manufacturer's Reference Book*: in 2 v. V. 1. *Rubbers and Ingredients*). Moscow: Tehinform MAI; 2012. P. 209 (in Russ.).
15. Blume A., Kiesewetter J. Determination of the crosslink density of tire tread compounds by different analytical methods. *Kautschuk Gummi Kunststoffe*. 2019;72(9):33–42.
16. Sperling L.H. *Introduction to Physical Polymer Science*. Hoboken, New Jersey: John Wiley & Sons Inc.; 2006. P. 504.
17. Litvinov I.A., Burmistrov V.V., Fayzullin R.R. Structure of some adamantyl-containing ureas and hydrogen bonds in their crystals. *J. Struct. Chem.* 2022;63(8):1274–1283. https://doi.org/10.1134/S002247662208008X
[Original Russian Text: Litvinov I.A., Burmistrov V.V., Fayzullin R.R. Structure of some adamantyl-containing ureas and hydrogen bonds in their crystals. *Zhurnal strukturnoi khimii.* 2022;63(8):96114 (in Russ.). https://doi.org/10.26902/JSC_id96114]

8. Хольшин С.В., Ягунов С.Е., Кандалинцева Н.В., Просенко А.Е. Синтез новых селенсодержащих аналогов фенозан-кислоты. *Известия Академии наук. Серия химическая*. 2019;(12):2374–2376.
9. Аверина А.Е., Лаптев А.Б., Нестеров А.С., Сарваева Г.А., Николаев Е.В. Применение квантово-химических расчетов для оценки процессов старения полиэтилентерефталата при воздействии климата. *Авиационные материалы и технологии*. 2020;3(60):47–56. https://doi.org/10.18577/2071-9140-2020-0-3-47-56
10. Valiev H.H., Vorobyev V.V., Karnet Yu.N., Kornev Yu.V., Yumaschev O.B. Application of quantum-chemical modeling results in experimental investigations of silicone composites. *Mater. Phys. Mechan.* 2017;32(3):293–297.
11. Siddique M.U.M., McCann G.J.P., Sonawane V., Horley N., Williams I.S., Joshi P., Chaudhuri B. Biphenyl urea derivatives as selective CYP1B1 inhibitors. *Org. Biomol. Chem.* 2016;14(38):8931–8936. https://doi.org/10.1039/C6OB01506A
12. Serrano J.L., Soeiro P.F., Reis M.A., Boto R.E.F., Silvestre S., Almeida P. Synthesis and process optimization of symmetric and unsymmetric barbiturates C5-coupled with 2,1-benzisoxazoles. *Mol. Diver*. 2020;24(1):155–166. https://doi.org/10.1007/s11030-019-09937-4
13. Кузнецов Я.П., Рассказова Е.В., Питушкин Д.А., Ештуков А.В., Васипов В.В., Бурмистров В.В., Бутов Г.М. Синтез и свойства 1,3-дизамещенных мочевин и их изостерических аналогов, содержащих полициклические фрагменты: XI. 1-[(Адамантан-1-ил)алкил]-3-арил селеномочевины. *Журн. орган. химии*. 2021;57(7):929–941. https://doi.org/10.31857/S0514749221070028
14. Резниченко С.В., Морозов Ю.Л. (ред.). *Большой справочник резинщика*: в 2-х ч. Ч. 1. *Каучуки и ингредиенты*. М.: ООО «Издательский центр «Техинформ» МАИ; 2012. С. 209.
15. Blume A., Kiesewetter J. Determination of the crosslink density of tire tread compounds by different analytical methods. *Kautschuk Gummi Kunststoffe*. 2019;72(9):33–42.
16. Sperling L.H. *Introduction to Physical Polymer Science*. Hoboken, New Jersey: John Wiley & Sons Inc.; 2006. P. 504.
17. Литвинов И.А., Бурмистров В.В., Файзуллин Р.Р. Строение некоторых адамантилсодержащих мочевин и водородные связи в их кристаллах. *Журн. структурн. химии*. 2022;63(8):96114. https://doi.org/10.26902/JSC_id96114
18. Ворончихин В.Д., Сороченко О.В., Семиколенов С.В., Иванов Д.П., Бабушкин Д.Э., Дубков К.А. Влияние олигомерного ненасыщенного поликетона на вулканизацию эластомерных композиций в присутствии сульфенамида Ц. *Известия Академии наук. Серия химическая*. 2020;11:2171–2176.

18. Voronchikhin V.D., Sorochenko O.V., Semikolenov S.V., *et al.* Influence of oligomeric unsaturated polyketone on the vulcanization of elastomeric compositions in the presence of sulfenamide C. *Russ. Chem. Bull.* 2020;69(11):2171–2176. https://doi.org/10.1007/s11172-020-3018-x
[Original Russian Text: Voronchikhin V.D., Sorochenko O.V., Semikolenov S.V., Ivanov D.P., Babushkin D.E., Dubkov K.A. Influence of oligomeric unsaturated polyketone on the vulcanization of elastomeric compositions in the presence of sulfenamide C. *Izvestiya Akademii nauk. Seriya khimicheskaya*. 2020;11:2171–2176 (in Russ.).]

About the Authors

Eugene S. Bochkarev, Cand. Sci. (Eng.), Senior Lecturer, Department of Technology of Macromolecular and Fibrous Materials, Volgograd State Technical University (28, pr. im. V.I. Lenina, Volgograd, 400005, Russia). E-mail: w_tovn@mail.ru. Scopus Author ID 57222574440, RSCI SPIN-code 6024-6675, https://orcid.org/0000-0002-2343-1562

Daria M. Zapravdina, Cand. Sci. (Chem.), Junior Researcher, Laboratory of Polymer, Composite and Hybrid Functional Materials, Volgograd State Technical University (28, pr. im. V.I. Lenina, Volgograd, 400005, Russia). E-mail: zapravdinadasha94@gmail.com. Scopus Author ID 57915518300, RSCI SPIN-code 2913-1891, https://orcid.org/0000-0002-8654-2382

Yaroslav P. Kuznetsov, Postgraduate Student, Volgograd State Technical University (28, pr. im. V.I. Lenina, Volgograd, 400005, Russia). E-mail: yroner@mail.ru. Scopus Author ID 572221849778, RSCI SPIN-code 3945-1938, https://orcid.org/0000-0002-1933-2684

Iurii M. Mkrtchian, Assistant, Department of Chemistry and Processing Technology of Elastomers, Volgograd State Technical University (28, pr. im. V.I. Lenina, Volgograd, 400005, Russia). E-mail: m.sc.yuri@vstu.ru. RSCI SPIN-code 1363-6544, https://orcid.org/0009-0008-6119-8125

Vladimir V. Burmistrov, Dr. Sci. (Chem.), Head of the Department of Organic Chemistry, Volgograd State Technical University (28, pr. im. V.I. Lenina, Volgograd, 400005, Russia). E-mail: vburmistrov@vstu.ru. Scopus Author ID 38861265800, ResearcherID M-4464-2015, RSCI SPIN-code 5404-0537, https://orcid.org/0000-0002-8547-9166

Marat A. Vaniev, Dr. Sci. (Eng.), Head of the Department of Chemistry and Processing Technology of Elastomers, Volgograd State Technical University (28, pr. im. V.I. Lenina, Volgograd, 400005, Russia). E-mail: vaniev@vstu.ru. Scopus Author ID 14063995400, RSCI SPIN-code 9260-2745, https://orcid.org/0000-0001-6511-5835

Об авторах

Бочкарёв Евгений Сергеевич, к.т.н., старший преподаватель, кафедра технологии высокомолекулярных и волокнистых материалов, ФГБОУ ВО «Волгоградский государственный технический университет» (400005, Россия, Волгоград, пр-т им. В.И. Ленина, д. 28). E-mail: w_tovn@mail.ru. Scopus Author ID 57222574440, SPIN-код РИНЦ 6024-6675, https://orcid.org/0000-0002-2343-1562

Заправдина Дарья Михайловна, к.х.н., младший научный сотрудник, лаборатория полимерных, композитных и гибридных функциональных материалов, ФГБОУ ВО «Волгоградский государственный технический университет» (400005, Россия, Волгоград, пр-т им. В.И. Ленина, д. 28). E-mail: zapravdinadasha94@gmail.com. Scopus Author ID 57915518300, SPIN-код РИНЦ 2913-1891, https://orcid.org/0000-0002-8654-2382

Кузнецов Ярослав Петрович, аспирант, ФГБОУ ВО «Волгоградский государственный технический университет» (400005, Россия, Волгоград, пр-т им. В.И. Ленина, д. 28). E-mail: yroner@mail.ru. Scopus Author ID 572221849778, https://orcid.org/0000-0002-1933-2684

Мкртчян Юрий Мушегович, ассистент, кафедра «Химия и технология переработки эластомеров», ФГБОУ ВО «Волгоградский государственный технический университет» (400005, Россия, Волгоград, пр-т им. В.И. Ленина, д. 28). E-mail: m.sc.yuri@vstu.ru. SPIN-код РИНЦ 1363-6544, https://orcid.org/0009-0008-6119-8125

Бурмистров Владимир Владимирович, д.х.н., заведующий кафедрой органической химии, ФГБОУ ВО «Волгоградский государственный технический университет» (400005, Россия, Волгоград, пр-т им. В.И. Ленина, д. 28). E-mail: vburmistrov@vstu.ru. Scopus Author ID 38861265800, ResearcherID M-4464-2015, SPIN-код РИНЦ 5404-0537, https://orcid.org/0000-0002-8547-9166

Ваниев Марат Абдурахманович, д.т.н., доцент, заведующий кафедрой «Химия и технология переработки эластомеров», ФГБОУ ВО «Волгоградский государственный технический университет» (400005, Россия, Волгоград, пр-т им. В.И. Ленина, д. 28). E-mail: vaniev@vstu.ru. Scopus Author ID 14063995400, SPIN-код РИНЦ 9260-2745, https://orcid.org/0000-0001-6511-5835

Translated from Russian into English by V. Glyanchenko
Edited for English language and spelling by Thomas A. Beavitt

Tonkie Khimicheskie Tekhnologii = Fine Chemical Technologies.
2025;20(3):253–263
ISSN 2686-7575 (Online)

Chemistry and technology of inorganic materials
Химия и технология неорганических материалов

UDC 546.05
https://doi.org/10.32362/2410-6593-2025-20-3-253-263
EDN JWGODK

RESEARCH ARTICLE

Synthesis of complex oxides Eu_2O_3–Gd_2O_3–$Zr(Hf)O_2$ using microwave radiation and study of their properties

Nikolay V. Grechishnikov ✉, **Elena E. Nikishina**
MIREA – Russian Technological University (Lomonosov Institute of Fine Chemical Technologies), Moscow, 119454 Russia
✉ *Corresponding author, e-mail: nklgrchshnkv@yandex.ru*

Abstract

Objectives. The authors synthesize complex oxide phases of the composition $Eu_{2-x}Gd_xZr_2O_7$ and $Eu_{2-x}Gd_xHf_2O_7$ at x = 0.5, 1.0, 1.5 under microwave heating conditions and investigate their phase composition, particle size distribution, and specific surface with the purpose of obtaining bulk ceramic materials on their basis and study their behavior when heated to 1473 K.

Methods. Using X-ray phase analysis, the phase composition of samples subjected to heat treatment at temperatures of 1473 and 1773 K was studied, and the cell parameters were calculated. The particle size of the obtained powders was analyzed by laser diffraction on a Fritsch Analysette 22 device. The specific surface area was studied by the Brunauer–Emmett–Teller method on a TriStar 3000 analyzer. Bulk ceramic materials were obtained by cold pressing with subsequent sintering at 1773 K. The coefficient of thermal expansion (CTE) of ceramic samples was studied on a Netzsch DIL 402C dilatometer in a temperature range of 300–1473 K.

Results. At a temperature of 1473 K, all synthesized samples were observed to form a fluorite structure; at a temperature of 1773 K, samples with the composition $Eu_{2-x}Gd_xHf_2O_7$ had an ordered pyrochlore structure. With an increase in the gadolinium content in the samples, a decrease in both the unit cell parameter and the CTE was observed. The particle size of almost all samples did not exceed 100 μm; the specific surface area did not exceed 1 m^2/g.

Conclusions. For the first time, compounds with the composition $Eu_{2-x}Gd_xZr_2O_7$ and $Eu_{2-x}Gd_xHf_2O_7$ were obtained using microwave processing at x = 0.5, 1.0, 1.5. As well as determining the dependence of the phase composition on the heat treatment temperature after microwave exposure, the dependence of the change in the unit cell parameters on the gadolinium content in the sample was studied, the particle size distribution was investigated. The CTEs of bulk ceramic samples obtained by cold pressing were additionally studied. The obtained data can be used in the development of thermal barrier coatings and technical ceramics used at high temperatures (up to 1473 K).

Keywords
zirconates, hafnates, thermal expansion, thermal barrier coatings, X-ray phase analysis

Submitted: 03.10.2024
Revised: 28.01.2025
Accepted: 11.04.2025

For citation
Grechishnikov N.V., Nikishina E.E. Synthesis of complex oxides Eu_2O_3–Gd_2O_3–$Zr(Hf)O_2$ using microwave radiation and study of their properties. *Tonk. Khim. Tekhnol. = Fine Chem. Technol.* 2025;20(3):253–263. https://doi.org/10.32362/2410-6593-2025-20-3-253-263

НАУЧНАЯ СТАТЬЯ

Синтез сложных оксидов Eu_2O_3–Gd_2O_3–$Zr(Hf)O_2$ с применением микроволнового излучения и исследование их свойств

Н.В. Гречишников ✉, **Е.Е. Никишина**

МИРЭА – Российский технологический университет (Институт тонких химических технологий им. М.В. Ломоносова), Москва, 119454 Россия

✉ *Автор для переписки, e-mail: nklgrchshnkv@yandex.ru*

Аннотация

Цели. Синтезировать сложнооксидные фазы состава $Eu_{2-x}Gd_xZr_2O_7$ и $Eu_{2-x}Gd_xHf_2O_7$ при x = 0.5, 1.0, 1.5 в условиях микроволнового нагрева, исследовать их фазовый состав, распределение частиц по размеру и удельную поверхность, получить на их основе объемные керамические материалы и изучить их поведение при нагревании до 1473 K.

Методы. С помощью рентгенофазового анализа проведено исследование фазового состава образцов, прошедших термическую обработку при разных температурах 1473 и 1773 K, а также рассчитаны параметры ячейки. Анализ размера частиц полученных порошков проводили методом лазерной дифракции на приборе Fritsch Analysette 22. Площадь удельной поверхности исследовали методом Брунауэра–Эммета–Теллера на анализаторе TriStar 3000. Объемные керамические материалы получали холодным прессованием с последующим спеканием при 1773 K. Исследование коэффициента линейного термического расширения (КЛТР) керамических образцов проводили на дилатометре Netzsch DIL 402C в интервале температур 300–1473 K.

Результаты. Установлено, что при температуре 1473 K у всех синтезированных образцов образуется структура флюорита, а при температуре 1773 K образцы с составом $Eu_{2-x}Gd_xHf_2O_7$ имеют упорядоченную структуру пирохлора. При увеличении содержания гадолиния в образцах наблюдается уменьшение как параметра элементарной ячейки, так и КЛТР. Размер частиц практически всех образцов не превышает 100 мкм, а площадь удельной поверхности не превышает 1 м^2/г.

Выводы. Впервые с применением микроволновой обработки получены соединения с составом $Eu_{2-x}Gd_xZr_2O_7$ и $Eu_{2-x}Gd_xHf_2O_7$ при x = 0.5, 1.0, 1.5, изучена зависимость фазового состава от температуры термообработки после микроволнового нагрева, изучена зависимость изменения параметров элементарной ячейки от содержания гадолиния в образце, исследовано распределение частиц по размерам, а также методом холодного прессования получены объемные керамические образцы, для которых изучен КЛТР. Полученные данные могут применяться при разработке термобарьерных покрытий и технической керамики, эксплуатируемой при высоких температурах (до 1473 K).

Ключевые слова

цирконаты, гафнаты, тепловое расширение, термобарьерные покрытия, рентгенофазовый анализ

Поступила: 03.10.2024
Доработана: 28.01.2025
Принята в печать: 11.04.2025

Для цитирования

Гречишников Н.В., Никишина Е.Е. Синтез сложных оксидов Eu_2O_3–Gd_2O_3–$Zr(Hf)O_2$ с применением микроволнового излучения и исследование их свойств. *Тонкие химические технологии*. 2025;20(3):253–263. https://doi.org/10.32362/2410-6593-2025-20-3-253-263

INTRODUCTION

In recent years, zirconates and hafnates of rare earth elements (REE) (Ln_2Zr/Hf_2O_7, where Ln = La–Lu) have been actively considered in the development of materials for parts of aggregates operating in aggressive environments and high temperatures. The most extensive area of practical application of these compounds is considered to be the creation of thermal barrier coatings, antioxidant coatings and high-temperature ceramics [1]. For such purposes, REE zirconates and hafnates with an ordered pyrochlore structure, in which the ratio of ionic radii $r(Ln^{3+})/r(Zr(Hf^{4+}))$ lies in the range 1.46–1.78 [2], are generally preferred. Such materials offer greater thermal stability, as well as thermal expansion coefficients close to those for most substrates and low thermal conductivity [3]. Zirconates and hafnates having a disordered fluorite structure also find application in the field of thermal barrier coatings and other areas of science and technology, for example, for the creation of solid electrolytes, due

to oxygen defects contained in the structure of these compounds [4].

At present, individual REE zirconates and hafnates have been quite well studied. A large number of works are devoted to the study of lanthanum zirconate and lanthanum hafnate, due to these substances offering the lowest fluorite→pyrochlore phase transition temperature (~1473 K) [2, 5], as well as europium hafnate [6], gadolinium zirconate [7]. Gadolinium zirconates and gadolinium hafnates are of particular interest due to the 1.46 ratio of the ionic radius of gadolinium to that of zirconium, which represents a boundary value for the possible formation of an ordered pyrochlore structure [2].

Due to the significant demand for REE zirconates and hafnates in various industries, the development of methods for obtaining such compounds containing two or more components while maintaining the required structure (fluorite or pyrochlore) is relevant. Works also describe the replacement of a part of REE ions by cations of another element in order to change the properties of the obtained material while preserving the ordered structure [8].

The most commonly used solid-phase method of synthesis is currently not preferred due to its high energy consumption: high sintering temperatures, long duration, since the rate is determined by the diffusion of components at the grain boundary, and preliminary preparation of initial reagents [9]. Such research is mainly focused on the development of "wet" methods for the synthesis of REE zirconates. Among such methods we can emphasize precipitation methods [10] and the sol–gel method [11]. Intermediate compounds formed as a result of the corresponding chemical reactions are transformed into REE zirconate and hafnate after thermal treatment.

In other studies, in addition to high temperatures, external influence on the reaction mixture is applied to obtain a single-phase product and increase the yield of the target phase. For example, an autoclave is used in the hydrothermal method to conduct synthesis at elevated pressures [12–14]. A simpler but no less effective method used in obtaining individual and complex oxides is microwave treatment [15, 16]. This approach provides fast and uniform heating of samples, which can be used to accelerate synthesis processes and reduce energy consumption. In some cases, the synthesis temperature can be reduced as compared with traditional methods [17]. Many studies consider microwave synthesis of compositions based on zirconium and hafnium dioxides, including in combination with sol–gel method [18–21].

The present study is based on the preparation of $Eu_{2-x}Gd_xZr_2O_7$ and $Eu_{2-x}Gd_xHf_2O_7$ compounds at $x = 0.5$, 1.0, 1.5 under microwave processing conditions to study the phase composition of the obtained products, the particle size and specific surface area of the obtained powders, as well as the coefficients of thermal expansion (CTE) of ceramic materials based on them.

MATERIALS AND METHODS

For the synthesis of REE zirconates and hafnates with the composition $Eu_{2-x}Gd_xZr_2O_7$ and $Eu_{2-x}Gd_xHf_2O_7$ at $x = 0.5$, 1.0, 1.5, zirconium oxychloride $ZrOCl_2 \cdot 2H_2O$ (*Lankhit*, Russia), hafnium oxynitrate $HfO(NO_3)_2 \cdot 2H_2O$ (*Lankhit*, Russia) were used as starting reagents along with dihydrates of europium acetate $Eu(CH_3COO)_3 \cdot 2H_2O$ (*Lankhit*, Russia) and gadolinium acetate $Gd(CH_3COO)_3 \cdot 2H_2O$ (*Lankhit*, Russia). Microwave treatment of the reaction mixture was carried out in a MS-6 sample preparation system (*Volta,* Russia). Thermal treatment was carried out in a SNOL 12/16 muffle furnace (*Snol*, Russia).

The process of synthesis of complex oxides included microwave treatment of a mixture of europium and gadolinium acetates with zirconium or hafnium hydroxide followed by heat treatment. For this purpose, zirconium or hafnium hydroxide was previously prepared by reactions (1) and (2), respectively:

$$ZrO(NO_3)_2 \cdot 8H_2O + 2NH_4OH = \\ = ZrO_x(OH)_{4-2x}\downarrow + 2NH_4NO_3 + (7 + x)H_2O \quad (1)$$

$$HfO(NO_3)_2 \cdot 8H_2O + 2NH_4OH = \\ = HfO_x(OH)_{4-2x}\downarrow + 2NH_4NO_3 + (7 + x)H_2O \quad (2)$$

To carry out these reactions, a solution containing a threefold excess of ammonia hydrate was first heated to 333 K, then zirconium oxychloride or hafnium oxynitrate was added with stirring for 40 min. The resulting precipitates were filtered off and dispersed with ethanol. A mixture of europium and gadolinium acetate containing a stoichiometric amount of REEs was added to the resulting suspensions to form a compound of the composition $Eu_{2-x}Gd_xZr_2O_7$, $Eu_{2-x}Gd_xHf_2O_7$. Next, the obtained reaction mixtures were subjected to microwave treatment with a power of 600 W and a frequency of 2.45 GHz, which lasted 15 min for the $Eu_{2-x}Gd_xZr_2O_7$ compound line and 18 min for the $Eu_{2-x}Gd_xHf_2O_7$ compound line. The influence of microwave treatment on the phase composition was considered in [22] on the example of europium zirconate. Heat treatment carried out on the obtained powders at different temperatures did not result in the formation of speck. Table 1 presents the synthesis conditions of these samples.

Table 1. Conditions for the synthesis of complex oxide phases $Eu_{2-x}Gd_xZr_2O_7$ and $Eu_{2-x}Gd_xHf_2O_7$

No.	Composition	Time of microwave processing, min	Temperature, K / Duration, h
1	$Eu_{1.5}Gd_{0.5}Zr_2O_7$	15	1473 / 6
2	$EuGdZr_2O_7$	15	
3	$Eu_{0.5}Gd_{1.5}Zr_2O_7$	15	
4	$Eu_{1.5}Gd_{0.5}Hf_2O_7$	18	
5	$EuGdHf_2O_7$	18	
6	$Eu_{0.5}Gd_{1.5}Hf_2O_7$	18	
7	$Eu_{1.5}Gd_{0,5}Zr_2O_7$	15	1773 / 1
8	$EuGdZr_2O_7$	15	
9	$Eu_{0.5}Gd_{1.5}Zr_2O_7$	15	
10	$Eu_{1.5}Gd_{0.5}Hf_2O_7$	18	
11	$EuGdHf_2O_7$	18	
12	$Eu_{0.5}Gd_{1.5}Hf_2O_7$	18	

X-ray phase analysis (XRD) of the obtained samples was performed on a D8 Advance diffractometer (*Bruker*, USA) with CuK_α-radiation (using a 0.12 mm Ni plate as a CuK_β-radiation filter, wavelength 1.5418 Å). The signal was recorded in air over a range of angles 2θ from 10° to 90° with the following parameters: step 2θ = 0.02°; signal acquisition time per step—0.4 s; sample rotation speed—20 rpm. Indication of the radiographs was performed using the PDF-2 rel. database 2011[1]. Processing and analysis of radiographs were performed using the HighScore Plus[2], Origin 8[3], and RTP32[4] software package.

The specific surface was investigated by the Brunauer–Emmett–Teller (BET) method on a TriStar 3000 adsorption analyzer of specific surface and porosity (*Micromeritics*, USA).

The particle size distribution was investigated using an Analysette 22 laser particle analyzer (*Fritsch*, Germany).

Bulk ceramic samples were obtained by cold pressing followed by sintering at a temperature of 1773 K for two hours. The heating rate did not exceed 180 K/h. The open porosity of all samples did not exceed 20%; the relative density of the samples was at least 92%. The dimensions of the samples were 5 × 5 × 26 mm.

Thermal expansion of ceramic samples was studied using a DIL 402C dilatometer (*NETZSCH*, Germany) in the temperature range from 273–1473 K.

RESULTS AND DISCUSSION

Figure 1 depicts the diffractograms of samples *1–6*, which show peaks characteristic of the fluorite structure (111), (200), (220), and (311).

XRD showed that despite the significant duration of heat treatment (6 h), the temperature of 1473 K was sufficient only for the formation of cubic fluorite structure $(Fm\bar{3}m)$ [23], the calculated parameters of the unit cell of which are presented in Table 2.

The value of the calculated unit cell parameter is characteristic of the fluorite structure. According to literature data, the parameter *a* in the pyrochlore structure lies in the range of 10.0–11.5 Å [24]. The decreased lattice parameter with an increase of gadolinium content in the obtained compound observed in these studies is explained by the smaller ionic radius of gadolinium ($r(Eu^{3+})$ = 1.066 Å (coordination number = 8); $r(Gd^{3+})$ = 1.053 Å (coordination number = 8)) than that of europium [25]. Figure 2 depicts the dependencies of the unit cell parameter *a* on the ionic radius ratio $Ln^{3+}/Zr(Hf)^{4+}$ for each composition. Taking into account the measurement error, the obtained dependence of the parameter *a* on the ratio of ionic radius $Ln^{3+}/Zr(Hf)^{4+}$ in the compound can be considered to have a linear character.

[1] International center for diffraction data (ICDD), USA, icdd.com

[2] *Malvern Pananalytical*, United Kingdom, malvernpanalytical.com

[3] *OriginLab Corporation*, USA, originlab.com

[4] Russia, slavic.me

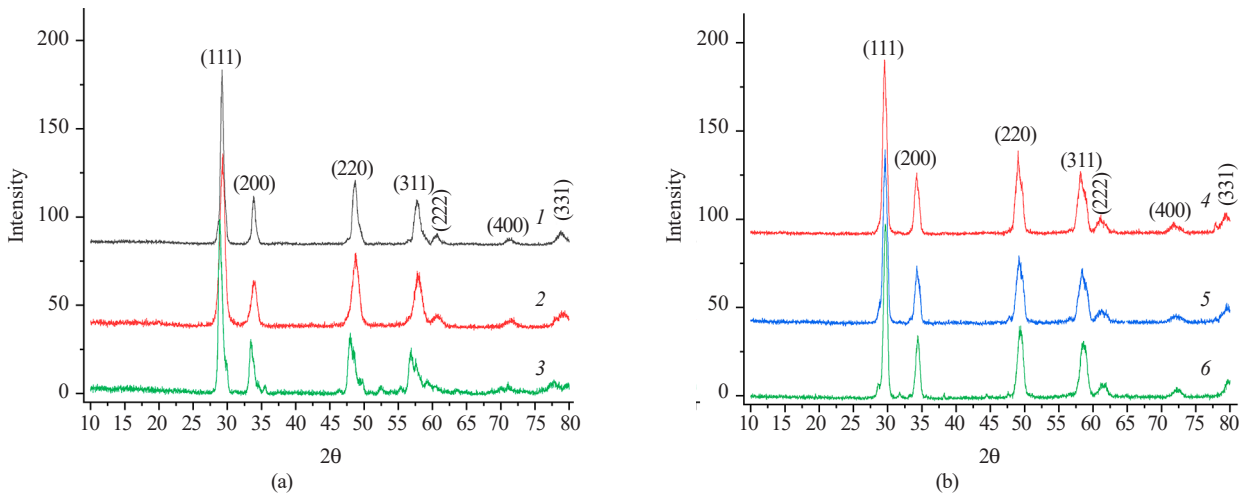

Fig. 1. Diffraction patterns of samples *1–3* (a) and *4–6* (b)

Table 2. Parameters of the unit cell of synthesized samples *1–6* (T = 1473 K)

Sample	Composition	Cell parameter a, Å	Cell volume V, Å^3
1	$Eu_{1.5}Gd_{0.5}Zr_2O_7$	5.324 ± 0.003	150.909 ± 0.226
2	$EuGdZr_2O_7$	5.292 ± 0.003	148.204 ± 0.222
3	$Eu_{0.5}Gd_{1.5}Zr_2O_7$	5.278 ± 0.003	147.031 ± 0.221
4	$Eu_{1.5}Gd_{0.5}Hf_2O_7$	5.243 ± 0.003	144.125 ± 0.216
5	$EuGdHf_2O_7$	5.236 ± 0.003	143.549 ± 0.215
6	$Eu_{0.5}Gd_{1.5}Hf_2O_7$	5.234 ± 0.003	143.384 ± 0.215

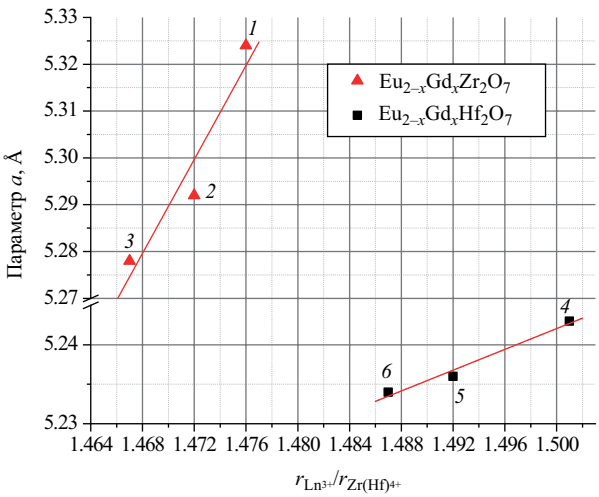

Fig. 2. Graph of the change in the cell parameter of the obtained samples of compounds *1–3* (markers ▲), *4–6* (markers ■)

Since the set temperature of 1473 K was sufficient only for crystallization of samples with fluorite structure, samples *7–12* were heat treated at 1773 K for 1 h.

Peaks on the diffractograms of samples *1–3* and *7–9* corresponding to the fluorite structure (Fig. 3) appear despite the temperature of 1773 K being sufficient for the structure ordering, i.e., the transition from the fluorite structure to the pyrochlore structure [26, 27]. This may be due to the fact that even a small amount of gadolinium ions is sufficient to distort the pyrochlore lattice and thus destabilize and disorder it to the fluorite structure, whose calculated unit cell parameters are presented in Table 2.

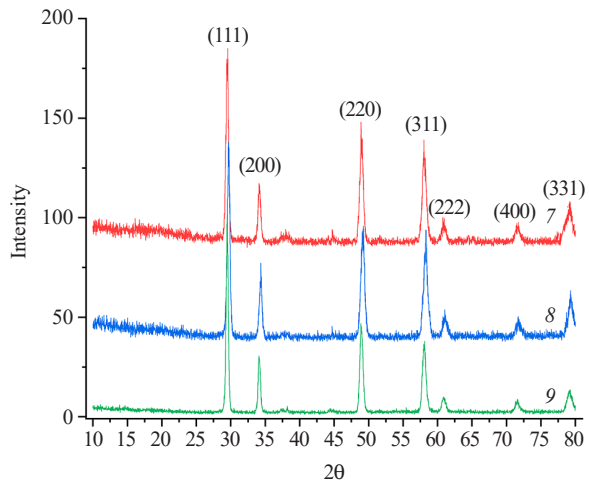

Fig. 3. X-ray diffraction pattern of samples *7–9*

Table 3. Parameters of the unit cell of synthesized samples *7–12* (T = 1773 K)

Sample	Composition	Cell parameter a, Å	Cell volume V, Å^3
7	$Eu_{1.5}Gd_{0.5}Zr_2O_7$	5.320 ± 0.002	150.569 ± 0.226
8	$EuGdZr_2O_7$	5.300 ± 0.003	148.877 ± 0.223
9	$Eu_{0.5}Gd_{1.5}Zr_2O_7$	5.276 ± 0.003	146.8637 ± 0.220
10	$Eu_{1.5}Gd_{0.5}Hf_2O_7$	10.49 ± 0.01	1154.321 ± 1.731
11	$EuGdHf_2O_7$	10.47 ± 0.01	1147.731 ± 1.721
12	$Eu_{0.5}Gd_{1.5}Hf_2O_7$	10.45 ± 0.01	1141.166 ± 1.711

The XRD results of samples *10–12* (Fig. 4) show that all samples are crystallized with the pyrochlore structure $(Fd\bar{3}m)$ [23] as indicated by the presence of additional weakly intense peaks characteristic of the pyrochlore structure: (111) at 2θ ~ 14°, (311) at 2θ ~ 19°, (331) at 2θ ~ 34°, (511) at 2θ ~ 47°. Here it is worth noting that the weak intensity of these reflexes is characteristic of this structure [26]. The calculated unit cell parameters of the obtained compounds are presented in Table 3. As indicated above, for the pyrochlore structure, the parameter a lies in the range of 10.0–11.5 Å, thus further confirming the formation of the pyrochlore structure in the compounds of the $Eu_{2-x}Gd_xHf_2O_7$ series (samples *10–12*).

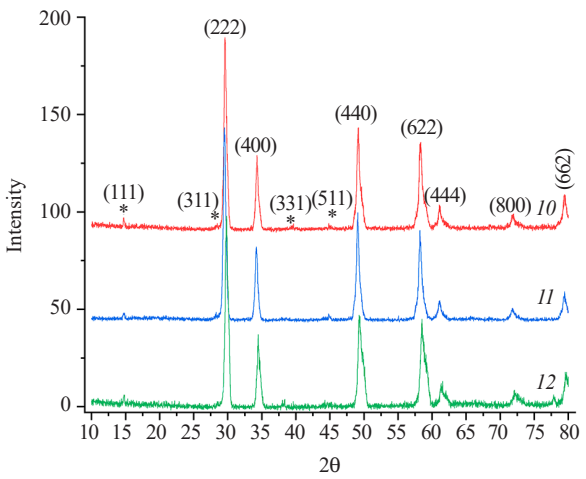

Fig. 4. X-ray diffraction pattern of samples *10–12*

The dependence of the parameter a on the ionic radius ratio $r(Ln^{3+})/r(Zr(Hf^{4+}))$ was plotted on the basis of the calculated parameters (Fig. 5). As in the case of samples *1–6*, in samples *7–12* there is an increase in the parameter a with increasing radius ratio in the compound, i.e., with decreasing gadolinium content in the sample.

The specific surface area of samples *7–12* was estimated by the BET method (Table 4).

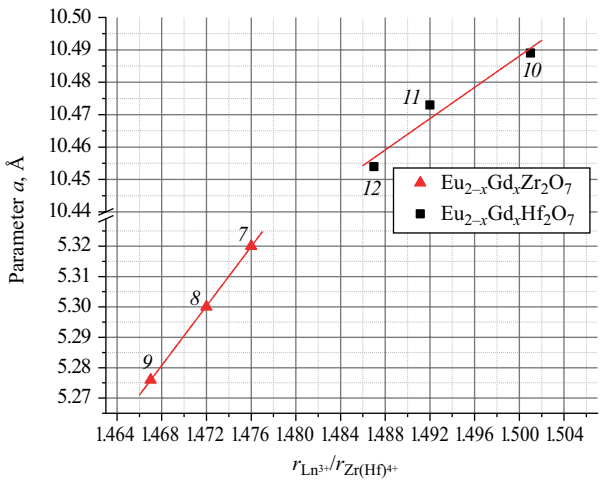

Fig. 5. Graph of the change in the cell parameter of the obtained samples of compounds *7–9* (markers ▲), *10–12* (markers ■)

Table 4. Specific surface area data for samples *7–12*

Sample	Composition	Specific surface area S, m^2/g
7	$Eu_{1.5}Gd_{0.5}Zr_2O_7$	0.600 ± 0.024
8	$EuGdZr_2O_7$	0.744 ± 0.029
9	$Eu_{0.5}Gd_{1.5}Zr_2O_7$	0.634 ± 0.025
10	$Eu_{1.5}Gd_{0.5}Hf_2O_7$	0.684 ± 0.027
11	$EuGdHf_2O_7$	0.987 ± 0.039
12	$Eu_{0.5}Gd_{1.5}Hf_2O_7$	0.890 ± 0.035

The highest value of the specific surface area in each of the rows of samples is observed for the sample corresponding to the composition $EuGd(Zr/Hf)_2O_7$. In general, the specific surface area of the obtained powders does not exceed 1 m^2/g. In [10], the specific surface area of gadolinium zirconate powder obtained by co-deposition method was 0.3 m^2/g.

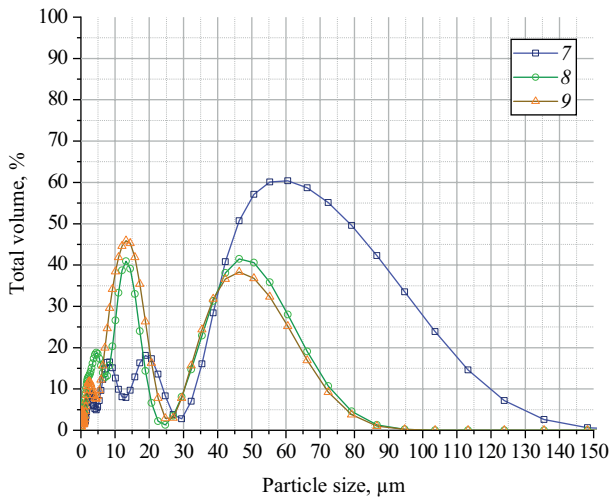

Fig. 6. Particle size distribution of samples *7* (marker •), *8* (marker ■), *9* (marker ▲)

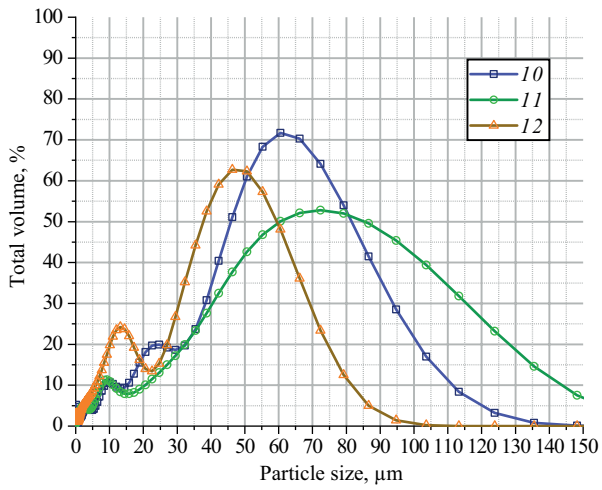

Fig. 7. Particle size distribution of samples *10* (marker •), *11* (marker ■), *12* (marker ▲)

The particle size distribution was investigated by laser diffraction method. The particle size distribution curves for samples *8* and *9* (Fig. 6) show the presence of two intense peaks, indicating that the samples predominantly contain particles having sizes between 15 ± 10 and 45 ± 15 μm. The curve characterizing sample *7* shows that most of the volume is occupied by particles with sizes between 45 ± 10 and 90 ± 15 μm. Particles >100 μm occupy no more than 20%, while for samples *8* and *9* there are no particles of this fraction (Fig. 6).

The particle size distribution for samples *10–12* (Fig. 7) has a different character from that presented above. The $Eu_{2-x}Gd_xHf_2O_7$ system predominantly contains particles having a size of 45 ± 15 μm for sample *12* and 60 ± 20 μm for sample *10*. Sample *11* has one broad peak with a maximum of about 70 μm, which covers almost the entire measurement range. For sample *12*, although the particle size does not exceed 100 μm, particles of this size account for about 20% of the sample and slightly more than 40% for sample *11*.

From a comparison of the two lines of samples, it can be concluded that samples *7–9* have a close to bimodal distribution of particles, while samples *10–12* tend rather to have one not highly intense but broad peak (monomodal distribution).

In order to investigate the CTEs, bulk ceramic samples were prepared. Measurements of the dimensional change of the samples were carried out in the temperature range of 300–1473 K. On the basis of the obtained data, the dependence of the ratio of the linear size difference to the initial size of the sample on the heating temperature was plotted (Fig. 8).

As can be seen from the presented dependencies, the difference in the behavior of samples *7–9* can be observed more clearly at temperatures above 700 K (Fig. 8), while the different behavior of samples *10–12* is more evident at temperatures above 600 K (Fig. 9).

The curves characterizing the dimensional change of samples *10–12* during heating (Fig. 9) have a linear character, which is practically useful for predicting the behavior of materials during utilization. Furthermore, the absence of jump-like changes in dimensions indicates the absence of phase transformations, i.e., the phase stability of samples at the main operating temperatures of materials based on them.

Using the obtained data, we calculated the CTEs of samples *7–12* (Table 5).

Table 5. CTE, $\alpha \cdot 10^{-6} \cdot K^{-1}$, of samples *7–12*

Sample	Composition	CTE, $\alpha \cdot 10^{-6} \cdot K^{-1}$
7	$Eu_{1.5}Gd_{0.5}Zr_2O_7$	9.17
8	$EuGdZr_2O_7$	9.02
9	$Eu_{0.5}Gd_{1.5}Zr_2O_7$	8.94
10	$Eu_{1.5}Gd_{0.5}Hf_2O_7$	9.83
11	$EuGdHf_2O_7$	9.81
12	$Eu_{0.5}Gd_{1.5}Hf_2O_7$	9.72

Figure 10 shows the dependence of CTE α on the ionic radius ratio $r(Ln^{3+})/r(Zr(Hf^{4+}))$.

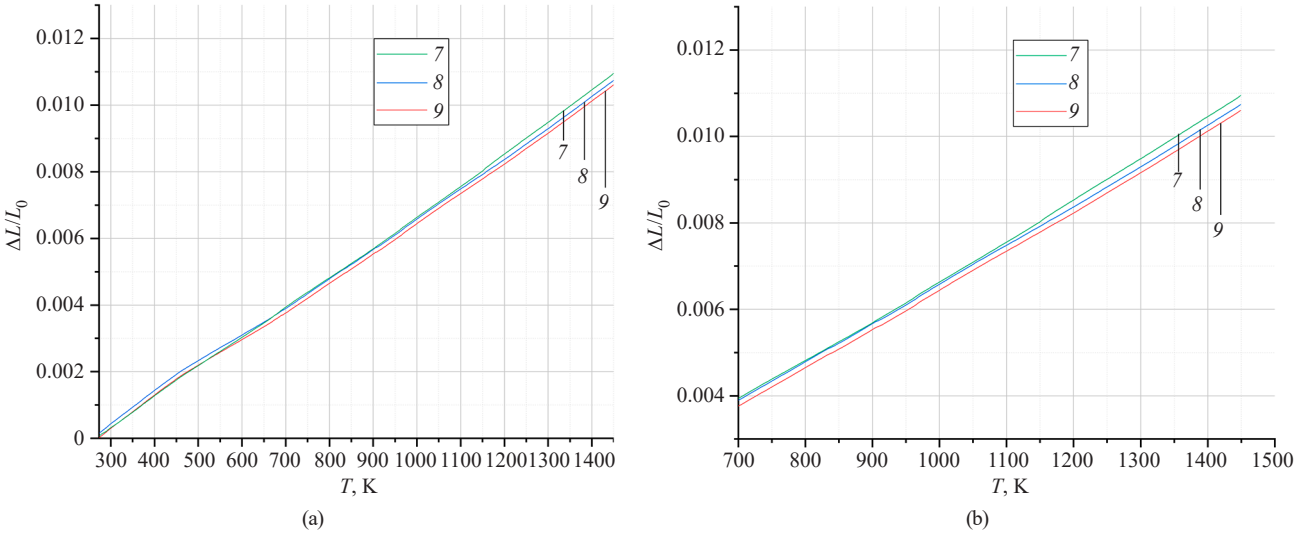

Fig. 8. Dependence of the ratio of the difference in sizes L to the initial size L_0 of the sample on the heating temperature T for samples *7–9* in the temperature range of 300–1473 K (a) and 700–1473 K (b)

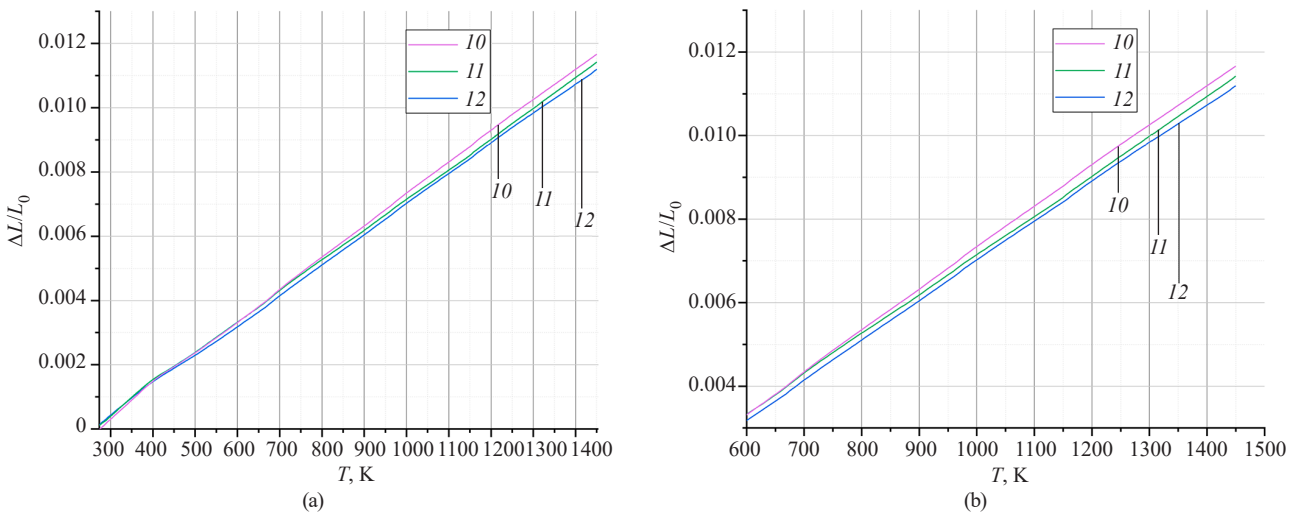

Fig. 9. Dependence of the ratio of the difference in sizes L to the initial size L_0 of the sample on the heating temperature T for samples *10–12* in the temperature range of 300–1473 K (a) and 600–1473 K (b)

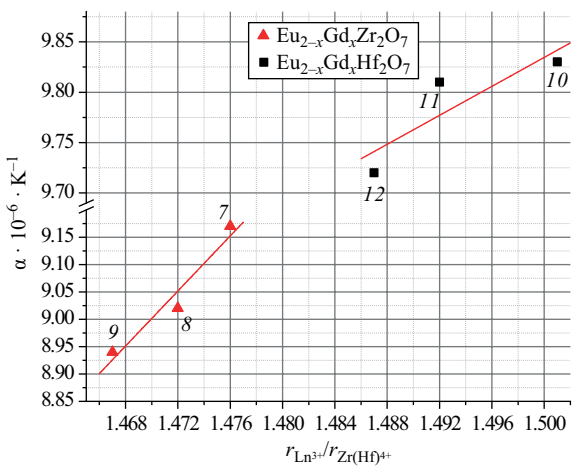

Fig. 10. CTE of samples *7–9* (markers ▲) and *10–12* (markers ■)

The presented graphs show an increase in CTE when the ratio of ionic radii in the samples increases, i.e., when the gadolinium content decreases (Fig. 10). This is due to the decreased parameter a of the unit cell fact that in samples with higher gadolinium content (and consequently decreased volume); as a consequence, the amplitude of its oscillation during heating decreases [28]. The difference of coefficients for different rulers of samples is also related to this: for samples *7–9* the average value of the unit cell parameter a is equal to ~5.3 Å (the fluorite structure is formed), while for samples *10–12* the average value of the unit cell parameter a is equal to ~10.5 Å (the value characteristic of the pyrochlore structure), which accounts for the different volume of the unit cell.

Since complex zirconates and hafnates have yet to be studied, the obtained CTE data can be compared with the literature data only for individual zirconates and hafnates of europium and gadolinium. Thus, in [29] CTE values are given for europium zirconate ($Eu_2Zr_2O_7$) of $10\cdot10^{-6}$ K^{-1} at 500 K, which increases to values of $11\cdot10^{-6}$ K^{-1} at 1500 K, as well as for gadolinium zirconate ($Gd_2Zr_2O_7$), which has the same values. In [30], the authors present the CTE curve for ceramic samples based on gadolinium zirconate, which has a parabolic character, where the CTE was $9\cdot10^{-6}$ K^{-1} at 673 K and $10.5\cdot10^{-6}$ K^{-1} at 1473 K temperature. For europium hafnate ($Eu_2Hf_2O_7$), the average value of CTE in the temperature range of 400–1200 K was $9.75\cdot10^{-6}$ K^{-1} [31], while the corresponding value for gadolinium hafnate ($Gd_2Hf_2O_7$) at 673 K of ~$12\cdot10^{-6}$ K^{-1} decreased to $11.3\cdot10^{-6}$ K^{-1} at 1473 K [32].

CONCLUSIONS

By contacting zirconium and hafnium hydroxides with europium and gadolinium acetates, single-phase REE zirconates and hafnates of the composition $Eu_{2-x}Gd_xZr_2O_7$ and $Eu_{2-x}Gd_xHf_2O_7$ were obtained under microwave heating conditions at x = 0.5, 1.0, 1.5. X-ray phase analysis confirmed the presence of fluorite structure in all samples following thermal treatment at 1473 K. Heat treatment at 1773 K leads to the formation of complex europium-gadolinium hafnates $Eu_{2-x}Gd_xHf_2O_7$ having a pyrochlore structure. The unit cell and volume parameters were calculated for all phases. The results demonstrate that the increased gadolinium content in the synthesized phases leads to a linear decrease in the unit cell parameter a and consequent decrease in its volume. At the same time, the specific surface of the obtained powders does not exceed 1 m^2/g. The results of CTE measurements demonstrated that the dependence of the ratio of the size difference to the initial size of the sample on the heating temperature, along with the linear decrease in CTE with increasing gadolinium content in the samples, has a linear character.

Acknowledgments

The study was conducted using the equipment of the Center for Collective Use at the RTU MIREA with support of the Ministry of Science and Higher Education of the Russian Federation.

The authors thank the staff of Laboratory No. 30 (Leading Researcher, Cand. Sci. (Chem.) L.I. Podzorova, Senior Researcher A.A. Ilyicheva, researchers O.I. Penkova and N.A. Mikhailina) for assistance in obtaining ceramic materials; Senior Researcher of the Laboratory No. 33, Cand. Sci. (Eng.) A.S. Lysenkov for assistance in studying the CTE; Senior Researcher of the Laboratory No. 4 at the A.A. Baikov Institute of Metallurgy of the Russian Academy of Sciences Cand. Sci. (Eng.) A.A. Konovalov for assistance in BET measurement.

Authors' contributions

N.V. Grechishnikov—conducting experimental studies, preparing the manuscript text, preparing materials for publication.

E.E. Nikishina—editing the manuscript text, preparing materials for publication, general supervision of the work.

The authors declare no conflict of interest.

REFERENCES

1. Lashmi P.G., Ananthapadmanabhan P.V., Unnikrishnan G., Aruna S.T. Present status and future prospects of plasma sprayed multilayered thermal barrier coating systems. *Eur. Ceram. Soc.* 2020;40(8):2731–45. https://doi.org/10.1016/j.jeurceramsoc.2020.03.016
2. Stanek C.R., Jiang C., Uberuaga B.P., Sickafus K.E., Cleave A.R., Grimes R.W. Predicted structure and stability of $A_4B_3O_{12}$ δ-phase compositions. *Phys. Rev. B.* 2019;80(17):174101. https://doi.org/10.1103/PhysRevB.80.174101
3. Sankar J., Kumar S. Synthesis of Rare Earth Based Pyrochlore Structured ($A_2B_2O_7$) Materials for Thermal Barrier Coatings (TBCs)-A Review. *Curr. Appl. Sci. Technol.* 2021;21(3):601–617. https://doi.org/10.14456/cast.2021.47
4. Salazar-Zertuche M., Díaz-Guillén J.A., Acosta-García J.O., Díaz-Guillén J.C., Montemayor S.M., Burciaga-Díaz O., Bazaldua-Medellin M.E., Fuentes A.F. Ionic conductivity of $Ln_4Zr_3O_{12}$ solid electrolytes synthesized by mechanochemistry. *Int. J. Hydrogen Energy.* 2019;44(24):12500–12507. https://doi.org/10.1016/j.ijhydene.2018.11.141
5. Popov V.V., Menushenkov A.P., Yaroslavtsev A.A., Zubavichus Y.V., Gaynanov B.R., Yastrebtsev A.A., Leshchev D.S, Chernikovet R.V. Fluorite-pyrochlore phase transition in nanostructured $Ln_2Hf_2O_7$ (Ln = La–Lu). *J. Alloys Compd.* 2016;689:669–679. https://doi.org/10.1016/j.jallcom.2016.08.019
6. Popov V.V., Menushenkov A.P., Zubavichus Y.V., *et al.* Studying processes of crystallization and cation ordering in $Eu_2Hf_2O_7$. *Russ. J. Inorg. Chem.* 2015;60(5):602–609. https://doi.org/10.1134/S0036023615050162
[Original Russian Text: Popov V.V., Menushenkov A.P., Zubavichus Y.V., Yaroslavtsev A.A., Veligzhanin A.A., Kolyshkin N.A., Kulik E.S. Studying processes of crystallization and cation ordering in $Eu_2Hf_2O_7$. *Zhurnal neorganicheskoi khimii.* 2015;60(5):672–680 (in Russ.). https://doi.org/10.7868/S0044457X15050165]
7. Popov V.V., Zubavichus Y.V., Menushenkov A.P., *et al.* Short- and long-range order balance in nanocrystalline $Gd_2Zr_2O_7$ powders with a fluorite-pyrochlore structure. *Russ. J. Inorg. Chem.* 2014;59(4):279–285. https://doi.org/10.1134/S0036023614040147

[Original Russian Text: Popov V.V., Zubavichus Y.V., Menushenkov A.P., Yaroslavtsev A.A., Kulik E.S., Petrunin V.F., Timofeeva N.N. Short- and long-range order balance in nanocrystalline $Gd_2Zr_2O_7$ powders with a fluorite-pyrochlore structure. *Zhurnal neorganicheskoi khimii*. 2014;59(4):431–438 (in Russ.).]

8. Sadykov V., Shlyakhtina A., Lyskov N., Sadovskaya E., Cherepanova S., Eremeev N., Skazka V., Goncharov V., Kharitonova E. Oxygen diffusion in Mg-doped Sm and Gd zirconates with pyrochlore structure. *Ionics* (*Kiel*). 2020;26(9):4621–4633. https://doi.org/10.1007/s11581-020-03614-5
9. Chernov I.O., Kushtym A.V., Malykhin S.V,. Synthesis of Materials Based on Compounds of Rare Earth Elements With Titanium, Hafnium and Zirconium As Promising Neutron Absorbers for Nuclear Reactors. *Probl. Atomic Sci. Technol*. 2024;2024(4):64–78. http://doi.org/10.46813/2024-152-064
10. Torres-Rodriguez J., Gutierrez-Cano V., Menelaou M., Kaštyl J., Cihlář J., Tkachenko S., Gonzalez J., Kalmar J., Fabian I., Lazar I., Celko L., Kaiser J. Rare-Earth Zirconate $Ln_2Zr_2O_7$ (Ln: La, Nd, Gd, and Dy) Powders, Xerogels, and Aerogels: Preparation, Structure, and Properties. *Inorg. Chem.* 2019;58(21):14467–14477. https://doi.org/10.1021/acs.inorgchem.9b01965
11. Zhang A., Lü M., Yang Z., Zhou G., Zhou Y. Systematic research on $RE_2Zr_2O_7$ (RE = La, Nd, Eu and Y) nanocrystals: Preparation, structure and photoluminescence characterization. *Solid State Sci.* 2008;10(1):74–81. https://doi.org/10.1016/j.solidstatesciences.2007.07.037
12. Matovic B., Maletaskic J., Zagorac J., Pavkov V., Maki R., Yoshida K., Yano T. Synthesis and characterization of pyrochlore lanthanide (Pr, Sm) zirconate ceramics. *J. Eur. Ceram. Soc.* 2020;40(7):2652–2657. https://doi.org/10.1016/j.jeurceramsoc.2019.11.012
13. Zeng J., Wang H., Zhang Y.C., Zhu M.K., Yan H. Hydrothermal synthesis and photocatalytic properties of pyrochlore $La_2Sn_2O_7$ nanocubes. *J. Phys. Chem. C*. 2007;111(32):11879–11887. https://doi.org/10.1021/jp0684628
14. Wang Q., Cheng X., Li J., Jin H. Hydrothermal synthesis and photocatalytic properties of pyrochlore $Sm_2Zr_2O_7$ nanoparticles. *J. Photochem. Photobiol. A: Chemistry*. 2016;321:48–54. https://doi.org/10.1016/j.jphotochem.2016.01.011
15. Perera S.S., Munasinghe H.N., Yatooma E.N., Rabuffetti F.A. Microwave-assisted solid-state synthesis of $NaRE(MO_4)_2$ phosphors (RE = La, Pr, Eu, Dy; M = Mo, W). *Dalton Trans.* 2020;49(23):7914–7919. https://doi.org/10.1039/D0DT00999G
16. Fetter G., Bosch P., Lopez T. ZrO_2 and Cu/ZrO_2 Sol–Gel Synthesis in Presence of Microwave Irradiation. *J. Sol- Gel Sci. Technol*. 2002;23:199–203. https://doi.org/10.1023/A:1013983211564
17. Vanetsev A.S., Tretyakov Y.D. Microwave-assisted synthesis of individual and multicomponent oxides. *Russ. Chem. Rev*. 2007;76(5):397–413. https://doi.org/10.1070/RC2007v076n05ABEH003650
[Original Russian Text: Vanetsev A.S., Tretyakov Y.D. Microwave-assisted synthesis of individual and multicomponent oxides. *Uspekhi khimii.* 2007;76(5):435–453 (in Russ.). https://doi.org/10.1070/RC2007v076n05ABEH003650]
18. Długosz O., Szostak K., Banach M. Photocatalytic properties of zirconium oxide–zinc oxide nanoparticles synthesised using microwave irradiation. *Appl. Nanosci*. 2020;10(3):941–954. https://doi.org/10.1007/s13204-019-01158-3
19. Kucio K., Sydorchuk V., Khalameida S., Charmas B. Mechanochemical and microwave treatment of precipitated zirconium dioxide and study of its physical–chemical, thermal and photocatalytic properties. *J. Therm. Anal. Calorim*. 2022;147:253–262. https://doi.org/10.1007/s10973-020-10285-x
20. Batool T., Bukhari B.S., Riaz S., Batoo K.M., Raslan E.H., Hadi M. Microwave assisted sol–gel synthesis of bioactive zirconia nanoparticles–correlation of strength and structure. *J. Mech. Behav. Biomed. Mater*. 2020;112:104012. https://doi.org/10.1016/j.jmbbm.2020.104012
21. Mahendran N., Johnson Jeyakumar S., Jothibas M., Ponnar M., Muthuvel A. Synthesis, characterization of undoped and copper-doped hafnium oxide nanoparticles by sol–gel method. *J. Mater. Sci.: Mater. Electron*. 2022;33(13):10439–10449. https://doi.org/10.1007/s10854-022-08031-0
22. Grechishnikov N.V., Nikishina E.E., Il'icheva A.A., Podzorova L.I. Effect of microwave treatment on the phase composition of europium zirconate during dilution synthesis. *Tsvetnye Metally*. 2023;10:51–55 (in Russ.). https://doi.org/10.17580/tsm.2023.10.06
23. Fuentes A.F., O'Quinn E.C., Montemayor S.M., Zhou H., Lang M., Ewing R.C.. Pyrochlore-type lanthanide titanates and zirconates: Synthesis, structural peculiarities, and properties. *Appl. Phys. Rev.* 2024;11(2):021337. https://doi.org/10.1063/5.0192415
24. Talanov M.V., Talanov V.M. Formation of breathing pyrochlore lattices: Structural, thermodynamic and crystal chemical aspects. *CrystEngComm.* 2020;22(7):1176–1187. https://doi.org/10.1039/C9CE01635J
25. Shannon R.D. Revised effective ionic radii and systematic studies of interatomic distances in halides and chalcogenides. *Acta Cryst. Sect. A*. 1976;32(5):751–767. https://doi.org/10.1107/S0567739476001551
26. Saradhi M.P., Ushakov S.V., Navrotsky A. Fluorite-pyrochlore transformation in $Eu_2Zr_2O_7$ – Direct calorimetric measurement of phase transition, formation and surface enthalpies. *RSC Adv.* 2012;2(8):3328–3334. https://doi.org/10.1039/c2ra00727d
27. Pavlyuchkov D., Seidel J., Dzuban A., Savinykh G., Schreiber G. Heat capacity for the $Eu_2Zr_2O_7$ and phase relations in the ZrO_2–Eu_2O_3 system: Experimental studies and calculations. *Thermochim. Acta*. 2013;558:74–82. https://doi.org/10.1016/j.tca.2013.02.009
28. Liu X., Wang H., Wang W., Fu Z.. A prediction model of thermal expansion coefficient for cubic inorganic crystals by the bond valence model. *J. Solid. State. Chem.* 2021;299:122111. https://doi.org/10.1016/j.jssc.2021.122111
29. Kutty K.V., Rajagopalan S., Mathews C.K., Varadaraju U.V. Thermal expansion behaviour of some rare earth oxide pyrochlores. *Mater. Res. Bull*. 1994;29(7):759–66. https://doi.org/10.1016/0025-5408(94)90201-1
30. Liu Z, Shen Z, Liu G, He L, Mu R, Xu Z. Sm-doped $Gd_2Zr_2O_7$ thermal barrier coatings: Thermal expansion coefficient, structure and failure. *Vacuum*. 2021;190:110314. https://doi.org/10.1016/j.vacuum.2021.110314
31. Hagiwara T., Nomura K., Kageyama H. Crystal structure analysis of $Ln_2Zr_2O_7$ (*Ln* = Eu and La) with a pyrochlore composition by high-Temperature powder X-ray diffraction. *J. Ceram. Soc. Japan.* 2017;125(2):65–70. https://doi.org/10.2109/jcersj2.16248
32. Yang P., An Y., Yang D., Li Y., Chen J. Structure, thermal properties and hot corrosion behaviors of $Gd_2Hf_2O_7$ as a potential thermal barrier coating material. C*eram. Int.* 2020;46(13):21367–21377. https://doi.org/10.1016/j.ceramint.2020.05.234

About the Authors

Nikolay V. Grechishnikov, Postgraduate Student, K.A. Bol'shakov Department of Chemistry and Technology Rare Elements, M.V. Lomonosov Institute of Fine Chemical Technologies, MIREA – Russian Technological University (78, Vernadskogo pr., Moscow, 119454, Russia). E-mail: nklgrchshnkv@yandex.ru. Scopus Author ID 58683791100, https://orcid.org/0009-0003-9591-391X

Elena E. Nikishina, Cand. Sci. (Chem.), Associate Professor, K.A. Bol'shakov Department of Chemistry and Technology Rare Elements, M.V. Lomonosov Institute of Fine Chemical Technologies, MIREA – Russian Technological University (78, Vernadskogo pr., Moscow, 119454, Russia). E-mail: nikishina@mirea.ru. Scopus Author ID 6602839662, ResearherID O-7115-2014, RSCI SPIN-code 9403-2325, https://orcid.org/0000-0003-3579-2194

Об авторах

Гречишников Николай Владимирович, аспирант, кафедра химии и технологии редких элементов им. К.А. Большакова, Институт тонких химических технологий им. М.В. Ломоносова, ФГБОУ ВО «МИРЭА – Российский технологический университет» (119454, Россия, Москва, пр-т Вернадского, д. 78). E-mail: nklgrchshnkv@yandex.ru. Scopus Author ID 58683791100, https://orcid.org/0009-0003-9591-391X

Никишина Елена Евгеньевна, к.х.н., доцент, кафедра химии и технологии редких элементов им. К.А. Большакова, Институт тонких химических технологий им. М.В. Ломоносова, ФГБОУ ВО «МИРЭА – Российский технологический университет» (119454, Россия, Москва, пр-т Вернадского, д. 78). E-mail: nikishina@mirea.ru. Scopus Author ID 6602839662, ResearherID O-7115-2014, SPIN-код РИНЦ 9403-2325, https://orcid.org/0000-0003-3579-2194

Translated from Russian into English by H. Moshkov
Edited for English language and spelling by Thomas A. Beavitt

Tonkie Khimicheskie Tekhnologii = Fine Chemical Technologies.
2025;20(3):264–275
ISSN 2686-7575 (Online)

Chemistry and technology of inorganic materials
Химия и технология неорганических материалов

UDC 621.318.12
https://doi.org/10.32362/2410-6593-2025-20-3-264-275
EDN QSOBYJ

RESEARCH ARTICLE

Formation of the microstructure and properties of strontium hexaferrite magnets using powder injection molding

Bogdan D. Chernyshev[1,2,✉], **Igor V. Schetinin**[2]
[1] *State Research and Design Institute of Rare Metal Industry "Giredmet," Moscow, 111524 Russia*
[2] *National University of Science and Technology MISIS, Moscow, 119049 Russia*
✉ *Corresponding author, e-mail: BDmChernyshev@rosatom.ru*

Abstract

Objectives. The study set out to investigate the possibility of production strontium hexaferrite permanent magnets using powder injection molding (PIM) technology, which involves casting granules highly filled with ceramic powder. After obtaining the initial granulate based on organic binders and strontium hexaferrite powder, the material was cast in an injection molding machine to create the first intermediate (*green*) parts, followed by removal of the primary binder to obtain *brown* parts and final sintering.

Methods. Strontium hexaferrite powder was obtained by the ceramic method. The material underwent grinding in a planetary ball mill to obtain a powder having an average particle size of 13.4 μm, which is considered optimal for the applied PIM technology. Granulate materials, consisting of the obtained strontium hexaferrite powder combined with primary paraffin and secondary polyamide binders, were prepared by manual mixing of the components and used for creation of green parts in injection molding machine. Brown parts obtained following removal of binder from the obtained green parts were characterized by their higher brittleness and open pore structure. Permanent magnets with dimensions of 10 × 10 × 5 mm were obtained following sintering of brown parts in an oxidizing atmosphere.

Results. The more than 70% higher strength of the magnetic properties of the obtained strontium hexaferrite samples compared to isotropic barium hexaferrite-based magnets manufactured in accordance with GOST 24063-80 is due to the presence of pores after sintering.

Conclusions. The possibility of using the ceramic method for producing strontium hexaferrite powder for use in granulate manufacturing was demonstrated. This raw material can then be used to obtain strontium hexaferrite permanent magnets via PIM technology having 80% density.

Keywords
permanent magnet, strontium hexaferrite, PIM technology, granulate, microstructure, magnetic properties

Submitted: 06.10.2024
Revised: 17.01.2025
Accepted: 02.04.2025

For citation
Chernyshev B.D., Schetinin I.V. Formation of the microstructure and properties of strontium hexaferrite magnets using powder injection molding. *Tonk. Khim. Tekhnol. = Fine Chem. Technol.* 2025;20(3):264–275. https://doi.org/10.32362/2410-6593-2025-20-3-264-275

НАУЧНАЯ СТАТЬЯ

Формирование структуры и свойств магнитов на основе гексаферрита стронция, полученных с помощью технологии Powder Injection Molding

Б.Д. Чернышев[1,2,✉], И.В. Щетинин[2]

[1] *Государственный научно-исследовательский и проектный институт редкометаллической промышленности «Гиредмет» имени Н.П. Сажина, Москва, 111524 Россия*

[2] *Национальный исследовательский технологический университет «МИСИС» (НИТУ МИСИС), Москва, 119049 Россия*

✉ *Автор для переписки, e-mail: BDmChernyshev@rosatom.ru*

Аннотация

Цели. Изучить возможность получения постоянных магнитов на основе гексаферрита стронция с помощью технологии Powder Injection Molding (PIM), заключающейся в литье гранулятов, высоконаполненных керамическим порошком. Данный процесс состоит из операций получения гранулята (исходного сырья на основе органического связующего и порошка гексаферрита стронция), литья гранулята в термопластавтомате для создания первых промежуточных («зеленых») деталей, последующего удаления связки из них, получения «коричневых» деталей и финального спекания.

Методы. Порошок гексаферрита стронция получен керамическим методом. Материал прошел стадию помола в планетарной шаровой мельнице до получения порошка со средним размером частиц 13.4 мкм, который считается оптимальным размером для PIM-технологии. На основе полученного порошка гексаферрита стронция, первичного связующего — парафина и вторичного — полиамида методом ручного смешивания компонентов подготовлен гранулят для создания «зеленых» деталей. Полученные детали подвергли операции удаления связующего — дебиндингу, в результате которого изготовили «коричневые» заготовки, отличающиеся более высокой хрупкостью и наличием структуры открытых пор. Постоянные магниты с размерами 10 × 10 × 5 мм получены методом спекания «коричневых» деталей в окислительной атмосфере.

Результаты. Уровень магнитных параметров образцов на основе гексаферрита стронция составил более 70% от значений, характерных для промышленных изотропных магнитов на основе гексаферрита бария в соответствии ГОСТ 24063-80, что обусловлено наличием пор в спеченных изделиях.

Выводы. Установлена возможность применения керамического метода для производства порошка гексаферрита стронция, который может быть использован при изготовлении гранулята. Использование данного сырья позволяет изготавливать магниты методом PIM-технологии с плотностью не менее 80%.

Ключевые слова

постоянный магнит, гексаферрит стронция, PIM-технология, гранулят, микроструктура, магнитные свойства

Поступила: 06.10.2024
Доработана: 17.01.2025
Принята в печать: 02.04.2025

Для цитирования

Чернышев Б.Д., Щетинин И.В. Формирование структуры и свойств магнитов на основе гексаферрита стронция, полученных с помощью технологии Powder Injection Molding. *Тонкие химические технологии*. 2025;20(3):264–275. https://doi.org/10.32362/2410-6593-2025-20-3-264-275

INTRODUCTION

Many areas of contemporary technical development rely on the use of hard magnetic materials. These materials are used to produce permanent magnets (PMs), which are used to create diverse products for special and general purposes, including electric motors, generators, sensors, acoustic systems and medical devices. Under industrial conditions, such materials are widely used in magnetic grippers, lifting mechanisms, mixers, and various kinds of sensor.

The strict quality requirements and continuous improvement of special-purpose products impose a number of limitations on magnetically hard materials for use in the creation of PMs. These include high operating—and consequent Curie point—temperatures, as well as higher values of tensile strength σ_B, relative elongation δ, and corrosion resistance. PMs based on rare-earth materials (REM) of Sm–Co system operate at temperatures of about 350–550°C. The class of magnetically hard materials based on alloys of

Fe–Cr–Co systems is characterized by the presence of an effective combination of magnetic parameters (residual induction B_r = 1.1 T and coercive force by induction H_C^B = 38 kA/m) and mechanical properties (tensile strength σ_B = 785 MPa and relative elongation δ = 3%) [1]. The achievement of a high level of magnetic properties of these types of PM is generally preceded by a stage of prolonged thermal and thermomagnetic processing.

Of all the PM materials produced onto the global market, Nd–Fe–B (neodymium) alloys have the highest magnetic energy product (the product of induction B and coercive force H $(BH)_{max}$), allowing the dimensions of manufactured equipment to be maximally reduced. This can be especially relevant in the production of various consumer goods. However, the significant disadvantages of materials of this system included its low operating temperatures (200–300°C, depending on the brand) as well as the high complexity of the production process, which is associated with the high activity of REMs [2, 3]. In view of these facts, a significant segment of the PM market (more than 25%) is occupied by products based on barium and strontium hexaferrites, which have a relatively low magnetic energy product compared to the Nd–Fe–B system, but are characterized by increased corrosion and chemical resistance. At the same time, the cost of raw materials for the production of ferrite PM is significantly lower as compared to REM-based materials, as well as those based on Co [4].

Strontium hexaferrite is a promising material for hyperthermic processes, which are only applicable in the case of nanosized particles [5]. In [6], particles having grain sizes of the order of 30–40 nm were obtained by using the sol–gel method. Nanoscale compositions can also be obtained by solution combustion of organo-nitrate precursors [7], synthesis from oxide glasses [8], self-propagating high-temperature synthesis [9], and hydrothermal methods [10]. However, the classical approach for obtaining strontium hexaferrite powders used in the creation of PMs is still the ceramic method, which consists of the operations of ferritization and grinding of the material to particles with the required fraction at the level of 1–10 μm [11].

PMs based on basic magnetically hard materials, among which the Nd–Fe–B, Sm–Co, Sr–Fe–O systems are distinguished, are generally produced using powder metallurgy methods [12, 13]. A number of materials based on Fe–Cr–Co and Al–Ni–Co alloys are obtained by investment casting [14]. The formation of a highly coercive state of these alloys is achieved in the process of spinodal decomposition of the main phase into strongly and weakly magnetic phases through the use of thermomagnetic processing technology. The use of these approaches is typical for the organization of large-scale production of magnets having predominantly simple shapes (ring, sector, etc.). However, miniaturization and complication of designs of existing devices and magnetic systems can complicate the product geometry [15]. When changing the configuration using traditional technological approaches, machining methods are applied. Their use not only requires the availability of facilities and a fairly large fleet of equipment, but also leads to a sharp decrease in the material utilization factor (MUF) to the level of about 40%. In order to reduce the costs of magnet manufacturing, the resulting large quantities of grinding waste containing expensive rare-earth metals must be re-extracted and reintroduced into the production cycle [16].

Powder injection molding (PIM) technologies are being widely introduced to increase MUF by reducing the need for machining. The PIM method is based on the pressing of products from a granulate consisting of an organic binder highly filled with metal or ceramic powder. Further, the pressed intermediate parts undergo binder removal (debinding) and sintering stages [17]. Using this approach, the production of complex configurations weighing up to 1 kg is ensured, allowing MUF to be increased to values of about 97–99% [18]. Consequently, it is rational to produce permanent magnets based on rare-earth metals using PIM technology.

Since this method is expedient for the production of large batches of products, it is possible to use additive manufacturing technologies to develop processes and obtain unique magnets on a laboratory scale. The results of using the selective laser melting method to create magnetic systems based on several materials have already been obtained [15]. The main disadvantage of selective laser melting is the cost of PM printing equipment, as well as high requirements as to the purity and size distribution of initial powders. The main competitor of this technology is stereolithography, which is successfully used to create ceramics by printing photopolymers highly filled with ceramic powders [19]. The process of adding the powder composition into the photopolymer, which is similar to the processes that take place during the preparation of granulates for PIM technology, can be performed using different methods for mixing the starting materials. Due to the high fluidity of photopolymers, this process does not require heating [20].

The aim of the present study is to investigate the microstructure and magnetic properties of powders based on strontium hexaferrite and permanent magnets obtained using PIM technology.

EXPERIMENTAL METHOD

Strontium hexaferrite powder was produced by solid-phase synthesis. At the first stage, initial components comprising hematite and strontium carbonate with a purity no less than 99.5 wt % were mixed in the Turbula mixer of the *Techno-Center* company (Russia), after which the synthesis of the required phase of strontium hexaferrite was carried out at 1200°C for 5 h. The obtained powder was milled in a planetary ball mill (*Techno-Center*, Russia) for at least 5 h. Control of the average size of powder compositions was carried out using an Analysette 22 MicroTec plus laser particle size analyzer (*Fritsch*, Germany). Analysis of magnetic properties of powder compositions was carried out using a VSM-250 vibromagnetometer (*Changchun*, China), which can analyze materials in fields up to 2 T.

The obtained strontium hexaferrite powder compositions were processed into a granulate to which a binder based on paraffin, polyamide, and additional technological additives was added manually and using an industrial granulator. Compacting of granulates was carried out on a thermoplastic automatic machine at the softening temperature of the binder. Investigation of the presence of internal defects of green parts was carried out using the tomography method.[1]

Removal of the primary paraffin-based binder from the intermediate parts was carried out by solution debinding methods. Acetone, hexane, and perchloroethylene (*Ekos-1*, Russia) were used as the main solvents. The change in the mass of parts and the amount of removed binder during debinding was determined using M-ER 123 ACFJR-600.01 Sensomatic TFT scales (*Mertech Equipment*, South Korea).

Sintering of the following intermediate parts, which are referred to as brown body samples, was carried out in an oxidizing environment in a PMV-1600p muffle furnace (*Bossert*, Russia) at a temperature not lower than 1210°C for 2 h. After binder removal and sintering, the samples had the shape of a parallelepiped with dimensions of 10 × 10 × 5 mm. The density of magnets after sintering was determined using a helium pycnometer (*Micromeritics*, USA).

The microstructure of the strontium hexaferrite powders, granulate, intermediate parts and sintered magnets was analyzed using TM-3000 scanning electron microscope (SEM) by *Hitachi* (Japan) and FEI quanta 200 F Feg 250 SEM (*FEI*, USA) with EDAX energy dispersive analyzer (*Octane Elect*, USA). Phase analysis was performed using a DRON-4 X-ray diffractometer (*Burevestnik*, Russia). Processing and analysis of the obtained data was carried out using a PDXL specialized software package (Rigaku[2]) and PDF-2 database[3]. Quantitative phase analysis was performed using the Rietveld method. Magnetic hysteresis loops of permanent magnet samples were measured using a MN-50 hysteresisgraph (*Walker Scientific Inc.*, USA). Chemical analysis of the samples was performed using an iCAP 6300 inductively coupled plasma atomic emission spectrometer (*Thermo Fisher Scientific*, USA). A LECO SC844 carbon and sulfur analyzer (USA) was used to study the contamination of permanent magnets with organic binder.

RESULTS AND DISCUSSION

According to the SEM analysis, the particle sizes of the powder, which passed the synthesis stage at 1200°C for 5 h, do not exceed 3–4 μm; the particles themselves often have the shape of hexagonal prisms (Fig. 1). However, in the process of high-temperature synthesis, sintering of the powder occurred with the formation of large agglomerates.

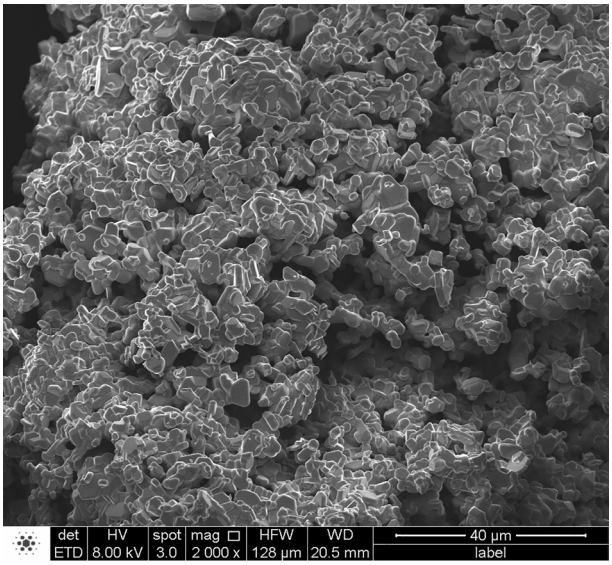

Fig. 1. Strontium hexaferrite microstructure after sintering during 5 h at temperature of 1200°C

[1] The names and manufacturers of the industrial pelletizer, thermoplastic automatic machine, tomograph, as well as the name and properties of the binder are trade secrets and cannot be published in the article.

[2] https://rigaku.com/. Accessed March 11, 2025.

[3] https://www.icdd.com/pdf-2/. Accessed March 11, 2025.

Since the use of the obtained material for obtaining products by PIM and stereolithography methods is impossible due to the obvious coarseness of the particles, their size should be reduced. For this purpose, fine grinding of the obtained materials was carried out. A snapshot of the microstructure of strontium hexaferrite powder after fine grinding is presented in Fig. 2.

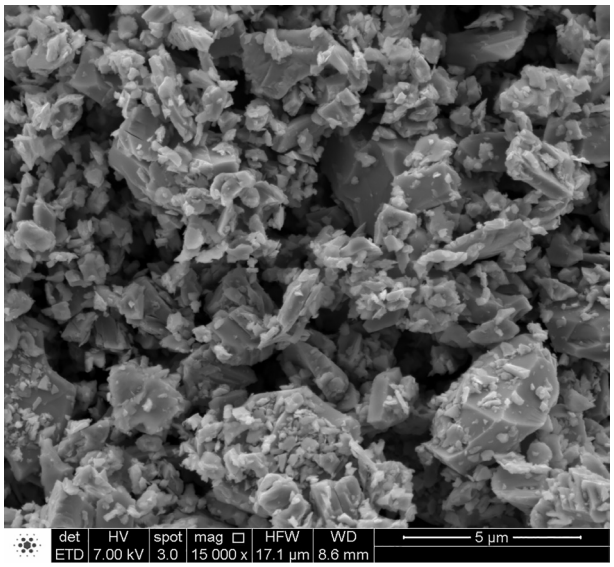

Fig. 2. Microstructure of strontium hexaferrite after grinding in a planetary ball mill

The shape of the powder based on strontium hexaferrite is predominantly splintered as a consequence of the material grinding process. It was found that crystallites with sizes less than 1 µm were formed during the grinding process, whose presence in the powder structure contributes to the achievement of high magnetic properties [21], which is due to the single-domain sizes of hexaferrite particles, which are in the range of 300–600 nm.

The magnetic properties of the strontium hexaferrite powder composition following fine grinding were as follows: specific saturation magnetization σ_s = 70.3 A·m^2/kg; specific residual saturation magnetization σ_r = 37.2 A·m^2/kg; coercive force by magnetization H_C^M = 303.9 kA/m (Fig. 3).

A laser particle analyzer was used to determine that the average particle size of the powder composition based on the material of the Sr–Fe–O system was 13.4 µm. The particle sizes of this powder composition are in the range from 500 nm to 25 µm. Powder with this particle size distribution is considered as an optimal raw material for the formation of feedstocks according to the PIM method. This is due to the fact that powders with sizes up to 20–25 µm can be used to produce granulates with the required yield parameters on their basis [20]. In this case, nanosized particles will fill the pores between

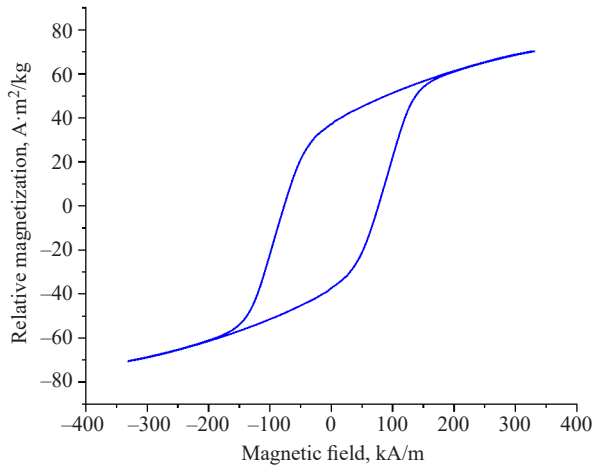

Fig. 3. Hysteresis loop of a strontium hexaferrite powder after fine grinding for 10 h

large particles. Powders of the obtained granulometric composition can also be used as a feedstock for the creation of photopolymers used in 3D printing of products by stereolithography. The particle size of this powder composition does not exceed the thickness of the printing layer, which is predominantly in the range of 20 to 50 µm [22, 23].

Figure 4 depicts an SEM image of the granulate showing particles of strontium hexaferrite powder located in a polymer matrix based on paraffin and polyamide. The contrast of light ceramic particles against the dark background of the binder shows a strong difference in the atomic numbers of chemical elements of the substances. From this it may be concluded that there are quite large areas in the feedstock structure, to which the powder was hindered in the mixing process. This is due to the peculiarities of granulate preparation, which was obtained by manual mixing of initial components.

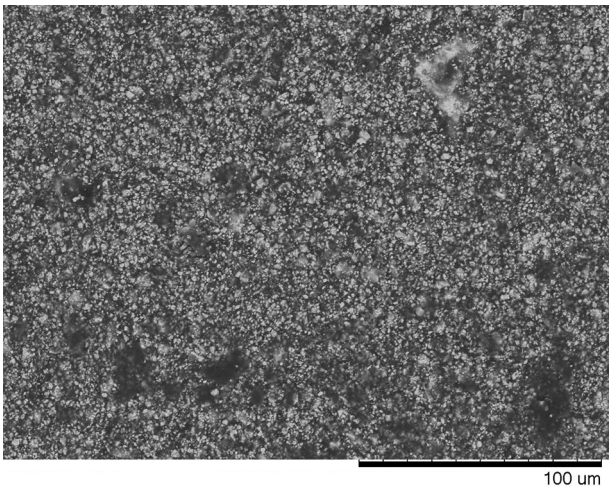

Fig. 4. Microstructure of granulate consist of strontium hexaferrite powder

The tomography results of the green body samples obtained from strontium hexaferrite are shown in Fig. 5.

Fig. 5. Tomography of strontium hexaferrite permanent magnet green body samples with lack of fusion (a, b) and without defects (c)

In the course of testing the process of obtaining green parts, the modes of granulate pouring into the mold of the injection molding machine were changed. Increasing the pressing pressure[4] allowed defects from the intermediate parts to be removed with lack of fusion, which were formed as a result of non-slip flows of molten binder of reduced liquid flowability (Figs. 5a and 5b). Green parts obtained under the modified regime were characterized by minimal porosity, indicating the possibility of their further use in order to obtain high-quality magnets at the final stage of the PIM process. Here, the magnetic (product of induction B and coercive force H $(BH)_{max}$, coercive force by induction H_C^B and magnetization H_C^M, residual induction B_r) and mechanical properties (tensile strength σ_B, relative elongation δ) will depend solely on the quality of the initial raw material. SEM images of the microstructure of the green parts, which were classified by tomography as having no internal defects, are presented in Fig. 6.

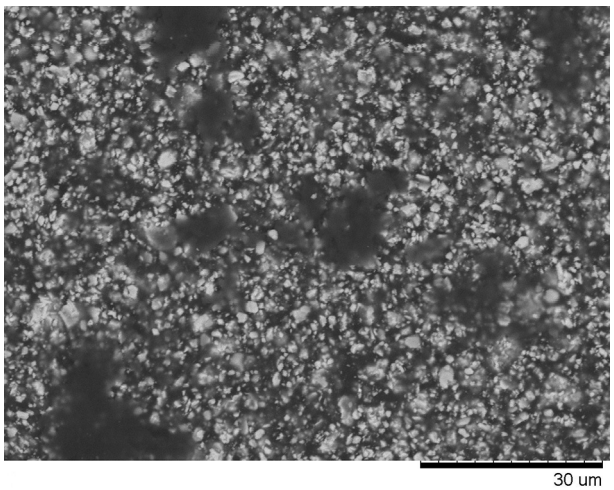

Fig. 6. Microstructure of strontium hexaferrite permanent magnet green body sample

These images show that the microstructure of the green part inherits the structure of the granulate: while particles of strontium hexaferrite powder are evenly distributed in the body of the intermediate part, there are significant areas to which the powder has not penetrated. The size of such areas reaches 30–40 μm in diameter. The presence of this defect is undesirable since the removal of the primary binder at the next stage of debinding can lead to the formation of large pores, which can not only remain in the final product, but also lead to warping and cracking of parts during shrinkage due to the weakening of the framework based on the secondary binder, mainly consisting of polyamide.

In the process of selecting the most effective medium and parameters for removing polyamide from the intermediate body samples, a plot of the green part mass variation was obtained over time, as shown in Fig. 7.

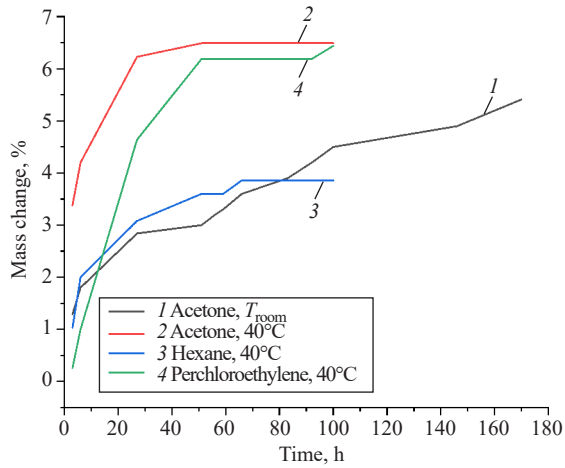

Fig. 7. Mass change of strontium hexaferrite permanent magnet green bodies samples during the debinding process depending on duration of debinding stage

Based on the obtained dependence, it can be concluded that the optimal media for removal of the primary binder are perchloroethylene and acetone. Nevertheless, it is desirable to accelerate the process of interaction between the green parts and the solvent by increasing the ambient temperature up to 40°C. Samples that underwent the debinding stage in acetone at room temperature (20°C) contained primary binder at the level of 1–2 wt % even after 170 h of exposure. In comparison with the results of works devoted to the study of effective debinding modes, the use of hexane did not lead to a positive result: soaking for 100 h allowed removal of only 4 wt % of the binder [24, 25]. Furthermore, the solvent interacted actively with the part, which led to the formation of a white scale on its surface. This is

[4] The nature of the change of granulate pouring modes and the value of increasing pressing pressure are commercial secrets and cannot be published in the article.

due to the fact that the dissolution of paraffin in hexane is a heterogeneous procedure, which is observed at the phase interface between liquid and solid substances with possible precipitation [26].

A snapshot of the microstructure of the brown body sample that was obtained from the green part during debinding is shown in Fig. 8.

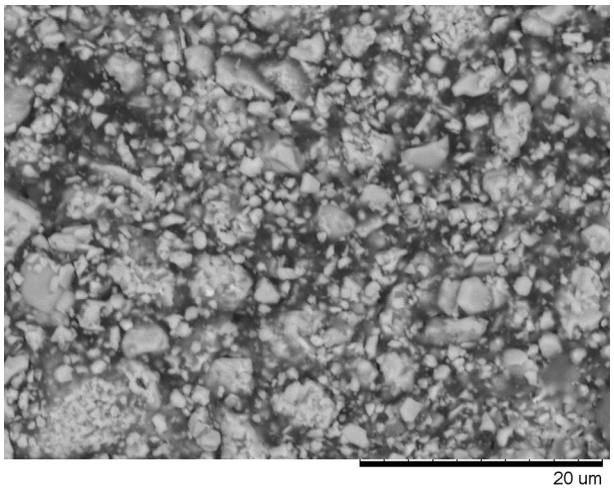

Fig. 8. Microstructure of strontium hexaferrite permanent magnet brown body sample

The resulting image shows that the second intermediate body samples also consist of strontium hexaferrite powder and organic binder. In contrast to the structure of the granulates and green parts, the brown body samples do not contain a primary binder. At this stage, the secondary binder acts as a framework, which makes the intermediate parts more brittle. The structure of the brown part is characterized by the presence of interconnected open pores necessary to ensure uniform shrinkage during the sintering stage.

Magnets with the required geometry of 10 × 10 × 5 mm were obtained by sintering of brown parts based on strontium hexaferrite. Analysis of the content of impurities in the samples after sintering showed that the material was not contaminated with carbon, which is often included in the parts made of various materials from the binder: its percentage was 0.014 wt %. This fact indicates that the binder based on paraffin and polyamide can be used to create clean materials by PIM technology.

The density of magnets based on strontium hexaferrite after sintering was 4.2 g/cm^3, which is 80% of the theoretical value [27]. It is likely that a density close to the theoretical one can be achieved by using industrial equipment for mixing powders and organic binder, which will permit uniform distribution of particles inside the granulate and green parts.

Magnetic properties of bulk samples based on strontium hexaferrite powder for the alloy obtained by PIM technology were as follows: residual induction B_r = 0.12 T; coercive force by induction H_C^B = 85.7 kA/m; coercive force by magnetization H_C^M = 298.4 kA/m. The magnetization coercive force exceeded the value established by the requirements of normative and technical documentation for isotropic permanent magnets based on barium hexaferrite[5]. However, the values of residual induction and coercive force by induction remained at the level of 70% of the values specified in the normative and technical literature. An increase in the level of coercive force can be achieved primarily by reducing the sintering time of magnets: by this means, the growth of individual crystallites, which in this case act as single-domain particles, will be prevented.

Despite the absence of major defects in the form of geometry changes or cracks in the parts based on strontium hexaferrite, the degradation of magnetic properties compared to the original powder is due to defects in the microstructure of the parts that have passed the sintering stage (Fig. 9).

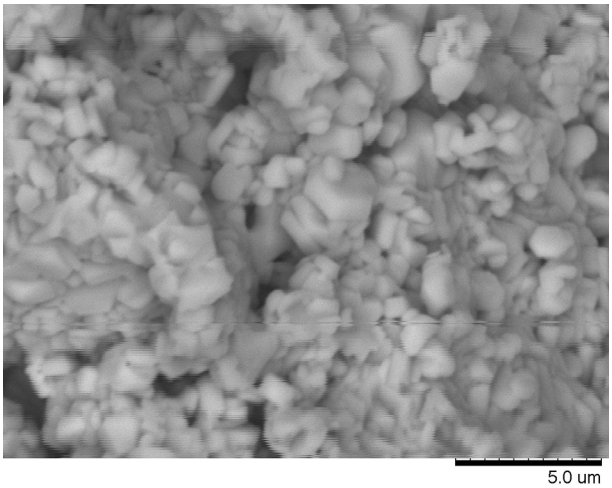

Fig. 9. Microstructure of sintered strontium hexaferrite permanent magnet obtained by PIM technology

The SEM images show that the final product is represented as a large number of large agglomerates, which are formed in the process of sintering of fine-grained single-domain powder. Between the agglomerates, pores with sizes of about 2–4 μm are noticeable, which could not be removed during high-temperature processing. The presence of pores, which negatively affect not only the

[5] GOST 24063-80. State Standard of the USSR. Magnetically hard ferrites. Brands and main parameters. Moscow: USSR State Committee for Standards; 1986. 14 p.

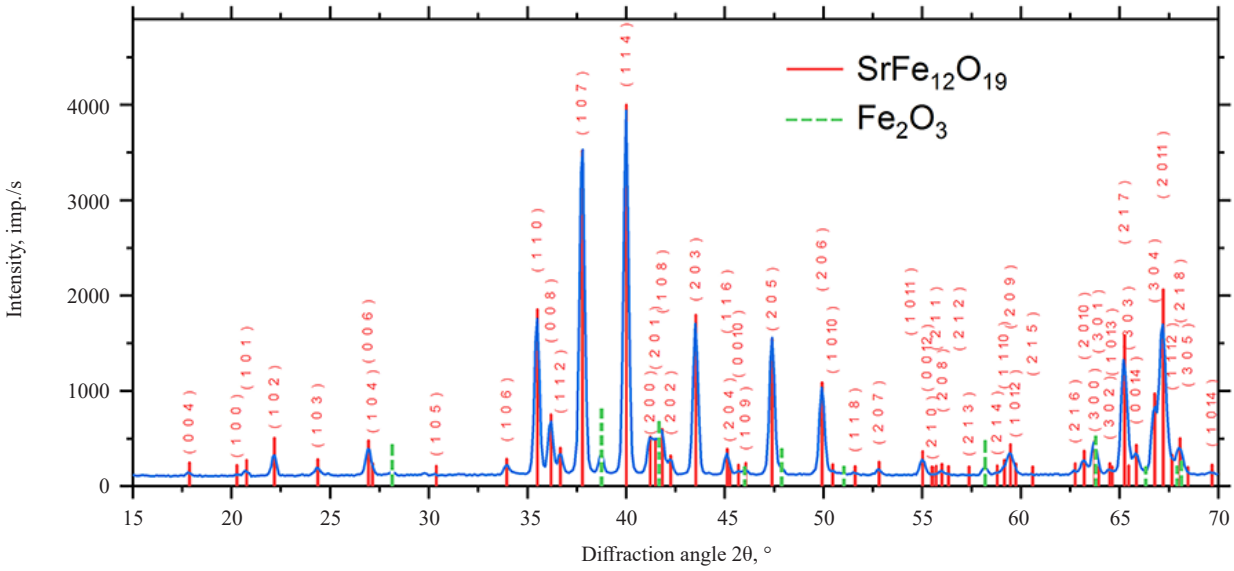

Fig. 10. X-ray diffraction of strontium hexaferrite permanent magnet obtained by PIM technology

mechanical and functional but also magnetic properties, can be prevented by preparing the raw material using sufficient powder quantity (from 4 kg) and industrial granulators. This problem can also be solved by hot isostatic pressing, which allows fixing microcracks and pores to increase the density and mechanical properties of the parts [28].

It is likely that magnetic parameters of the sintered product can be further enhanced by reducing the time of holding the material in the sintering process. This will prevent the growth of single-domain crystallites and preserve the structure of the final part to be more similar to that of the initial raw material.

In the process of studying the phase composition of magnets after sintering, an additional factor of magnetic properties reduction was revealed. On the X-ray diffractogram of the sample of permanent magnet based on strontium hexaferrite, as shown in Fig. 10, there are additional lines of hematite Fe_2O_3, the content of which in the sample was equal to 2 wt %. The amount of the main ferromagnetic phase $SrFe_{12}O_{19}$ amounted to 98 wt %.

CONCLUSIONS

In the process of studying the microstructure and magnetic properties of strontium hexaferrite powder, it was confirmed that the proposed technology used to obtain this material can be used for manufacturing raw materials for PIM technology and stereolithography.

The control of intermediate and final parts obtained by injection molding of granulates highly filled with ceramic powder led to the conclusion that the PIM method is a promising technology for the production of permanent magnets based on strontium hexaferrite. However, for the industrial implementation of this method, the granulate production processes will need to be optimized. This will be realized in further research through the use of specialized equipment for granulate production. Industrial equipment for production of raw materials, which should work in a continuous mode, requires powder loading in the amount of 2–3 kg to provide a more uniform distribution of strontium hexaferrite particles in the binder based on polyamide and paraffin. Furthermore, in comparison with the method of manual mixing, the use of a granulator will eliminate human influence on the homogeneity of the distribution of powder particles to obtain a high quality granulate. The sintering mode of brown parts may also be optimized in order to prevent the formation of pores and growth of single-domain particles of strontium hexaferrite. This can be achieved by lowering the sintering temperature and reducing the heating rate in the section up to 500°C, during which the removal of secondary binder and technological additives takes place.

By developing this process using granulate filled with strontium hexaferrite powders and solving the above problems, it will probably be possible to use this material as a binder for the development of feedstock based on Sm–Co alloy powders and for the production of grade KS25 rare-earth permanent magnets.

Acknowledgments

The work was financially supported by the Russian Science Foundation, project No. 23-73-00114.

Authors' contributions

B.D. Chernyshev—synthesis of strontium hexaferrite powder, production of permanent magnets by PIM technology, processing the results, and writing the text of the article.

I.V. Schetinin—analysis of the microstructure, phase composition, and magnetic properties of samples.

The authors declare no conflicts of interest.

REFERENCES

1. Altafia M., Sharifia E.M., Ghasemi A. The effect of various heat treatments on the magnetic behavior of the Fe-Cr-Co magnetically hard alloy. *J. Magn. Magn. Mater*. 2020;507:166837. https://doi.org/10.1016/j.jmmm.2020.166837
2. Takagi K., Soda R., Jinno M., Yamaguchi W. Possibility of high-performance $Sm_2Fe_{17}N_3$ sintered magnets by low-oxygen powder metallurgy process. *J. Magn. Magn. Mater*. 2020;506:166811. https://doi.org/10.1016/j.jmmm.2020.166811
3. Pandian S., Chandrasekaran V., Markandeyulu G., Iyer K.J.L., Rama Rao K.V.S. Effect of Co, Dy and Ga on the magnetic properties and the microstructure of powder metallurgically processed Nd–Fe–B magnets. *J. Magn. Magn. Mater*. 2004;364(1–2):295–303. https://doi.org/10.1016/S0925-8388(03)00541-3
4. Luk P.C.-K., Abdulrahem H.A., Xia B. Low-cost high-performance ferrite permanent magnet machines in EV applications: A comprehensive review. *eTransportation*. 2020;6: 100080–100093. https://doi.org/10.1016/j.etran.2020.100080
5. Najafinezhad A., Abdellahi M., Samandari S.S., Ghayour H., Khandan A. Hydroxyapatite- M-type strontium hexaferrite: A new composite for hyperthermia applications. *J. Alloys Compound.* 2018;734:290–300. https://doi.org/10.1016/j.jallcom.2017.10.138
6. Kumar S.S., Kumar R.S., Kumari P., Ranga N., Manash A., Kumari R. Structural, ferromagnetic, ferroelectric, and bio-medical behaviour of yttrium doped strontium hexaferrite ($SrFe_{12-x}Y_xO_{19}$) nano materials, assisted with sol–gel cost effective technique. *Physica Scripta.* 2023;98(11):115015. https://doi.org/10.1088/1402-4896/acfce7
7. Ostroushko A.A., Gagarin I.D., Kudyukov E.V., *et al.* Preparation of strontium hexaferrite based materials by solution combustion: the effect of charges arising in precursors and an external magnetic field. *Russ. J. Inorg. Chem.* 2024;69(2): 141–150. https://doi.org/10.1134/s003602362360301x [Original Russian Text: Ostroushko A.A., Gagarin I.D., Kudyukov E.V., Zhulanova T.Y., Permyakova A.E., Russkikh O.V. Preparation of strontium hexaferrite based materials by solution combustion: the effect of charges arising in precursors and an external magnetic field. *Journal of Inorganic Chemistry = Zhurnal neorganicheskoi khimii*. 2024;69(2): 143–154 (in Russ.). https://doi.org/10.31857/S0044457X24020013]
8. Zaitsev D.D., Kazin P.E., Gravchikova E.A., Trusov L.A., Kushnir S.E., Tretyakova Y.D., Jansen M. Synthesis of magnetic glass ceramics containing fine $SrFe_{12}O_{19}$ particles. *Mendeleev Communications.* 2004;14(4):171–173. https://doi.org/10.1070/MC2004v014n04ABEH001971
9. Jing Y., Jia L., Zhenga Y., Zhanga H. Hydrothermal synthesis and competitive growth of flake-like M-type strontium hexaferrite. *RSC Adv.* 2019;57(9):33388–33394. https://doi.org/10.1039/C9RA06246G
10. Shirmahd H., Aboutalebi M., Seyedein S.H., Adeli M. Synthesis of strontium hexaferrite ($SrFe_{12}O_{19}$) by self-propagating high-temperature synthesis (SHS) method and investigation of the effect of milling on morphology and magnetic properties. *Ceram. Int.* 2024;50(20):38542–38549. https://doi.org/10.1016/j.ceramint.2024.07.222

СПИСОК ЛИТЕРАТУРЫ

1. Altafia M., Sharifia E.M., Ghasemi A. The effect of various heat treatments on the magnetic behavior of the Fe-Cr-Co magnetically hard alloy. *J. Magn. Magn. Mater*. 2020;507:166837. https://doi.org/10.1016/j.jmmm.2020.166837
2. Takagi K., Soda R., Jinno M., Yamaguchi W. Possibility of high-performance $Sm_2Fe_{17}N_3$ sintered magnets by low-oxygen powder metallurgy process. *J. Magn. Magn. Mater*. 2020;506:166811. https://doi.org/10.1016/j.jmmm.2020.166811
3. Pandian S., Chandrasekaran V., Markandeyulu G., Iyer K.J.L., Rama Rao K.V.S. Effect of Co, Dy and Ga on the magnetic properties and the microstructure of powder metallurgically processed Nd–Fe–B magnets. *J. Magn. Magn. Mater*. 2004; 364(1–2):295–303. https://doi.org/10.1016/S0925-8388(03)00541-3
4. Luk P.C.-K., Abdulrahem H.A., Xia B. Low-cost high-performance ferrite permanent magnet machines in EV applications: A comprehensive review. *eTransportation*. 2020;6: 100080–100093. https://doi.org/10.1016/j.etran.2020.100080
5. Najafinezhad A., Abdellahi M., Samandari S.S., Ghayour H., Khandan A. Hydroxyapatite- M-type strontium hexaferrite: A new composite for hyperthermia applications. *J. Alloys Compound.* 2018;734:290–300. https://doi.org/10.1016/j.jallcom.2017.10.138
6. Kumar S.S., Kumar R.S., Kumari P., Ranga N., Manash A., Kumari R. Structural, ferromagnetic, ferroelectric, and bio-medical behaviour of yttrium doped strontium hexaferrite ($SrFe_{12-x}Y_xO_{19}$) nano materials, assisted with sol–gel cost effective technique. *Physica Scripta.* 2023;98(11):115015. https://doi.org/10.1088/1402-4896/acfce7
7. Остроушко А.А., Гагарин И.Д., Кудюков Е.В., Жуланова Т.Ю., Пермякова А.Е., Русских О.В. Получение материалов на основе гексаферрита стронция методом растворного горения: воздействие возникающих в прекурсорах зарядов и внешнего магнитного поля. *Журн. неорган. химии.* 2024;69(2):143–154. https://doi.org/10.31857/S0044457X24020013
8. Zaitsev D.D., Kazin P.E., Gravchikova E.A., Trusov L.A., Kushnir S.E., Tretyakova Y.D., Jansen M. Synthesis of magnetic glass ceramics containing fine $SrFe_{12}O_{19}$ particles. *Mendeleev Communications.* 2004;14(4):171–173. https://doi.org/10.1070/MC2004v014n04ABEH001971
9. Jing Y., Jia L., Zhenga Y., Zhanga H. Hydrothermal synthesis and competitive growth of flake-like M-type strontium hexaferrite. *RSC Adv.* 2019;57(9):33388–33394. https://doi.org/10.1039/C9RA06246G
10. Shirmahd H., Aboutalebi M., Seyedein S.H., Adeli M. Synthesis of strontium hexaferrite ($SrFe_{12}O_{19}$) by self-propagating high-temperature synthesis (SHS) method and investigation of the effect of milling on morphology and magnetic properties. *Ceram. Int.* 2024;50(20):38542–38549. https://doi.org/10.1016/j.ceramint.2024.07.222
11. Yu Z., Zhou N., Sun Y., Chen Z., Gong H., Shen B. Preparation of high-performance M-type strontium hexaferrites by ceramic method by optimizing the particle size of raw materials. *Solid State Sci*. 2023;144:107309. https://doi.org/10.1016/j.solidstatesciences.2023.107309

11. Yu Z., Zhou N., Sun Y., Chen Z., Gong H., Shen B. Preparation of high-performance M-type strontium hexaferrites by ceramic method by optimizing the particle size of raw materials. *Solid State Sci*. 2023;144:107309. https://doi.org/10.1016/j.solidstatesciences.2023.107309
12. Green M.L. Powder metallurgy processing of CrCoFe permanent magnet alloys containing 5–25 wt. % Co. *J. Appl. Phys.* 1982;53(3):2398–2400. https://doi.org/10.1063/1.330824
13. Shatsov A.A. Powder materials of the Fe – Cr – Co system. *Met. Sci. Heat Treat.* 2004;46(3–4):152–155. https://doi.org/10.1023/B:MSAT.0000036668.48856.02
14. Kaneko H., Sherwood R.C., Wong C.C. New Ductile Permanent Magnet of Fe-Cr-Co System. *AIP Conf. Proc*. 1972;5(1):1088–1092. https://doi.org/10.1063/1.2953814
15. Volegov A.S., Andreev S.V., Selezneva N.V., Ryzhikhin I.A., Kudrevatykh N.V., Mädler L., Okulov I.V. Additive manufacturing of heavy rare earth free high-coercivity permanent magnets. *Acta Materialia*. 2020;188:733–739. https://doi.org/10.1016/j.actamat.2020.02.058
16. Shumkin S.S., Sitnov V.V., Kamynin A.V., Chernyshov B.D., Semenov M.Y., Nikolaichik V.I. Composition and Operating Properties of Hard Magnetic Materials Based on Alloys of the Sm – Co – Cu – Fe – Zr System Obtained with the Use of Recoverable Resources. *Met. Sci. Heat Treat.* 2022;63:479–485. https://doi.org/10.1007/s11041-022-00715-y
17. Parkhomenko A.V., Amosov A.P., Samboruk A.R. Science intensive technology of metallic parts powder injection molding (MIM technology). *Naukoemkie tekhnologii v mashinostroenii = High-Tech Technologies in Mechanical Engineering.* 2012;12(18):8–13 (in Russ.).
18. Baidarov S.Yu., Kamynin A.V., Kraposhin V.S., Chernyshev D.L. Problems of development of MIM technology in Russia as applied to production of permanent magnets. *Met. Sci. Heat Treat.* 2020;61(9–10):559–562. https://doi.org/10.1007/s11041-020-00461-z
[Original Russian Text: Baidarov S.Yu., Kamynin A.V., Kraposhin V.S., Chernyshev D.L. Problems of development of MIM technology in Russia as applied to production of permanent magnets. *Metallovedenie i termicheskaya obrabotka metallov* 2019;9(771):34–37 (in Russ.).]
19. Malas A., Isakov D., Couling K., Gibbons G.J. Fabrication of High Permittivity Resin Composite for Vat Photopolymerization 3D Printing: Morphology, Thermal, Dynamic Mechanical and Dielectric Properties. *Materials.* 2019;12(23):3818–3833. https://doi.org/10.3390/ma12233818
20. Kostin D.V., Amosov A.P., Samboruk A.R., Chernyshev B.D. Influence of metal powder production method on microstructure and fluidity of magnetically alloy granulate. *Naukoemkie tekhnologii v mashinostroenii = High-Tech Technologies in Mechanical Engineering.* 2021;9(123):3–7 (in Russ.).
21. Kostishin V.G., Andreev V.G., Chitanov D.N., *et al.* Analysis of the effect of crushing of strontium hexaferrite powders in a vibratory mill on the properties of magnets on their basis. *Tech. Phys.* 2015;60(8):1194–1197 . https://doi.org/10.1134/S1063784215080149
[Original Russian Text: Kostishin V.G., Andreev V.G., Chitanov D.N., Timofeev A.V., Adamtsov A.Yu., Alekseev A.A. Study of the influence of grinding modes of strontium hexaferrite powders in a vibration mill on the properties of magnets based on them. *Zhurnal tekhnicheskoi fiziki.* 2015;8:91–93 (in Russ.).]
22. Ermakova L.V., Kuznetsova D.E., Poplevin D.S., *et al*. Effect of Acrylate Monomer on the Characteristics of Photopolymerizable Suspensions for Obtaining Ceramic from Stabilized ZrO_2. *Glass Ceram.* 2023;79:395–400. https://doi.org/10.1007/s10717-023-00520-w

12. Green M.L. Powder metallurgy processing of CrCoFe permanent magnet alloys containing 5–25 wt. % Co. *J. Appl. Phys.* 1982;53(3):2398–2400. https://doi.org/10.1063/1.330824
13. Shatsov A.A. Powder materials of the Fe – Cr – Co system. *Met. Sci. Heat Treat.* 2004;46(3–4):152–155. https://doi.org/10.1023/B:MSAT.0000036668.48856.02
14. Kaneko H., Sherwood R.C., Wong C.C. New Ductile Permanent Magnet of Fe-Cr-Co System. *AIP Conf. Proc*. 1972;5(1):1088–1092. https://doi.org/10.1063/1.2953814
15. Volegov A.S., Andreev S.V., Selezneva N.V., Ryzhikhin I.A., Kudrevatykh N.V., Mädler L., Okulov I.V. Additive manufacturing of heavy rare earth free high-coercivity permanent magnets. *Acta Materialia*. 2020;188:733–739. https://doi.org/10.1016/j.actamat.2020.02.058
16. Shumkin S.S., Sitnov V.V., Kamynin A.V., Chernyshov B.D., Semenov M.Y., Nikolaichik V.I. Composition and Operating Properties of Hard Magnetic Materials Based on Alloys of the Sm – Co – Cu – Fe – Zr System Obtained with the Use of Recoverable Resources. *Met. Sci. Heat Treat.* 2022;63:479–485. https://doi.org/10.1007/s11041-022-00715-y

17. Пархоменко А.В., Амосов А.П., Самборук А.Р. Наукоемкая технология инжекционного порошкового формования металлических изделий (MIM-технология). *Наукоемкие технологии в машиностроении.* 2012;12(18):8–13.
18. Байдаров С.Ю., Камынин А.В., Крапошин В.С., Чернышев Д.Л. Проблемы развития MIM-технологии в России в области производства постоянных магнитов. *Металловедение и термическая обработка металлов.* 2019;9(771):34–37.

19. Malas A., Isakov D., Couling K., Gibbons G.J. Fabrication of High Permittivity Resin Composite for Vat Photopolymerization 3D Printing: Morphology, Thermal, Dynamic Mechanical and Dielectric Properties. *Materials.* 2019;12(23):3818–3833. https://doi.org/10.3390/ma12233818

20. Костин Д.В., Амосов А.П., Самборук А.Р., Чернышев Б.Д. Влияние способа получения металлических порошков на микроструктуру и текучесть гранулята магнитотвердого сплава. *Наукоемкие технологии в машиностроении.* 2021;9(123):3–7. https://doi.org/10.30987/2223-4608-2021-9-3-7
21. Костишин В.Г., Андреев В.Г., Читанов Д.Н., Тимофеев А.В., Адамцов А.Ю., Алексеев А.А. Исследование влияния длительности измельчения порошков гексаферрита стронция на микроструктуру и свойства магнитов на их основе. *Журн. технической физики*. 2015;8:91–93.
22. Ермакова Л.В., Кузнецова Д.Е., Поплевин Д.С., Смыслова В.Г., Карпюк П.В., Соколов П.С., Досовицкий Г.А., Чижевская С.В. Влияние акрилатного мономера на характеристики фотополимеризуемых суспензий для получения керамики из стабилизированного ZrO_2. Стекло и керамика. 2022;95(10):03–10. https://doi.org/10.14489/glc.2022.10.pp.003-010
23. Hostaša J., Schwentenwein M., Toci G., Esposito L., Brouczek D., Piancastelli A., Pirri A., Patrizi B., Vannini M., Biasini V. Transparent laser ceramics by stereolithography. *Scr. Mater.* 2020;187:194–196. https://doi.org/10.1016/j.scriptamat.2020.06.006
24. Rolere S., Soupremanien U., Bohnke M., Dalmasso M., Delafosse C., Laucournet R. New insights on the porous network created during solvent debinding of powder injection-molded (PIM) parts, and its influence on the thermal debinding efficiency. *J. Mater. Process. Technol.* 2021;295:117163–117173. https://doi.org/10.1016/j.jmatprotec.2021.117163
25. Basir A., Sulong A.B., Jamadon N.H., Muhamad N. Feedstock properties and debinding mechanism of yttria-stabilized zirconia/stainless steel 17-4PH micro-components fabricated via two-component micro-powder injection molding process. *Ceram. Int.* 2021;47(14):20476–20485. https://doi.org/10.1016/j.ceramint.2021.04.057

[Original Russian Text: Ermakova L.V., Kuznetsova D.E., Poplevin D.S., Smyslova V.G., Karpyuk P.V., Sokolov P.S., Dosovitskii G.A., Chizhevskaya S.V. Effect of Acrylate Monomer on the Characteristics of Photopolymerizable Suspensions for Obtaining Ceramic from Stabilized ZrO_2. *Steklo i keramika*. 2022;95(10):03–10 (in Russ). https://doi.org/10.14489/glc.2022.10.pp.003-010]

23. Hostaša J., Schwentenwein M., Toci G., Esposito L., Brouczek D., Piancastelli A., Pirri A., Patrizi B., Vannini M., Biasini V. Transparent laser ceramics by stereolithography. *Scr. Mater.* 2020;187: 194–196. https://doi.org/10.1016/j.scriptamat.2020.06.006
24. Rolere S., Soupremanien U., Bohnke M., Dalmasso M., Delafosse C., Laucournet R. New insights on the porous network created during solvent debinding of powder injection-molded (PIM) parts, and its influence on the thermal debinding efficiency. *J. Mater. Process. Technol.* 2021;295: 117163–117173. https://doi.org/10.1016/j.jmatprotec.2021.117163
25. Basir A., Sulong A.B., Jamadon N.H., Muhamad N. Feedstock properties and debinding mechanism of yttria-stabilized zirconia/ stainless steel 17-4PH micro-components fabricated via two-component micro-powder injection molding process. *Ceram. Int.* 2021;47(14):20476–20485. https://doi.org/10.1016/j.ceramint.2021.04.057
26. Maryisheva M.A., Aleksanyan I.Yu., Nugmanov A.H.-H., Titova L.M., Maksimenko Y.A. Kinetics of technical paraffin dissolution in hexane and the specific heat of vaporization of a hexane-paraffin composition in the production of food paraffin. *Scientific journal NRU ITMO Series "Processes and Food Production Equipment."* 2022;1:12–21. https://doi.org/10.17586/2310-1164-2022-15-1-12-21
27. García-Martín E., Granados-Miralles C., Ruiz-Gómez S., Pérez L., Campo A., Guzmán-Mínguez J.C., Fernández C.J., Quesada A., Fernández J.F., Serrano A. Dense strontium hexaferrite-based permanent magnet composites assisted by cold sintering process. *J. Alloys Compound*. 2022;917:165531. https://doi.org/10.48550/arXiv.2309.16038
28. Benzing J., Hrabe N., Quinn T., White R., Rentz R., Ahlfors M. Hot isostatic pressing (HIP) to achieve isotropic microstructure and retain as-built strength in an additive manufacturing titanium alloy (Ti-6Al-4V). *Mater. Lett*. 2019;257: 126690–126695. https://doi.org/10.1016/j.matlet.2019.126690

26. Maryisheva M.A., Aleksanyan I.Yu., Nugmanov A.H.-H., Titova L.M., Maksimenko Y.A. Kinetics of technical paraffin dissolution in hexane and the specific heat of vaporization of a hexane-paraffin composition in the production of food paraffin. *Scientific journal NRU ITMO Series "Processes and Food Production Equipment."* 2022;1:12–21 (in Russ.). https://doi.org/10.17586/2310-1164-2022-15-1-12-21
27. García-Martín E., Granados-Miralles C., Ruiz-Gómez S., Pérez L., Campo A., Guzmán-Mínguez J.C., Fernández C.J., Quesada A., Fernández J.F., Serrano A. Dense strontium hexaferrite-based permanent magnet composites assisted by cold sintering process. *J. Alloys Compound*. 2022;917:165531. https://doi.org/10.48550/arXiv.2309.16038
28. Benzing J., Hrabe N., Quinn T., White R., Rentz R., Ahlfors M. Hot isostatic pressing (HIP) to achieve isotropic microstructure and retain as-built strength in an additive manufacturing titanium alloy (Ti-6Al-4V). *Mater. Lett*. 2019;257: 126690–126695. https://doi.org/10.1016/j.matlet.2019.126690

About the Authors

Bogdan D. Chernyshev, Postgraduate Student, Department of Physical Materials Science, National University of Science and Technology MISIS (NUST MISIS) (4-1, Leninskii pr., Moscow, 119049, Russia); Research Scientist, Laboratory of Metallurgical Processes, Giredmet (2-1, Electrodnaya ul., Moscow, 111524, Russia). E-mail: BDmChernyshev@rosatom.ru. Scopus Author ID 57219974902, RSCI SPIN-code 5059-3811, https://orcid.org/000-0003-4129-3420

Igor V. Schetinin, Cand. Sci. (Eng.), Associate Professor, Department of Physical Materials Science, National University of Science and Technology MISIS (NUST MISIS) (4-1, Leninskii pr., Moscow, 119049, Russia). E-mail: ingvvar@gmail.com. Scopus Author ID 36053563600, ResearcherID A-2270-2012, RSCI SPIN-code 8382-7666, https://orcid.org/0000-0002-0281-2497

Об авторах

Чернышев Богдан Дмитриевич, аспирант кафедры физического материаловедения, ФГАОУ ВО «Национальный исследовательский технологический университет «МИСИС» (НИТУ МИСИС) (119049, Россия, Москва, Ленинский пр-т, д. 4, стр. 1); научный сотрудник лаборатории металлургических процессов, АО «Государственный научно-исследовательский и проектный институт редкометаллической промышленности «Гиредмет» им. Н.П. Сажина» (АО «Гиредмет») (111524, Россия, Москва, ул. Электродная, д. 2, стр. 1). E-mail: BDmChernyshev@rosatom.ru. Scopus Author ID 57219974902, SPIN-код РИНЦ 5059-3811, https://orcid.org/000-0003-4129-3420

Щетинин Игорь Викторович, к.т.н., доцент кафедры физического материаловедения, ФГАОУ ВО «Национальный исследовательский технологический университет «МИСИС» (НИТУ МИСИС) (119049, Россия, Москва, Ленинский пр-т, д. 4, стр. 1). E-mail: ingvvar@gmail.com. Scopus Author ID 36053563600, ResearcherID A-2270-2012, SPIN-код РИНЦ 8382-7666, https://orcid.org/0000-0002-0281-2497

Translated from Russian into English by H. Moshkov
Edited for English language and spelling by Thomas A. Beavitt

Tonkie Khimicheskie Tekhnologii = Fine Chemical Technologies.
2025;20(3):276–288
ISSN 2686-7575 (Online)

Analytical methods in chemistry and chemical technology
Аналитические методы в химии и химической технологии

UDC 615.072
https://doi.org/10.32362/2410-6593-2025-20-3-276-288
EDN DNWEEB

RESEARCH ARTICLE

Quantitative determination of 8-methoxypsoralene in mild dosage form by high-performance liquid chromatography

Adnan Alsayed, Anastasiya A. Prezhedromirskaya✉, Elizaveta A. Shnyak, Stanislav A. Kedik
MIREA – Russian Technological University (M.V. Lomonosov Institute of Fine Chemical Technologies), Moscow, 119454 Russia
✉ *Corresponding author, e-mail: a.a.pregedromirskaya@ipt.ru.com*

Abstract

Objectives. To develop and validate a method for the quantitative determination of 8-methoxypsoralen in a soft dosage form in accordance with the requirements of the State Pharmacopoeia of the Russian Federation, 15th edition, and the Pharmacopoeia of the Eurasian Economic Union.

Methods. Quantitative determination of 8-methoxypsoralen was performed by high-performance liquid chromatography on a Chromaster 5000 (*Hitachi*, Japan) with a diode array detector. Chromatography was performed on a Kromasil EternityXT-5-C18, 5 µm, 250 × 4.6 mm column in isocratic mode with a mobile phase of acetonitrile/water in a ratio of 50 : 50% (*v*/*v*). The flow rate was 1.0 mL/min, while the detection wavelength was 250 nm.

Results. The optimal condition for the extraction of 8-methoxypsoralen was found to be ultrasonic gel extraction at 40°C for 15 min using acetonitrile. The best peak resolution of 8-methoxypsoralen was achieved during gel analysis at 250 nm using a reversed-phase sorbent with an octadecyl phase (C18) grafted onto silica gel. The acetonitrile/water mixture was used as a mobile phase in a volume ratio of 50 : 50% to minimize chromatography time while maintaining optimal resolution. From the validation procedures, it was confirmed that the method is specific, linear ($R^2 > 0.997$) and reproducible (relative standard deviation was ≤3.0%). The accuracy of the analytical method was from 98.26% to 101.02%, while the values of the detection and quantitative determination limits were 0.006 and 0.020 µg/mL, respectively. The developed quantitative determination method demonstrated its stability when varying as the column temperature and flow rate by ±5%.

Conclusions. As effectively implemented using the high-performance liquid chromatography method, the method for quantitative determination of 8-methoxypsoralen has a number of advantages over the previously described methods, including reduced analysis time, as well as increased sensitivity and effectiveness, which makes it possible to apply the developed method in assessing the quantitative content of 8-methoxypsoralen in a soft dosage form—gel for the treatment of psoriasis.

Keywords

8-methoxypsoralen, methoxalen, 8-MOP, mild dosage form, gel, quantitative determination, high-performance liquid chromatography, validation

Submitted: 31.10.2024
Revised: 15.01.2025
Accepted: 03.04.2025

For citation

Alsayed A., Prezhedromirskaya A.A., Shnyak E.A., Kedik S.A. Quantitative determination of 8-methoxypsoralene in mild dosage form by high-performance liquid chromatography. *Tonk. Khim. Tekhnol. = Fine Chem. Technol.* 2025;20(3):276–288. https://doi.org/10.32362/2410-6593-2025-20-3-276-288

НАУЧНАЯ СТАТЬЯ

Количественное определение 8-метоксипсоралена в мягкой лекарственной форме методом высокоэффективной жидкостной хроматографии

А. Алсайед, А.А. Прежедромирская✉, Е.А. Шняк, С.А. Кедик

МИРЭА – Российский технологический университет (Институт тонких химических технологий им. М.В. Ломоносова), Москва, 119454 Россия

✉ *Автор для переписки, e-mail: a.a.pregedromirskaya@ipt.ru.com*

Аннотация

Цель. Разработка и валидация методики количественного определения 8-метоксипсоралена в мягкой лекарственной форме в соответствии с требованиями Государственной Фармакопеи Российской Федерации XV издания и Фармакопеи Евразийского экономического союза.

Методы. Количественное определение 8-метоксипсоралена проводили методом высокоэффективной жидкостной хроматографии на приборе «Chromaster 5000» (*Hitachi*, Япония) с диодно-матричным детектором. Хроматографирование выполняли на колонке Kromasil EternityXT-5-C18, 5 мкм, 250 × 4.6 мм в изократическом режиме с подвижной фазой ацетонитрил/вода в соотношении 50 : 50% (об/об). Скорость потока составляла 1.0 мл/мин, длина волны детектирования — 250 нм.

Результаты. Установлено, что экстракция активного вещества из геля под действием ультразвука при температуре 40°C в течение 15 мин с использованием ацетонитрила является наиболее оптимальным условием для извлечения 8-метоксипсоралена. Наилучшее пиковое разрешение 8-метоксипсоралена было достигнуто при анализе геля на длине волны 250 нм с помощью обращенно-фазового сорбента с октадецильной фазой (C_{18}), привитой к силикагелю. Использование в качестве подвижной фазы смеси ацетонитрил/вода в объемном соотношении 50 : 50% позволило обеспечить минимальное время хроматографирования при сохранении оптимального разрешения. По данным валидационных процедур уставлено, что методика специфична, линейна ($R^2 > 0.997$) и воспроизводима (относительное стандартное отклонение составило ≤ 3.0%). Точность аналитической методики составила от 98.26% до 101.02%, а значения пределов обнаружения и количественного определения — 0.006 и 0.020 мкг/мл соответственно. Разработанная методика количественного определения показала свою устойчивость при варьировании как температуры колонки, так и скорости потока на ±5%.

Выводы. Методика количественного определения 8-метоксипсоралена была эффективно реализована с использованием метода высокоэффективной жидкостной хроматографии и обладает рядом преимуществ по сравнению с ранее описанными методиками. Эти преимущества заключаются в сокращении времени анализа, увеличении чувствительности и эффективности, что позволяет применять разработанную методику для оценки количественного содержания 8-метоксипсоралена в мягкой лекарственной форме — геле при лечении псориаза.

Ключевые слова

8-метоксипсорален, метоксален, 8-МОП, мягкая лекарственная форма, гель, количественное определение, высокоэффективная жидкостная хроматография, валидация

Поступила: 31.10.2024
Доработана: 15.01.2025
Принята в печать: 03.04.2025

Для цитирования

Алсайед А., Прежедромирская А.А., Шняк Е.А., Кедик С.А. Количественное определение 8-метоксипсоралена в мягкой лекарственной форме методом высокоэффективной жидкостной хроматографии. *Тонкие химические технологии*. 2025;20(3):276–288. https://doi.org/10.32362/2410-6593-2025-20-3-276-288

INTRODUCTION

Psoralenes are natural furanocoumarins found in medicinal plants such as *Psoralea corylifolia* L., *Ficus carica* L. and *Ficus petiolaris* L., *Ammi majus* L., and *Heracleum sosnowskyi* L. They have found wide application in photochemotherapy (Psoralen UltraViolet A (PUVA)), which uses psoralen as a photosensitizer combined with ultraviolet radiation in the 320–400 nm wavelength region [1]. Indications for phototherapy include epidermal diseases such as atopic dermatitis [2], psoriasis [3], vitiligo [4], photodermatoses, mycosis fungoides [5], and diseases due to deep cutaneous lesions (e.g., scleroderma).

The most commonly used photosensitizer when taking this approach is 8-methoxypsoralen (8-MOP). Considered one of the best generators of singlet oxygen and superoxide radicals among psoralens [6], 8-MOP is activated by ultraviolet radiation (UV) to form pyrimidine compounds inside cells (Fig. 1). After intercalating one psoralen molecule into the DNA double strand, one photon of light is absorbed under UV irradiation, followed by binding of a thymine base and absorption of an additional photon of light, binding of another thymine base, and so on. DNA-psoralen cross-linking inhibits DNA replication and causes cell cycle arrest [7]. This induces a number of antipolyferative, antiangiogenic, apoptotic and immunosuppressive effects [8].

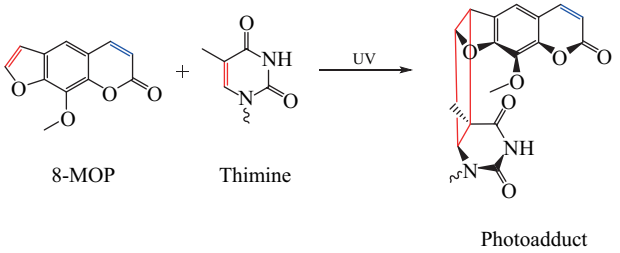

Fig. 1. Chemical structure of 8-MOP and its photoaddition to DNA

In studies comparing the efficacy of treatment methods, oral administration of PUVA solution was found to be more effective than parenteral administration [9]. However, gastrointestinal side effects, psychiatric disorders, optic nerve damage, and increased risk of melanoma and squamous cell cancer are possible [10]. Furthermore, 8-MOP is virtually insoluble in water and thus exhibits uneven absorption from the gastrointestinal tract, including inter-subject variability in plasma concentration [11]. Hence, the proposed topical therapy of 8-MOP is a more effective approach to enhance the bioavailability of the drug.

Various delivery systems designed to ensure the required level of resorption of 8-MOP, such as niosomes [12], nanoemulsions [13], microemulsions [14], and solid lipid nanoparticles [15], have been previously prepared and investigated to improve the transdermal penetration of 8-MOP. Conventional dosage forms such as ointments, creams and gels can be used as a carrier for 8-MOP nanosystems for topical application.

In addition to the necessity for research on the selection of drug delivery systems, it is important to develop and validate analytical techniques for detecting and quantifying 8-MOP content in soft dosage forms. High performance liquid chromatography (HPLC) equipped with a spectrophotometric detector, such as the Diode Array Detector (DAD), is one of the most commonly used quantification methods due to its versatility and ease of use [16, 17].

HPLC, namely its reversed-phase variation, is the simplest and most sensitive method for the quantification of 8-MOP, based on the peculiarities of its structure and physicochemical properties. Various parameters for instrumental analysis of 8-MOP have been described in the literature. Pitzanti *et al.* used a chromatograph with fluorescence detector at wavelengths of 317 and 445 nm. The analysis was an isocratic elution on an X Terra RP18 column (3.5 µm, 4.6 × 100 mm, *Waters*, USA). The mobile phase used was water, methanol and acetonitrile in a volume ratio of 40 : 40 : 20. Mahmoud *et al.* performed detection using UV detector to determine the 8-MOP content [18]. The researchers selected the conditions for the determination of 8-MOP on ACE® C18 column (5 µm, 4.6 × 150 mm, *Advanced Chromatography Technologies*, United Kingdom) in isocratic elution mode with methanol/water mobile phase in the volume ratio of 60 : 40. Detection was performed at a wavelength of 300 nm. Ageev *et al.* proposed a technique using a spectrophotometric detector [19]. This approach used a Symmetry Shield C18-RP column (5 µm, 250 × 4.6 mm, *Waters*, USA) with a mobile phase consisting of phosphate buffer with pH 5.6 and acetonitrile in a volume ratio of 50 : 50, and detection was performed at a wavelength of 285 nm. Kulikov *et al*. modified the previously described technique and used an acetonitrile/water system in a volume ratio of 50 : 50 as the mobile phase [20]. Barradas *et al*. used a chromatograph with UV detector and a NovaPak C18 column (150 × 3.9 mm, *Waters*, USA) [13]. The mobile phase was water and methanol in the ratio of 65 : 35. Detection was performed at a wavelength of 300 nm.

These methods have a number of disadvantages: the use of salt buffers in the mobile phase can lead to an increase in the working pressure of the equipment

and, accordingly, additional efforts to maintain the performance of the device. An additional disadvantage pertains to the use of methanol, which belongs to the group of particularly dangerous poisons and is under strict control and accounting. For this reason, the development of new analytical techniques for the determination of 8-MOP is still an urgent task[1].

Thus, the aim of the present study the development and validation of a new, more accurate, reproducible, selective, stable, highly sensitive methodology for the determination of the quantitative content of 8-MOP in a soft dosage form of the gel used in psoriasis therapy. In this case, the analytical methodology and validation procedures was carried out in accordance with the guidelines of good manufacturing practice and in compliance with the recommendations of the rules of production and quality control of medicines[2] and the 15th Edition of the State Pharmacopoeia of the Russian Federation[3].

MATERIALS AND METHODS

Reagents and materials

In the study to determine the quantitative content of 8-MOP in soft dosage form, 8-MOP substance (*Henan Tianfu Chemical Co.*, China) was used, as well as the following reagents: acetonitrile (highest purity, *Cryochrom*, Russia), water for chromatography (deionized water with electrical conductivity >0.18 mOhm/m).

The object of the study was a laboratory sample in the form of a gel with 8-MOP (hereinafter, "the gel"), whose composition is presented in Table 1.

Equipment

For sample preparation, Pioneer PA214C electronic analytical scales (China) were used. Preparation of water for chromatography was carried out using a Vodoley-M water deionizer (*Khimelektronika*, Russia). The studied samples were prepared using an ultrasonic bath (*Sapfir*, Russia). The study was carried out using a Chromaster 5000 chromatograph (*Hitachi*, Japan), equipped with a PUMP Chromaster 5160 universal pump module, 5430 Diode Array detector, 5310 Column Oven column thermostat and automatic dosing device, 5260 Autosampler. Control and data processing were carried out using the MultiChrome version 3.4 software[4].

Statistical processing of the results was carried out in accordance with General Pharmacopoeia Article (GPA) 1.1.0013.15 "Statistical processing of chemical experiment results"[5] using Microsoft Office Excel 2016 software.

Chromatography conditions

The chromatographic analysis conditions and chromatographic system suitability requirements are presented in Table 2.

Table 1. Composition of gel with 8-MOP

Components	Manufacturer	Concentration, wt %/wt
8-Methoxypsoralen	*Henan Tianfu Chemical Co.*, China	0.67
Clove oil	*Naturalnye masla*, Russia	7.95
Pluronic F68	*Sigma-Aldrich*, USA	1.06
Hydroxyethyl cellulose 250 HHX	Natrosol™ 250 G PHARM, *Ashland*, USA	1.4
Purified water (PA.2.2.0020)	–	88.92

1 https://regulation.eaeunion.org/upload/iblock/4ec/jsw9jphfi1xvwlf9vt4otsb8y2lz5322/ria_30062017_mdoc.pdf/. Accessed March 11, 2025.

2 https://meganorm.ru/Data2/1/4293828/4293828749.pdf/. Accessed March 11, 2025.

3 https://pharmacopoeia.regmed.ru/pharmacopoeia/izdanie-15/1/1-1/validatsiya-analiticheskikh-metodik/. Accessed March 11, 2025.

4 https://multichrom.ru/documentation/manuals/. Accessed March 11, 2025.

5 https://pharmacopoeia.ru/wp-content/uploads/2016/11/OFS.1.1.0013.15-Statisticheskaya-obrabotka-rezultatov-eksperimenta.pdf. Accessed March 11, 2025.

Table 2. Chromatographic parameters

Parameter	Value
Column	Kromasil EternityXT-5-C18, 5 µm, 250 × 4.6 mm, (*Nouryon*, No. X05CLA25)
Elution	Isocratic
Mobile phase	Acetonitrile : water (50 : 50% *v/v)*
Flow rate	1.0 mL/min
Temperature of column	25°C
Detection wavelength	250 nm
Injection volume	20 µL
Run time	10 min
System suitability requirements Number of theoretical plates (*N*) Relative standard deviation (RSD) Asymmetry Factor (As)	 At least 5000 At least 3.0% 0.8 < As < 1.5

Sample preparation methods

8-MOP reference standard sample solution (0.67 mg/mL)

67.0 mg (exact weighing) of 8-MOP substance was placed in a 100-mL volumetric flask, dissolved in acetonitrile, brought to the mark with the same solvent, and mixed.

8-MOP standard sample solution (0.067 mg/mL)

1.0 mL of the initial solution of 8-MOP standard sample was taken into a 10-mL volumetric flask, dissolved in acetonitrile, brought to the mark with the same solvent, and mixed. The resulting standard sample solution was filtered through a 33-mm Millipore Millex-HN Nylon 0.45 µm syringe filter (*Merck Millipore*, Germany) and transferred to a chromatographic vial.

Gel solution (10 mg/mL)

1.0 g (exact weighing) of gel was placed in a 100-mL measuring flask, 85 mL of acetonitrile was added; following treatment with ultrasound for 30 min, the volume of the solution was brought to the mark with acetonitrile. The resulting solution was filtered using a 33-mm Millipore Millex-HN Nylon 0.45 µm syringe filter and transferred to a chromatography vial.

Course of analysis

To determine the quantitative content of 8-MOP in the gel, sequential chromatographic analysis of the working solution of 8-MOP standard sample (at least 5 times) and the gel solution injected in triplicate was carried out.

Calculations

The content of 8-MOP ($C_{8\text{-MOP}}$, mg/g) in the soft dosage form was determined according to formula (1).

$$C_{8\text{-MOP}} = \frac{S_{gel} \cdot a_{8\text{-MOP}} \cdot V_{st.s.} \cdot 100 \cdot P}{S_{8\text{-MOP}} \cdot 100 \cdot 10 \cdot a_{gel} \cdot 100} = \frac{S_{gel} \cdot a_{8\text{-MOP}} \cdot 1 \cdot 100 \cdot P}{S_{8\text{-MOP}} \cdot 100 \cdot 10 \cdot a_{gel} \cdot 100} = \frac{S_{gel} \cdot a_{8\text{-MOP}} \cdot P}{S_{8\text{-MOP}} \cdot a_{gel} \cdot 1000}, \quad (1)$$

where $S_{8\text{-MOP}}$ and S_{gel} are average values of 8-MOP peak areas on chromatograms of 8-MOP standard sample solution and gel solution, respectively; $a_{8\text{-MOP}}$ is the 8-MOP standard sample weight, which was used to prepare a stock solution of 8-MOP standard sample, mg; $V_{st.s.}$ is the aliquot of the stock solution of 8-MOP standard sample used for final dilution, mL; a_{gel} is gel weight, g; P is a content of the main substance in the standard sample, %.

Method validation

Specificity

The specificity of the methodology for the quantification of 8-MOP in the gel was proved by comparing the chromatograms obtained by analyzing the solvent (acetonitrile), 8-MOP standard sample solution and gel solution.

Linearity and analytical domain

The linearity and analytical range of the methodology for the quantification of 8-MOP was established using 8-MOP standard sample solutions with concentration levels of 80%, 90%, 100%, 110%, and 120% of the nominal loading. The solutions were prepared by diluting the stock solution with a concentration of 0.67 mg/mL. The analysis was carried out in threefold repetition. According to the obtained results, a graph of the dependence of the peak area of 8-MOP on concentration was plotted. Using the mathematical dependence, the linear regression was calculated, and the correlation coefficient was determined (R^2).

Limit of detection and limit of quantification

As recommended by the State Pharmacopoeia, the limit of detection (LOD) and limit of quantification (LOQ) were determined by the ratio of analytical signal height to noise level. These parameters are determined using equations (2) and (3), respectively:

$$\mathrm{LOD} = \frac{3 \cdot h}{H} \cdot C, \quad (2)$$

$$\mathrm{LOQ} = \frac{10 \cdot h}{H} \cdot C, \quad (3)$$

where h is the background noise level, H is the 8-MOP peak height, C is the 8-MOP solution concentration.

Correctness

The correctness of the method was evaluated by the additive method by analyzing 9 individually prepared solutions of 8-MOP standard sample with concentration levels of 80%, 100%, 120% of the nominal loading in three repetitions each. The solutions were prepared by diluting the stock solution (concentration 0.67 mg/mL).

According to the results of the analysis, the response factor (RF) was calculated by formula (4).

$$\mathrm{RF} = \frac{\text{experimental value}}{\text{real value}} \cdot 100\%. \quad (4)$$

Based on the nine calculated values of the response factor, the relative standard deviation (RSD) and confidence interval were determined using equations (5) and (6), respectively.

$$\mathrm{RSD} = \frac{s}{x_{\mathrm{av}}} \cdot 100\%, \quad (5)$$

where s is the standard deviation of the measurement series and x_{av} is the average value of the variable being changed.

$$\Delta x = \frac{t(P, f) \cdot s}{\sqrt{n}}, \quad (6)$$

where $t(P, f)$ is the tabular value of Student's criterion at P (confidence level) = 95%, f (number of degrees of freedom) = 8; s is the standard deviation of the measurement series; n is the number of measurements.

Precision (repeatability)

To assess the precision (repeatability) of the methodology, we used a variant in which we prepared six solutions of 8-MOP standard sample with a concentration level of 100% of the nominal loading (the preparation procedure is described in the *Linearity* section).

According to the results of measurements, the relative standard deviation of peak areas of 8-MOP was calculated by formula (5).

Intra-laboratory (intermediate) precision

To assess the intra-laboratory precision of the methodology, six solutions of 8-MOP standard sample were prepared each with a concentration level of 100% of the nominal loading (the preparation procedure is described in the *Linearity* section). Two chemists analyzed the prepared solutions through a complete analytical procedure from sample preparation to results on different days.

From the measurements of each of the two analytical sessions, the relative standard deviation of the 8-MOP peak areas was calculated using formula (5). Fisher's criterion (F) for two analytical sessions was calculated by formula (7).

$$F = \frac{s_1^2}{s_2^2}, \quad (7)$$

where s^2 are dispersions of the first and second series of measurements.

Stability

To assess stability, a solution of 8-MOP standard sample was prepared with a concentration level of 100% of the nominal loading (the preparation procedure is described in the *Linearity* section). The solution was chromatographically analyzed at column temperatures differing by ±5% from the temperature stated

in the methodology, i.e., at 23.5 and 26.5°C, respectively. The flow rate was also varied by ±5% from the value stated in the method.

The relative standard deviation of the peak areas of 8-MOP at different chromatography conditions was calculated from the results of measurements according to formula (5).

RESULTS AND DISCUSSION

Development of a quantitative determination methodology

Despite the many techniques already developed and validated for the quantification of 8-MOP, previous studies have not provided evidence of the reproducibility and performance of these approaches during routine laboratory analysis.

When developing the methodology for quantitative determination of 8-MOP in soft dosage form by HPLC, several variants of chromatographic columns differing in the type of filler were used. The low solubility of the detected substance in aqueous media was taken into account during the selection of the stationary phase to indicates the preferable use of sorbent with octadecyl phase (C_{18}) grafted to silica gel [21]. Since the properties of the stationary phase can change over time during use or simply storage [22], two columns with similar stationary phase characteristics were used in the development process: a Luna C18(2) 5 µm, 250 × 4.6 mm column (*Phenomenex*, USA) and a Kromasil Eternity XT-5-C18, 5 µm, 250 × 4.6 mm column. From the evaluation of the suitability of the chromatographic system, the efficiency of the Luna C18(2) column was found to be 1400 theoretical plates, which did not meet the suitability requirements for the chromatographic system. Since the Kromasil EternityXT-5-C18 column demonstrated higher efficiency (15000 theoretical plates) under otherwise identical conditions, it was selected as the primary column for the analytical methodology for the quantification of 8-MOPs.

Further, the effect of introducing acetonitrile and methanol as an organic modifier into the mobile phase was evaluated. The use of acetonitrile resulted in optimal resolution in a short period of time (less than 10 min), while the use of methanol as a component of the mobile phase caused a change in the asymmetry of the peak of the detected substance, which does not meet the requirements of the suitability of the chromatographic system. In the course of further studies, we varied the volume content of acetonitrile in water for chromatography in the range of 20–50% due to the insufficient dissociation of the lower water content in the silanol groups [23]. Eluents with higher water content (more than 50%) cause dehydration of the stationary phase [24]. Under these conditions, a hydrocarbon film formed due to dispersion interactions between the alkyl groups of the stationary phase becomes stronger than when interacting with the eluent, which actually blocks the interaction of the synol groups with 8-MOP. Optimal sensitivity and resolution were achieved at an acetonitrile/water ratio of 50 : 50% (*v*/*v*) and a mobile phase flow rate of 1.0 mL/min.

Evaluation of the electronic absorption spectrum of 8-MOP (Fig. 2) using DAD, showed that the maximum response is observed at absorption of radiation with a wavelength of 250 nm.

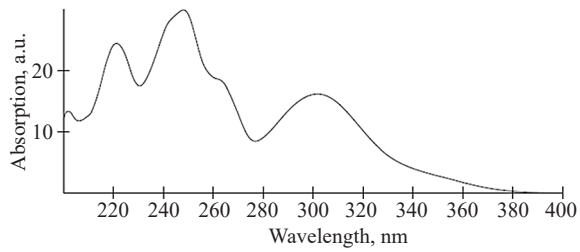

Fig. 2. Spectral analysis of 8-MOP

Method validation

Validation of the method was performed in accordance with GPA.1.1.0012.15 "Validation of Analytical Methods"[6] and the document "Guide for Validation of Analytical Methods"[7] for the following characteristics: specificity, LOD, LOQ, linearity, analytical range, correctness, repeatability (convergence), intra-laboratory (intermediate) precision.

Specificity

To assess the specificity of the methodology for the quantification of 8-MOP, the following model samples were analyzed: solvent (acetonitrile), 8-MOP standard sample solution and gel solution.

The chromatograms of the solvent (Fig. 3), 8-MOP standard sample solution (Fig. 4), and gel solution (Fig. 5) are as presented below.

In the chromatogram of the blank sample (solvent), there are no peaks with retention times corresponding

6 https://pharmacopoeia.ru/ofs-1-1-0012-15-validatsiya-analiticheskih-metodik/. Accessed March 11, 2025.

7 https://regulation.eaeunion.org/upload/iblock/4ec/jsw9jphfi1xvwlf9vt4otsb8y2lz5322/ria_30062017_mdoc.pdf/. Accessed March 11, 2025.

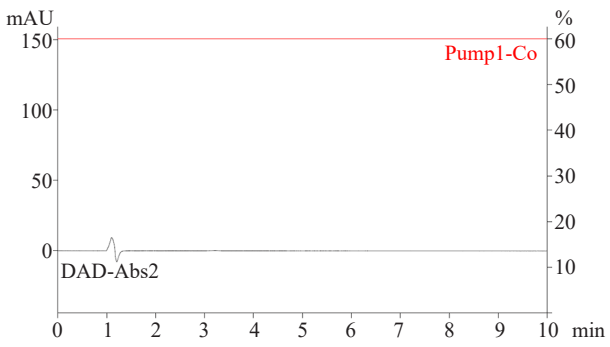

Fig. 3. Chromatogram of solvent

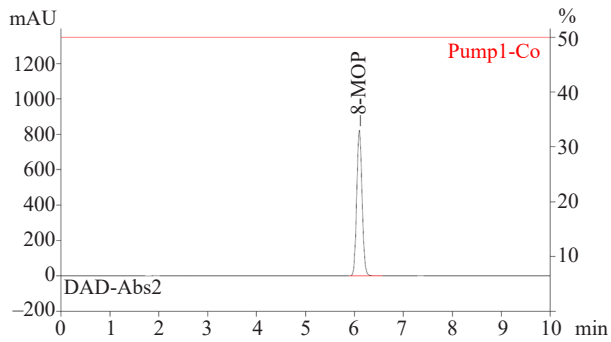

Fig. 4. Chromatogram of reference standard 8-MOP solution (0.067 mg/mL)

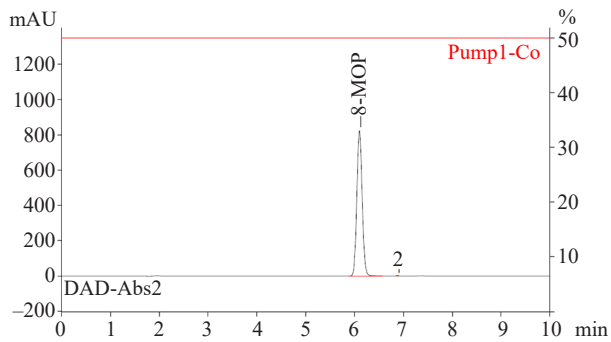

Fig. 5. Chromatogram of gel solution (10 mg/mL)

to a retention time of 8-MOP that could interfere with the determination of the analyte. The retention time of 8-MOP on the chromatogram of the standard sample solution (Fig. 4) is identical to that of the analyte peak on the chromatogram of the gel solution (Fig. 5). Thus, it is experimentally confirmed that the presence of accompanying components and impurities does not affect the analytical result and the technique is specific.

LOD and LOQ

The LOD of 8-MOP was 0.006 μg/mL and the LOQ was 0.02 μg/mL, allowing qualitative and quantitative compositional evaluation of samples with low analyte content.

Linearity and analytical domain

To confirm the linearity of the developed methodology, chromatography of 8-MOP standard sample solutions was performed with concentration levels of 80%, 90%, 100%, 110%, and 120% of the nominal value of 8-MOP concentration in the standard sample solution (Table 3). Solutions of each concentration level were analyzed in triplicate.

Table 3. Linearity parameters

Concentration, %	Concentration of 8-MOP, mg/mL	Peak area, mAU·s
80	5.36	2732.56
	5.36	2712.03
	5.36	2756.31
90	6.03	3074.36
	6.03	3098.33
	6.03	3058.87
100	6.7	3436.12
	6.7	3415.33
	6.7	3485.13
110	7.37	3757.21
	7.37	3788.99
	7.37	3741.22
120	1.2	4098.22
	1.2	4134.12
	1.2	4107.84
Slope		514.15
Segment cut off by a straight line on the *y* axis		−18.364
Linear correlation (R^2)		0.9979

Based on the results obtained, a calibration plot of the dependence of the peak area of 8-MOP on the concentration of 8-MOP in the standard sample solutions was constructed (Fig. 6). Linear regression was calculated using the mathematical dependence. The correlation coefficient was 0.9979, which indicates a linear relationship between concentrations and peak area values of 8-MOP.

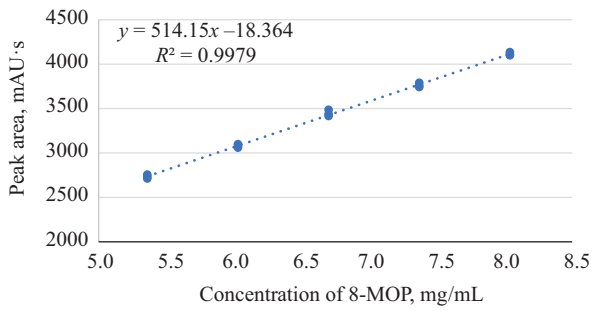

Fig. 6. Linear calibration curve

Correctness

To confirm the correctness of the methodology, nine solutions were analyzed: three solutions having a concentration level of 100% of the nominal value of 8-MOP concentration in the standard sample solution and three solutions each with a concentration level limiting the linear range of the methodology, i.e., 80% and 120% of the nominal value of 8-MOP concentration in the standard sample solution, respectively (Table 4).

The average value of the method opening parameter used to evaluate the correspondence between the results obtained with this analytical technique and the value taken as true was 99.42%. All values of the response factor are in the range of 95–105%, corresponding to the limits required in the 15th Edition of the State Pharmacopoeia of the Russian Federation.

Precision (repeatability)

The intra-laboratory precision of the 8-MOP quantification technique was determined by analyzing six similar solutions of 8-MOP standard sample at the same concentration but on different days and by two chemists (Table 5).

Precision was assessed by processing the experimental data obtained during two analytical sessions by calculating the relative standard deviation of the concentrations found. The relative standard deviation of the 8-MOP peak area for each analytical session conducted on different days, by different chemists, was ≤3.0%. The statistical equivalence of the results obtained from the two analytical sessions of the results was assessed by calculating Fisher's criterion

Table 4. Accuracy parameters

Concentration, %	Amount taken, mg/mL	Peak area, mAU·s	Amount found, mg/mL	Response, %
80	5.36	2732.56	5.31	99.01
80	5.36	2712.03	5.27	98.26
80	5.36	2756.31	5.35	99.87
100	6.7	3436.12	6.67	99.60
100	6.7	3415.33	6.63	99.00
100	6.7	3485.13	6.77	101.02
120	8.04	4098.22	7.96	98.99
120	8.04	4134.12	8.03	99.86
120	8.04	4107.84	7.98	99.22

Statistical characteristics	Results	Eligibility criteria
Average, %	99.42	95–105
RSD, %	0.79	≤3.0
The upper limit of the confidence interval (P = 95%), %	101.02	100
The lower limit of the confidence interval (P = 95%), %	98.26	

Table 5. Precision parameters

No.	Chemist 1		Chemist 2	
	Peak area, mAU·s	Found concentration, mg/mL	Peak area, mAU·s	Found concentration, mg/mL
1	3426.24	6.65	3455.36	6.71
2	3355.69	6.52	3498.33	6.79
3	3512.67	6.82	3412.85	6.63
4	3478.98	6.76	3512.65	6.82
5	3504.22	6.80	3459.36	6.72
6	3400.25	6.60	3425.22	6.65
RSD, %		1.81	1.13	
Fisher's criterion *F* (95; 5; 5)			2.54	

(*F*-test). The value of Fisher's criterion is less than the tabulated value of Fisher's criterion *F* (95, 5, 5) = 99.01, indicating an insignificant difference between the results of the two analytic sessions at 95% confidence level. Thus, the conducted validation studies demonstrate that the methodology provides comparable results under the influence of additional random factors.

Stability

To assess the stability of the methodology for quantitative determination of 8-MOP, the standard sample solution was chromatographed by varying the column temperature by ±5% from the temperature stated in the methodology, i.e., at 23.5 and 26.5°C, respectively. The deviation from the eluent flow rate stated in the method was ±5% (Table 6).

Table 6. Robustness parameters

Column temperature, °C	Flow rate, mL/min	Peak area, mAU·s
23.5	1.0	3456.51
		3524.12
		3489.22
25.0	1.0	3512.36
		3497.36
		3524.98
26.5	1.0	3552.14
		3547.56
		3485.22
25.0	0.95	3458.69
		3541.22
		3567.54
25.0	1.05	3478.29
		3500.27
		3466.88
RSD, %		1.01

Changes in flow rate and column temperature values by ±5% do not significantly affect the obtained results. The relative standard deviation of the 8-MOP peak area on the chromatograms of the standard sample solution of less than 3.0% meets the requirements of the suitability of the chromatographic system.

CONCLUSIONS

The described technique for the quantitative determination of 8-MOP by HPLC offers a number of significant advantages over most of the previously described methods. The use of acetonitrile instead of methanol as an organic modifier of the mobile phase allows working in acetonitrile/water mixture at a wavelength corresponding to the maximum response of the detector at absorption of radiation by the substance. Elution of the analyte in the presence of acetonitrile occurs earlier than in the presence of methanol in the mobile phase. This significantly reduces the analysis time, which is the most important factor for routine analysis. Unlike existing techniques, no salt buffers were used in the mobile phase; such approaches are undesirable due to increased working pressure and the considerable effort required to maintain instrument performance.

The technique was validated according to the guidelines set forth in the 15th Edition of the State Pharmacopoeia of the Russian Federation, which confirms its accuracy, precision, selectivity, and reliability. Considering the sensitivity of the methodology, its efficiency and ability to meet all validity parameters, it represents a reliable platform for the quantification of 8-MOP in finished dosage form.

Authors' contribution

All the authors took an active part in the discussion, analysis, and development of the experiment, processing the results, writing the text of the article and discussing it.

The authors declare no conflicts of interest.

REFERENCES

1. Bishnoi A., Parsad D. Phototherapy for vitiligo: A narrative review on the clinical and molecular aspects, and recent literature. *Photoderm. Photoimm. Photomed*. 2024;40(3):12968. https://doi.org/10.1111/phpp.12968
2. Molla A. A Comprehensive Review of Phototherapy in Atopic Dermatitis: Mechanisms, Modalities, and Clinical Efficacy. *Cureus.* 2024;16(3):e56890. https://doi.org/10.7759/cureus.56890
3. Barros N., Sbroglio L., Buffara M., Baka J., Pessoa A., Azulay-Abulafia L. Phototherapy. *An. Bras. Dermatol*. 2021;96(4):397–407. https://doi.org/10.1016/j.abd.2021.03.001
4. Wełniak A., Białczyk A., Kamińska B., Czajkowski R. Phototherapy in the management of vitiligo – an updated narrative review. *Eur. J. Clin. Exp. Med*. 2024;22(3):668–676. https://doi.org/10.15584/ejcem.2024.3.26
5. Zengarini C., Baruffaldi G., Piraccini B.M., Bardazzi F., Mussi M., Stancic B., Pileri A. Nb-UVB and PUVA therapy in treating early stages of Mycosis Fungoides: A single-center cross-sectional study. *Photoderm. Photoimm. Photomed*. 2023;39(5):435–440. https://doi.org/10.1111/phpp.12873
6. Serrano-Pérez J.J., González-Luque R., Merchán M., *et al*. The family of furocoumarins: Looking for the best photosensitizer for phototherapy. *J. Photochem. Photobiol. A: Chem.* 2008;199(1): 34–41. https://doi.org/10.1016/j.jphotochem.2008.04.013
7. Diekmann J., Theves I., Thom K.A., Gilch P. Tracing the Photoaddition of Pharmaceutical Psoralens to DNA. *Molecules.* 2020;25(22):5242. https://doi.org/10.3390/molecules25225242
8. Vieyra-Garcia P., Wolf P. A deep dive into UV-based phototherapy: Mechanisms of action and emerging molecular targets in inflammation and cancer. *Pharmacol. Ther*. 2021;222:107784. https://doi.org/10.1016/j.pharmthera.2020.107784
9. Schalla W., Schaefer H., Kammerau B., Zesch A. Pharmacokinetics of 8-methoxypsoralen (8-MOP) after oral and local application. *J. Invest. Dermatol*. 1976;66:258–259.
10. Lapolla W., Yentzer B.A., Bagel J., Halvorson C.R., Feldman S.R. A review of phototherapy protocols for psoriasis treatment. *J. Am. Acad. Dermatol.* 2011;64(5):936–949. https://doi.org/10.1016/j.jaad.2009.12.054
11. Hönigsmann H., Szeimies R., Knobler R. Chapter 238. Photochemotherapy and Photodynamic Therapy. In: Goldsmith L.A., Katz S.I., Gilchrest B.A., Paller A.S., Leffell D.J., Wolff K. (Eds.). *Fitzpatrick's Dermatology in General Medicine*. 8th Edition. TMcGraw-Hill Companies; 2012.
12. Kassem A.A., Abd El-Alim S.H., Asfour M.H. Enhancement of 8-methoxypsoralen topical delivery via nanosized niosomal vesicles: formulation development, *in vitro* and *in vivo* evaluation of skin deposition. *Int. J. Pharm*. 2017; 517(1–2):256–268. https://doi.org/10.1016/j.ijpharm.2016.12.018
13. Barradas T.N., Senna J.P., Cardoso S.A., de Holanda e Silva K.G., Mansur C.R.E. Formulation characterization and *in vitro* drug release of hydrogel-thickened nanoemulsions for topical delivery of 8-methoxypsoralen. *Mater. Sci. Eng. C Mater. Biol. Appl*. 2018;92:245–253. https://doi.org/10.1016/j.msec.2018.06.049
14. Wu J.Y., Li Y.J., Liu T.T., *et al.* Microemulsions vs chitosan derivative-coated microemulsions for dermal delivery of 8-methoxypsoralen. *Int. J. Nanomed*. 2019;14:2327–2340. https://doi.org/10.2147/IJN.S191940
15. Pitzanti G., Rosa A., Nieddu M., *et al.* Transcutol® P containing SLNs for improving 8-methoxypsoralen skin delivery. *Pharmaceutics.* 2020;12(10):973. https://doi.org/10.3390/pharmaceutics12100973
16. Chew Y.L., Khor M.A., Lim Y.Y. Choices of Chromatographic Methods as Stability Indicating Assays for Pharmaceutical Products: A Review. *Heliyon*. 2021;7(3):e06553. https://doi.org/10.1016/j.heliyon.2021.e06553
17. Araujo P. Key Aspects of Analytical Method Validation and Linearity Evaluation. *J. Chromatogr. B. Anal. Technol. Biomed. Life Sci.* 2009;877(23):2224–2234. https://doi.org/10.1016/j.jchromb.2008.09.030
18. Mahmoud D., ElMeshad A., Fadel M., Tawfik A., Ramez S. Photodynamic therapy fortified with topical oleyl alcohol-based transethosomal 8-methoxypsoralen for ameliorating vitiligo: Optimization and clinical study. *Int. J. Pharm*. 2022;614:121459. https://doi.org/10.1016/j.ijpharm.2022.121459

19. Ageev V.P., Shlyapkina V.I., Kulikov O.A., Zaborovskiy A.V., Tararina L.A. Qualitative and quantitative analysis of the main psoralen derivatives in the juice of Sosnovsky's hogweed. *Farmatsiya = Pharmacy*. 2022;71(3):10–17 (in Russ.). https://doi.org/10.29296/25419218-2022-03-02
20. Kulikov O., Ageev V., Brodovskaya E., Shlyapkina V., Petrov P., Zharkov M., Yakobson D., Maev I., Sukhorukov G., Pyataev N. Evaluation of photocytotoxicity liposomal form of furanocoumarins Sosnowsky's hogweed. *Chem. Biol. Interact*. 2022;357:109880. https://doi.org/10.1016/j.cbi.2022.109880
21. Ahmed A., Skinley K., Zhang H. Column technology for liquid chromatography. In: Fanali S., Haddad P.R., Poole C., Lloyd D.K. (Eds.). *Liquid Chromatography: Fundamentals and Instrumentation*. Volume 1 in *Handbooks in Separation Science*. 2023. P. 37–60. https://doi.org/10.1016/B978-0-323-99968-7.00007-2
22. Bachhav H., Shirsath G., Badhe S., Kurne D., Sonawane S. AI-driven data analysis for identification of impurities in HPLC chromatograms & artificial intelligent system for HPLC column selection and method development. *World J. Pharmac. Res*. 2024;13(13)238–263.
23. García-Alvarez-Coque M., Torres-Lapasió J., Ruiz-Angel M., Navarro-Huerta J. Secondary chemical equilibria in reversed-phase liquid chromatography. In: Fanali S., Haddad P.R., Poole C., Lloyd D.K. (Eds.). *Liquid Chromatography: Fundamentals and Instrumentation*. Volume 1 in *Handbooks in Separation Science*. 2023. P. 121–143. https://doi.org/10.1016/B978-0-323-99968-7.00012-6
24. Žuvela P., Skoczylas M., Jay Liu J., Bączek T., Kaliszan R., Wong M.W., Buszewski B. Column Characterization and Selection Systems in Reversed-Phase High-Performance Liquid Chromatography. *Chem. Rev*. 2019;119(6):3674–3729. https://doi.org/10.1021/acs.chemrev.8b00246

About the Authors

Adnan Alsayed, Process Engineer, Department of Biotechnology and Industrial Pharmacy, M.V. Lomonosov Institute of Fine Chemical Technologies, MIREA – Russian Technological University (78, Vernadskogo pr., Moscow, 119454, Russia). E-mail: Adnanalsayed00@gmail.com. https://orcid.org/0009-0004-8265-934X

Anastasiya A. Prezhedromirskaya, Engineer, Department of Biotechnology and Industrial Pharmacy, M.V. Lomonosov Institute of Fine Chemical Technologies, MIREA – Russian Technological University (78, Vernadskogo pr., Moscow, 119454, Russia). E-mail: a.a.pregedromirskaya@ipt.ru.com. https://orcid.org/0009-0001-5985-3900

Elizaveta A. Shnyak, Can. Sci. (Pharm.), Associate Professor, Department of Biotechnology and Industrial Pharmacy, M.V. Lomonosov Institute of Fine Chemical Technologies, MIREA – Russian Technological University (78, Vernadskogo pr., Moscow, 119454, Russia). E-mail: elizaweta__@mail.ru. ResearcherID H-9402-2013, RSCI SPIN-code 7112-7197, https://orcid.org/0000-0001-8560-7060

Stanislav A. Kedik, Dr. Sci. (Eng.), Professor, Head of the Department of Biotechnology and Industrial Pharmacy, M.V. Lomonosov Institute of Fine Chemical Technologies, MIREA – Russian Technological University (78, Vernadskogo pr., Moscow, 119454, Russia). E-mail: doctorkedik@yandex.ru. Scopus Author ID 7801632547, https://orcid.org/0000-0003-2610-8493

Об авторах

Алсайед Аднан, инженер-технолог, кафедра биотехнологии и промышленной фармации, Институт тонких химических технологий им. М.В. Ломоносова, ФГБОУ ВО «МИРЭА – Российский технологический университет» (119454, Москва, пр-т Вернадского, д. 78). E-mail: Adnanalsayed00@gmail.com. https://orcid.org/0009-0004-8265-934X

Прежедромирская Анастасия Александровна, инженер, кафедра биотехнологии и промышленной фармации, Институт тонких химических технологий им. М.В. Ломоносова, ФГБОУ ВО «МИРЭА – Российский технологический университет» (119454, Москва, пр-т Вернадского, д. 78). E-mail: a.a.pregedromirskaya@ipt.ru.com. https://orcid.org/0009-0001-5985-3900

Шняк Елизавета Александровна, к.фарм.н., доцент, кафедра биотехнологии и промышленной фармации, Институт тонких химических технологий им. М.В. Ломоносова, ФГБОУ ВО «МИРЭА – Российский технологический университет» (119454, Москва, пр-т Вернадского, д. 78). E-mail: elizaweta__@mail.ru. ResearcherID H-9402-2013, SPIN-код РИНЦ 7112-7197, https://orcid.org/0000-0001-8560-7060

Кедик Станислав Анатольевич, д.т.н., профессор, заведующий кафедрой биотехнологии и промышленной фармации, Институт тонких химических технологий им. М.В. Ломоносова, ФГБОУ ВО «МИРЭА – Российский технологический университет» (119454, Россия, Москва, пр-т Вернадского, д. 78). E-mail: doctorkedik@yandex.ru. Scopus Author ID 7801632547, https://orcid.org/0000-0003-2610-8493

Translated from Russian into English by H. Moshkov
Edited for English language and spelling by Thomas A. Beavitt

ISSN 2686-7575 (Online)

Erratum

Исправления

https://doi.org/10.32362/2410-6593-2025-20-3-289
EDN FJFAXB

Erratum to the article "Production of the recombinant hemagglutinin protein of the swine influenza virus A/H1N1 and analysis of its physicochemical and antigenic properties"

Elena D. Avdonina, Kristina A. Pervoykina, Ludmila V. Verkhovskaya, Dmitriy N. Shcherbinin, Natalia Yu. Viskova, Irina S. Kruzhkova, Maria A. Ilina, Larisa V. Kudriavtseva, Lyudmila V. Kolobukhina, Maksim M. Shmarov, Natalya A. Antipyat, Alexander L. Gintsburg, Igor N. Tyurin

Tonk. Khim. Tekhnol. = Fine Chem. Technol. 2025;20(2):107–118. https://doi.org/10.32362/2410-6593-2025-20-2-107-118

Page 110, line 11, instead of:

"The obtained swH1-His gene (full sequence is given in Table 2) was cloned by simple linear iterative clustering (SLIC) into the shuttle plasmid...".

should read:

"The obtained swH1-His gene (full sequence is given in Table 2) was cloned by sequence and ligation-independent cloning (SLIC) into the shuttle plasmid...".

The original article can be found under https://doi.org/10.32362/2410-6593-2025-20-2-107-118

MIREA – Russian Technological University
78, Vernadskogo pr., Moscow, 119454, Russian Federation.
Publication date *June 30, 2025.*
Not for sale

МИРЭА – Российский технологический университет
119454, РФ, Москва, пр-т Вернадского, д. 78.
Дата опубликования *30.06.2025.*
Не для продажи

www.finechem-mirea.ru